Editor Board

THE CONTENTS

FIRST AXIS: MATHEMATICS RESEARCH

SECOND AXIS: COMPUTING RESEARCH

THIRD AXIS: STATISTICS RESEARCH

Some Properties of Fuzzy AB-ideal of AB-algebras

Areej Tawfeeq Hameed   **Baneen Najah Abaas**

Department of Mathematics, Faculty of Education for Girls, University of Kufa.
areej238@gmail.com   areejtawfeeq@uokufa.edu.iq

Abstract:

In this research we have introduced the concept of fuzzy AB-ideal of AB-algebra and also we proved some relevant characteristics and theories. We also studied the fuzzy relations on AB-algebras and fuzzy derivations   AB-ideals. We presented the characteristics and theories that illustrat the two concepts that is promted us to study Cartesian Product of fuzzy derivations AB-ideals.

Keywords:

Fuzzy derivation AB-ideal of AB-algebras, Cartesian Product of Fuzzy Derivations AB-ideals .

Mathematics Subject Classification: 06F35, 03G25, 03B52.

Introduction:

The notion of BCC-algebras was proposed by W.A. Dudek in ([9],[10],[11]). S.S. Ahn and H.S. Kim have introduced the notion of QS-algebras. A.T. Hameed and et al ([7],[8]) introduced the notions of QS-ideal and fuzzy QS-ideal of QS-algebra. A.T. Hameed, and et al have introduced the notion of fuzzy QS-ideal of QS-algebra in [1]. A.T. Hameed introduce new of abstract algebras: is called KUS-algebras and define its ideals as KUS-algebras in ([5]). In 2017, A.T. Hameed and B.N. Abbas. introduced the notion of AB-ideals in AB-algebras, described connections between such ideal and congruences and some properties of AB-algebra in ([2],[3]). A.T. Hameed and B.N. Abbas, considered the fuzzification of AB-ideals in

AB-algebras [4]. In this paper, we introduce the notion of fuzzy derivation on AB-algebras and obtain some of related properties and we characterized Cartesian Product of Fuzzy Derivations AB-ideals .

1.Preliminaries:

We review some definitions and properties that will be useful in our results.

Areej .T /Baneen .N

Definition 1.1.([2],[3]) Let X be a set with a binary operation "∗" and a constant 0.Then (X, ∗, 0) is called **an AB-algebra** if the following axioms satisfied: for all x, y, z ∈X:

(i) $((x * y) * (z * y)) * (x * z) = 0$,

(ii) $0 * x = 0$,

(iii) $x * 0 = x$,

Note that: Define a binary relation (≤) on X by $x * y = 0$ if and only if, $x \leq y$. Then(X, ≤) is a partially ordered set.

Proposition 1.2.([2],[3]) In any AB-algebra X, for all x, y, z ∈ X, the following properties hold:

(1) $(x * y) * x = 0$.

(2) $x \leq y$ *implies* $x * z \leq y * z$.

(3) $x \leq y$ *implies* $z * y \leq z * x$.

Remark 1.3.([2],[3]) An AB-algebra is satisfies for all x, y, z ∈X

(1) $(x * y) * z = (x * z) * y$

(2) $(x * (x * y)) * y = 0$.

Definition 1.4.([2],[3]) Let X be an AB-algebra and I ⊆ X. I is called **an AB-ideal of X** if it satisfies the following conditions:

(i) $0 \in$ I,

(ii) $(x * y) * z \in$ I and $y \in$I imply $x * z \in$I.

Definition 1.5.([2],[3]) For an AB-algebra X, we denote $x \wedge y = y * (y * x)$, for all x, y ∈X,

$x \wedge y \leq x$, y.

Definition 1.6.([2],[3]) An AB-algebra is said to be **commutative** if and only if, satisfies for all x, y ∈ X, $x * (x * y) = y * (y * x)$, i.e, $x \wedge y = y \wedge x$.

Definition 1.7.([2],[3]) Let X be an AB-algebra. A mapping d : X → X is a left-right derivation (briefly,(l,r)-derivation) of X,

if it satisfies the identity
 $d(x * y) = (d(x) * y) \wedge (x * d(y))$, for all x, y ∈ X,

if d satisfies the identity $d(x * y) = (x * d(y)) \wedge (d(x) * y)$, for all x, y ∈ X.

Then d is a right-left derivation (briefly, (r, l)-derivation) of X.

Moreover, if d is both a (l,r) and (r,l)-derivation, then d is a derivation of X.

Example 1.8. Let X = {0,1,2,3} be an AB-algebra in which the operation (*) is defined as follows:

*	0	1	2	3
0	0	0	0	0
1	1	0	1	0
2	2	2	0	0
3	3	3	1	0

Define a map d : G → G by
$$d(x) = \begin{cases} 0 & if\ x = 0,1,3, \\ 2 & if\ x = 2. \end{cases}$$

And define a map d* : G → G
by$d^*(x)\begin{cases} 0 & if\ x = 0,1, \\ 2 & if\ x = 2,3. \end{cases}$

Then it is easily checked that d is both a (l,r) and (r,l)-derivation of G and d* is a(r,l)-derivation but not a (l,r)-derivation of G.

Definition1.9.([2],[3]) A derivation of an AB-algebra is said to be **regular** if d(0) = 0.

Definition 1.10.([4]) A fuzzy subset μ of AB-algebra X is called **a fuzzy AB-subalgebra of X**
if $μ(x * y) \geq$ min{ μ (x), μ (y)}, for all x, y ∈ X.

Areej .T /Baneen .N

Definition 1.11.([4]) A fuzzy subset μ of AB-algebra X is called **a fuzzy AB-ideal of X** if it satisfies :

FAB$_1$) $\mu(0) \geq \mu(x)$;

FAB$_2$) $\mu(x * z) \geq \min\{\mu(x * (y * z)), \mu(y)\}$,

for all x, y, z ∈ X.

Definition 1.12. [6]. A fuzzy μ is called a fuzzy relation on any set S, if μ is a fuzzy subset

μ: X× X→ [0,1].

Definition 1.13. [6]. If μ is a fuzzy relation on a set S and is a fuzzy subset of X, then μ is a fuzzy relation on β if $\mu\{x, y\} \leq \min$ ($\beta(x)$, $\beta(y)$), $\forall x, y \in$ X.

Definition 1.14 [6]. Let μ and β be a fuzzy subset of a set X, the Cartesian product of μ and β is defined by ($\mu \times \beta$)(x, y) = min{ $\mu(x), \beta$ (y)}, $\forall$ x, y∈ X.

Lemma 1.15 [6]. Let μ and β be a fuzzy subset of a set X, then

(i) $\mu \times \beta$ a fuzzy relation on X,

(ii) $(\mu \times \beta)_t = \mu_t \times \beta_t$, $\forall$ t∈[0,1].

2.(Fuzzy) Derivations AB-Ideals on AB-Algebras:

We review the definition of fuzzy derivations AB-algebra and study some properties of it.

Definition 2.1. Let $(X, *, 0)$ be an AB-algebra. and $d : X \to X$ be a self map. A non-empty subset A of an AB-algebra X is called **left derivations AB-ideal of X,** If it satisfies the following conditions:

 1) $0 \in A$,
 2) $d(x) * (y * z) \in$ A, and $d(y) \in$ A implies $d(x * z) \in$ A.

Definition2.2. Let $(X, *, 0)$ be an AB-algebra. and $d : X \to X$ be a self map. A non-empty subset A of an AB- algebra X is called **right derivations AB-ideal of X,** If it satisfies the following conditions:

1) $0 \in$ A,
2) $x * d(y * z) \in$ A, and $d(y) \in$ A implies $d(x * z) \in$ A.

Definition 2.3. Let(X ;*,0)be an AB-algebra. and $d : X \to X$ be a self map. A non-empty subset A of an AB- algebra X is called derivations   AB-ideal of If it satisfies the following conditions:

 1) $0 \in$ A,
 2) $d((x * y) * z) \in$ A, and $d(y) \in$ A implies $d(x * z) \in$ A.

Definition 2.4. Let $(X, *, 0)$ be an AB-algebra. and $d : X \to X$ be a self map. A non-empty subset A of an AB-algebra X is called **a fuzzy derivations AB-ideal of X** If it satisfies the following conditions:

 1) $\mu(0) \geq \mu(x)$;
 2) $\mu(d(x*z)) \geq \min\{\mu(d(x*(y*z)), \mu(d(y))\}$" , for all x, y, z ∈ X

Example 2.5. Let X={0,1,2,3} be an AB-algebra in which the operation (*) is defined as follows:

*	0	1	2	3
0	0	0	0	0
1	1	0	1	0
2	2	2	0	0
3	3	3	1	0

Define a map d : X→X by

$d(x) = \begin{cases} 0 & if\ x = 0,1,3, \\ 2 & if\ x = 2. \end{cases}$

Define a fuzzy setμ: X $\to$ [0,1] by μ(d (0))=t$_0$, μ(d (1))= t$_1$, μ(d (2) = μ(d (3)) =t$_2$

Where $t_0, t_1, t_{2,} \in$[0,1], with

$t_0 > t_1 > t_2$. Routine calculations give that μ is not fuzzy left (right)- derivations AB-ideal of AB-algebra.

Areej .T /Baneen .N

Example 2.6. Consider the set X = {0, 1, 2, 3, 4, 5} with the operation defined by the following table:

*	0	1	2	3	4	5
0	0	0	0	0	0	0
1	1	0	0	0	0	1
2	2	2	0	0	1	1
3	3	2	1	0	1	1
4	4	4	4	4	0	1
5	5	5	5	5	5	0

define d(x): X → X by $d(x) = \begin{cases} 0 & \text{if } x = 0,1,2,3,4 \\ 5 & \text{if } x = 5 \end{cases}$

define a fuzzy set μ: X → [0,1] by μ(d (0))= t_0, μ(d (1)), μ(d (1)) = μ(d (2)) = t_2, μ(d (3))= μ(d (4)) = t_3.

Where $t_0, t_1, t_2, t_3, \in$[0,1],with $t_0 > t_1 > t_2 > t_3$. Routine calculations give that μ is a fuzzy derivations AB-ideal of AB-algebra.

Theorem 2.7. Let μ be a fuzzy derivations AB-ideal of AB-algebra X.

(1) If $x \leq d(y)$, then μ(d (x)) ≥ μ(d (y)),

(2) If $x * y \leq d(y)$, then

μ(d (x * y)) ≥ μ(d (y)),

(3) If $(x * y) * (z * y) \leq d(x * z)$, then μ(d ((x * y) * (z * y))) ≥ μ(d (z * x)),

(4) If μ(d (x * y)) = μ(d (0)), then

μ(d (x)) ≥ μ(d (y))

Proof :
(1) Let $x \leq d(y)$, and since $d(y) \leq y$, hence $x \leq y$, i.e. $x * y = 0$, then

μ(d (x)) = μ(d (x * 0))

≥ min\{μ(d (x * y) * 0), μ(d (y))\}

(from Definition (2.4(2)))

= min\{μ(d (x * y)), μ(d (y))\}

= min\{μ(d (0), μ(d (y))\} = μ(d (y))

(2) Let $x * y \leq d(y)$, Then by Theorem (2.7(1)) we get, μ(d (x * y)) ≥ μ(d (x))

(3) Let $(x * y) * (z * y) \leq d(x * z)$, by (Theorem (2.7(1)) we get,

μ(d ((x * y) * (z * y))) ≥ μ(d (z * x))

(4) Let μ(d (x * y)) = μ(d (0)), then

μ(d (x)) = μ(d (x * 0)) ≥ min\{μ(d (x * y) * 0), μ(d (y))\} = min\{μ(d (x * y)), μ(d (y))\}

= min\{μ(0), μ(d (y))\} = μ(d (y)).

Proposition 2.8.   The intersection of any set of fuzzy derivations AB-ideals of AB-algebra X is also fuzzy left derivations AB-ideal.

Proof:
Let { μ_i} be a family of fuzzy derivations AB-ideals of AB-algebra X, then

∀x, y, z ∈X($\cap\mu_i$)(0) = inf ($\cap\mu_i$(0))

≥ inf (μ_i (d (x)) = ($\cap\mu_i$)(d (x)) and

($\cap\mu_i$)(d (x * z)) = inf (μ_i(d(x * z))

≥ inf (min\{μ_i (d (x * y) * z)), μ_i (d (y))\}

= min\{inf (μ_i (d (x * y) * z)), μ_i (d (y))\}

= min\{($\cap\mu_i$)(d(x * y) * z), ($\cap\mu_i$)(d(y))\}.

Theorem 2.9. Let μ be a fuzzy set in X, then μ is a fuzzy derivations AB-ideal of X if and only if it satisfies : ∀ α∈[0, 1]), U(μ , α) ≠ φ implies U(μ ,α) is AB-ideal of X, where U (μ , α) = {x ∈ X / μ (d(x)) ≥ α}.

Proof: Assume that μ is a fuzzy derivations AB-ideal of X, let $\alpha\in$ 0,1 be such that U (μ, α) ≠φ and x, y ∈X, such that

x ∈U (μ,α) then μ (d(x)) ≥ α, and so by (fl_2)   μ($d(0)$) = μ($d(0 * y)$) ≥ min\{ μ(d(0 * x) * y),   μ(d(x))   = min\{ μ(d(0) * y), μ(d(x))

= min\{ μ(0 * y), μ(d(x)) = min\{ μ(0), μ(d(x)) = α, hence 0∈U(μ , α).

Let $d(x * (y * z))$ ∈U(μ , α) and $d(y)$ ∈ U(μ , α), by (FL_2) μ($d(x * z)$) ≥ min\{ μ($d(x * y) * z$), μ($d(y)$)\} = α, so that x*z ∈ U(μ , α) .

4

Areej .T /Baneen .N

Hence $U(\mu, \alpha)$ is AB-ideal of X.
Conversely, Let $U(\mu, \alpha)$ is AB-ideal of X, let
x, y, z $\in$X be such that
$\mu(d(x*z)) > \min\{ \mu(d(x*y)*z), \mu(d(y))\}$,
taking$\beta_0 = \frac{1}{2}\{\mu(d(x*z)) + \min\{\mu(d(x*y)*z), \mu(d(y))\}\}$, we have $\beta_0 \in [0,1]$,
$\mu(d(x*z))$
$< \beta_0 < \min\{\mu(d(x*y)*z), \mu(d(y))\}\}$, it
follows that $d(x*y)*z \in U(\mu, \beta_0)$ and
y $\in U(\mu, \beta_0)$, this this is a contradiction and
therefore μ is a fuzzy derivations AB-ideal of
X.

3. Cartesian Product of Fuzzy Derivations AB-ideals:

The following definitions introduce the
notion of Cartesian Product of Fuzzy
Derivations AB-ideals and some Properties
of it.

Definition 3.1. Let μ and β be a fuzzy
derivations subset of a set X,**the Cartesian
product of μ and β is** defined by
$(\mu \times \beta)(d(x,y))$
$= \min\{\mu(d(x)), \beta(d(y))\}, \forall$x, y $\in$ X.

Definition 3.2. If β is a fuzzy derivations
subset of a set X, the strongest fuzzy relation
on X, that is a **fuzzy derivations relation on β
is μ_β** given by
$\mu_\beta(d(x,y)) = \min\{\beta(d(x)), \beta(d(y))\}$,
$\forall$ x, y $\in$ X.

Proposition 3.3. For a given fuzzy derivations
subset β of AB-algebra X, let μ_β be the
strongest fuzzy derivations relation on X. If μ_β
is a fuzzy derivations AB-ideal of X $\times$X then
$\beta(d(x)) \le \beta(d(0)) = \beta(0), \forall$x$\in$X.
Proof:
Since $\mu_\beta$is a fuzzy derivation AB-ideal of X
$\times$X it follows from (F_1) that
μ_β(x,x) = $\min\{\beta(d(x)), \beta(d(x))\} \le \beta(d(0,0))$
$= \min\{\beta(d(0)), \beta(d(0)\}$ where (0,0)$\in$X $\times$X
then $\beta(d(x)) \le \beta(d(0)) = \beta(0)$.

Remark 3.4. Let X and Y be AB-algebras, we
define $*$ on X $\times$Y by
$(x,y)*(u,v)(x*u, y*v), \forall(x,y), (u,v)$
$\in$ X$\times$Y then clearly (X $\times$Y,$*$,(0,0)) is an
AB-algebra.
Theorem 3.5. Let μ and β be a fuzzy
derivations AB-ideals of AB-algebra X, then μ
$\times \beta$ is a fuzzy derivations AB-ideal of X $\times$X.
Proof:
(1) $(\mu \times \beta)(d(0,0))$ = $\min\{\mu(0), \beta(0)$
$\ge \min\{\mu(d(x)), \beta(d(x))\} = \mu \times \beta(d(x,y))$
$\forall$x, y $\in$X $\times$X.
(2) Let $(x_1, x_2), (y_1, y_2), (z_1, z_2) \in$X$\times$X, then

$\mu \times \beta(x_1*z_1, x_2*z_2) = \min\{\mu(d(x_1, z_1)*\beta(d(x_2, z_2))$
$\ge \min\{\mu(d(x_1*(y_1*z_1)), \mu(d(y_1)),$
$\beta(d(x_2*(y_2*z_2)), \beta(d(y_2))\}$
$= \min\{\min\{\mu(d(x_1*(y_1*z_1)),$
$\beta(d(x_2*(y_2*z_2))\}, \min\{\mu(d(y_1)), \beta(d(y_2))\}$
$= \min\{\mu \times \beta((d(x_1*(y_1*z_1)),$
$(d(x_2*(y_2*z_2))), \mu \times \beta(d(y_1)), (d(y_2)))\}$
Hence $\mu \times \beta$ is a fuzzy derivations AB-ideal of
X$\times$X .

Theorem 3.6. Let β be a fuzzy derivations
subset of AB-algebra X and let μ_β be the
strongest fuzzy derivations relation on then βis
a fuzzy derivations AB-ideal of X if and only
if $\mu_\beta$is a fuzzy derivations AB-ideal of X $\times$X.
Proof:
Let β be a fuzzy derivations AB-ideal of X .
(1) From (F_1), we get $\mu_\beta(0,0)$
$= \min\{\beta(d(0)), \beta(d(0))\} = \min\{\beta(0), \beta(0)\}$
$\ge \min\{\beta(d(x)), \beta(d(y))\} = \mu_\beta(d(x)), d(y)),$
$\forall$x, y $\in$X $\times$X.
(2) $\forall(x_1, x_2), (y_1, y_2), (z_1, z_2) \in$X$\times$X, we
have from (F_2)
$\mu_\beta(x_1*z_1, x_2*z_2) = \min\{\beta(d(x_1*z_1), \beta(d(x_2*z_2))\}$
$\ge \min\{\beta(d(x_1*(y_1*z_1)), \beta(d(y_1)),$
$\beta(d(x_2*(y_2*z_2)), \beta(d(y_2))\}$
$= \min\{\min\{\beta(d(x_1*(y_1*z_1)),$
$\beta(d(x_2*(y_2*z_2))\}, \min\{\beta(d(y_1)), \beta(d(y_2))\}\}$
$= \min\{\mu_\beta((d(x_1*(y_1*z_1)),$
$(d(x_2*(y_2*z_2))), \mu_\beta(d(y_1)), (d(y_2)))\}$

Areej .T /Baneen .N

Hence μ_β is a fuzzy derivations AB-ideal of $X \times X$.

Conversely, let μ_β be a fuzzy derivations AB-ideal of $X \times X$,

(1) $\forall (x, y) \in X \times X$, we have,

$\min\{ \beta(0), \beta(0)\} = \mu_\beta(x, y) = \min\{ \beta(x), \beta(y)\}$,

It follows that $\beta(0) \geq \beta(x)\ \forall x \in X$,

(2) Let $(x_1, x_2), (y_1, y_2), (z_1, z_2) \in X \times X$, then

$\min\{ \beta(d(x_1 * z_1), \beta(d(x_2 * z_2))\}$

$= \mu_\beta(d(x_1 * z_1), d(x_2 * z_2))$

$\geq$

$\min\{\mu_\beta(d(x_1, x_2)*((y_1, y_2)*(z_1, z_2))), \mu_\beta(d(y_1), d(y_2))\}$

$= \min\{\mu_\beta(d(x_1 * (y_1 * z_1)), d(x_2 * (y_2 * z_2))), \mu_\beta(d(y_1), d(y_2))\}$

$= \min\{\min\{\beta(d(x_1 * (y_1 * z_1)), \beta(d(x_2 * (y_2 * z_2))\}, \min\{ \beta(d(y_1)), \beta(d(y_2))\}\}$

$= \min\{\beta(d(x_1 * (y_1 * z_1)), \beta(d(y_1)), \beta(d(x_2 * (y_2 * z_2)), \beta(d(y_2))\}$

In particular, if we take $x_2, y_2, z_2 = 0$, then

$\beta(d(x_1 * z_1) \geq \min\{\beta(d(x_1 * (y_1 * z_1)), \beta(d(y_1))\}$.

Hence β be a fuzzy derivations AB-ideal of X.

Conclusions and discussion

1)   we presented some properties related to fuzzy AB-ideal of AB- algebra, among these properties, derivations AB-ideals, Cartesian Product of Fuzzy Derivations AB-ideals.

2)   We recommend finding other properties for this type of algebra.

References

[1] A.T. Hameed, A.A. Alfatlawi and A.K. Alkurdi, **Fuzzy QS-ideals of QS-algebras**, International Journal of Algebra, 11, 1(2017), 43-52.

[2] A.T. Hameed and B.N. Abbas, **AB-ideals of AB-algebra**, Applied Mathematical Sciences, 11,35(2017), 1715-1723.

[3] A.T. Hameed and B.N. Abbas, **Some Properties of AB-ideals of AB-algebra**, Algebra Letters, To apper, 2017.

[4] A.T. Hameed and B.N. Abbas, **Fuzzy AB-ideals of AB-algebra**, To apper, 2017.

[5] A.T. Hameed, **Fuzzy ideals of some algebras**, PH. Sc. Thesis, Ain Shams University, Faculty of Sciences, Egypt , 2015.

[6] P. Bhattacharye and N.P. Mukheriee, **Fuzzy relation and fuzzy group in form**, Sci, 36(1985), 267-282.

[7] S.M. Mostafa, A.T. Hameed and A.H. Abed, **Fuzzy KUS-ideals of KUS-algebra**, Basra, Journal of Science (A), 34, 2 (2016), 73-84.

[8] S.M. Mostafa, M.A. Abdel Naby, F. Abdel-Halim and A.T. Hameed, **On KUS-algebra**, 7, 3 (2013), 131-144.

[9] W.A. Dudek, **A new characterization of ideals in BCC-algebras**, Novi Sad J. Math. , 29(1999),139 − 145.

[10]   W.A. Dudek, and J. Thomys, **On some generalizations of BCC-algebras**, Intern. J. Computer Math., 89(2012), 1596-1606.

[11]   W.A. Dudek, **On BCC-algebras**, Logique et Analyse ,129-131(1991), 103-111.

بعض خصائص المثاليات الضبابية الى الجبر -AB

أريج توفيق حميد   بنين نجاح عباس

جامعة الكوفة، كلية التربية للبنات، قسم الرياضيات

المستخلص :

و كذلك برهنا بعض الخصائص والنظريات ذات الصلة بالموضوع AB- في هذا البحث قدمنا مفهوم المثالي الضبابي الى الجبر وقدمنا الخصائص والنظريات التي توضح المفهومين AB- وكذلك درسنا العلاقات الضبابية واشتقاقات المثاليات الضبابية الى الجبر AB- مما دفعنا الى دراسة الضرب الديكارتي الى اشتقاقات المثاليات الضبابية الى الجبر

On second-order differential subordination and superordination of analytic functions involving the Komatu integral operator

Abdul Rahman S. Juma   Raad Awad Hameed   Mustafa Ibrahim Hameed

University of Anbar   University of Tikrit
Department of Mathematics   Department of Mathematics
Ramadi-Iraq   Iraq
dr_juma@hotmail.com   awad.raad2@gmail.com   mustafa8095@yahoo.com

Abstract

In the present paper by using properties of the Komatu integral operator, we derive some properties of subordinations and superordinations associated with the Hadamard product concept.

Key words: Differential subordination, Differential superordination, Univalent function, Convex function, Komatu integral operator, Hadamard product.

Mathematics Subject Classification: 30C45, 30A10, 30C80.

1. Introduction and Definitions

Let $U = \{z \in C : |z| < 1\}$ be an open unit disc in C (complex plane) and $\overline{U} = \{z \in C : |z| \leq 1\}$.

Let H(U) be the class of analytic functions in U and let H[a, k] be the subclass of H(U) of the form

$$f(z) = a + a_n z^n + a_{n+1} z^{n+1} + \cdots ,$$

where $a \in C$ and $n \in N$ with $H_0 \equiv H[0, 1]$ and $H \equiv H[1, 1]$. Let A_p be the class of all analytic functions of the form

$$f(z) = z^p + \sum_{n=p+1}^{\infty} a_n z^n , (z \in U)$$
(1.1)

in the open unit disk U. For functions $f \in A_p$ given by equation (1.1) and $g \in A_p$ defined by

$$g(z) = z^p + \sum_{n=p+1}^{\infty} b_n z^n \quad , \quad (z \in U)$$

The Hadamard product(convolution) of f and g is defined by

$$(f * g)(z) = z^p + \sum_{n=p+1}^{\infty} a_n b_n z^n = (g * f)(z) .$$

Let f and F be members of H(U).The function f is said to be subordinate to a function F or F is said to be superordinate to f, if there exists a Schwarz function w analytic in U, with w(0) = 0 and |w(z)| < 1, (z ∈ U), such that f(z) = F(w(z)).

We denote this subordination by

$$f(z) \prec F(z) \text{ or } f \prec F.$$

Furthermore, if the function F is univalent in U, then we have the following equivalence [6, 12]

$$f(z) \prec F(z) \Leftrightarrow f(0) = F(0) \text{ and } f(U) \subset F(U).$$

Abdul Rahman .S/Raad .A/Mustafa. I

The method of differential subordinations (also known as the admissible functions method) was first introduced by Miller and Mocanu in 1978 [3] and the theory started to develop in 1981 [4]. For more details see [5].

Let Ω and Δ be sets in C, let $\psi : C^3 \times U \to C$ and h be univalent in U. If p is analytic in U with p(0) = a with generalizations of implication

$$\{\psi(p(z), zp'(z), zp''(z); z\,)\} \subset \Omega \Longrightarrow p(U) \subset \Delta,$$

with satisfies the second-order differential subordination

$\psi(\, p(z),\, zp'\,(z),\, zp''(z);\, z\,) \prec h(z),$
(1.2)

then p is called a solution of the differential subordination. The univalent function q is called a dominant of the solution of the differential subordination or more simply dominant, if $p \prec q$ for all p satisfying (1.2). A dominant $\tilde{q}$ satisfying $\tilde{q} \prec q$ for all dominants (1.2) is said to be the best dominant of (1.2). And if p and $\Psi(\, p(z),\, zp'\,(z),\, zp''(z);\, z\,)$ are univalent in U with satisfies the second-order differential subordination

$h(z) \prec \psi(\, p(z),\, zp'\,(z),\, zp''(z);\, z\,),$
(1.3)

then p is called a solution of the differential superordination. An analytic function q is called a subordinant of the solutions of the differential superordination or more simply dominant, if $q \prec p$ for all p satisfying (1.3). A univalent subordinant $\tilde{q}$ that satisfies $q \prec \tilde{q}$ for all subordinants q of (1.3) is said to be the best subordinant.

by using (1.3) we get

$$\Omega \subset \{\psi(p(z), zp'(z), zp''(z);\ z\,)\}.$$

For functions f and g $\in$ A(p), The Komatu integral operator$D_{m,p}^{\lambda}$:A(p) $\to$ A(p) $(\lambda \geq 0, m \in N \cup \{0\}\ and\ N = \{1, 2, 3, \dots\ \})$ defined as follows:[10].

$D_{m,p}^{\lambda}$ (f $*$ g)(z) =

$\frac{m^{\lambda}}{\Gamma(\lambda)} \int_0^1 t^{m-2} \left(\log \frac{1}{t}\right)^{\lambda-1}$ (f $*$ g)(z) (tz)dt,
(1.4)

 where the symbol Γ stands for the gamma function.

Thus, we get

$D_{m,p}^{\lambda}(\text{f} * \text{g})(z) =$
$z^p + \sum_{n=p+1}^{\infty} \left(\frac{m}{m+n-1}\right)^{\lambda} a_n b_n z^n.$
(1.5)

For λ, $\alpha \geq 0$, we obtain

$$D_{m,p}^{\lambda}(\, D_m^{\alpha}(\text{f} * \text{g})(z)\,) = \ D_{m,p}^{\lambda+\alpha}(\text{f} * \text{g})(z)\ .$$

From (1.5) we have

$\frac{z}{p}\left(D_{m,p}^{\lambda}(\text{f} * \text{g})(z)\right)' =$
$mD_{m,p}^{\lambda+1}(\text{f} * \text{g})(z) - (m-1)D_{m,p}^{\lambda}(\text{f} * \text{g})(z).$
(1.6)

The operator $D_m^{\lambda}(\text{f} * \text{g})(z)$ is related to the transformation of the multiplier studied by Flett [8] Several interesting proposals were examined by the operator D_m^{λ} have been studied by Jung et al. [9] and Liu [11].

In order to prove our main results , we need the following definitions and lemmas.

Definition 1.1. ([13]) We denote by Q the set of functions q that are analytic and injective on $\overline{U}/E(q)$, where

$$E(q) = \{x \,\epsilon\, \partial U\ ;\ \lim_{Z \to x} q(z) = \,\infty\},$$

and are such that $q'(x\,) \neq 0$ for $x \,\epsilon\, \partial U/E(q)$. The subclass of Q for which $q(0) = a$ is denoted by Q(a).

Definition 1.2. ([13]) Let Ω be a set in C, q(z) $\in$ Q and n be a positive integer. The class of admissible functions $\Psi_n[\Omega, q]$ consists of those functions ψ: $C^3 \times U \to$ C that satisfy the admissibility condition
$$\psi(\text{r, s, t; z}) \notin \Omega,$$

whenever r = q(x), s = yxq(x),

$$\Re e\left\{1 + \frac{t}{s}\right\} \geq y\Re e\left\{1 + \frac{xq''(x)}{q'(x)}\right\},$$

where z $\in$ U, $x \,\epsilon\, \partial U/E(q)$ and y $\geq$ n.

we get $\Psi_1[\Omega, q] = \ \Psi[\Omega, q].$

Abdul Rahman .S/Raad .A/Mustafa. I

In particular, when q(z) = $M\frac{Mz+a}{M+\bar{a}z}$, with   M > 0 and $|a| < M$, then q(U) = U_M = $\{w : |w| < M\}$,   q(0) = a, E(q) = $\emptyset$ and q $\in$ Q.

In this case, we set $\Psi_n[\Omega, M, a]$ = $\Psi[\Omega, q]$, and in the special case when $\Omega = U_M$, the class is simply denoted by $\Psi_n[M, \alpha]$.

Definition 1.3. ([14]) Let Ω be a set in C and q $\in$ H[a,n] with $q'(z) \neq 0$. The class of admissible functions $\Psi'[\Omega, q]$ consist of this functions $\psi : C^3 \times U \to C$ that satisfy the admissibility condition

$$\psi(r, s, t; x) \in \Omega,$$

whenever r = q(z), s = $\frac{zq'(z)}{j}$ for z $\in U$ and

$$\Re e\left\{1 + \frac{t}{s}\right\} \leq \frac{1}{j} \Re e\left\{1 + \frac{zq''(z)}{q'(z)}\right\},$$

for   z $\in U, x \in \partial U$ and j $\geq$ n $\geq$ 1. We write $\Psi_1[\Omega, q]$ = $\Psi[\Omega, q]$.

Lemma 1.4. ([13]) Let $\psi \in \Psi_n[\Omega, q]$ wtih q(0) = a. If the analytic function

$$p(z) = a + a_n z^n + a_{n+1} z^{n+1} + ...,$$

(z $\in U$) satisfies the following inclusion relationship $\psi(p(z), zp'(z), zp''(z); z) \in \Omega$,

then

$$p(z) \prec q(z)   (z \in U).$$

Lemma 1.5. ([14]) Let $\psi \in \Psi_n[\Omega, q]$ wtih q(0) = a . If p $\in Q(a)$ and $\psi(p(z), zp'(z), zp''(z); z)$ is univalent in U, then

$$\Omega \subset \psi(p(z), zp'(z), zp''(z); z),$$
implies

$$q(z) \prec p(z).$$

In the present work, we get some results of differential subordination and superordination of Oros [15], [16] , we shall the study of the class of admissible functions involving the Komatu integral operator $D_{m,p}^{\lambda}(f * g)(z)$ de fined by (1.5) . We remark in passing that some interesting developments on differential subordination and superordination for various operators in connection with the Komatu integral operator were obtained by Ali *et al.* [1],[2] and Cho *et al.* [7].

2. Differential subordination results

Definition 2.1. Let Ω be a set in C,q $\in Q_0 \cap$ H[0,p]. The class of admissible functions Φ_n [Ω, q] consists of those functions $\phi : C^3 \times U \to C$ that satisfy the admissibility condition

$$\phi(u, v, w; z; x) \notin \Omega,$$

Whenever

$$u = q(x),$$
$$v = \frac{yxq'(x) + p(m-1)q(x)}{pm}$$

and

$$\Re e\left\{\frac{m^2p^2w - p^2(m-1)^2u}{pcv - p(m-1)u} - 2p(m-1)\right\}$$
$$\geq y\Re e\left\{1 + \frac{xq''(x)}{q'(x)}\right\},$$

for   z $\in U, x \in \partial U/E(q), \lambda \geq 1$ and y $\geq$ p.

Theorem 2.2. Let $\phi \in \Phi_n[\Omega, q]$. If $f \in A(p)$ satisfies

$$\left\{\phi\begin{pmatrix} D_{m,p}^{\lambda}(f*g)(z), D_{m,p}^{\lambda+1}(f*g)(z), \\ D_{m,p}^{\lambda+2}(f*g)(z); z \end{pmatrix}; z \in U\right\} \subset \Omega, \quad (2.1)$$

then

$$D_{m,p}^{\lambda}(f * g)(z) \prec q(z).$$

Proof. Let $g(z) \in$ U define by

$$g(z) = D_{m,p}^{\lambda}(f * g)(z). \quad (2.2)$$

In view of relation (1.6) with from (2.2), we have

$$D_{m,p}^{\lambda+1}(f * g)(z) = \frac{zg'(z) + p(m-1)g(z)}{pm}. \quad (2.3)$$

Abdul Rahman .S/Raad .A/Mustafa. I

Based on that

$D_{m,p}^{\lambda+2}(f * g)(z) =$
$\frac{z^2 g''(z)+2p(m-1)zg'(z)+p^2(m-1)^2g(z)}{p^2m^2}$.   (2.4)

Define the transformation from C^3 to C by

$u(r,s,t) = r, v(r,s,t) = \frac{s+p(m-1)r}{pm}, w(r,s,t) =$
$\frac{t+2p(m-1)s+p^2(m-1)^2r}{p^2m^2}$.   (2.5)

Let

$\psi(r,s,t;z) = \phi(u,v,w;z)$

$= \phi\left(r, \frac{s+p(m-1)r}{pm}, \frac{t+2p(m-1)s+p^2(m-1)^2r}{p^2m^2}; z\right)$.   (2.6)

The proof shall get use of Lemma 1.4 .Using equations (2.2), (2.3) amd (2.4), from (2,6), we have

$\psi(g(z), zg'(z), z^2g''(z); z)$
$= \phi(D_{m,p}^{\lambda}(f * g)(z), D_{m,p}^{\lambda+1}(f * g)(z), D_{m,p}^{\lambda+2}(f * g)(z); z)$.   (2.7)

Therefore, (2.1) we have

$\psi(g(z), zg'(z), z^2g''(z); z) \in \Omega$.   (2.8)

See that

$$1 + \frac{t}{s} = \frac{m^2p^2w - p^2(m-1)^2u}{pcv - p(m-1)u} - 2p(m-1),$$

and since the admissibility condition for $\psi \in \Psi_n[\Omega, q]$. By Lemma 1.4,

$g(z) \prec q(z),$ or $D_{m,p}^{\lambda}(f * g)(z) \prec q(z)$.

Theorem 2.3. Let $\phi \in \Phi_n[h, q]$ with q(0) = 1. If $f \in A(p)$ satisfies

$\phi\left(\begin{matrix} D_{m,p}^{\lambda}(f * g)(z), D_{m,p}^{\lambda+1}(f * g)(z), \\ D_{m,p}^{\lambda+2}(f * g)(z) ; z \end{matrix}\right) \prec h(z)$
    (2.9)

then
$D_{m,p}^{\lambda}(f * g)(z) \prec q(z) . (z \in U)$

The next is an extension of Theorem 2.2 to the case where the behavior of q(z) on ∂U is unknown.

Corollary 2.4. $\Omega \in C$ and let q(z) be univalent in U with q(0) =1. Let $\phi \in \Phi_n[\Omega, q_\rho]$ for some $\rho \in (0,1)$, where $q_\rho(z) = q(\rho z)$. If $f(z) \in A(P)$ and

$\phi\left(\begin{matrix} D_{m,p}^{\lambda}(f * g)(z), D_{m,p}^{\lambda+1}(f * g)(z), \\ D_{m,p}^{\lambda+2}(f * g)(z) ; z \end{matrix}\right) \in \Omega,$

then
$D_{m,p}^{\lambda}(f * g)(z) \prec q(z).$

Proof. By Theorem 2.2 we have $D_{m,p}^{\lambda}(f * g)(z) \prec q(\rho z)$. The result now deduced from the following subordination relationship $q_\rho(z) \prec q(z)$.

Theorem 2.5. Let h(z) and q(z) be univalent in U, with q(0) = 1 and set $q_\rho(z) = q(\rho z)$ and $h_\rho(z) = h(\rho z)$. Let $\phi : C^3 \times U \to C$ satisfy one of the following conditions:
(1) $\phi \in \Phi_n[h, q_\rho]$, for some $\rho \in (0,1)$, or
(2) there exists $\rho_0 \in (0,1)$ such that $\phi \in \Phi_n[h_\rho, q_\rho]$, for all $\rho \in (\rho_0, 1)$.If $f(z) \in A(P)$ satisfy (2.9),
then
$D_{m,p}^{\lambda}(f * g)(z) \prec q(z).$

Proof. Case (1). By applying Theorem 2.2, we get $D_{m,p}^{\lambda}(f * g)(z) \prec q_\rho(z),$ since $q_\rho(z) \prec q(z)$, we deduce $D_{m,p}^{\lambda}(f * g)(z) \prec q(z)$.

Case (2). If we let $g_\rho(z) = D_{m,p}^{\lambda}(f * g)_\rho(z) = D_{m,p}^{\lambda}(f * g)(\rho z) = g(\rho z),$

then

$\phi(g_\rho(z), zg_\rho'(z), z^2g_\rho''(z); \rho z) =$
$\phi(g(\rho z), zg'(\rho z), z^2g''(\rho z); \rho z) \in h_\rho(U).$

By using Theorem 2.2 and the comment associated with (2.8) where $w(z) = \rho z$ is any mapping U in to U, we get

$g_\rho(z) \prec q_\rho(z)$ for $\rho \in (\rho_0, 1)$. By letting $\rho \to 1^-$, we obtain $g(z) \prec q(z)$.

Hence,
$D_{m,p}^{\lambda}(f * g)(z) \prec q(z).$

Abdul Rahman .S/Raad .A/Mustafa. I

Now, the next result we need the best dominant of the differential subordination (2.9).

Theorem 2.6. Let $h(z)$ be univalent in U and let $\phi : C^3 \times U \to C$. Suppose that the differential equation

$$\phi\left(q(z), \frac{zq'(z)+p(m-1)q(z)}{pm}, \frac{z^2q''(z)+2p(m-1)zq'(z)+p^2(m-1)^2q(z)}{p^2m^2}; z\right) = h(z).$$
(2.10)

has a solution q(z) with q(0) = 0 and satisfy one of the following conditions:
(1) $q(z) \in Q_0$ and $\phi \in \Phi_n[h, q]$.
(2) $q(z)$ is univalent in U and $\phi \in \Phi_n[h, q_\rho]$ for some $\rho \in (0,1)$, or
(3) $q(z)$ is univalent in U and there exists $\rho_0 \in (0,1)$ such that $\in \Phi_n[h_\rho, q_\rho]$ for all $\rho \in (\rho_0, 1)$.
If $f(z) \in A(p)$ satisfies (2.9), then $D_{m,p}^\lambda(f * g)(z) \prec q(z)$ and q(z) is the best dominant.

Proof. By applying Theorem 2.3 and 2,5, we deduce that q(z) is a dominant of (2.9). Since q(z) satisfies (2.10), it is a solution of (2.9) and therefore q(z) will be dominated by all dominants of (2.9).
Hence, q(z) is the best dominant of (2.9).
In the particular case q(z) = Mz, M > 0, and in view of the Definition 1.2, the class of admissible function $\Phi_n[\Omega, q]$ denoted by $\Phi_n[\Omega, M]$ is described below.

Definition 2.7. Let Ω be a set in C, $\Re e\{m\} > 0$, $\lambda \geq 1$ and M > 0. The class of admissible functions $\Phi_n[\Omega, M]$ consists of those functions $\phi : C^3 \times U \to C$ that satisfy the admissibility condition:

$$\phi\left(Me^{i\theta}, \frac{y+p(m-1)Me^{i\theta}}{pm}, \frac{L+[2p(m-1)y+p^2(m-1)^2Me^{i\theta}]}{p^2m^2}; z\right) \notin \Omega,$$
(2.11)

whenever $\theta \in R, R(Le^{i\theta}) \geq y(y-1)M, y \geq 1$ and $z \in U$.

Corollary 2.8. Let $\phi \in \Phi_n[\Omega, M]$. If $f(z) \in A(P)$ satisfy the following inclusion relationship

$$\phi\left(\begin{matrix} D_{m,p}^\lambda(f * g)(z), D_{m,p}^{\lambda+1}(f * g)(z), \\ D_{m,p}^{\lambda+2}(f * g)(z) ; z \end{matrix}\right) \in \Omega,$$

then

$$D_{m,p}^\lambda(f * g)(z) \prec Mz.$$

Now, in the special case $\Omega = q(U) = \{w : |w| < M\}$, the class $\Phi_n[\Omega, M]$ is denoted by $\Phi_n[M]$.

Corollary 2.9. Let $\phi \in \Phi_n[M]$. If $f(z) \in A(P)$ satisfies

$$\left|\phi\left(\begin{matrix} D_{m,p}^\lambda(f * g)(z), D_{m,p}^{\lambda+1}(f * g)(z), \\ D_{m,p}^{\lambda+2}(f * g)(z) ; z \end{matrix}\right)\right| < M,$$

then

$$\left|D_{m,p}^\lambda(f * g)(z)\right| < M.$$

Theorem 3.2. Let $\phi \in \Phi_n[\Omega, q]$. If $f(z) \in A(P), D_{m,p}^\lambda(f * g)(z) \in Q_0$ and

$$\phi\left(\begin{matrix} D_{m,p}^\lambda(f * g)(z), D_{m,p}^{\lambda+1}(f * g)(z), \\ D_{m,p}^{\lambda+2}(f * g)(z) ; z \end{matrix}\right) \text{ is}$$
univalent in U, then

$$\Omega \subset \phi\left(\begin{matrix} D_{m,p}^\lambda(f * g)(z), D_{m,p}^{\lambda+1}(f * g)(z), \\ D_{m,p}^{\lambda+2}(f * g)(z) ; z \end{matrix}\right),$$
(3.1)

implies
$$q(z) \prec D_{m,p}^\lambda(f * g)(z). \quad (z \in U)$$

Proof. By using (2.7) and (3.1) we get

$$\Omega \subset \psi(g(z), zg'(z), z^2g''(z); z), (z \in U)$$

From (2.5), we note that the admissibility condition for $\phi \in \Phi'_n[\Omega, q]$ is equivalent to the admissibility condition for ψ as given in Definition 1.3. therefore, and by Lemma 1.5 we get

$$q(z) \prec g(z) \text{ or } q(z) \prec D_{m,p}^\lambda(f * g)(z).$$
$$(z \in U)$$

Abdul Rahman .S/Raad .A/Mustafa. I

Theorem 3.3. Let $h(z)$ is analytic on U and $\phi \in \Phi'_n[h,q]$. If $f(z) \in A(P)$, $D_{m,p}^{\lambda}(f * g)(z) \in Q_0$ and $\phi : C^3 \times U \to C$ with

$$\phi\left(\begin{matrix} D_{m,p}^{\lambda}(f * g)(z), D_{m,p}^{\lambda+1}(f * g)(z), \\ D_{m,p}^{\lambda+2}(f * g)(z) \; ; z \end{matrix}\right) \text{ is}$$

univalent

in U, then

$$h(z) \prec \phi\left(\begin{matrix} D_{m,p}^{\lambda}(f * g)(z), D_{m,p}^{\lambda+1}(f * g)(z), \\ D_{m,p}^{\lambda+2}(f * g)(z) \; ; z \end{matrix}\right),$$
$$(3.2)$$

implies

$$q(z) \prec D_{m,p}^{\lambda}(f * g)(z).$$

Proof. By using relationship (3,2) we obtain

$$h(z)$$
$$= \Omega$$
$$\subset \phi\left(\begin{matrix} D_{m,p}^{\lambda}(f * g)(z), \\ D_{m,p}^{\lambda+1}(f * g)(z), D_{m,p}^{\lambda+2}(f * g)(z) \; ; z \end{matrix}\right),$$

and from Theorem 3,2, we have

$$q(z) \prec D_{m,p}^{\lambda}(f * g)(z).$$

Collect Theorem 2.3 and 3.3, we get the following sandwich type Theorem.

Theorem 3.4. Let $h_1(z)$ and $q_1(z)$ be analytic functions in U, $h_2(z)$ be univalent function in U, $q_2(z) \in Q_0$ with $q_1(0) = q_2(0) = 0$ and $\phi \in \Phi_n[h_2, q_2] \cap \Phi'_n[h_1, q_1]$. If $f(z) \in A(P)$, $D_{m,p}^{\lambda}(f * g)(z) \in Q_0 \cap H[0, P]$ and
$\phi\left(D_{m,p}^{\lambda}(f * g)(z), D_{m,p}^{\lambda+1}(f * g)(z), D_{m,p}^{\lambda+2}(f * g)(z) \; ; z\right)$ is univalent in U,

then

$$h_1(z) \prec \phi\left(\begin{matrix} D_{m,p}^{\lambda}(f * g)(z), D_{m,p}^{\lambda+1}(f * g)(z), \\ D_{m,p}^{\lambda+2}(f * g)(z) \; ; z \end{matrix}\right)$$

$$\prec h_2(z),$$

implies that

$$q_1(z) \prec D_{m,p}^{\lambda}(f * g)(z) \prec q_2(z).$$

References

[1]   R. M. Ali, V. Ravichandran and N. Seenivasagan, Subordination and superordination of the Liu-Srivastava linear operator on meromorphic functions, Bull. Malays. Math. Soc., 31, (2008), 193-207.
[2]   R. M. Ali, V. Ravichandran and N. Seenivasagan, On subordination and superordination of the multiplier transformation of meromorphic functions, Bull. Malays. Math. Soc., 33, (2010), 311-324.
[3]   S. Altınkaya and S. Yalcın, Coefficient estimates for two new subclasses of biunivalent functions with respect to symmetric points, J. Funct. Spaces, 2015, (2015), 5 pages.
[4]   S. Altınkaya and S. Yalcın, General properties of multivalent concave functions involving linear operator of carlson-shaffer type, Comptes rendus de lacademie bulgare des Sciences, 69, (2016), 1533–1540.
[5]   M. K. Aouf and A. O. Mostafa, Sandwich theorems for analytic functions defined by convolution, Acta. Univ. Apulensis Math. Inform., 21, (2010), 7–20.
[6]   T. Bulboaca, Differential subordinations and superordinations, Recent Results, House of Scientific Book Publ. Cluj-Napoca, (2005).
[7]   N. E. Cho, O. S. Kwon and H. M. Srivastava, Strong differential subordination and superordination for multivalently meromorphic functions involving the Liu-Srivastava operator, Integral Transforms Spec. Funct., 21, (2010), 589-601.
[8]   T. M. Flett, The dual of an inequality of Hardy and Littlewood and some related inequalities, J. Math. Anal. Appl., 38, (1972), 746-765.
[9]   I. B. Jung, Y. C. Kim and H. M. Srivastava, The Hardy space of analytic functions associated with certain one-parameter families of integral operators, J. Math. Anal. Appl., 176, (1993), 138-147.
[10]   Y. Komatu, Distortion Theorems in Relation to Linear Integral Operators, Kluwer Academic, Dordrecht, (1996).
[11]   J. L. Liu, A linear operator and strongly starlike functions, J. Math. Soc. Jpn., 54, (2002), 975-981.
[12]   S. S. Miller and P. T. Mocanu, Differential subordinations and univalent functins, Michigan Math. J., 28, (1981), 157-171.

Abdul Rahman .S/Raad .A/Mustafa. I

[13] S.S. Miller and P.T. Mocanu, Differential subordination. Theory and Applications, Series on Monographs and Textbooks in Pure and Applied Mathematics, Vol. 225, Marcel Dekker Inc., New York and Basel. 2000.

[14] S.S. Miller and P.T. Mocanu, Subordination of differential superordinations, complex varibals Theory Appl., 10, (2003), 815-826.

[15] G. I. Oros and G. Oros, Strong differential subordination, Turk. J. Math., 33, (2009), 249-257.

[16] G. I. Oros, Strong differential superordination. Acta. Univ. Apulensis, Mat. Inform, 19, (2009), 101-106.

<div dir="rtl">

حول التابعية وفوق التابعية التفاضلية من الدرجة الثانية بأستخدام المؤثرالتكامل كوماتو

عبد الرحمن سلمان جمعه   رعد عواد حميد   مصطفى ابراهيم حميد

جامعة الانبار   جامعة تكريت
كلية التربية للعلوم الصرفة   كلية التربية للعلوم الصرفة
قسم الرياضيات   قسم الرياضيات

المستخلص :
في هذا البحث بأستخدام خصائص مؤثر كوماتو استطعنا ان نشتق بعض خواص التابعية التفاضلية وفوق التابعية بالأعتماد على مفهوم ضرب هادمرد.

</div>

On The Enumeration of The Transitive and Acyclic Digraphs Having a Fixed Support Set

Khalid Shea Khairalla Al'Dzhabri

University of Al-Qadisiyah, College of Education, Department of mathematics

Khalid.aljabrimath@qu.edu.iq

Abstract: In previous works of the author, the concept of a binary reflexive adjacency relations was introduced on the set of all binary relations of the set X , and an algebraic system consisting of all binary relations of the set X and of all unordered pairs of adjacent binary relations was defined. If X is a finite set, then this algebraic system is a graph (graph of binary relations G). The current paper introduces the notion of a support set for acyclic and transitive digraphs. This is the collections $S(\sigma)$ and $S'(\sigma)$ consisting of the vertices of the digraph $\sigma \in G$ that have zero indegree and zero outdegree, respectively. It is proved that if G_σ is a connected component of the graph G containing   the   acyclic   or   transitive   digraph $\sigma \in G$,   then $\{S(\tau) : \tau \in G_\sigma\} = \{S'(\tau) : \tau \in G_\sigma\}$. A formula for the number of acyclic and   transitive digraphs having a fixed support set is obtained.

Keywords: Enumeration of graphs, acyclic digraph, transitive digraph.
Mathematics subject classification :05C30

Khalid .S

1.Definitions and auxiliary propositions:

Definition 1.1 Any "binary relation $\sigma \subseteq X^2$ (X – arbitrary set) , generates a

charcteristic   function" $\sigma' : X^2 \to \{0,1\}$,(if

$(x, y) \in \sigma$,   then $\sigma'(x, y) = 1$,   otherwise

$\sigma'(x, y) = 0)$, and this mpping is bijectve.

Remarks 1.2 1) From the definition(1.1) we called

the   subset $\sigma \subseteq X^2$ as   the   relationsships   and

functions (someetimes digraphs).

2) If X finite set then the characeteristic function can be interepreted as a binaary matrix (the matrix consisiting of 0 and 1). **Definition 1.3** The relations

$\sigma, \tau \subseteq X^2$ called adjaceent if there exists a disjoint

of union of two subsets $X = Y \cup Z$, such that:

i) $\sigma(x, y) = 0$ for all $(x, y) \in Y \times Z$;

ii) $\tau(x, y) = 0$ for all $(x, y) \in Z \times Y$;

iii) $\tau(x, y) + \sigma(y, x) = 1$ for   all

$(x, y) \in Y \times Z;$

iv) $\sigma(x, y) = \tau(x, y).$ for   all

$(x, y) \in Y^2 \cup Z^2$.

Remark 1.4 From the definiition (1.3), that if

the relation τ adjaceent with a relation σ , then

σ adjaceent with a relation τ , and this fact we

write in the form of a diagaram

$\sigma \xleftrightarrow{Y \times Z} \tau$.

$= \sigma \xleftrightarrow{Y \times Z} \tau =$
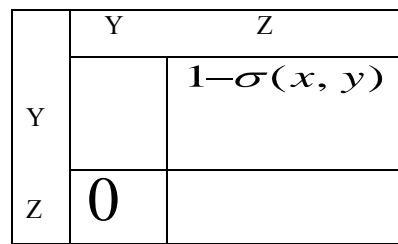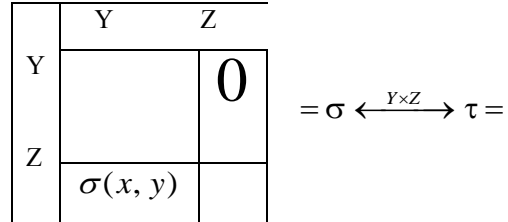
Example 1.5: For $X = \{1, 2, 3, 4\}$ we have the

following adjaceent relations:

$$\begin{bmatrix} 1 & 0 & 0 & 0 \\ 0 & 1 & 0 & 0 \\ 1 & 1 & 1 & 1 \\ 1 & 1 & 0 & 1 \end{bmatrix} \xleftrightarrow{\{1\} \times \{2,3,4\}} \begin{bmatrix} 1 & 1 & 0 & 0 \\ 0 & 1 & 0 & 0 \\ 0 & 1 & 1 & 1 \\ 0 & 1 & 0 & 1 \end{bmatrix}$$

$$\xleftrightarrow{\{2,4\} \times \{1,3,\}} \begin{bmatrix} 1 & 0 & 0 & 0 \\ 0 & 1 & 0 & 0 \\ 0 & 0 & 1 & 0 \\ 1 & 1 & 0 & 1 \end{bmatrix} \xleftrightarrow{\{2,3\} \times \{1,4\}}$$

$$\begin{bmatrix} 1 & 0 & 0 & 0 \\ 1 & 1 & 0 & 0 \\ 1 & 0 & 1 & 1 \\ 1 & 0 & 0 & 1 \end{bmatrix}$$

16

Khalid .S

Example1.6:

$$X = \{1,...,6\}, \ Y=\{1,2\}, \ Z=\{3,4,5,6\},$$

then the adjaceent relation is:

"Thus, the set X generatees a pair $\langle 2^{X^2}, E(X) \rangle$,

where 2^{X^2} is the set of vertices, consist of the set of all binary relations of the set X , and $E(X)-$ is a set of edeges, consist of all unordered distinct pairs of adjaceent of binary relations of the set X . The pair $G(X) \doteq \langle 2^{X^2}, E(X) \rangle$ will be called "undirected graph of binary relations of the set X ".

The following theorem proved that in our work [3].

Theorem   1.7:   If $card \ X \neq 1,$ then $diam(G(X)) = 2$.

Remark 1.8: we denoted the "connected component of the graph" $G(X)$ by $G_\sigma(X)$, which contaiins the given relation $\sigma \in 2^{X^2}$.

2. Arithmetic properties of some subgraphs of the graph of binary relations. "We denoted that the collection of all partial orders defined on the set X by $V_0(X)$. And the collection of all reflexivie – transitive relations defined on the set X by $V(X)$ and where X finiite sets the collection of all acyclic relations by $A(X)$."

In [1],[2] and [3] we proved that if $\sigma, \tau \in 2^{X^2}$ are adjaceent then:

1. $\sigma \in V_0(X)$ if and only if $\tau \in V_0(X)$;

2. $\sigma \in V(X)$ if and only if $\tau \in V(X)$;

3. $\sigma \in A(X)$ if and only if $\tau \in A(X)$.

Therefore, in the garaph $\langle 2^{X^2}, E(X) \rangle$ define the following subgrphs:

$$\langle V_0(X), E(X) \rangle, \quad \langle V(X), E(X) \rangle, \quad \langle A(X), E(X) \rangle....$$
$$.......................(1)$$

Continue to suggeset that $card \ X < \infty$ (i.e $X = \{1,...,n\}$) . Then we get the following remakes:

Remakes 2.1: 1) If replacing the unit elements $\sigma(x,x),$ zeros, then we get a one-to-one corresepondence between the set $V_0(X)$ and the set of all labeled transitive digraphs denoted by $V_0^0(X)$.

2) There exist a one-to-one corresepondence between the set $V_0(X)$ and the seet of all labeeled $T_0 -$ topoology denoted by $T_0(X)$.

Khalid .S

3)   Let

$$T_0(n) = card \ T_0(X) = card \ V_0(X) = card \ V_0^0(X).$$

Additional suggest that $T_0(0) = 1$.

In [1] we proved that the number of "connected component of the graph " $\langle V_0(X), E(X) \rangle$ equal to $T_0(n-1)$. We note that for any nataural number n the following equaliities are hold:

$$T_0(n) = \sum_{p_1+...+p_k=n} \frac{n!}{p_1!+...+p_k!} V(p_1,...,p_k),$$
...............................(2)

$$T_0(n) = \sum_{p_1+...+p_k=n} (-1)^{n-k} \frac{n!}{p_1!+...+p_k!} w(p_1,...,p_k),$$

where the summation is over all ordered sets $(p_1,...,p_k)$ of positivee integers such that $p_1 +...+ p_2 = n$. The first formula see [4],[5] and [6] and second in [7]. The number of $V(p_1,...,p_k)$ and $W(p_1,...,p_k)$ denote the number of partial orders of a special form, which depends on a set of $(p_1,...,p_k)$ see below (4).

4)   If $X = \{1,...,n\}$. Then:

$$cardV(X) = \sum_{m=1}^{n} S(n,m)T_0(m) \quad \text{see [4],[8]}$$

and [9] where $S(n,m) -$ This Stiriling numbers of the 2nd kind in our work [2] we proveed that the number of coonnected component of the graph

$\langle V(X), E(X) \rangle$ equal   to

$$\sum_{m=1}^{n} S(n,m)T_0(m-1).$$

Remark 2.2 From above there exists a one to one correseponded between the set of all transitive-reflexive relations $V(X)$ and the set of all labeled topologies $T(X)$ defined on the set X.

If $A_n = A(X)$ and $X = \{1,...,n\}$ a cording to [10] the following equality holds:

$$cardA(X) = \sum_{p_1+...+p_k=n} (-1)^{n-k} \frac{n!}{p_1!...p_k!} 2^{(n^2-p_1^2-...-p_k^2)/2}, ...$$
..........................(3)

In our work [3] we proveed that the number of connected   component   of   the   graph $\langle A(X), E(X) \rangle$ equal   to

$$\sum_{p_1+...+p_k=n} (-1)^{n-k} \frac{(n-1)!}{(p_1-1)!p_2!...p_k!} 2^{(n^2-p_1^2-...-p_k^2)/2}.....$$
..........................(4)

In both cases, the summation is over all ordered sets $(p_1,...,p_k)$ of natural numbers such that $p_1 + p_2 +...+ p_k = n$.

Remark 2.3 We note that the formulass (2) and (3) have the same struccture, and in the second case if the formula has a finisihed appearance, then in the first formula remains a problem of calculation of numbers $W(p_1,...,p_k)$.

Journal of AL-Qadisiyah for computer science and mathematics   Vol.10   No.1   Year 2018
ISSN (Print): 2074 – 0204   ISSN (Online): 2521 – 3504

Khalid .S

In the work [10] the following (more general) assertions are proved. We denote by $A_n(x) = \sum_r A_{nr} x^r$ a polynomial whose coefficient A_{nr} is equal to the number of labeled acyclic digraphs of order n having exactly r arcs. It is clear that $A_n = A_n(1)$. We use the agreement $A_0(x) = A_0 = 1$. The polynomial $A_n(x)$ for $n \in \square$ is given by the formula:

$$A_n(x) = \sum_{p_1+\ldots+p_k=n} (-1)^{n-k} \frac{n!}{p_1!\ldots p_k!} (1+x)^{(n^2-p_1^2-\ldots-p_k^2)/2}$$

(compare with the formula (3) . For any $n \geq 0$, we have the following :

$$\sum_{m=0}^{n} (-1)^m \binom{n}{m}(1+x)^{m(n-m)} A_m(x) = \delta_{n0}.$$

Now from the formulass above we give the following example:

3. Examples of subgraphs of the graph of binary relations.

Let $X = \{1,2,3\}$.Then we get 3 "connected components of the graph" $\langle V_0(X), E(X) \rangle$, contains 19 partial orders:

………(5)
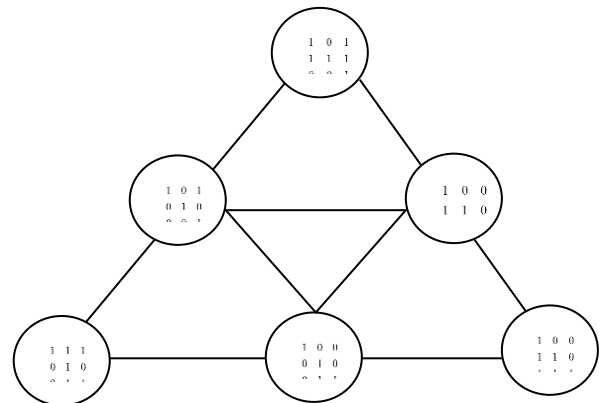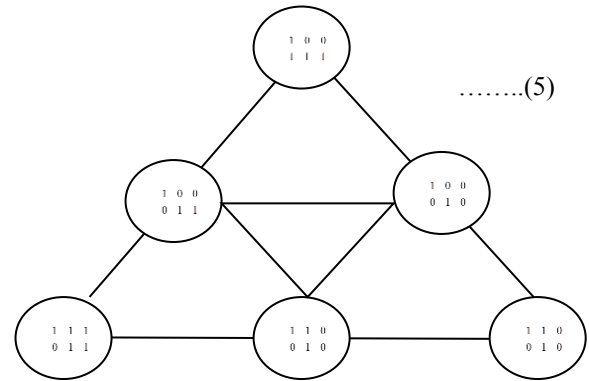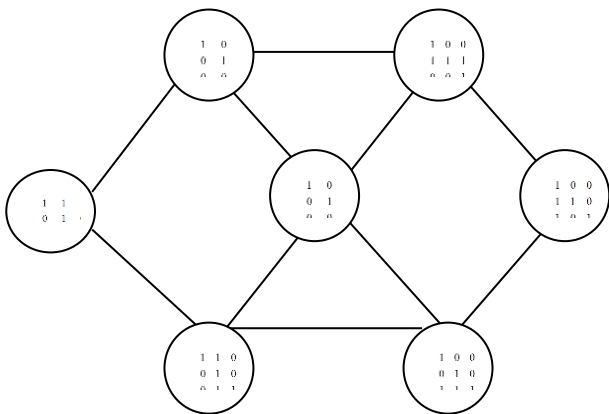
And the graph $\langle V(X), E(X) \rangle$, contains 29 reflexive- transitive relations. It has 7 conneected componeents: 3 components of the graph (4) above and 4 components as:

Journal of AL-Qadisiyah for computer science and mathematics   Vol.10   No.1   Year 2018
ISSN (Print): 2074 – 0204   ISSN (Online): 2521 – 3504

Khalid .S
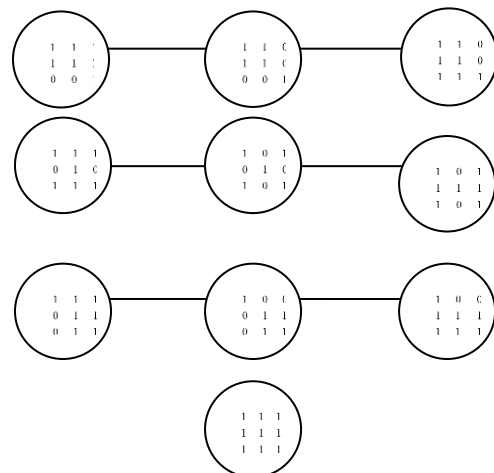
And the graph $\langle A(X), E(X)\rangle$ contaiins 25 acyclice relations . It has 5 connected components : 3 components of the grapha (4) above (in them should be replaced the elementes of the set $V_0(X)$ by the elements of the set $V_0^0(X)$) 2 componenets as follows:

"Where $X = \{1, 2, 3, 4\}$ in subgraphs of the form (1) there is a 219, 355 and 543 vertices respectively and the number of connected components of these subgrags in (1) equal to 19, 45, and 79 respectively."

...........(6)
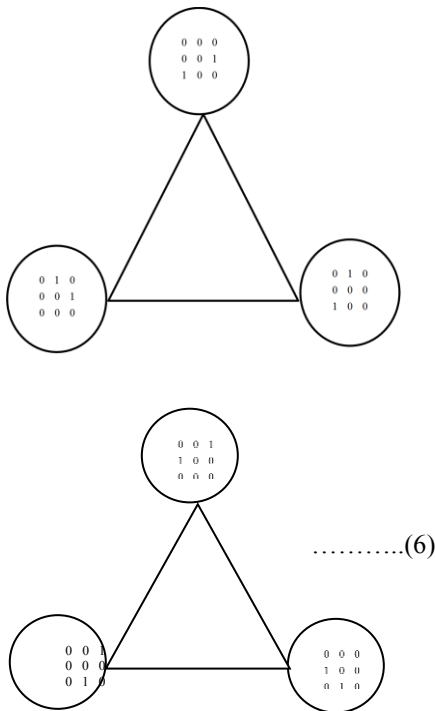
4. Definition of numbers $W(p_1, ..., p_k)$ **and** $V(p_1, ..., p_k)$**:** We fix $(p_1, ... p_k) \in \Box^{\;k}$, and let $n = p_1 + ... + p_k$, $X = \{1, ..., n\}$. The set $(p_1, ..., p_k)$ Will be called a partition of the number n . The partition $(p_1, ..., p_k)$ corresponds to representation of a relation $\sigma \in V_0(X)$ in block form

$$\begin{vmatrix} \sigma^{11} & \sigma^{12} & \cdots & \sigma^{1k} \\ \sigma^{21} & \sigma^{22} & \cdots & \sigma^{2k} \\ \cdots & \cdots & \cdots & \cdots \\ \sigma^{k1} & \sigma^{k2} & \cdots & \sigma^{kk} \end{vmatrix} \quad ....(7)$$

In which at the intersection of the ith horizontal and j^{th} vertical bands cost a block σ^{ij} with p_i rows and p_j columns recording the relation $\sigma \in V_0(X)$ in the form (7) will be called a block representation of type $(p_1, ..., p_k)$. Through $w(p_1, ..., p_k)$ we denote the set of all relations $\sigma \in V_0(X)$ for which in the block representation (7) of type $(p_1, ..., p_k)$：

1-   All blocks σ^{ij}, $1 \le j < i \le k$, consist of zeros;All diagonal blocks σ^{ii}, $i = 1, ..., k, -$ identity matrices. And let $W(p_1, ..., p_k) = cardw(p_1, ..., p_k)$.

Through $v(p_1, ..., p_k)$ we denote the set of all relations $\sigma \in \omega(p_1, ..., p_k)$ such that in block representation (7) of type $(p_1, ..., p_k)$ in super-diagonal blocks $\sigma^{i-1,i}, i = 2, ..., k$ in each column there is at least number one we call such blocks (nondegenerate). We note that, by virtue of transitivity σ all blocks $\sigma^{sr}, s = 1, ... k - 1, \; r = s + 1, ..., k$ nondegenerate. We use the notation $V(p_1, ..., p_k) = cardv(p_1, ..., p_k)$.

Journal of AL-Qadisiyah for computer science and mathematics   Vol.10   No.1   Year 2018
ISSN (Print): 2074 – 0204   ISSN (Online): 2521 – 3504

Khalid .S

5. Comparison of the formulas (2) and (3):

Inclusion $v_0^0(X) \subset A(X)$ it is well known that formulas (2) and (3) for calculating numbers $card\, v_0^0(X)$ and $card\, A(X)$ have the same structure. However, if in the second case the formula has a completed form, then in the first the problem persists calculation of numbers $W(p_1,...,p_k)$. In the framework of studies of this problem in the works [7,11] obtained family of equations of connection between the individual numbers $W(p_1,...,p_k)$:

$$W(p_{\pi(1)},...,p_{\pi(k)}) = W(p_1,...,p_k), \quad \pi \in D_k,$$

Where $D_k -$ is the dihedral group, generated by substitutions:

$$\begin{pmatrix} 1 & 2 & ... & k-1 & k \\ 2 & 3 & ... & k & 1 \end{pmatrix}, \begin{pmatrix} 1 & 2 & ... & k-1 & k \\ k & k-1 & ... & 2 & 1 \end{pmatrix},$$

$$\sum_{q_1+...+q_r=m} (-1)^{m-r} \frac{m!}{q_1!...q_r!} W(p+1,q_1,...,q_r) =$$

$$\sum_{q_1+...+q_r=m} (-1)^{m-r} \frac{m!}{q_1!...q_r!} (r+1) W(p+1,q_1,...,q_r)$$

$$W(p,1,q,1) = \sum_{r=0}^{q} \binom{q}{r}(2^{q-r}+1)^p W(p,r,1)$$

$$+ \sum_{r=0}^{p} \binom{p}{r}(2^{p-r}+1)^q W(r,q,1).$$

Formulas $\quad W(n)=1, \; W(p,q)=2^{pq} \quad$ are obvious. B [11], the following explicit formulas are proved:

$$W(p,1,q) = \sum_{r=0}^{q} \binom{q}{r}(2^r + 2^q)^p,$$

$$W(p,2,q) = \sum_{q_1+...+q_4=q} \frac{q!}{q_1!...q_4!}(2^{q_1} + 2^{q_1+q_2} + 2^{q_1+q_3} + 2^q)^p,$$

$$W(p,1,1,q) - W(p,2,q) =$$

$$= \sum_{q_1+q_2+q_3=q} \frac{q!}{q_1!.q_2.q_3!}(2^{q_1} + 2^{q_1+q_2} + 2^q)^p.$$

The above relations allow us to calculate the numbers $T_0(n)$ for all $n \le 7$ (without the use

of a computer, by solving a system of linear equations with respect to quantities $W(p_1,...,p_k))$. In [11] it was noted that to calculate the number $T_0(8)$ of these relations is not sufficient (only three equations are

missing with respect to the quantities $W(p_1,...,p_k)$ generating the required rank of the matrix of the system). We assume that the existence of some general patterns, generating new relations equation. Note also that due to the development of effective algorithms

Computer calculations [12] currently known value $T_0(n)$ for all $n \le 18$.

6. The number of transitive and acyclic digraphs having a fixed support set.

Let $(p_1, p_2) \in N^2$, $p = p_1$, $m = p_2$,

$$X = \{1,...,p+m\}, \; M = \{p+1,...,p+m\}.$$

through $w(p;m)$ we denote the set of all relations $\sigma \in v_0(X)$, for which in the block representation (7) of type (p_1, p_2).

Khalid .S

1.   The diagonal block σ^{11} is the identity matrix,

2.   In the block σ^{12} consists of zeros,

3.   The diagonal block σ^{22} is a partial order (belongs to $v_0(M)$,

And let $W(p;m)=cardw(p;m).$ In addition, we assume:

$$W(0;m)=T_0(m),\ m=0,1,...,\quad W(p;0)=1,\ p=0,1,...$$
..................(8)

through $v(p,m)$ we denote the set of all relations $\sigma \in w(p,m)$ Such   that   in   the   block representation (7) of type $(p_1,p_2)\ (=(p,m))$ the block $\sigma^{12}-$nondegenerate. We use the notation $V(p;m)=cardv(p;m)$ and we assume, by definition,

$$V(0;m)=\delta_{0m},\ m=0,1,...,\quad V(p;0)=1\ \ p=0,1,....$$
..................(9)

For a relation $\sigma \in v_0(X)$ (in which, in contrast to the relations of $v_0^0(X),$ for all $x \in X$ justly $\sigma(x,x)=1$) support sets are the collections:

$$S(\sigma)=\{y \in X : \sigma(x,y)=\delta_{xy}\ for\ all\ x \in X\},$$
$$S^{'}(\sigma)=\{x \in X : \sigma(x,y)=\delta_{xy}\ for\ all\ y \in X\}.$$
It is clear that the set $v(p,m)$ coincides with the set of all those relations $\sigma \in v_0(X),$ in which $S(\sigma)=\{1,...,p\}.$

Theorem 6.1 For integer $p \geq 0$ and $m \geq 0$ the following equalities are hold:

$$W(p;m)=\sum_{r=0}^{m}\binom{m}{r}V(p+r;m-r),\ ....$$
..................(10)

$$V(p;m)=\sum_{r=0}^{m}(-1)^r\binom{m}{r}W(p+r;m-r).$$
..................(11)

Proof: Let $p \geq 1,\ m \geq 1$. It is easy to see that if $\sigma \in w(p;m)$ then the set $P=\{1,...,p\}$ is contained in the support set $S(\sigma).$ For any $\alpha \subseteq M$, $w_\alpha(p;m)$ we denoted the set of all those   relations $\sigma \in w(p;m)$,   which $S(\sigma)=P \bigcup \alpha$, thus breaking up the set of $w(p;m)$ to   pairwise   disjoint   classes $w_\alpha(p;m)$ .Therefore,

$$W(p;m)=cardw(p;m)=\sum_{\alpha \subseteq M}cardw_\alpha(p;m).$$
Obviously,   when $\alpha=\varnothing$ the   equalities $w_\varnothing(p;m)=v(p;m)$,and

$w_\varnothing(p;m)=V(p;m).$ It is also easy to understand that if non-empty $\alpha,\beta \subseteq M$ such that $|\alpha|=|\beta|$, then:

$$cardw_\alpha(p;m)=cardw_\beta(p;m)=cardw_\gamma(p;m),$$
where
$$\gamma=\{p+1,...,p+r\} \subseteq M,\ r=|\alpha|=|\beta| \in [1,m].$$

Khalid .S

Since for all $\sigma \in w_{\gamma}(p;m)$ we have the equality

$$S(\sigma) = \{1,...,p+r\}, \text{ then :}$$

$$w_{\gamma}(p;m) = v(p+r;m-r), \text{ therefore:}$$

$$cardw_{\gamma}(p;m) = V(p+r;m-r),$$

which proves (10). With the introduction of agreements (8) and (9) it is easy to verify that the equation (10) holds also for $p=0$ and $m=0$.

Let Δ we denoted the right-hand side of the formula (11) then by the formula (10) we have the equality:

$$\Delta = \sum_{r=0}^{m}(-1)^{r}\binom{m}{r}\sum_{s=0}^{m-r}\binom{m-r}{s}V(p+r+s;m-r-s).$$

Replacing the index s by $t = r + s$ and changing the order of summation, we obtain the following chain of equalities:

$$\Delta = \sum_{t=0}^{m}[\sum_{r=0}^{t}(-1)^{r}\binom{t}{r}]\binom{m}{t}V(p+t;m-t) =$$

$$= \sum_{t=0}^{m}\delta_{t0}\binom{m}{t}V(p+t;m-t) = V(p;m).$$

Theorem 6.2 For integer $p \geq 1$ and $m \geq 0$ the following equality are hold:

$$V(p;m) = \sum_{\substack{p_1+...+p_k=p+m \\ p_1 \geq p}}(-1)^{m+1-k}\frac{m!}{(p_1-p)!p_2!...p_k!}W(p_1,...,p_k).$$

Proof: Suppose that $m \geq 1.$ By formula (11) the following equality holds:

$$V(p;m) = (-1)^{m} + \sum_{q=0}^{m-1}(-1)^{q}\binom{m}{q}W(p+q;m-q).$$

In accordance with Lemma (3) in [7] for all $q = 0,1,...,m-1$ we have the equality:

$$W(p+q;m-q) = \sum_{q_1+...+q_r=m-q}(-1)^{m-q-r}\frac{(m-q)!}{q_1!...q_r!}W(p+q,q_1,...,q_r),$$

therefore

$$V(p;m)-(-1)^{m} = \sum_{q=0}^{m-1}(-1)^{q}\binom{m}{q}\sum(-1)^{m-q-r}\frac{(m-q)!}{q_1!...q_r!}W(p+q,q_1,...,q_r) =$$

$$= \sum_{\substack{q+q_1+...+q_r=m \\ 0 \leq q \leq m}}(-1)^{m-r}\frac{m!}{q!q_1!...q_r!}W(p+q,q_1,...,q_r).$$

Passed to the summation of all the variables simultaneously. Let $q_0 = p + q,$ then:

$$V(p;m)-(-1)^{m} = \sum_{\substack{q_0+q_1+...+q_r=p+m \\ p \leq q_0 < p+m}}(-1)^{m-r}\frac{m!}{(q_0-p)!q_1!...q_r!}W(q_0,q_1,...,q_r).$$

The proof completes the change of variables

$$k = r+1, \; p_i = q_{i-1}, \; i=1,...,k.$$ The case

$$m = 0$$ is valid by virtue of the formula (9).

Remark 6.3: For any $n \in N$ and $p = 1,...,n$

through $A_n^{(p)}$ (through $T_0^{(p)}(n)$) denote the number of all labeled acyclic digraphs $\sigma \in A(X)$ (respectively labeled transitive digraphs $\sigma \in v_0^0(X)$) defined on the sets $X = \{1,...,n\}$ and such that $S(\sigma) = \{1,...,p\}.$ It is clear that

$$T_0^{(p)}(n) = V(p;n-p).$$

Thus, by virtue of Lemma (2), we can proof that the following theorem:

Theorem 6.4 : For any $n \in N$ and $p = 1,...,n$

we have the following equality:

$$T_0^{(p)}(n) = \sum_{\substack{p_1+...+p_k=n \\ p_1 \geq p}} (-1)^{n-p+1-k} \frac{(n-p)!}{(p_1-p)!p_2!...p_k!} W(p_1,...,p_k),$$

$$A_n^{(p)}(n) = \sum_{\substack{p_1+...+p_k=n \\ p_1 \geq p}} (-1)^{n-p+1-k} \frac{(n-p)!}{(p_1-p)!p_2!...p_k!_1} 2^{(n^2-p_1^2-...p_k^2)/2}.$$

The second formula is proved in Lemma 4 of (compare also with the expression (4).

Reference

[1] Al'Dzhabri Kh.Sh., Rodionov V.I. , The graph of partial orders, Vestn. Udmurt. Univ. Mat. Mekh. Komp'yut. Nauki, 2013, issue 4, pp. 3-12 (in Russian). DOI: 10.20537/vm130401

[2] Al'Dzhabri Kh.Sh. ,The graph of reflexive-transitive relations and the graph of finite topologies, Vestn. Udmurt. Univ. Mat. Mekh. Komp'yut. Nauki, 2015, Vol. 25, issue 1, pp. 3-11 (in Russian). \\ DOI: 10.20537/vm150101

[3] Al' Dzhabri Kh.Sh., Rodionov V.I. ,The graph of acyclic digraphs, Vestn. Udmurt. Univ. Mat. Mekh. Komp'yut. Nauki, 2015, Vol. 25, issue 4, pp. 441-452 (in Russian). DOI: 10.20537/vm150401

[4] Comtet L. , Recouvrements, bases de filtre et topologies d'un ensemble fini , C. R. Acad. Sci., 1966, Vol. 262, pp. A1091-A1094.es

[5] Erne M. , Struktur- und anzahlformeln fur topologien auf endlichen mengen, Manuscripta Math., 1974, Vol. 11, No. 3, pp. 221-259. DOI: 10.1007/BF01173716

[6] Borevich Z.I. "Enumeration of finite topologies", J. Sov. Math., 1982, Vol. 20, issue 6, pp. 2532-2545. \\ DOI: 10.1007/BF01681470

[7] Rodionov V.I. , On enumeration of posets defined on finite set, Siberian Electronic Mathematical Reports, 2016, Vol. 13, pp. 318-330 (in Russian). DOI: 10.17377/semi.2016.13.026

[8] Evans J.W., Harary F., Lynn M.S. , On the computer enumeration of finite topologies, Comm. ACM, 1967, Vol. 10, issue 5, pp. 295-297. DOI: 10.1145/363282.363311

[9] Gupta H. , Number of topologies on a finite set, Research Bulletin of the Panjab University (N.S.)}, 1968, Vol. 19, pp. 231-241.

[10] Rodionov V.I. , On the number of labeled acyclic digraphs, Discrete Mathematics, 1992, Vol. 105, No. 1-3, pp. 319--321. DOI: 10.1016/0012-365X(92)90155-9

[11] Rodionov V.I. , On recurrence relation in the problem of enumeration of finite posets, Siberian Electronic Mathematical Reports, 2017, Vol. 14, pp. 98-111 (in Russian). DOI: 10.17377/semi.2017.14.011

[12] Brinkmann G., McKay B.D. , Posets on up to 16 points, Order, 2002, Vol. 19, issue 2, pp. 147-179. \\ DOI: 10.1023/A:1016543307592.

حول اعداد البيانات المباشرة المتعدية والدائرية بوجود المجموعة الداعمة

خالد شياع خيرالله الجبري
جامعة القادسية
كلية التربية
قسم الرياضيات
Khalid.aljabrimath@qu.edu.iq

المستخلص :

في الأعمال السابقة للمؤلف قدم مفهوم العلاقات الانعكاسية الثنائية الملاصقة من العلاقات الثنائية للمجموعة X وللنظام الجبري الذي يحوي كل العلاقات الثنائية للمجموعة X وقدم جميع الأزواج غير مرتبة من العلاقات الثنائية الملاصقة . اذا كانت الـ X مجموعة منتهية بالتالي يمكن اعتبار هذا النظام الجبري هو بيان (بيان من العلاقات الثنائية للبيان G) .

في البحث الحالي قدم مفهوم المجموعة الداعمة للبيانات المباشرة الدائرية والمتعدية حيث المجموعات $S(\sigma)$ و $S'(\sigma)$ التي تحتوي على كل الرؤوس من البيان المباشر $\sigma \in G$ والتي تمتلك (zero indegree and zero outdegree) على التوالي وبرهنا بانه اذا كانت G_σ مركبات متصلة للبيان G والذي يحوي البيانات الدائرية والمتعدية المباشرة فأن $\{S(\tau): \tau \in G_\sigma\} = \{S'(\tau): \tau \in G_\sigma\}$ وكذلك أوجدنا وبرهنا الصيغة التي تحسب كل هذه البيانات الدائرية والمتعدية المباشرة بوجود مفهوم المجموعة الداعمة .

الكلمات المفتاحية : تعداد الرسم البياني ، البيانات المباشرة الدائرية، البيانات المتعدية المباشرة.

Dihedral Cryptographic Technique

Zainab Fahad Mhawes

Al-Qadisiya university-College of education-Department of Mathematics

zainab.alnaseri@qu.edu.iq

Abstract:

This paper focuses on a new technique of cryptography in abstract algebra. We first give the necessary review on Dihedral group and cryptography .We definition a new alphabetic of characters by additive character "blank" ,thus we have (27) characters {26 letters and "blank" },therefore we use modular 27 instead 26 such that we use the reflection and rotation which exists in Dihedral group to change the arrange of vectors of characters in plain text.

Keywords : Dihedral group, Cryptography ,Caesar Cipher ,Encryption Processes, Decryption processes.

Mathematics Subject Classification: 68P25

Introduction: Cryptography is one of the most important applications of algebra and number theory where the process is to change important information to another unclear one . The main goal of cryptography is to keep the integrity and security of this information there are many types of Cryptography techniques and we will try to consider some of them in this paper .

This paper consists of three paragraphs ,where one includes some necessary definitions on dihedral groups . In second, we defined some necessary definitions on Cryptography. Third includes a suggested technique and some example and analysis of this technique . The programs of this paper write by using V.B. language .

Zainab .F

1. Preliminary definitions in algebra:

1.1   Definition [4]:

We say that $*: S \times S \to S$, which defined by $(x,y) \to x$ is a binary opration on a nonempty set S if it is map .

1.2   Definition[5]:

A group $(G,*)$ is a nonempty set G with a binary operation * such that the following conditions are hold:

(i) $(x* y)* z = x* (y* z)$, for all $x,y,z \in G$

(ii) There exists an element e such that:

$$x * e = x = e * x \text{ , for all } x \in G,$$

(iii) For all $x \in G$ there is an element x^{-1} in G such that:

$$x^{-1} * x = e = x * x^{-1}.$$

1.3   Definition[4]:

The set $D_n = \{r^0, r, r^2, \ldots , r^{n-1}, s, sr, sr^2 , \ldots , sr^{n-1} \}$ is called the dihedral group and has order 2n with property $sr = r^{-1}s$.

1.4 Remarks[4]:

$r^n = r^0$, $s^2 = r^0$

2. Preliminary definitions in Cryptography:

2.1 Definition[3]:

Encryption is the process of changing the text of the content (data) to the symbols and Numbers are difficult to understand using the many and varied mathematical algorithms .

2.2 Goals of Cryptography [1]:

- Data privacy (confidentiality).
- Data Authenticity (it came from where it claim).
- Data integrity(it has not been modified on the way) in the digital world.

2.3   The   fundamental   objects   of Cryptography [2]:

- Plaint text is the original data.
- Cipher text is the message changed by using some algorithms .
- Encryption is the processes which are changing the plaintext to cipher text.
- Decryption is the processes which are changing the cipher text to plaintext.

2.4 Definition [4]:

Let   A= $\begin{bmatrix} a_1 \\ a_2 \\ \vdots \\ a_{n-1} \\ a_n \end{bmatrix}$ be a vector then the

cryptography transpose (CT) of A is

$$A^{CT} = \begin{bmatrix} a_n \\ a_{n-1} \\ \vdots \\ a_2 \\ a_1 \end{bmatrix}$$

We will introduce a new term in the following definition, that is the transpose of element.

Zainab .F

2.5 Definition:

Let $\quad A=\begin{bmatrix} a_0 \\ a_1 \\ \vdots \\ . \\ a_{n-1} \end{bmatrix}$ be a vector and a_k

be an element of A, then the transport of a_k is $(a_k)^T = a_{(n-1)} - k$

We will define a new operation in the following definition, which it very import in our paper.

2.6 Definition:

Let $\quad D_n = \{r^0, r, \ldots, r^{n-1}, s, sr, \ldots, sr^{n-1}\}$ be a dihedral group then we can define the new operation :

$$r^k a = a+k \bmod 27$$
$$r^{-k} a = a-k \bmod 27$$
$$sa = a^T \bmod 27$$
$$sr^k a = (a+k)^T \bmod 27$$

3. The suggested algorithm :

Here we consider the blank is character , i.e the alphabet is 27 chars .

- i- Encryption process :
    1- Take positive integer number n .
    2- Construction Dihedral group D_n .
    3- Cut block of plain text with length 2n character as :

$$P = \begin{bmatrix} p_1 \\ p_2 \\ \vdots \\ . \\ p_{2n} \end{bmatrix} = \begin{bmatrix} A \\ B \end{bmatrix} \quad , A = \begin{bmatrix} p_1 \\ \vdots \\ . \\ p_n \end{bmatrix}, B = \begin{bmatrix} p_{n+1} \\ \vdots \\ . \\ p_{2n} \end{bmatrix}$$

4- Apply the Dihedral operations (r,s):

$$D_n p = \begin{bmatrix} (r^k a_{k+1}) \bmod 27 \\ (sr^k b_{k+1}) \bmod 27 \end{bmatrix} \quad , k=0,1,\ldots,n-1$$

$$DnP = \begin{bmatrix} \left(\begin{bmatrix} 0 \\ 1 \\ \vdots \\ n-2 \\ n-1 \end{bmatrix} + \begin{bmatrix} p_1 \\ \vdots \\ . \\ p_n \end{bmatrix} \right) \bmod 27 \\ \left(\begin{bmatrix} 0 \\ 1 \\ \vdots \\ n-2 \\ n-1 \end{bmatrix} + \begin{bmatrix} p_{n+1} \\ \vdots \\ . \\ p_{2n} \end{bmatrix} \right)^T \bmod 27 \end{bmatrix}$$

For enhanced this technical we must encryption the first letter of plaintext because the first letter by using this technical stay the same letter always.

Encryption the first letter

$$C_1 = p_1 + (2*n) \bmod 27$$

ii) Decryption process:

$$P_i = C_i - (2*n) \bmod 27$$

$$D_n C = \begin{bmatrix} (r^{-k} a_{k+1}) \bmod 27 \\ (r^{-k} s B_{k+1}^T) \bmod 27 \end{bmatrix}$$

3.1 Example:

Take plain text="hello"

Encryption by using Dihedral Cryptographic Technique

Zainab .F

Solution

1- Encrption

Let n=2

$D_n=D_2=\{r^0,r,s,sr\}, |D_2|=4$

Hello={Hell}+{o_ _ _}

"Hell"$\rightarrow P_1=\begin{bmatrix}7\\4\\11\\11\end{bmatrix}=\begin{bmatrix}A\\B\end{bmatrix}$, $A=\begin{bmatrix}7\\4\end{bmatrix}$

, $B=\begin{bmatrix}11\\11\end{bmatrix}$

$D_1P_1=\begin{bmatrix}\begin{bmatrix}0\\1\end{bmatrix}&+&\begin{bmatrix}7\\4\end{bmatrix}\\(\begin{bmatrix}0\\1\end{bmatrix}&+&\begin{bmatrix}11\\11\end{bmatrix})\ _T\end{bmatrix}=$

$\begin{bmatrix}\begin{bmatrix}7\\5\end{bmatrix}\\(\begin{bmatrix}11\\12\end{bmatrix})\ _T\end{bmatrix}=\begin{bmatrix}\begin{bmatrix}7\\5\end{bmatrix}\\\begin{bmatrix}15\\14\end{bmatrix}\end{bmatrix}=\begin{bmatrix}7\\5\\15\\14\end{bmatrix}\rightarrow$HFPO=$C_1$

The first letter:

H $\rightarrow 7 \rightarrow 7+4=11\rightarrow$ L

"O"$\rightarrow$"O---"$\rightarrow P_2\rightarrow\begin{bmatrix}14\\26\\26\\26\end{bmatrix}\rightarrow\begin{bmatrix}\begin{bmatrix}14\\26\end{bmatrix}\\\begin{bmatrix}26\\26\end{bmatrix}\end{bmatrix}$

$D_2P_2=\begin{bmatrix}\begin{bmatrix}0\\1\end{bmatrix}&+&\begin{bmatrix}14\\26\end{bmatrix}\\(\begin{bmatrix}0\\1\end{bmatrix}&+&\begin{bmatrix}26\\26\end{bmatrix})\ _T\end{bmatrix}=$

$\begin{bmatrix}\begin{bmatrix}14\\0\end{bmatrix}\\(\begin{bmatrix}26\\0\end{bmatrix})\ _T\end{bmatrix}=\begin{bmatrix}14\\0\\0\\26\end{bmatrix}\rightarrow C_2$=OAA-

Then

O$\rightarrow 14\rightarrow 14+4=18\rightarrow$S

P="Hello"$\rightarrow$C="LFPOSAA-"

2-Decryption :

C=" LFPOSAA-"

C_1="LFPO" ,C_2="SAA-"

C_1:

L $\rightarrow$ 11-4=7 $\rightarrow$H

$D_2C_1=D_n=\begin{bmatrix}\begin{bmatrix}7\\5\end{bmatrix}\\\begin{bmatrix}15\\14\end{bmatrix}\end{bmatrix}=$

$\begin{bmatrix}-\begin{bmatrix}0\\1\end{bmatrix}&+&\begin{bmatrix}7\\5\end{bmatrix}\\-\begin{bmatrix}0\\1\end{bmatrix}&+&\begin{bmatrix}15\\14\end{bmatrix}^T\end{bmatrix}=$

$\begin{bmatrix}-\begin{bmatrix}0\\1\end{bmatrix}&+&\begin{bmatrix}7\\5\end{bmatrix}\\-\begin{bmatrix}0\\1\end{bmatrix}&+&\begin{bmatrix}11\\12\end{bmatrix}\end{bmatrix}=\begin{bmatrix}7\\4\\11\\11\end{bmatrix}$

$\rightarrow$"HELL"=P_1

C_2:

S$\rightarrow$ 18-4=14$\rightarrow$O

$D_nC_2=D_n=\begin{bmatrix}\begin{bmatrix}14\\0\end{bmatrix}\\\begin{bmatrix}0\\26\end{bmatrix}\end{bmatrix}=$

$\begin{bmatrix}-\begin{bmatrix}0\\1\end{bmatrix}&+&\begin{bmatrix}14\\0\end{bmatrix}\\-\begin{bmatrix}0\\1\end{bmatrix}&+&\begin{bmatrix}0\\26\end{bmatrix}^T\end{bmatrix}=$

$\begin{bmatrix}-\begin{bmatrix}0\\1\end{bmatrix}&+&\begin{bmatrix}14\\0\end{bmatrix}\\-\begin{bmatrix}0\\1\end{bmatrix}&+&\begin{bmatrix}26\\0\end{bmatrix}\end{bmatrix}=\begin{bmatrix}14\\-1\\26\\-1\end{bmatrix}=\begin{bmatrix}14\\26\\26\\26\end{bmatrix}$

$\rightarrow$"O---"=P_2

Then   p="Hello---"

3.2 Example:

Encryption the text:

College of education university of al Qadisiya

Solution:

P=" College of education university of al Qadisiya"

C=" GPPOIHW SGAVHVYZXJMMDVNRZFJHMUC SGAZPAKZHJIRBBA"

Zainab .F

3.3 Example:

In example (3.1) and example (3.2) we take n=1, now we will change value of n and compare between them:

P="Hello"

n=1 → C=" LFPOSAA-"

n=100→C="

SFNOSEFGHIJKLMNOPQRSTUVWXYZ ABCDEFGHIJKLMNOPQRSTUVWXYZ ABCDEFGHIJKLMNOPQRSTUVWXYZ ABCDEFGHIJKLMNOPQRA ZYXWVUTSRQPONMLKJIHGFEDCBA ZYXWVUTSRQPONMLKJIHGFEDCBA ZYXWVUTSRQPONMLKJIHGFEDCBA ZYXWVUTSRQPONMLKJ"

n=10→C=" AFNOSEFGHIA ZYXWVUTS"

P=" College of education university of al Qadisiya"

n=1→C="GPPOIHW SGAVHVYZXJMMDVNRZFJHMUC SGAZPAKZHJIRBBA"

n=10→C="

WPNOILKGWOAVVDUVBLEETVPLZJXZ QBC   KSXVJUCRXJULBFFGHIA ZYXWVUTS"

n=100→C="

NPNOILKGWOJPPGQPIZFFTOIESCQSJVA DTLGIUJAMQWGYOSSTUVWXYZ ABCDEFGHIJKLMNOPQRSTUVWXYZ ABCDEFGHIJKLMNOPQRA ZYXWVUTSRQPONMLKJIHGFEDCBA ZYXWVUTSRQPONMLKJIHGFEDCBA ZYXWVUTSRQPONMLKJIHGFEDCBA ZYXWVUTSRQPONMLKJ"

We note that the complexity of cryptography increasing when the value n increasing.

3.4 Frequency analysis:

A	8.89%	P	6.67%	F	2.22%	W	2.22%
H	8.89%	J	6.67%	C	2.22%	X	2.22%
Z	8.89%	R	4.44%	K	2.22%		
V	6.67%	S	4.44%	U	2.22%		
G	6.67%	B	4.44%	D	2.22%		
M	6.67%	I	4.44%	Y	2.22%		
O	2.22%						
N	2.22%						

FREQUENCY ANALYSIS
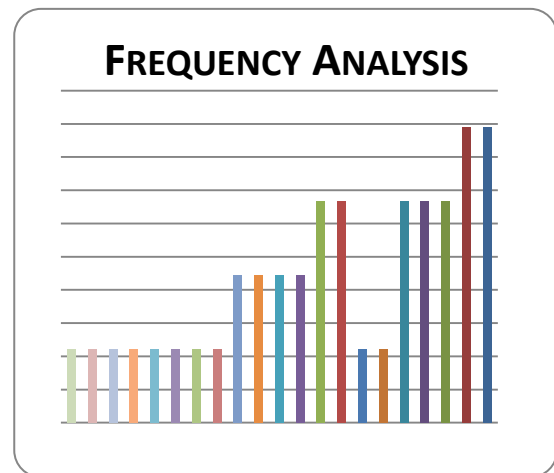
4. Conclusions:

1. The technique consists of an algebraic concept depends on recycling and displacement in forming the elements which led to the raising

Confidentiality and complexity level.

2. technical included some original ideas, whether in design or implementation making

Her privacy.

3. encryption keys used random and difficult to detect.

References

1- Alfred M. and paul v. ,A, Handbook of Applied Cryptography , CRC press ,2001.

2- Jonathan K. and Lindell Y., Introduction to modern Cryptography,CRC press, New york,2007 .

3- Neal K. ,A course in number theory and Cryptography , spinger , 1994 .

4-

5- Schneier B., Applied Cryptography ,John wiley and son press ,New York ,1996.

6- Thomas W.,Abstract algebra , Austin state university , 2010.

تقنية التشفير ثنائي السطوح

زينب فهد مهوس

جامعة القادسية ـ كلية التربية ـ قسم الرياضيات

zainab.alnaseri@qu.edu.iq

المستخلص :

يركز هذا البحث على تقنية جديدة في التشفير في الجبر المجرد. في البداية اعطينا عرض ضروري عن زمر السطوح الثنائية و التشفير. عرفنا ابجدية جديدة للرموز بأضافة "الفراغ" ، لذلك اصبح لدينا (٢٧) رمز (٢٦ رمز و الفراغ) ، لذلك استخدمنا معيار ٢٧ بدل ٢٦ حيث استخدمنا الانقلابات و التدوير الموجودة في زمرة السطوح الثنائية لتغيير ترتيب متجهات الرموز في لانص الصريح.

Application of Modified Adomian Decomposition Method to (2+1)-dimensional Non-linear Wu-Zhang system

Ahmed F. Qasim

College of Computer Sciences and Mathematics
University of Mosul
Republic of Iraq
E-mail: ahmednumerical@yahoo.com

Zead Y. Ali

College of physical education and sport scinces
University of Mosul
Republic of Iraq
E-mail: zyaa_77@yahoo.com

Abstract

In this paper, the Domain decomposition method (ADM) with modified polynomials is applied for nonlinear (2+1) – dimensional Wu-Zhang system . we compared the solution of the system with MVIM, HPM and RDTM [17,13,15]. The numerical results obtained by this polynomial are very effective, convenient and quite accurate to system of partial differential equations. A comparative between the modifications method and the other methods is present from some examples to show the efficiency of each method.

Keywords: Modified Adomian decomposition method, Wu- Zhang system.

Mathematics Subject Classification: **65M99,35G50 .**

1. Introduction

The nonlinear partial differential equations (NPDEs) are encountered in various disciplines, such as physics, mechanics, chemistry, biology, mathematics and engineering. Many efforts have been made on the study of NPDEs. Long wave in shallow water is a subject of broad interests and has along colorful history.

Wu and Zhang derived three sets of model equations for modeling nonlinear and dispersive long gravity waves travelling in two horizontal directions on shallow waters of uniform depth [16]. One of these equations, Wu-Zhang equation (which describes (2+1)-dimensional dispersive long wave), can be written as[16]

Ahmed .F/ Zead .Y

$$u_t + u\,u_x + v\,u_y + w_x = 0 \;,$$
$$v_t + u\,v_x + v\,v_y + w_y = 0 \;, (1)$$
$$w_t + (u\,w)_x + (v\,w)_y +$$
$$\tfrac{1}{3}(u_{xxx} + u_{xyy} + u_{xxy} + u_{yyy}) = 0 \;,$$

where w is the elevation of the water, u is the surface velocity of water along x-direction, and v is the surface velocity of water along y-direction. The explicit solutions of Eq. (1) are very helpful for costal and civil engineers to apply the nonlinear water wave model in harbor and coastal design. Recently introduced some new methods and are applied to nonlinear equations such as Variation Iteration Method [11], Homotopy Perturbation Method [10,13], the homogeneous balance method [9], the differential transform method (DTM) [5]. Among all of the methods, the reduced differential transform method (RDTM), employed for solving the nonlinear partial differential equations [12]. The RDTM is presented to overcome the demerit of complex calculation of DTM. This technique doesn't require any discretization, linearization or small perturbations and therefore it reduces significantly the numerical computation.

Ma Z.Y [13], used Homotopy perturbation method (HPM) for the Wu-Zhang equation in fluid dynamics. Extended tanh method and exp-function method and its application to (2+1)_dimensional dispersive long wave nonlinear equations [4]. Application to Reduced differential Transform method to the Wu-Zhang equation is presented in [15], and the solution of Wu-Zhang equations using the modified variational iteration method obtained by [17]. solitons and other solution Wu-Zhang system are discussed in [14].

At the beginning of the 1980, a so-called Adomian decomposition method (ADM) [1] has been used to solve effectively, easily, and accurately a large class of linear and nonlinear equations, solutions partial, deterministic or stochastic differential equations with approximates which converge rapidly.

Several studies have been proposed to modify the regular Adomian decomposition method for initial value problems in ordinary and partial differential equations [3,6]. Error analysis of Adomian series solution to a class of nonlinear differential equation is introduction in [7]. Alkresheh ,H. A. [2] , proposed two new adomian decomposition method, and [8] used the ADM to solve coupled system of nonlinear physical equations, coupled system of diffusion-reaction equation and integro-differential diffusion-reaction equation.

This paper is organized as follows. In section 2, the basic ideas of the modified Adomian decomposition method are described, in section 3, is devoted to solving a nonlinear (2+1)-dimensional Wu-Zhang system by MADM, the results and comparisons of

the numerical solutions are presented in section 4 and concluding remarks are given in section 5.

Ahmed .F/ Zead .Y

2. The modified Adomian decomposition method (MADM)

Let us consider the following equation

$$Lu + Nu + Ru = f(x) \quad (2)$$

where L is an invertible linear operator, N represents the nonlinear operator and R is the remaining linear part, from equation (2) we have

$$Lu = f(x) - Nu - Ru, \quad (3)$$

Now, applying the inverse operator L^{-1} to both sides of equation (3) then use the initial conditions we find

$$u = g(x) - L^{-1} Nu - L^{-1} Ru, (4)$$

where $L^{-1} = \int_0^x (.) \, ds$, and $g(x)$ represents the terms having from integrating the remaining term $f(x)$ and from using the given initial or boundary conditions. The ADM assumes that the nonlinear operator $N(u)$ can be decomposed by an infinite series of polynomials given by

$$N(u) = \sum_{n=0}^{\infty} A_n(u_o, u_1, \dots, u_n)$$

where A_n are the Adomian's polynomials [1] defined as:

$$A_n = \frac{1}{n!} \frac{d^n}{d\lambda^n} \left[N\left(\sum_{i=0}^{\infty} \lambda^i u_i \right) \right]_{\lambda=0}$$
$$, \quad n = 0,1,2, \dots \quad (5)$$

El-Kalla [7] introduce a new formula for Adomian polynomials, he claimed that the Adomian solution using this new formula converges faster than using Adomian polynomials (5). Kalla polynomial given in the following form:

$$A_n = N(S_n) - \sum_{i=0}^{n-1} A_i(u_o, u_1, \dots, u_{n-1}) \quad (6)$$

Where $S_n = u_o + u_1 + \cdots + u_n$ and A_n can be given as :

$$A_0 = N(u_o)$$
$$A_1 = \frac{d}{dx}(N(u_o))u_1 +$$
$$\frac{1}{2}\frac{d^2}{dx^2}(N(u_o))u_1^2 +$$
$$\frac{1}{6}\frac{d^3}{dx^3}(N(u_o))u_1^3 +$$
$$\frac{1}{24}\frac{d^4}{dx^4}(N(u_o))u_1^4 + \cdots$$
$$A_2 = \frac{d}{dx}(N(u_o))u_2 +$$
$$\frac{1}{2}\frac{d^2}{dx^2}(N(u_o))[2u_1 u_2 + u_2^2] +$$
$$\frac{1}{6}\frac{d^3}{dx^3}(N(u_o)) [3u_1^2 u_2 +$$
$$3u_1 u_2^2 + u_2^3] + \cdots$$
$$\vdots$$

And so on. These formulas are easy to compute by using Maple 13 software.

3. Application MADM to the Wu-Zhang system

This section is devoted to study the analytical solution of the Wu-Zhang system (1) using MADM, we make a comparison for the corresponding absolution error between the using of the proposed polynomial in MADM and the methods in [13,15,17].

let us consider the standard form of equation (1) in an operator form:

$$L_t u + u L_x u + v L_y u + L_x w = 0 ,$$
$$L_t v + u L_x v + v L_y v + L_y w = 0 ,(7)$$
$$L_t w + u L_x u + w L_x u + v L_y w +$$
$$w L_y v + \frac{1}{3}\left(L_{xxx} u + L_{xyy} u + L_{xxy} v + L_{yyy} v \right) = 0 ,$$

$$u(x,y,o) = g_1(x,y), \; v(x,y,o) = g_2(x,y), \; w(x,y,o) = g_3(x,y),$$

Where the notations $L_t = \frac{\partial}{\partial t}, L_x = \frac{\partial}{\partial x}, L_y = \frac{\partial}{\partial y}, L_{xxx} = \frac{\partial^3}{\partial x^3}, L_{xyy} = \frac{\partial^3}{\partial x \partial y^2}, \; L_{xxy} = \frac{\partial^3}{\partial x^2 \partial y}, and \; L_{yyy} = \frac{\partial^3}{\partial y^3},$ Symbolize the linear differential operator.

Ahmed .F/ Zead .Y

Assuming l_t^{-1} the inverse of the operator l_t exists and can conveniently by taken as definite integrate with respect to (t):

Define $l_t^{-1} = \int_0^t (.) dt$ than the system (7) becomes :

$$u(x,y,t) = g_1(x,y) - l_t^{-1}(\vartheta_1(u) + \vartheta_2(u,v) + l_x w),$$

$$v(x,y,t) = g_2(x,y) - l_t^{-1}(\vartheta_3(u,v) + \vartheta_4(v) + l_y w),$$

$$w(x,y,t) = g_3(x,y) - l_t^{-1}\left(\vartheta_5(u,w) + \vartheta_6(u,w) + \vartheta_7(v,w) + \vartheta_8(v,w) + \frac{1}{3}(L_{xxx} u + L_{xyy} u + L_{xxy} v + L_{yyy} v)\right),$$

Where
$\vartheta_1(u) = u\,u_x$, $\vartheta_2(u,v) = v\,u_y$, $\vartheta_3(u,v) = uv_x$
$\vartheta_4(v) = v\,v_x$, $\vartheta_5(u,w) = u\,w_x$, $\vartheta_6(u,w) = w\,u_x$
$\vartheta_7(v,w) = v\,w_y$, $\vartheta_8(u,w) = w\,v_y$

The MADM assumes an infinite series for the unknown functions $u(x,y,t), v(x,y,t)$ and $w(x,y,t)$ in the $form$
$$u(x,y,t) = \sum_{n=0}^{\infty} u_n(x,y,t)$$
$$v(x,y,t) = \sum_{n=0}^{\infty} v_n(x,y,t)$$
$$w(x,y,t) = \sum_{n=0}^{\infty} w_n(x,y,t)$$

We can write $\vartheta_1, \vartheta_2 \dots\dots\dots, \vartheta_8$ by an infinite series of Adomian polynomial in the form
$\vartheta_1(u) = \sum_{n=0}^{\infty} A_n$, $\vartheta_2(u,v) = \sum_{n=0}^{\infty} B_n$, $\vartheta_3(u,v) = \sum_{n=0}^{\infty} C_n$
$\vartheta_4(v) = \sum_{n=0}^{\infty} D_n$, $\vartheta_5(u,w) = \sum_{n=0}^{\infty} E_n$, $\vartheta_6(u,w) = \sum_{n=0}^{\infty} F_n$
$\vartheta_7(v,w) = \sum_{n=0}^{\infty} G_n$, $\vartheta_8(v,w) = \sum_{n=0}^{\infty} H_n$

Where $A_n, B_n, C_n, D_n \dots\dots, H_n$ are the appropriate modified Adomian polynomials

$$A_n(u_0, u_1, \dots\dots\dots u_n) = \frac{1}{n!}\frac{d^n}{d\rho^n}[\varphi_1(\sum_{k=0}^{\infty} \rho^k u_k)]_{\rho=0} , n \geq 0$$

$$B_n(u_0, u_1, \dots, u_n, v_0, v_1, \dots, v_n) = \frac{1}{n!}\frac{d^n}{d\rho^n}\left[\varphi_2\left(\sum_{k=0}^{\infty} \rho^k u_k, \sum_{k=0}^{\infty} \rho^k v_k\right)\right]_{\rho=0} , n \geq 0$$

$\vdots$ (8)

$$H_n(v_0, v_1, \dots, v_n, w_0, w_1, \dots, w_n) = \frac{1}{n!}\frac{d^n}{d\rho^n}[\varphi_8(\sum_{k=0}^{\infty} \rho^k v_k, \sum_{k=0}^{\infty} \rho^k w_k)]_{\rho=0} ,$$
$n \geq 0$

For examples, the first polynomials using formulas (8) are computed be:
$$A_o = u_o \frac{\partial u_o}{\partial x}$$
$$A_1 = u_o \frac{\partial u_1}{\partial x} + u_1 \frac{\partial u_o}{\partial x} + u_1 \frac{\partial u_1}{\partial x}$$
$$A_2 = u_o \frac{\partial u_2}{\partial x} + u_2 \frac{\partial u_o}{\partial x} + u_2 \frac{\partial u_1}{\partial x} + u_1 \frac{\partial u_2}{\partial x} + u_2 \frac{\partial u_2}{\partial x}$$
$$A_3 = u_3 \frac{\partial u_o}{\partial x} + u_o \frac{\partial u_3}{\partial x} + u_3 \frac{\partial u_1}{\partial x} + u_1 \frac{\partial u_3}{\partial x} + \cdots$$
$$A_4 = u_4 \frac{\partial u_o}{\partial x} + u_o \frac{\partial u_4}{\partial x} + \cdots$$
$\vdots$

$$B_o = v_o \frac{\partial u_o}{\partial y}$$
$$B_1 = v_o \frac{\partial u_1}{\partial y} + v_1 \frac{\partial u_o}{\partial y} + v_1 \frac{\partial u_1}{\partial y}$$
$$B_2 = v_o \frac{\partial u_2}{\partial y} + v_2 \frac{\partial u_o}{\partial y} + v_2 \frac{\partial u_1}{\partial y} + v_1 \frac{\partial u_2}{\partial y} + v_2 \frac{\partial u_2}{\partial y}$$
$$B_3 = v_3 \frac{\partial u_o}{\partial y} + v_o \frac{\partial u_3}{\partial y} + v_3 \frac{\partial u_1}{\partial y} + v_1 \frac{\partial u_3}{\partial y} + \cdots$$
$\vdots$

$$C_o = u_o \frac{\partial v_o}{\partial x}$$
$$C_1 = u_o \frac{\partial v_1}{\partial x} + u_1 \frac{\partial v_o}{\partial x} + u_1 \frac{\partial v_1}{\partial x}$$
$$C_2 = u_o \frac{\partial v_2}{\partial x} + u_2 \frac{\partial v_o}{\partial x} + u_2 \frac{\partial v_1}{\partial x} + u_1 \frac{\partial v_2}{\partial x} + u_2 \frac{\partial v_2}{\partial x}$$
$$C_3 = u_3 \frac{\partial v_o}{\partial x} + u_o \frac{\partial v_3}{\partial x} + u_3 \frac{\partial v_1}{\partial x} + u_1 \frac{\partial v_3}{\partial x} + \cdots$$

Ahmed .F/ Zead .Y

$\vdots$

$$D_o = v_o\ \frac{\partial v_o}{\partial y}$$

$$D_1 = v_o\ \frac{\partial v_1}{\partial y} +\ v_1 \frac{\partial v_o}{\partial y} + v_1 \frac{\partial v_1}{\partial y}$$

$$D_2 = v_o\ \frac{\partial v_2}{\partial y} +\ v_2 \frac{\partial v_o}{\partial y} + v_2 \frac{\partial v_1}{\partial y} +$$
$$v_1 \frac{\partial v_2}{\partial y} + v_2 \frac{\partial v_2}{\partial y}$$

$$D_3 = v_3\ \frac{\partial v_o}{\partial y} +\ v_o \frac{\partial v_3}{\partial y} + v_3 \frac{\partial v_1}{\partial y} +$$
$$v_1 \frac{\partial v_3}{\partial y} + \cdots$$

$\vdots$

$$E_o = u_o\ \frac{\partial w_o}{\partial x}$$

$$E_1 = u_o\ \frac{\partial w_1}{\partial x} +\ u_1 \frac{\partial w_o}{\partial x} + u_1 \frac{\partial w_1}{\partial x}$$

$$E_2 = u_o\ \frac{\partial w_2}{\partial x} +\ u_2 \frac{\partial w_o}{\partial x} + u_2 \frac{\partial w_1}{\partial x} +$$
$$u_1 \frac{\partial w_2}{\partial x} + u_2 \frac{\partial w_2}{\partial x}$$

$$E_3 = u_3\ \frac{\partial w_o}{\partial x} +\ u_o \frac{\partial w_3}{\partial x} + u_3 \frac{\partial w_1}{\partial x} +$$
$$u_1 \frac{\partial w_3}{\partial x} + \cdots$$

$\vdots$

$$F_o = w_o\ \frac{\partial u_o}{\partial x}$$

$$F_1 = w_o\ \frac{\partial u_1}{\partial x} +\ w_1 \frac{\partial u_o}{\partial x} + w_1 \frac{\partial u_1}{\partial x}$$

$$F_2 = w_o\ \frac{\partial u_2}{\partial x} +\ w_2 \frac{\partial u_o}{\partial x} + w_2 \frac{\partial u_1}{\partial x} +$$
$$w_1 \frac{\partial u_2}{\partial x} + w_2 \frac{\partial u_2}{\partial x}$$

$$F_3 = w_3\ \frac{\partial u_o}{\partial x} +\ w_o \frac{\partial u_3}{\partial x} + w_3 \frac{\partial u_1}{\partial x} +$$
$$w_1 \frac{\partial u_3}{\partial x} + \cdots$$

$\vdots$

$$G_o = v_o\ \frac{\partial w_o}{\partial y}$$

$$G_1 = v_o\ \frac{\partial w_1}{\partial y} +\ v_1 \frac{\partial w_o}{\partial y} + v_1 \frac{\partial w_1}{\partial y}$$

$$G_2 = v_o\ \frac{\partial w_2}{\partial y} +\ v_2 \frac{\partial w_o}{\partial y} + v_2 \frac{\partial w_1}{\partial y} +$$
$$v_1 \frac{\partial w_2}{\partial y} + v_2 \frac{\partial w_2}{\partial y}$$

$$G_3 = v_3\ \frac{\partial w_o}{\partial y} +\ v_o \frac{\partial w_3}{\partial y} + v_3 \frac{\partial w_1}{\partial y} +$$
$$v_1 \frac{\partial w_3}{\partial y} + \cdots$$

$\vdots$

$$H_o = w_o\ \frac{\partial v_o}{\partial y}$$

$$H_1 = w_o\ \frac{\partial v_1}{\partial y} +\ w_1 \frac{\partial v_o}{\partial y} + w_1 \frac{\partial v_1}{\partial y}$$

$$H_2 = w_o\ \frac{\partial v_2}{\partial y} +\ w_2 \frac{\partial v_o}{\partial y} + w_2 \frac{\partial v_1}{\partial y} +$$
$$w_1 \frac{\partial v_2}{\partial y} + w_2 \frac{\partial v_2}{\partial y}$$

$$H_3 = w_3\ \frac{\partial v_o}{\partial y} +\ w_o \frac{\partial v_3}{\partial y} + w_3 \frac{\partial v_1}{\partial y} +$$
$$w_1 \frac{\partial v_3}{\partial y} + \cdots$$

$\vdots$

And so on, the nonlinear system (7) is constructed as:

$$u_0(x,y,t) = g_1(x,y),\ v_0(x,y,t) = g_2(x,y), w_0(x,y,t) = g_3(x,y),$$

$$u_{n+1}(x,y,t) = l_t^{-1}\left[l_x\ w + A_n\ + B_n\ \right];$$
$$n \geq 1,$$
$$v_{n+1}(x,y,t) = l_t^{-1}\left[l_y\ w + C_n\ + D_n\ \right];$$
$$n \geq 1, (9)$$

$$w_{n+1}(x,y,t) = l_t^{-1}\left[\frac{1}{3}\left(L_{xxx}\ u \right.\right.$$
$$+ L_{xyy}\ u + L_{xxy}\ v$$
$$\left. + L_{yyy}\ v\right) + E_n\ + F_n$$
$$\left. + G_n\ + H_n\ \right];$$
$$n \geq 1,$$

Where   The   functions $g_1(x,y), g_2(x,y), and\ g_3(x,y)$,Are initial conditions. We construct the solution $u(x,y,t)$, $v(x,y,t)$ And $w(x,y,t)$ as follow:

$\lim_{n \to \infty} \varphi_n = u(x,y,t),$
$\lim_{n \to \infty} \widetilde{\varphi_n} = v(x,y,t)$ and
$\lim_{n \to \infty} \widehat{\varphi_n} = w(x,y,t)$
$\varphi_n(x,y,t) = \sum_{k=0}^{\infty} u_k(x,y,t),$
$\widetilde{\varphi_n}(x,y,t) = \sum_{k=0}^{\infty} v_k(x,y,t),$
$\widehat{\varphi_n}(x,y,t) = \sum_{k=0}^{\infty} w_k(x,y,t)$

And the recurrence relation is given as in (9).

Ahmed .F/ Zead .Y

4. Applications

We consider the Solutions of the system (9) with the initial and conditions [13,15,17].

$$u_o(x,y,t) = -\frac{K_3 + K_2 bb_0}{K_1} + \frac{2}{3}\sqrt{3}k_1 \tanh(k_1 x + k_2 y),$$

$$v_o(x,y,t) = bb_0 + \frac{2}{3}\sqrt{3}k_2 \tanh(k_1 x + k_2 y),$$

(10)

$$w_o(x,y,t) = \frac{2}{3}(k_1^2 + k_2^2)\,sech(k_1 x + k_2 y)^2$$

Where

b_0, k_1, k_2 and k_3 are arbitrary constants . To calculate the terms of the MADN for $u(x,y,t), v(x,y,t)$ and $w(x,y,t)$, we substitute the initial conditions (10) into the system (9) and using Maple 13 language , the solutions of the system (9) can be obtained as follows:

$$u_1(x,y,t) = \frac{2}{3}\frac{K_1 t\sqrt{3}K_3}{\cosh(K_1 x + K_2 y)^2}$$

$$v_1(x,y,t) = \frac{2}{3}\frac{K_2 t\sqrt{3}K_3}{\cosh(K_1 x + K_2 y)^2}$$

$$w_1(x,y,t) = -\frac{4}{3}\frac{t\sinh(K_1 x + K_2 y)K_3(K_1^2 x + K_2^2 y)}{\cosh(K_1 x + K_2 y)^3}$$

$$u_2(x,y,t) = -\frac{2}{9}\frac{1}{\cosh(K_1 x + K_2 y)^5}(k_1 k_3^2 t^2 \sinh(k_1 x + k_2 y)^{-4K_1^2 t - 4tK_2^2 + 3}\sqrt{3}\cosh(k_1 x + k_2 y)^2))$$

$$v_2(x,y,t) = -\frac{2}{9}\frac{1}{\cosh(K_1 x + K_2 y)^5}(k_1 k_3^2 t^2 \sinh(k_1 x + k_2 y)^{-4K_1^2 t - 4tK_2^2 + 3}\sqrt{3}\cosh(k_1 x + k_2 y)^2))$$

$$w_2(x,y,t) = -\frac{2}{27}\frac{1}{\cosh(K_1 x + K_2 y)^5}(K_3^2 t^2$$

$$(-20k_1^4 t\sqrt{3} - 40k_2^2 k_1^2 t\sqrt{3} - 20k_2^4 t\sqrt{3} + 27k_1^2 \cosh(k_1 x + k_2 y)^2 + 27k_2^2 \cosh(k_1 x + k_2 y)^2 - 18 k_1^2 \cosh(k_1 x + k_2 y)^4 - 18 k_2^2 \cosh(k_1 x + k_2 y)^4 + 16\sqrt{3}\, t\, k_1^4 \cosh(k_1 x + k_2 y)^2 + 16\sqrt{3}\, t\, k_2^4 \cosh(k_1 x + k_2 y)^2 + 32\sqrt{3}\, t\, k_1^2 k_1^2 \cosh(k_1 x + k_2 y)^2))$$

$$u(x,y,t) = u_o(x,y,t) + u_1(x,y,t) + u_2(x,y,t) + \cdots$$
$$= \frac{-1}{2835}\frac{1}{k_1 \cosh(k_1 x + k_2 y)^{11}}(2835 \cosh(k_1 x + k_2 y)^{11} k_2 bb_0 \ldots \ldots$$

$$v(x,y,t) = v_o(x,y,t) + v_1(x,y,t) + v_2(x,y,t) + \cdots$$
$$= \frac{1}{2835}\frac{1}{\cosh(k_1 x + k_2 y)^{11}}(2835\, bb_0 \cosh(k_1 x + k_2 y)^{11} - 1890 \ldots$$

$$w(x,y,t) = w_o(x,y,t) + w_1(x,y,t) + w_2(x,y,t) + \cdots$$
$$= \frac{2}{8505}\frac{1}{\cosh(k_1 x + k_2 y)^{12}}(55040 k_3^4 t^7 \sqrt{3}k_2^2 k_1^6 \cosh(k_1 x + k_2 y)^2 - 20480 \ldots$$

The approximate solutions of the system (1) are obtained as follows

$$u(x,y,t) = u_0(x,y,t) + u_1(x,y,t) + u_2(x,y,t) + \cdots$$
$$v(x,y,t) = v_0(x,y,t) + v_1(x,y,t) + v_2(x,y,t) + \cdots$$
$$w(x,y,t) = w_0(x,y,t) + w_1(x,y,t) + w_2(x,y,t) + \cdots$$

This solution is convergent to the exact solution [13]

$$u(x,y,t) = -\frac{K_3 + K_2 b_0}{K_1} + \frac{2\sqrt{3}}{3}k_1 \tanh(k_1 x + k_2 y + k_3 t),$$

Ahmed .F/ Zead .Y

$v(x,y,t) = b_0 + \frac{2\sqrt{3}}{3}k_2 \tanh(k_1 x + k_2 y + k_3 t),$

$w(x,y,t) = \frac{2}{3}(k_1^2 + k_2^2) sech^2(k_1 x + k_2 y + k_3 t),$

We comparisons   the absolute errors and mean square error for the MADN results for

$u(x,y,t), v(x,y,t)$ and $w(x,y,t)$,for the first three approximations with HPM [13] ,RDTM [15], and MVIM [17], when

$b_0 = k_1 = 0.1, k_2 = k_3 = 0.01 ,$
$t = 5, y = 20$

$for\ the\ solution\ of\ the\ Wu\ Zhang\ system\ (1)$
$with\ the\ initial\ conditions\ (10).$

Table 1: Comparison of absolute errors using u_3 for various values of x in Wu-Zhang system between MADM and MVIM [17] when

$b_0 = k_1 = 0.1 , k_2 = k_3 = 0.01 , t = 5 , and\ y = 20$

x	u_{exact}	u_{MADM}	$\|u_{exact} - u_{MVIM}\|$	$\|u_{exact} - u_{MADM}\|$
-50	0.225452768	0.225452769	1.6451825 E-6	10.39242830 E-10
-40	0.225342395	0.225342395	1.2148126 E-5	4.330797530 E-10
-30	0.224530095	0.224530099	8.9315718 E-5	3.594419403 E-9
-20	0.218700684	0.218700708	6.3605735 E-4	2.448538578 E-8
-10	0.183340683	0.183340786	3.6024380 E-3	1.023749896 E-7
0	0.0817192288	0.0817189240	6.4447985 E-3	3.048061683 E-7
10	0.0120486423	0.120487416	1.9107842 E-4	8.922341521 E-3
20	0.002932728	0.002932733	2.9196656 E-4	5.192973059 E-9
30	0.005123370	0.005123372	4.0172038 E-5	1.372972068 E-9
40	0.005423074	0.005423074	5.44887493 E-6	2.078596792 E-10
50	0.005463694	0.005463694	7.37648418 E-7	5.196177359 E-11
MSE			5.00446211 E-6	1.018121171 E-14

Ahmed .F/ Zead .Y

Table 2: Comparison of absolute errors using v_3 for various values of x in Wu-Zhang system

between MADM and MVIM [17] when

$b_0 = k_1 = 0.1$, $k_2 = k_3 = 0.01$, $t = 5$, and $y = 20$

x	v_{exact}	v_{MADM}	$\|v_{exact} - v_{MVIM}\|$	$\|v_{exact} - v_{MADM}\|$
-50	0.0884547231	0.884547231	8.08571164 E-9	1.039242830 E-11
-40	0.0884657604	0.0884657604	5.96388798 E-8	6.330797530 E-11
-30	0.0885469904	0.0885469900	4.34887678 E-7	3.394419403 E-10
-20	0.0891299315	0.0891299291	2.91626141 E-6	2.438538578 E-9
-10	0.0926659316	0.0926659213	1.07971370 E-5	1.027749896 E-8
0	0.102828077	0.102828107	5.875I9681 E-6	3.050061683 E-8
10	0.109795135	0.109795126	7.18185473 E-6	8.962341521 E-9
20	0.111293272	0.111293273	1.30807366 E-6	5.392973059 E-10
30	0.111512337	0.111512337	1.84431598 E-7	1.072972068 E-10
40	0.111542307	0.111542307	2.50992772 E-8	2.078596792 E-11
50	0.111546369	0.111546369	3.39937593 E-9	5.196177359 E-12
MSE			1.93743805 E-11	1.018378476 E-16

Table 3: Comparison of absolute errors using w_3 for various values of x in Wu-Zhang system

between MADM and MVIM [17] when

$b_0 = k_1 = 0.1$, $k_2 = k_3 = 0.01$, $t = 5$, and $y = 20$

x	w_{exact}	w_{MADM}	$\|w_{exact} - w_{MVIM}\|$	$\|w_{exact} - w_{MADM}\|$
-50	2.01570751 E-6	2.01569976 E-6	3.705249242 E-7	7.749880486 E-12
-40	1.448799414 E-5	1.48798843 E-5	2.73I8146111 E-6	5.708491389 E-11
-30	1.09176198 E-4	1.09175786 E-4	1.986047907 E-5	4.118114838 E-10
-20	7.66334776 E-4	7.66332142 E-4	1.302774181 E-4	2.634558628 E-9
-10	4.01701111 E-3	4.01701120 E-3	4.145730832 E-4	8.8787905 E-11
0	6.32943331 E-3	6.32939492 E-3	1.153652836 E-4	3.839847338 E-8
10	1.88812677 E-3	1.88814161 E-3	2.265746793 E-5	1.484359887 E-8
20	2.92663787 E-4	2.92663846 E-4	6.972254850 E-7	5.892963187 E-11
30	4.03711466 E-5	4.03709936 E-5	1.991078199 E-7	1.529342660 E-10
40	5.47785204 E-6	5.47782786 E-6	2.877 10754 E-8	2.418224902 E-11
50	7.41607526 E-7	7.41604188 E-7	3.9511 0044 E-9	3.337771675 E-12
MSE			1.84607383 E-8	1.547236655 E-16

Ahmed .F/ Zead .Y

The absolute error for u(x,y,t)	The numerical solution for u(x,y,t)
The absolute error for v(x,y,t)	The numerical solution for v(x,y,t)
The absolute error for w(x,y,t)	The numerical solution for w(x,y,t)

Figure 1: The absolute error for the first three approximation between MADM and the exact

solution, for various values of x and y when

$$b_0 = 0.1 , k_1 = 0.1, k_2 = 0.01 , k_3 = 0.01 , and t = 5.$$

Ahmed .F/ Zead .Y

Table 4: Comparison of absolute errors and mean square error using u_3 for Wu-Zhang system between MADM with HPM [13] and RDTM [15], for various values of x and y when $b_0 = 0.1$, $k_1 = 0.05$, $k_2 = 0.1$, $k_3 = 0.3$, $and \ t = 2.5$

(x,y)	u_{exact}	u_{MADM}	$\|u_{exact} - u_{HPM}\|$ $\|u_{exact} - u_{MVIM}\|$	$\|u_{exact} - u_{MADM}\|$
(0.001,-40)	6.25756167 E-0	6.25757298 E-0	1.13049917 E-5	1.13094127 E-5
(0.002,-30)	6.25646611 E-0	6.25654557 E-0	7.92908229 E-5	7.94573088 E-5
(0.003,-20)	6.24897325 E-0	6.24936663 E-0	3.85696522 E-4	3.93378218 E-4
(0.004,-10)	6.21412953 E-0	6.21299676 E-0	1.26708625 E-3	1.13277326 E-3
(0.005,0)	6.16332105 E-0	6.16444944 E-0	1.49035435 E-3	1.12839583 E-3
(0.006,10)	6.14564769 E-0	6.14581428 E-0	5.73725768 E-5	1.66595217 E-4
(0.007,20)	6.14273462 E-0	6.14247428 E-0	2.65974103 E-4	2.60340360 E-4
(0.008,30)	6.14232875 E-0	6.14228437 E-0	4.45040837 E-5	4.43855200 E-5
(0.009,40)	6.14227361 E-0	6.14226742 E-0	6.19002050 E-6	6.18845786 E-6
(0.01,50)	6.14226614 E-0	6.14226530 E-0	8.41789424 E-7	8.41763456 E-7
MSE			4.057899493 E-7	2.815176595 E-7

Table 5: Comparison of absolute errors and mean square error using v_3 for Wu-Zhang system between MADM with HPM [13] and RDTM [15], for various values of x and y when $b_0 = 0.1$, $k_1 = 0.05$, $k_2 = 0.1$, $k_3 = 0.3$, $and \ t = 2.5$

(x,y)	v_{exact}	v_{MADM}	$\|v_{exact} - v_{HPM}\|$ $\|v_{exact} - v_{MVIM}\|$	$\|v_{exact} - v_{MADM}\|$
(0.001,-40)	1.51233361 E-2	1.51459522 E-2	2.26099488 E-5	2.2616027 E-5
(0.002,-30)	1.29322262 E-2	1.30911405 E-2	1.58587648 E-4	1.58914298 E-4
(0.003,-20)	2.05349994 E-3	1.26674403 E-3	7.71401056 E-4	7.86755912 E-4
(0.004,-10)	7.17409386 E-2	7.40064832 E-2	2.53417253 E-3	2.26554453 E-3
(0.005,0)	1.73357903 E-1	1.71101111 E-1	2.98071071 E-3	2.25679205 E-3
(0.006,10)	2.08704626 E-1	2.08371441 E-1	1.14747188 E-4	3.33185019 E-4
(0.007,20)	2.14530751 E-1	2.15051429 E-1	5.31948231 E-4	5.20677749 E-4
(0.008,30)	2.15342497 E-1	2.15431265 E-1	8.90041228 E-5	8.87677480 E-5
(0.009,40)	2.15452784 E-1	2.15465160 E-1	1.23800410 E-5	1.23756930 E-5
(0.01,50)	2.15467717 E-1	2.15469398 E-1	1.68148224 E-6	1.68139959 E-6
MSE			1.62316013 E-6	1.12607062 E-6

Ahmed .F/ Zead .Y

Table 6: Comparison of absolute errors and mean square error using v_3 for Wu-Zhang system between MADM with HPM [13] and RDTM [15], for various values of x and y when $b_0 = 0.1$, $k_1 = 0.05$, $k_2 = 0.1$, $k_3 = 0.3$, $and \ t = 2.5$

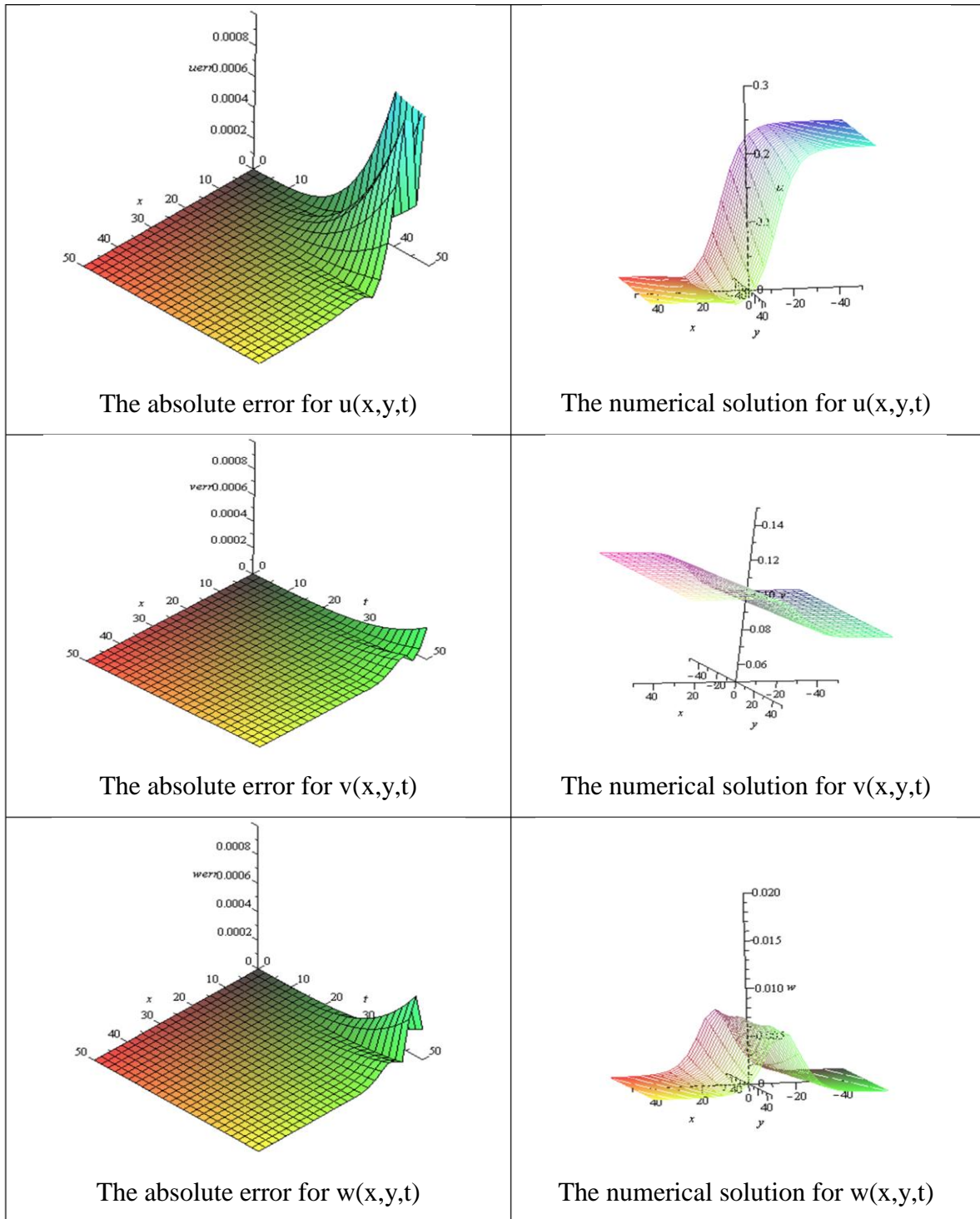| (x,y)	w_{exact}	w_{MADM}	$\|w_{exact} - w_{HPM}\|$ $\|w_{exact} - w_{MVIM}\|$	$\|w_{exact} - w_{MADM}\|$
(0.001,-40)	4.99692720 E-5	4.67304813 E-5	3.23703114 E-6	3.23879066 E-6
(0.002,-30)	3.62278514 E-4	3.40688032 E-4	2.14972816 E-5	2.15904817 E-5
(0.003,-20)	2.33738529 E-3	2.28043656 E-3	5.29010050 E-5	5.69487325 E-5
(0.004,-10)	7.83422424 E-3	8.54191973 E-3	7.31802585 E-4	7.07695496 E-4
(0.005,0)	4.96996963 E-3	3.63168325 E-3	1.32491691 E-3	1.33828638 E-3
(0.006,10)	9.47898572 E-4	1.37068310 E-3	3.99459208 E-4	4.22784533 E-4
(0.007,20)	1.35025275 E-4	8.08732586 E-5	5.71504440 E-5	5.41520164 E-5
(0.008,30)	1.84010586 E-5	6.03244902 E-6	1.24360974 E-5	1.23686096 E-5
(0.009,40)	2.49244365 E-6	7.14467502 E-7	1.77924640 E-6	1.77797617 E-6
(0.01,50)	3.37325458 E-7	9.47861898 E-8	2.42562615 E-7	2.42539268 E-7
MSE			2.457202663 E-7	2.477398551 E-7
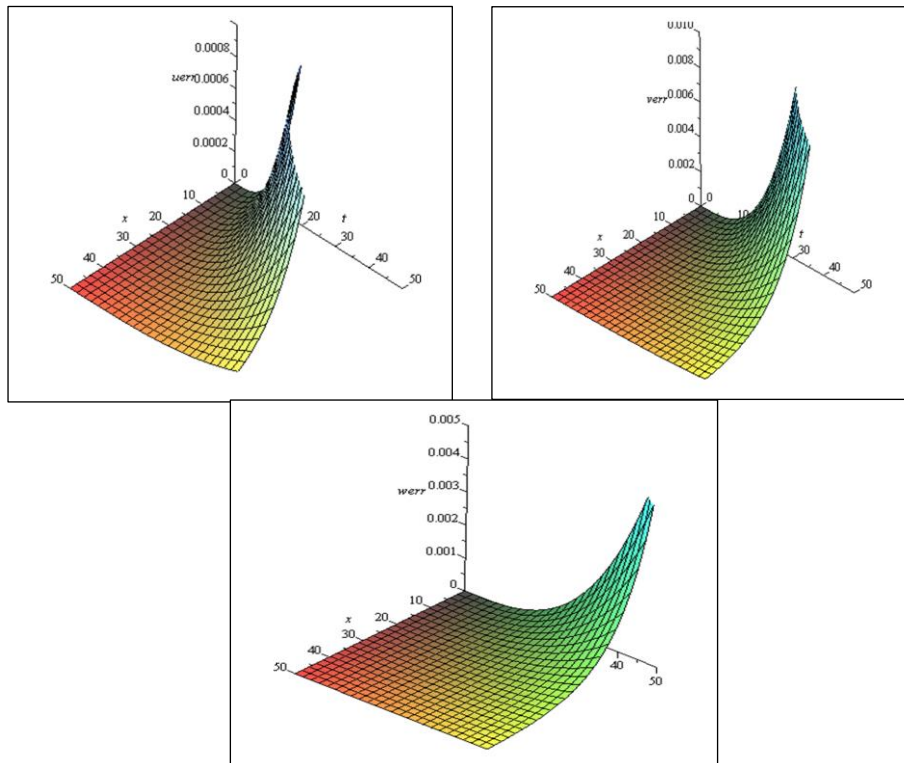
Figure 2: The absolute error for the first three approximation between MADM and the exact solution, for various values of x and t when
$$b_0 = 0.1 , k_1 = 0.05, \qquad k_2 = 0.1 , k_3 = 0.3 , \qquad and \ y = 50$$

Ahmed .F/ Zead .Y

5. conclusions

The powerful modified adomian decomposition method was employed for analytic treatment of the nonlinear (2+1)- dimensional Wu-Zhang system , the MADN can be used directly and in a straight forward manner with rapid convergence successive approximations without any restrictive assumptions that may change in the physical behavior of the problem. Comparison at the MADM with several other methods that have been advanced for solving this system, shows that the new technique is reliable , powerful ,and promising as shown in the tables (1)-(6). The MADM provides analytic, verifiable, rapidly convergent approximation that yields insight into the character and the behavior of the solution just as in the closed form solution as shown in the figures (1) and (2). All the computations were carried out with the aid of maple 13 software.

REFERENCES

[1]   Adomian, G., (1986), "Non-linear Stochastic Operator Equations", Academic Press, San Diego, CA.

[2]   Al-kresheh , H. A., (2016) "New classes of Adomian polynomials for the Adomian decomposition method ", International Journal of Engineering Science Invention, Volume 5, Issue 3, PP. 37-44.

[3]   Al-mazmumy , M., Hendi , F. A., Bakodah , H. O., Alzumi, H. , (2012), "Recent Modifications of Adomian Decomposition Method for Initial Value Problem in Ordinary Differential Equations", *American Journal of Computational Mathematics*, 2, pp. 228-234.

[4]   Asgari, A., Ganji, D. D., and Davodi, A. G., (2010), "Extended Tanh method and Exp-Function method and its application to (2+1)-dimensional dispersive long wave nonlinear equations", journal of the applied mathematics, statistics and informatics (JAMSI), 6, No. 1.

[5]   Ayaz, F., (2003), "On the two-dimensional differential transform method", Applied Mathematics and Computation, 143:, Pp. 361-374.

[6]   Bakodah, H. O., (2012), "Some Modifications of Adomian Decomposition Method Applied to Nonlinear System of Fredholm Integral Equations of the Second Kind ", Int. J. Contemp. Math. Sciences, Vol. 7, No. 19, 929 – 942.

[7]   El-Kalla, I. L., (2007), "Error Analysis of Adomian Series Solution to A Class of Nonlinear Differential Equations", Applied Mathematics E-Notes, 7, pp. 214-221.

[8]   El-Wakil, S. A., and Abdou, M. A., (1998), "New applications of Adomian decomposition method", Chaos Solitons Fractals 33(2), pp. 513-522, 2007.

[9]   Fan, E., H. Zhang, (1998), "A note on the homogeneous balance method", Phys. Letters, A246:, Pp. 403-406.

[10]   Ganji, D.D., (2006), "The application of He's homotopy perturbation method to nonlinear equations arising in heat transfer", Physics Letters A, A355:, Pp. 337-341.

[11]   He, J. H., (2000), "A coupling method of a homotopy technique and a perturbation technique for non-linear problems", International Journal of Non-Linear Mechanics, 35:, Pp. 37-43.

[12]   Keskin, Y., G. Oturanc, (2010), "Numerical solution of Regularized Long Wave equation by reduced differential transform method", Applied Mathematical Sciences, 4:, Pp. 1221- 1231.

[13]   Ma, Z. Y., (2008), "Homotopy Perturbation method for the Wu-Zhang equation in fluid dynamics", Journal of physics; conference series 96, 012182.

[14]   Mirzazadeh, M., and al., (2017), "Solitons and other solutions to Wu-Zhang system", Nonlinear analysis: modeling and control, Vol. 22, No. 4, Pp. 441-458.

[15]   Taghizadeh, N., Akbari, M. and Shahidi, M., (2011), "Application of Reduced Differential Transform method to the Wu-Zhang equation", Australian journal of basic and applied sciences, 5 (5); Pp. 565-571.

[16]   Wu, T.Y., J.E. Zhang, (1996), "On modeling nonlinear long wave", in: L.P. Cook, V. Roytbhurd, M. Tulin (Eds.), Mathematics is for Solving Problems, SIAM, pp: 233.

[17]   Zayed, E. M. E. and Abdel Rahman, H. M., (2009), " On solving the Kdv-Burger's equation and the Wu-Zhang equations using the modified variational iteration method", International Journal of Nonlinear Sciences and Numerical Simulation, 10 (9), Pp. 1093-1103.

Ahmed .F/ Zead .Y

تطبيق طريقة تحليل ادوميان المحسنة لحل نظام Wu-Zhang غير الخطي ببعدين

احمد فاروق قاسم
جامعة الموصل
كلية علوم الحاسوب والرياضيات

زياد يحيى علي
جامعة الموصل
كلية علوم الرياضة والتربية البدنية

المستخلص

في هذا البحث، طريقة ادرمين المحسنة (MADM) استخدمت لحل نظام WU-Zhang غير الخطي ببعدين. نحن نقارب الحل للنظام مع طرائق MVIM و HPM وRDTM [17 ,13 ,15]، النتائج العددية التي حصلنا عليها هي ذات كفاءة عالية وملائمة ودقة كبيرة لحل انظمة المعادلات التفاضلية الجزئية. كذلك تمت مقارنة النتائج بين الطريقة المقترحة والطرائق الأخرى في بعض الأمثلة لإظهار كفاءة كل طريقة.

On Edge Addition Problem with some graphs

Alaa A. Najim   Zainab A. H. Al-Hassan

Departement of Mathematics

University of Basrha College of Science

Abstract

The two questions that: how many edges at least have to be added to the network to ensure the message d within the effective bounds, and how large message delay will be increased when faults occur, can re-write this problem as: What the minimum diameter of a connected graph obtained from a graph of diameter d after adding t extra edges, this problem called "Edge Addition Problem". In this paper we find some exact values to above problem by using some special graphs (Line Graph, Bipartite graph, and complete Bipartite graph).

Key words: diameter; altereded graph; edge addition problem.

Computer subject classification : 33C80,03F05,65Q05.

Introduction

Graph Theory is a basic and powerful mathematical tool for a wide rang of application. Many emerging problems in various fields, such as chemistry, industrial and electrical engineering, management of transport planning, marketing and education can pose graph theory problems [1, 2]. In network communication, the topology of the delivery network can be modeled by a graph. Conversely, any graph can also be considered as a topological structure for some interconnection networks [3, 4]. Historically,

the first paper on the graph theory was written by Euler in 1736 [2]. W, Rose [5] in 1892, submitted the first representation of the problem as a graph in order to solved. More historical information about the graph theory can be found in F R. K. Chung and M. R. Garey (1984), where they introduction the " Edge Addition Problem" and "Edge Deletion Problem"[6]. There are many authors tried to prove the two problems by find the exact values or bound to these problems, for example A. A. Schoone et.el. (1987) [7], Z. G. Deng and J.-M. Xu (2004) [8], H. –X. Ye and C.

Alaa .A/ Zainab .A

Yang (2009) [9], A. A. Najim (2005) [10], Y.-Z. Wu (2006) [11], S. A. AL-Bachary (2009) [12]. S. A. AL-Maliky (2013) [13]. In this paper we will find exact values to $P(t,d)$ for some t and d by using new teachings. All the authors use the path of graph (with some diameter) to prove the edge addition problem, i.e. the problem became "find a minimum diameter of a connected graph obtained from a graph of diameter d after adding t extra edges".

Theorem (1):- $P(t,7) = 2, t = 4,5$

Proof:- Let $t = 4$, $d = 7$ and $P = (x_0, x_1, ..., x_7)$ be simple path of length 7. The vertices x_1, x_2, x_4, x_6 partion P in to five segments

$$P_1 = P(x_0, x_1), P_2 = P(x_1, x_2),$$

$$P_3 = P(x_2, x_4), P_4 = P(x_4, x_6),$$

$$P_5 = P(x_6, x_7)$$

Let G be altereded graph obtain from path plus four extra edges.

$e_1 = (x_0, x_4), e_2 = (x_4, x_7), e_3 = (x_2, x_6),$
$e_4 = (x_1, x_6)$
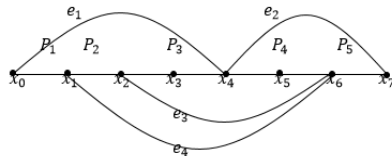
Define seven cycles as follows:

$C^1 = P_1 \cup P_2 \cup P_3 + e_1$, $C^2 = P_1 \cup P_4 + e_4 + e_1$, $C^3 = P_1 \cup P_5 + e_4 + e_2 + e_1$, $C^4 = P_2 + e_3 + e_4$, $C^5 = P_3 \cup P_4 + e_3$, $C^6 = P_3 \cup P_5 + e_3 + e_2$, $C^7 = P_4 \cup P_5 + e_2$

It is easy to see that,

$\varepsilon(P_i) = 1$ for $i = 1,2,5$, and

$\varepsilon(P_i) = 2$ for $i = 3,4$

Thus we have

$\varepsilon(C^i) = 5$ for $i = 1,2,3,5,6$

$\varepsilon(C^i) = 4$ for $i = 7$

$\varepsilon(C^i) = 3$ for $i = 4$

It is easy to see that any two vertices x and y of G, are connected in some cycle C^i as define above. $\text{Max}\{d(C^i) : 1 \leq i \leq 7\} \leq \left\lceil \frac{5}{2} \right\rceil = 2$. We get, $P(4,7) \leq d(G) \leq 2$. Now from [8] ($\left\lceil \frac{d}{t+1} \right\rceil \leq P(t,d) \leq \left\lceil \frac{d}{t+1} \right\rceil + 1$) ……………................. (1) we have $P(4,7) \geq \left\lceil \frac{7}{5} \right\rceil$. Thus, $P(4,7) = 2$. From [12] ($P(t,d) \geq P(t',d)$ if $t \leq t'$),

we get: $P(5,7) = 2$

Theorem (2):- $P(5,8) = 3$

Proof:- Let $P = (x_0, x_1, ..., x_8)$ be an (x_0, x_8)-path and G an altereded graph obtained from P pluse 5 extra edges and having diameter $d(G) = P(5,8)$. Assum to the contrary $d(G) \leq 2$. If $d(G) = 1$, then the number of the extra edges is equal to $t \geq 7 + 6 + \cdots + 1 = 28$, this is contradiction.

Now assume $d(G) = 2$. Let x_i be a smallest numbered vertex that G has no edge (x_i, x_j) with $j > i + 1$. Thus, for each $j = 0,1, ..., i - 1$, there exists an $j'(\geq j + 2)$ such that $(x_{j'}, x_j) \in E(G)$ is extra edge, and so such edges are at least i.

Since $d(G) = 2$, we must be able to reach every other vertex in two steps from x_i. Hence we need edges (x_i, x_j) for all $i + 3 \leq j \leq 8$ for some $j' \leq j - 2$. Then we have two case:

a) suppose (x_{i-1}, x_j) is no extra edge but $(x_i, x_{j'})$ is an extra for some $j' \leq i + 1$. Then $(x_i, x_{j'})$ and $(x_{j'}, x_j)$ are extra edges thus $t \geq i + (9 - (i + 3)) = t + 1$,

this is contradiction.
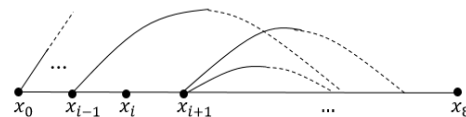
b) suppose (x_{i-1}, x_j) and (x_i, x'_j) are extra edges for some $j' = i - 1$. Then some vertices $(x_{i+2}, x_{i+3}, ..., x_8)$ need at least one new extra edges to reached any other vertex of the path by at most 2 steps. Thus we have

$$t \geq i + (9 - (i + 3) - 1) + 1 = t + 1$$

Journal of AL-Qadisiyah for computer science and mathematics   Vol.10 No.1   Year 2018
ISSN (Print): 2074 – 0204   ISSN (Online): 2521 – 3504

Alaa .A/ Zainab .A
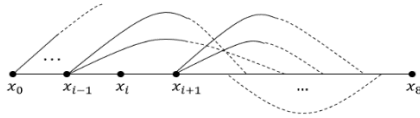
where the appearance of (-1) is because that there is an extra edge (x_{i-1}, x_j) in the first (i) extra edge when $j' = i - 1$.

But this is contradiction. Thus $P(5,8) \geq 3$ from inequality (1) $P(5,8) \leq \lceil \frac{8}{6} \rceil + 1 = 3$. Thus $P(5,8) = 3$.

■

Theorem (3):- $P((n-1)^2, 2n - 1) = 2$,

$$n \geq 2$$

Proof:-Let $K_{n,n}$ be an equally complete bipartite graph with bipartion $\{X, Y\}$, $X = \{x_1, x_2, \dots, x_n\}$, $Y = \{y_1, y_2, \dots, y_n\}$, $|X| = n, |Y| = n$,

$E(K_{n,n}) = n^2, V(K_{n,n}) = 2n, d(K_{n,n}) = 2$

$$K_{n,n}$$

$$K_{6,6}$$
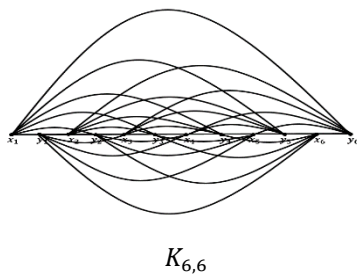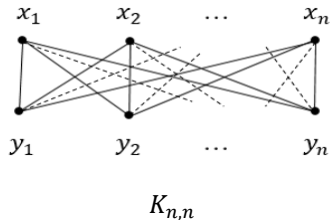
Let $P = (x_1, y_1, x_2, y_2, \dots, x_n, y_n)$. Then P is a longest path in $K_{n,n}$.

$$d(P) = V(K_{n,n}) - 1 = 2n - 1$$

G an altereded graph with diameter $d(G) = P(t, d)$ optained from the path P pluse t extra edges such that $G \cong K_{n,n}$ then $d(G) = 2$ and $t = E(K_{n,n}) - d(P) = n^2 - 2n + 1$

$$= (n-1)^2$$

Now we wanted to prove that $P((n-1)^2, 2n - 1) = 2$ by two ways

1) $d(K_{n,n}) = 2 \rightarrow P((n-1)^2, 2n - 1) \leq 2$

Either $P((n-1)^2, 2n - 1) = 1$ or

$$P((n-1)^2, 2n - 1) = 2$$

If $P((n-1)^2, 2n - 1) = 1$ this is contradiction (since the graph not complete).

Then $P((n-1)^2, 2n - 1) = 2$.

2) If $n = 2$ then from [8] (for $d \geq 2$, $P(1, d) = \lceil \frac{d+1}{2} \rceil$), $P(1,3) = 2$

If $n = 3$ then from [13] (for $t = 4,5$ and $4 \leq d \leq t + 1$, $P(t, d) = 2$), $P(4,5) = 2$

If $n \geq 4$ then $P((n-1)^2, 2n - 1) \leq \lceil \frac{2n-3}{(n-1)^2 + 1} \rceil + 1 = \lceil \frac{2n-3}{n^2 - 2n + 2} \rceil + 1$

Since $n \geq 4$

$n^2 \geq 4n \rightarrow n^2 > 4n - 3$

$$\rightarrow n^2 - 2n > 2n - 3$$

$$\rightarrow n^2 - 2n + 2 > 2n - 3$$

Then from [12] (for $\frac{r(r-1)}{2} \leq t \leq \frac{(r-1)(r+2)}{2}, r \geq 4$ and $r + 1 \leq d \leq t + 3$,

$$P(t, d) = 2 \dots \dots \dots \dots \dots \dots \dots \dots \dots \dots (1))$$

$$P((n-1)^2, 2n - 1) \leq 2.$$

Either $P((n-1)^2, 2n - 1) = 1$ or

$$P((n-1)^2, 2n - 1) = 2$$

If $P((n-1)^2, 2n - 1) = 1$ this is contradiction, (since the graph not complete).

Then $P((n-1)^2, 2n - 1) = 2$

■

Theorem (4):- $P(n(n-1), 2n) = 2$,

$$for \ n \geq 2$$

Alaa .A/ Zainab .A

Proof:-

Let $K_{n,n+1}$ be a complete bipartite graph with bipartion $\{X,Y\}$, $X = \{x_1, x_2, \dots, x_n\}$, $Y = \{y_1, y_2, \dots, y_{n+1}\}$, $|X| = n$, $|Y| = n+1$,

$$V(K_{n,n+1}) = 2n+1,$$

$$E(K_{n,n+1}) = n(n-1), d(K_{n,n+1}) = 2.$$
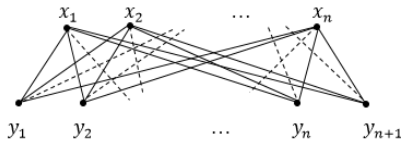
$$K_{n,n+1}$$
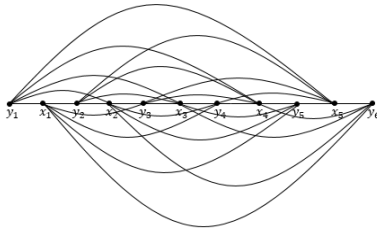
$$K_{5,6}$$

Let $P = (y_1, x_1, y_2, x_2, \dots, y_n x_n, y_{n+1})$. Then P is alongest path in $K_{n,n+1}$

$$d(P) = V(K_{n,n+1}) - 1 = 2n$$

G an altereded graph with diameter $d(G) = P(t,d)$ optained from the path P pluse t extra edges such that $G \cong K_{n,n+1}$ then $d(G) = 2$ and

$$t = E(K_{n,n+1}) - d(P) = n^2 + n - 2n$$

$$= n(n-1)$$

Now we wanted to prove that

$P(n(n-1),2n) = 2$ by two ways

1) $d(K_{n,n}) = 2 \to P(n(n-1), 2n) \leq 2$

Either $P(n(n-1), 2n) = 1$ or

$P(n(n-1), 2n) = 2$

If $P(n(n-1), 2n) = 1$ this is contradiction, (since the graph not complete).

Then $P(n(n-1), 2n) = 2$

If $n = 2$ then from [7] (for $d \geq 3$, $P(2,d) = \lceil \frac{d+1}{3} \rceil$) $P(2,4) = \lceil \frac{5}{3} \rceil = 2$

If $n \geq 3$ then $P(n(n-1),2n) \leq \lceil \frac{2n-2}{n(n-1)+1} \rceil + 1 = \lceil \frac{2n-2}{n^2-n+1} \rceil + 1$

Since $n \geq 3$

$$n^2 \geq 3n \to n^2 > 3n - 2$$

$$\to n^2 - n > 2n - 2$$

$$\to n^2 - n + 1 > 2n - 2$$

Then from equation (1) $P(n(n-1),2n) \leq 2$.

Either $P(n(n-1), 2n) = 1$ or

$$P(n(n-1), 2n) = 2$$

If $P(n(n-1), 2n) = 1$ this is contradiction, (since the graph not complete).

Then $P(n(n-1), 2n) = 2$

■

Remark:-

The symbol "$a \gg b$" is mean, the number a is too big of number b.

Lemma:-

1) $P(t', d') < P(t, d)$, if $t' - t \gg d' - d$

2) $P(t', d') > P(t, d)$, if $d' - d \gg t' - t$

Proof:-

1) Let $P(t, d)$ be minimum diameter of an altereded graph G obtained from a path $P = (x_0, x_1, \dots, x_d)$ of diameter d with t extra edges and let $P(t', d')$ be minimum diameter of an altereded graph G' obtained from path $P' = (x_0, x_1, \dots, x_{d'})$ of diameter d' with t' extra edges.

Now wanted to prove $P(t', d') < P(t, d)$, if $t' - t \gg d' - d$ since $t' - t \gg d' - d$ this mean

$d' - d$ be too small compare with $t' - t$,

So, $d' \approx d$ and t' is greater than t, then $P(t', d') < P(t, d)$, from [12].

In the same way we prove 2.

■

Alaa .A/ Zainab .A

Theorem (5):-

For $t \geq 2$ and $d = (t + 1) + 5$, let G and G' be two graphs such that $d(G) = P(t, d)$, $G' = L(G)$, $d(G') = P(t', G')$.

Then $P(t', d') < P(t, d)$.

Proof:-

Let $m \geq 0, r = 1,2,3$ for $t \geq 2, d = (t + 1) + 5, P(t, d) = 3$ from [13] ($P(t, d) = k + 2$, for $t \geq 2, k \geq 1$ and $d = k(t + 1) + 5$),
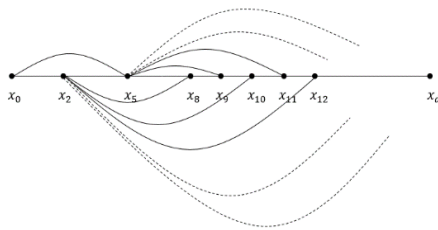
since $t \geq 0, m \geq 0$ and $r = 1,2,3$, then

$t = 2m + r + 1, d = 2m + r + 7$

Let G' is line graph of G where $V(G') = t + d$ and

$$E(G') = \frac{1}{2} \sum_{x \in V(P(t,d))} \left(d_{p(t,d)}(x)\right)^2 - E(P(t,d))$$

$P(t', d')$ is minimum diameter of an altereded graph G'

$d' = V(G) - 1 = t + d - 1 = 4m + 2r + 7,$

and $t' = E(G') - d' = m^2 + 6m + mr + 4r$

$t' - t = m^2 + 4m + mr + 3r - 1$

$d' - d = 2m + r$

Then, $(t' - t) - (d' - d) = m^2 + 2m + mr + 2r - 1 \gg 0.$

So, $t' - t \gg d' - d$

from   lemma $P(t', d') < P(t, d)$
∎

Conclusions

A minimum diameter of a connected graph obtained from a graph of diameter d after adding t extra edges, this problem called "Edge Addition Problem". We find exact values to problem for some t and d by using some special graph that is:

1. $P(t, 7) = 2, t = 4,5$

2. $P(5,8) = 3$

2. $P((n - 1)^2, 2n - 1) = 2, n \geq 2$

4. $P(n(n - 1), 2n) = 2, for \ n \geq 2$

5. For $t \geq 2$ and $d = (t + 1) + 5$, let G and G' be two graphs such that $d(G) = P(t, d)$, $G' = L(G)$, $d(G') = P(t', G')$.

Then $P(t', d') < P(t, d)$.

References

[1] J. M. Aldous and R. J. Wilson, "*Graphs and Application: An Introductory Approach*", Springer-Verlag London Berlin Heideberg, 2003.

[2] N. L. Biggs, E. K. Lloyed and R. J. Wilson, "Graph Theory ١736-١936", Clarendon Press. Oxford, 1998.

[3] J.-C. Bermond, N. Homobono and C. Peyyrat, "*Large Fault-Tolerant Interconnection Networks*", Journal of Graphs and Combinatorics, Vol. 5, PP. 107-123, 1989.

[4] J.-M. Xu, "*Topological Structure and Analysis of Interconnection Network*" Kluwer Academic Pulbishers, 2001.

[5] W. W. Rouse Ball, Mathematical Recreations and Problems of Pas and Present Time (later entitled Mathematical Recreations and Essays), Macmillan, London, 1892.

[6] F R. K. Chung and M. R. Garey, "*Diameter bounds for altered graphs*", Journal of Graph Theory. Vol, 8, No 4. PP 511.534, 1984.

[7] A. A. Schoone, H. L. Bodlaender and V. J. Leeunwen "*Diameter increase caused by edge deletion*" Journal of Graph Theory, Vol 11, No. 3 PP. 409-427, 1987.

[8] Z. G. Deng and J. M. Xu, "*On Diameters of Altered Graphs*", Journal of Mathematical study. Vol 37, No.1, PP 35.4L 2004.

[9] H.-X. Ye, C. Yang, J.-M. Xu, "Diameter vulnerability of graphs by edge deletion", Journal of Discrete Mathematics, Vol. 309, PP. 1001-1006, 2009.

[10] A. A. Najim, J. -M. Xu, "*On edge Addition of Altered graphs*" Journal of University of Science and Technology China Vol 35, No.6, PP, 725-731, 2005.

[11] Y.-Z. Wu, and J. -M. Xu, "*Diameters of Altered graphs*" Journal of Mathematical Research and Exposition, Vol. 26, No. 3. PP 502-508, 2006.

[12] S.A. AL-Bachary "*On Edge addition and Edge deletion problems of graphs*", M.Sc. thesis, university of Basrah, 2009.

[13] S.A.A. AL-Maliky "*On Edge addition problems of graphs*", M.Sc. thesis, university of Basrah, 2013.

<div dir="rtl">

حول مسألة أضافة الحافات مع بعض البيانات

علاء عامر نجم   زينب عبد الأمير حمزة الحسن

قسم الرياضيات

جامعة البصرة كلية العلوم

المستخلص :

السؤالين اقل عدد من الحواف التي يجب ان تضاف الى الشبكة لضمان تأخير الرسالة ضمن حدود فعالة، وكيف سيتم زيادة تأخير رسالة عندما تحدث أخطاء يمكن إعادة كتابة هذه المشكلة على النحو التالي: ما الحد الأدنى للقطر من رسم بياني متصل تم الحصول عليه من رسم بياني للقطر بعد إضافة حواف إضافية، هذه المشكلة تسمى "مسالة إضافة الحافات". في هذا البحث وجدنا بعض القيم الدقيقة للمسألة أعلاه باستخدام بعض البيانات الخاصة (البيان الخطي، بيان التجزئة، بيان التجزئة الكامل).

</div>

Paper Currency Detection based Image Processing Techniques: A review paper

Shaimaa H. Shaker   **Mohammed Gheni Alwan**
Department of Computer sciences -University of Technology, Baghdad, Iraq
(sh_n_s2004@yahoo.com)   (mgaz_mgaz@yahoo.com)

Abstract:
The currency has a great meaning in everyday life. Thus currency recognition has gained a great interest for many researchers. The researchers have suggested diverse approaches to improve currency recognition. Based on strong literature survey, image processing can be considered as the most widespread and effective technique of currency recognition. This paper introduces some close related works of paper-currency recognition. This paper has explained a variety of different currency recognition systems. The applications have used the power of computing to differentiate between different types of currencies with the appropriate layer. Choosing the proper feature would improve overall system performance. The main goal of this work is to compare previous papers and literatures through reviews these literatures and identify the advantages and disadvantage for each method in these literatures. The results were summarized in a comparison table that presented different ways of reviewing the technology used in image processing to distinguish currency papers.

Keywords: Currency recognition, Digital image processing, classifier, distinguish banknotes.

1.   Introduction

Individuals cannot easily have the ability to recognize different currencies coming from different countries. Since the currency is vital in enabling the overall management of the countries' economies, automatic currency recognition tools turn out to be a major area of concern for researchers and developers. Currency recognition system is an image processing practice used to identify the currency note of different countries. This system is used to identify the currency note in businesses, banks, malls, railways, organizations, etc. but it is mainly recognized using a hardware device. Common man also doesn't always have the ability to use it as a hardware. Therefore, there is a need to computerize the human effort to recognize the currency. Let us consider the example of the bank scenario. The employees need to recognize the labels from each note using a device that consists of ultraviolet light. The bank staff keeps a currency note on the device and tries to find whether the watermark icon, serial number and some other characteristics of the notes are suitable for getting the label and verifying it. This increases the banking business. As an alternative, if the bank uses the currency recognition system and computes its work, apparently the result will be much more accurate and reliable. The same can be applied to areas such as malls and investment companies where these systems can be tested. So there is a necessity to have a straightforward and easy way to recognize banknotes. The system is based on scanners, computers, and workbooks. Based on image processing techniques and algorithms [1]. See Figure (1).

Shaimaa .H / Mohammed .G
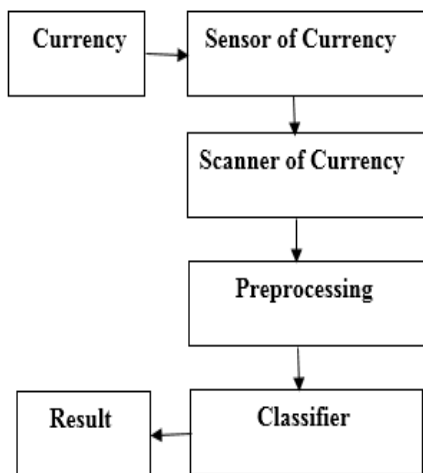
Figure (1): The General Structure of the Recognition System.

The programming software will do the job of extracting the features of the test images. Once they are extracted the features will be coordinated with the stored ones in MAT file. The features in MAT file are the ones of the train images. If the features of test image will be matched with those in MAT file, the software will return the class of that currency note. If the test image features don't match with any of those in Mat file, the software will display the output revealing that it is doesn't belong to any class.

The aim of this work is to introduce a comparison table in different ways and algorithms based on image processing to recognize the currency.

Section 2 deals with some related works to currency recognition, section 3 and 4 represent the steps of currency recognition system based on image processing, section 5 presents the discussion and conclusion.

2.   Some Related Works
There are many of the previous literatures on the subject of this research paper, which can be included in a chronological order as follows:

2.1 Currency Recognition:
Y. Mitsukura et al. in 2000 introduced a method depend on Artificial Intelligence methods and adaptive systems, combining Neural Network methods with the Simulated Annaling method.

The simulation results was achieved by the author indicating to developed small size neural network for coin recognition by using genetic algorithm and simulated annealing and coin recognition system is low cost with a recognition rate results of 99.68%[1].

R. Primanathan et al. in 2005 proposed a system focusing only on numbers rather than using other images found on the front and back of the coin. Extracting a digital image from a particular coin image and using the result to perform character recognition. The important thing of this work was that could easily be applied in any real-time business transactions. The produced system from this research recognized the numbers using neurosurgery with a success rate of 92.43% of the tested data [2].

A. Khashman et al. in 2006 reported a Smart Currency recognition System that used currency arrangements of recognition to help preventing misperception between different currencies with similar physical dimensions. Based on multilayer of neural network and limited number of images [3].

L. J. P. Van der Maten et al. in 2006 introduced a currency classification method called "Sween-O-Matik" especially to achieve trustworthy classification of different coin groups. "Coin-O-Matek" technique used currency images and sensor information in the currency recognition. "Coin-O-Matek" system accomplished in these stages:

Stage 1. It includes separating a coin from the coin photograph background.

Stage 2. It is engaged to get efficient and specific features from the coin images. The outputs features can be employed in the classifier training process.

Stage 3. The selection of likely coin classes depend on area and thickness.

Stage 4. Classifying one currency, the nearest neighbors approach is applied. Depending on coin images of the two sides are categorized

Stage 5. It includes checking whether the two images may have the same symbol. The accuracy efficiency was about 72% [4].

K. K. Debnath et al. in 2010 offered a system for recognizing the currency using the Neural Network (NN), especially for the currency of Bangladesh. Neural network band (N) which was actually seeded and trained by passive link learning. Based on the experience of individuals neural network on different parts of input in a group. This technique was capable of identifying a very noisy or old image of "Taka" and could recognize the "Teka" even if the input were confusion [5].

H. R. Al-Zoubi et al. in 2010 offered a recognition system of Jordanian coins employing a statistical procedure. It used two features: the first one was the color of the coin, and second one was the area of the coin [6].

S. Modi in 2011 introduced Actress Artificial Neural Network (ANN) based on automated identification of the currency recognition system of the Indian currencies for the label `1,` 2, `5 and 10. This process was able to recognize the coins from the two faces as images from both faces of the currency. Conversion techniques were used to extract the features of the images. The extracted features were then passed as inputs to the trained neural network. It has been observed that the system provided results accuracy of about 97.74% [7].

S. Das et al. in 2013 presented a system for the classification of recently discharged Indian coins. The system was based on the "Hissian Harris" algorithm, which used size, weight, surface etc. of the currency as parameters, also using the concept of rotation stability. This work produced a low-cost system having a rate of nearly 100% recognition [8].

2.2 Paper Currency Recognition:
M. Aoba et al. in **2003** suggested a Euro recognition system. Three layers perception and Radial Basis Function (RBF) were employed to the recognition process. The noticeable features of the method are: [9]
1. Used 3 stages perception for the classification and RBF for the checking the correctness.
2. RBF network was efficiently to refuse unacceptable data because it detect the likelihood distribution of the data.

A. AHMADI et al. in 2003 assumed a method for removing nonlinear dependencies between variables and extracting important geographies of the data. Firstly, the area is divided into pieces using organizing map model, and IKA is implemented in each piece. The Learning Vector Quantization network (LVQ) is used as is employed to as major part of the system. The outstanding charcristics of the method are [10]:
1. Employed a simple linear mode for data-complexity.
2. The rate of correctness was 100%.

D. Gunnaratna et al. in 2008 reported "Celeric" system with a shift operation which was eliminate noise patterns without disturbing the unique images of the coin paper and repairing the pictures. The neural network was trained with color brightness, noise, dust, impact, etc. "Canny" algorithm was employed for the edge recognition because of its low fault average and good

capability to localised edge points correctly. The outstanding characteristics of this method are [11]:
1. Many layers back propagation neural network is employed for the classification.
2. The author perform several tests, acquired good classification results and varying image conditions.

J. Guo et al. 2010 used a Local Binary Pattern (LBP) algorithm to extract characteristic paper currency. The anticipated currency recognition system was the form creation phase, that consisted of preparing a model for paper then extracting the feature using a Block-Core Algorithm and other phase was the verification phase. In this way the higher classification accuracy using the block algorithm of the pulp [12].

Velu et al. in 2011 presented a perfect image which was used for currency learning and appreciation.
The correct rating for accepting a currency was very high. This paper could be expanded to classify coins issued over different periods of time. Also, it included coin stands, type of coin-metal etc...
Classification using the measure of coin-similarity, size and tops locations in the space [13].

B. V. Chetan et al. in 2012 proposed the side of the precious paper currency recognition method. It is a two-stage:
1. Matching database notes
2. Matching using correlating the edges of input.

The results showed that the method of identification of paper currencies, "Gabor Muweijeh", an accuracy of 65%. the method of subtraction image gave a resolution of 51.52%, and the method based on the Local Binary Pattern (LBP) gave accuracy of 52.5%. While the suggested technique gave very high rate exceed to ninety nineand half percentage accuracy for a particular set of currency [14].

A. Rajai et al. in 2012 introduced a method to extract the texture profiles of the currency memo pictures. Using Discrete-Wavelet-Transform (DWT) with a group of statistical measures extracted from the approximate matrix[15].

Althafiri et al. in 2012 forwarded a new image technique based on "Birhani" identification based on euclidean distance based some values and neural network. So   deals with varity kinds of paper currency and convert them to the binary image then using "Prewette Mask"; and using the "Kani mask".

Shaimaa .H / Mohammed .G

The characters were then obtained by finding the total pixel for each of the these images. It ended after finishing the extraction of the paper extraction features using various techniques such as the Euclidian Welded Distance (EWD) and Neural Networks. This was done by feedback forward again. The least distance was obtained for the method of classification was taken by the weighted Euclidean distance showing accuracy of 96.4%. On the other hand the neural network with the posterior propagation classification system gave approximately 85.1% accuracy in the optimum choice. So, the author revealed that the weighted euclidean approach was better than the neural network. Figure (2) domnstrates the comparison of the different paper-recognition techniques[16].

F. Lamont, et al. in 2012 suggested a system to identify the Mexican currency. The input images were suffering from different lighting change. Color and texture are extracted from the bank notes. Using local binary model to characteristic the texture [17].

Jain in 2013 suggested a method to extract the amount of currency paper. The extracted Reign of Interest (ROI) and neural networks for matching. At the beginning, got the input by means of a scanner to achieve the image. Few filters were useful for extracting the observation range assessment. Different pixel levels were used in different quantity notes [18].

Manzoor and Ali in 2013 proposed a technique for currency recognition using image processing. Their research was the lowest cost machine to identify the Pakistani-paper -currency. Different images of currency was test on this system so the efficiency rate was 100% [19].

Nayak and Danti in 2014 worked on Indian paper currency note recognition and reported some vital characteristics such as the denomination, year of print, etc... Based on geometrical shape, and amount of currency were identified and Neural Network classifier. And demonstrated the efficiency of the approach [20].

    A. B. Sargano et al. in 2014 proposed smart systems to recognize the Pakistani-paper currency. After finding the features, they suggest to use multi-layers of forward feed Propagation Neural Network (PNN) for classification. The technique was simple and consumed relatively less time making them suitable for real-time application. The results indicated that the system had the ability to recognize 99% efficient of captured images [21].

K. Vora et al. in 2015 proposed an algorithm based on the method of extracting the frequency band feature and discussed the currency detector. 2-Dimensional "Moji" Discrete Wavelet Transform (2D-DWT) and a group of statistical moments used. Extracted features could be used to identify, classify and retrieve bank notes. The result of the classification would facilitate the recognition of the counterfeit currency based on the serial number extraction mainly through the implementation of OCR [22].

S. Sahu and et al. in 2016 reported an image processing technique used to recognize the paper currency of different countries. A booming approach to determine the paper currency depending on the pre-processing, extracting feature and classification of those currency images was discovered. The step for the currency identification system of different processing steps for analyzing the definition of paper currency were pre-treatment, morphological filtration, analysis, induction analysis, fragmentation and extraction of properties. [23].

Figure (2): shows graphical representation of comparison between various papers Techniques.

PAPER CURRENCY RECOGNITION TECHNIQUES

	Ensemble Neural N/W	Hidden Markov Model	Radial Basic Function	BlocK-LPB	Fast Adaboost Algorithm	Image Substraction Method	Side Invariance Method	Weight Euclidean Distance Method	Feed Forward of Back Propagation
	100	95	100	100	97	51.25	99.5	94.4	85.1
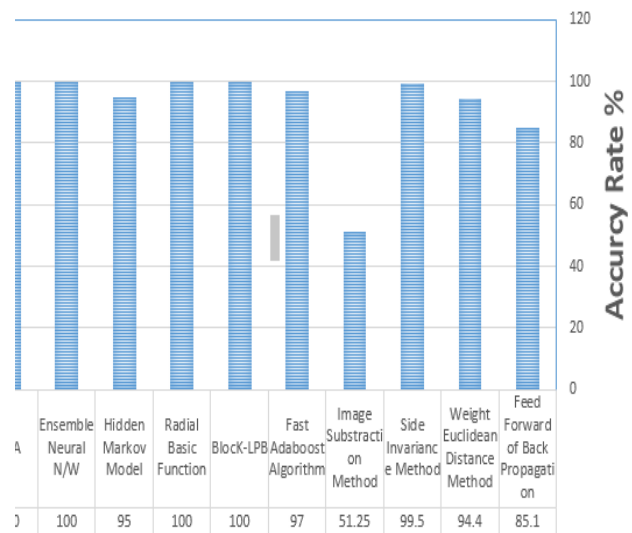
): comparison between Accuracy of Various Paper Currency Recognition Techniques.

Shaimaa .H / Mohammed .G

3.   Typical Construction of a Paper Currency Recognition System

The image is acquired from the input device has to be of high quality. The similar images (size and quality) are stored in the database.

The system consists of: image acquisition, pre-processing including noise removal, feature extraction, classification and recognition. Figure (3) shows the construction of currency recognition system.
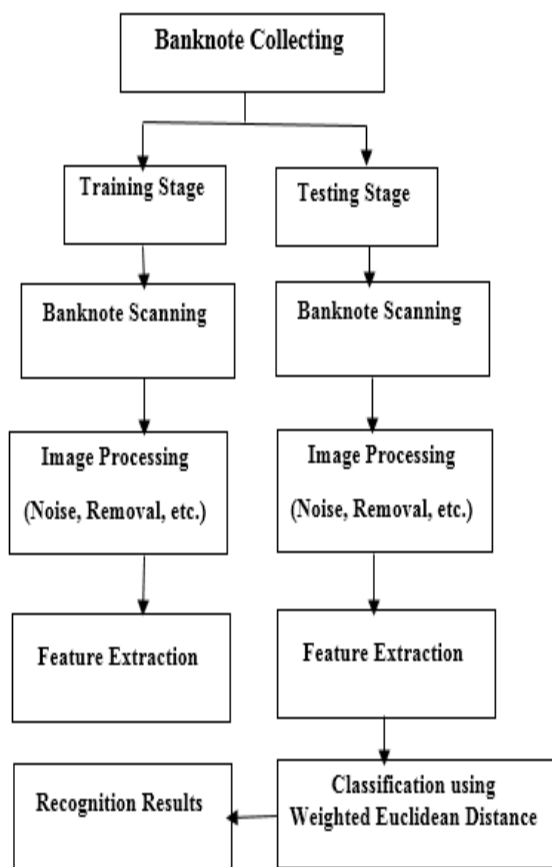
Figure (3): Construction of a Currency Recognition.

3.1   Steps for Paper Currency Recognition:

In any Currency Recognition System, the following steps are performed:

First Stage 1- Image Acquisition:

It is the formation of digital images, and is generally acquired by using digital camera. The image is then saving in order to be processed [24].

Second Stage-preprocessing:

In this stage undesired noise has to be removed to be able to process. Smoothing of image is applied to remove noise from the images using median filter. Median filter of 3*3 neighborhoods is applied to find the median, Figure (4) shows an example of a median filter.
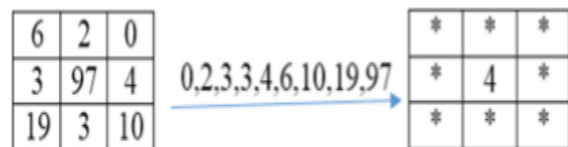
Figure (4): Example of 3*3 of Median Filter.

After that the image enhancement stage is used to improve the images of low contrast. Based on reviewing the histogram of a gray scale image, discovering that it is a gray level where clustered toward 0, then it is a dark image. Brighter images will have the gray level clustered mostly at the upper end, towards 255. An example exhibits this in figure (3) for the sample currency [25] .

Third Stage-Edge Detection:

Edge detection aims at identifying points in digital image at which the image intensity changes strongly. The edge detection is essential to restrict the currency note that is the region of interest [26].

Fourth stage-Image Segmentation:

This subdivides the image into its ingredient regions or substances. Segmentation algorithm for dull images generally are based on two properties:

    a.   Discontinuity

    b.   Similarity.

Image segmentation, bwlabel operation has been applied to marker the connected components in an image or part of an image. All set of pixels be a connected group [25]. Each connected component is given a sole label to be visualized in an image. Figure (5) shows an example that the binary image has three connected components.

Shaimaa .H / Mohammed .G
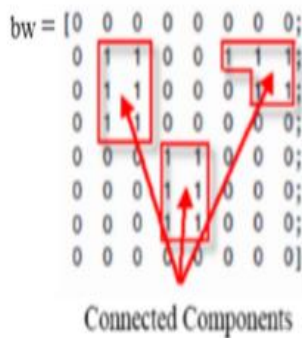
Figure (5): Three Connected Components of Binary Image.

Fifth Stage-Feature Extraction:

Include currency gratitude system, this stage is the most difficult tasks. The purpose of this stage is to recognize the single and individual geographies of each denomination under the diversity of challenging situations such as old notes, damaged notes and also under different illumination and environment [27].

Sixth Stage-Matching Algorithm:

This step recognizes or classifies currency notes of different denomination based on a variety of exceptional features extracted.

4. Discussion:

Table 1 introduces a comparison of the previous literature according to some criteria. This paper presents some methods and works to recognize the paper currency which is described by applying image processing. Through the first stage, notice variations among images and this leads to enhance the recognition rate. Basic features are extracted including identification the paper-currency. The procedure begins from data acquisition and later compare between features. The extraction is using sobel or canny operator which works well in the whole system with less computation time for segmentation. Assessment of the various approaches is based on classifier accuracy, and correspondence measurements of paper currency and coin currency.

Table (1): summarize the previous literature according some criteria.

Researchers	Year	Type of currency	Algorithm	Accuracy recognition	Recognition speed
Y. Mitsukura et al.	2000	coin	Three-Layered Neural Networks, Genetic algorithm and simulated annealing.	-	99.68%
M. Aoba et al.	2003	Paper	The 3 layers perception and Radial Basis Functions, (RBF) and RBF network	effectively	-
A. Ahmadi et al.	2003	paper	(simple linear mode) Self-Organizing Map (SOM) model and PCA	-	100%
R. Bremananth et al.	2005	coin	character recognition procedure	-	92.43%
A. Khashman et al.	2006	1 TL and 2 EURO coins	Intelligent Coin Identification System (ICIS) used pattern averaging and neural network	-	-
L.J.P. van der Maaten et al.	2006	coin	Classification of coins edge angle distance distribution has been used for feature extraction and the nearest-neighbor approach for classification.	-	72%.
D.. Gunaratna	2008	Currency Notes	Three layer back propagation neural network	-	100%
K. K. Debnath et al.	2010	TAKA	Ensemble Neural Network (ENN) and Hidden Markov Model (HMM)	-	-
J. Guo et al	2010	paper currency	Algorithm of block LBP	-	High
H. R. Al-Zoubi et al.	2010	coin	Color of the coin and its area	-	97%
S. Modi	2011	coins	Artificial Neural Network(ANN), Hough Transformation and Pattern Averaging	-	97.74%
Velu et al.	2011	coin	Image coin learning and appreciation, the Robert's, Laplacian and Canny edge detection methods, the planned ML-CPNN and ML-CPNN	99.6%	-
B. V. et al.	2012	paper currency	Two phases approach (matching dimension database notes are identified and the template matching is achieved by correlating the edges of input and matching dimension database note images.	-	-
A. Rajai et al.	2012	paper notes	feature extraction of currency, Discrete Wavelet Transform (DWT)	-	-
Ibtesam Althafiri et al.	2012		Two classifiers: Euclidean distance and Neural Network.	-	96.4%
F. Lamont, et.al	2012	banknotes	RGB space to extract color and the local binary patterns to extract texture	-	-
S. das.Y.M et al.	2013	coins	Advanced Harris-Hessian Algorithm and Hough Transformation	-	-
Jain	2013	Paper currency	Region of Interest (ROI) Neural Networks matching method	-	-
Manzoor and Ali	2013	paper currency	image processing techniques	-	100%
Nayak and Danti	2014	Currency Notes	Neural Network and OCR techniques.	-	efficiency
Malik et al	2014	coin	Fourier Transform	-	very fast
Allah Bux Sargano et al	2014	paper currency	three layers feed forward back Propagation Neural Network	-	99%
k. Vora, Ami Shah and Jay Mehta,	2015	Paper currency	2D Discrete Wavelet Transform (2D-DWT) and OCR	superior	-
S. Sahu and Toran Verma	2016	paper currency	image processing technique	efficient	-

5. Conclusion

A detail review has been reported in this paper about coin recognition and paper currency recognition. A number of findings have been obtained from the previous literatures. The most important conclusion is the use of various algorithms to classify and get optimum results using image processing. Both coin recognition and paper currency recognition methods have been investigated distinctly. Finally, their works have been summarized in tabular form which are very useful to be reviewed quickly. Further research works are needed to be done on this topic where still there are some other improved matters related to the accuracy and efficiency of the process. Thus accomplishing maximum efficiency and getting higher accuracy for the heterogeneous currency. When the physical state of the currency is not optimum, then it will always be possible to have a new challenge for researchers.

Shaimaa .H / Mohammed .G

References:

1. Y. Mitsukura, M. 'ukumi, N. Akamatsu ، "Design and Evaluation of Neural Networks for Coin Recognition by Using GA and SA" in proceedings of the   EEE-INNS-ENNS International Joint Conference on Neural Networks, Vol. 5, Pp. 178 –183, 2000, IJCNN 2000.

2. R. Bremananth, B. Balaji, M. Sankari and A. Ch0itra, "A new approach to coin recognition using neural pattern analysis" IEEE Indicon 2005 Conference, Chennai, India, 11- 13 Dec. 2005.

3. Kh. A., S. B. And D. K., "Intelligent Coin Identification System", Proceedings of the IEEE .International Symposium on Intelligent Control (ISIC'06), Munich, Germany, 4-6 October 2006.

4. L. J.P., V. der Maaten and P. J. Boon "Coin – o - matic: A fast system for reliable coin classification" in Proceedings of the MUSCLE CIS Coin Computation Workshop, Germany, pp. 7-17, Sep. 1, 2006.

5. K. Kumar Debnath, S. Uddin Ahmed, Md . Shahjahan, "A Paper Currency Recognition System Using Negatively Correlated Neural Network Ensemble", Journal Of Multimedia, Vol. 5, No. 6, Pp. 560-567, December 2010.

6. Al-Z. H. .R. "Efficient coin recognition using a statistical approach", 2010 IEEE International Conference on Electro/Information Technology (EIT), 2010.

7. Sh. Modi, Dr. S. Bawa, "Automated Coin Recognition System using ANN" International Journal of Computer Applications (0975 – 8887) Volume 26–   No.4, Pp. 13-18, July 2011.

8. S. das. Y. M, R. Pugazhenthi, "Harris-Hessian Algorithm for Coin Apprehension", International Journal of Advanced Research in Computer Engineering & Technology (IJARCET) Volume 2, No 5, May 2013.

9. M. Aoba, T. Kikuchi, Y. Takefuji ، "Euro banknote recognition system using a three layer perceptron and RBF networks", IPSJ Transaction on Mathematical Modeling and Its Application, Vol 44, No . SIG 7 (TOM 8), Pp. 99-109, May2003.

10. A. Ahmadi, S. Omatu, T. Kosaka, "A Reliable Method for Recognition of Paper Currency by Approach to Local PCA) used local principal component analysis PCA", in IEEE proceedings of the International Joint Conference on Neural Networks, 20-24 ,Vol. 2, Pp. 1258 – 1262., July 2003.

11. D. A. K. S. Gunaratna, N. D. Kodikara and H. L . Premaratne, "ANN Based Currency Recognition System using Compressed Gray Scale and Application for Sri Lankan Currency Notes-SLCRec", in proceedings of world academy of science, engineering and technology ، vol. 35,ISSN 2070-3740, Pp. 235-240,Nov 2008.

12. J. Guo, Y. Zhao, A. Cai, "A reliable method for paper currency recognition based on LBP" in proceeding of 2nd IEEE International Conference on Network Infrastructure and Digital Content, 24-26, Pp. 359 – 363 ,Sept . 2010.

13. Velu, C.M., Vivekanadan, P., and Kashwan, K. R.2011. Indian Coin Recognition and Sum Counting System of Image Data Mining Using Artificial Neural Networks. International Journal of Advanced Science and Technology, Vol. 31, pp. 67-80, 2011.

14. Ch. B. V., Dr. P. A. Vijaya, "A Robust Side Invariant Technique of Indian Paper Currency Recognition ،"International Journal of Engineering Research & Technology (IJERT), Vol. 1 Issue 3, Pp. 1-7, May – 2012,.

15. A. Rajaei, E. Dallalzadeh, M. Imran "Feature Extraction of Currency Notes: An Approach Based on Wavelet Transform" in IEEE proceedings of Second International Conference on Advanced Computing & Communication Technologies , 7-8 Jan. 2012 ,Pp. 255 – 258, 2012.

16. E. Althafiri, M. Sarfraz, M.Alfarras, "Bahraini Paper Currency Recognition " Journal of Advanced Computer Science and Technology Research, Vol. 2 No.2, Pp. 104-115, June 2012.

17. F. García-Lamont et.al. "Recognition of Mexican banknotes via their color and texture features", Elsevier, Expert Systems with Applications page no.9651–9660, 2012.

18. J., V.K.,.Indian Currency Denomination Identification Using Image Processing Technique", Vipin Kumar Jain et al, (IJCSIT) International Journal of Computer Science and Information Technologies., Vol. 4, No.1, PP. 126-128, 2013.

19. A., A., and M., M." Recognition System for Pakistani Paper Currency. Research Journal of Applied Sciences, Engineering and Technology." Vol. 6(16). pp. 3078-3085, 2013.

20. D, A., and N., K." Grid Based Feature Extraction for the Recognition of Indian Currency Notes. International Journal of Latest Trends in Engineering and Technology (IJLTET), Vol.4, Iss. 1, 2014.

21. A. Sargano, M. Sarfrazb, and N. Haq."An intelligent system for paper currency recognition with robust features Journal of Intelligent & Fuzzy Systems" 27, 1905–191, 2014.

22. K. Vora, A. Shah and J. Mehta," A Review Paper on Currency Recognition System" International Journal of Computer Applications" (0975 – 8887) Volume 115 – No. 20, April 2015

23. S. Sahu and T. Verma " Identification of Paper Currency Techniques: A Survey.IJSTE - International Journal of Science Technology & Engineering Volume 2 | Issue 12, " June 2016.

24. M. Deborah and C. Prathap, "Detection of Fake Currency using Image Processing", International Journal of Innovative Science, Engineering & Technology, vol. 1, no. 10, December 2014.

25. R. C. Gonzalez and R. E. Woods, "Digital Image Processing (3rd Edition)", Prentice-Hall, Inc., Upper Saddle River, NJ, USA, 2006.

26. M. Thakur and A. Kaur, "Various Fake Currency Detection Techniques", International Journal of Engineering Science and Technology, vol. 1, no.11, pp. 1309-1313, July 2014.

27. M. Akbar, A. Sedayu, A. Putra and S. Widyarto, "Original and Counterfeit Money Detection Based on Edge Detection", Information Technology and Biomedical Engineering, Indonesia, November 2013.

التعرف على العملة الورقية بالاعتماد تقنيات معالجة الصورة: بحث استعراضي

شيماء حميد شاكر   محمد غني علوان

قسم علوم الحاسوب / الجامعة التكنولوجيا / العراق – بغداد

mgaz_mgaz@yahoo.com   sh_n_s2004@yahoo.com

المستخلص :

في الحياة اليومية العملة لها معنى كبير . وبالتالي ابدى الكثير من الباحثيين اهتماماً كبيراً للتعرف على العملة النقدية. وقد اقترح الباحثون نهجا مختلفاً لتحسين التعرف على العملة النقدية.واستنادا إلى استعراض الادبيات ، يمكن اعتبار معالجة الصور أكثر التقنيات انتشارا وفعالية في التعرف على العملات النقدية. يقدم البحث بعض من هذه الأعمال القريبة والمتعلقة بالاعتراف بالعملة النقدية الورقية. هذا البحث اوضح مجموعة متنوعة من أنظمة مختلفة للتعرف على العملة النقدية.وقد استخدمت تطبيقات الحوسبة للتمييز بين أنواع مختلفة من العملات النقدية.واختيار الميزة المناسبة للأداء العام الجيد للنظام. والهدف الرئيسي من هذا العمل هو لمقارنة البحوث والآدبيات السابقة من خلال استعراض هذه الأدبيات وتحديد مزايا وعيوب لكل طريقة في هذه الأدبيات. تم تلخيص النتائج بجدول مقارنة للطرق المختلفة في استعراض التكنولوجيا المستخدمة في معالجة الصور للتمييز بين العملة الورقية.

Comparison Between The Efficient Of Routing Protocol In Flying Ad-Hoc Networks (FANET)

Hadeel M. Taher Alnuami
University of Anbar- Iraq.
hadeilmt@yahoo.com

Abstract

Flying Ad-Hoc Networks (FANETs) is a crowd of Unmanned Air Vehicles (UAVs). The role of the UAV is very developing speedily. Through the advancement of technologies various interesting tasks are likewise related like growth and maintenance cost and incorporation. This technology area is present, which are used for communication purpose. The main characteristics of FANET are flexible, low-cost besides fast to arrange or organize a network. On the other hand, there are the main problems in this category of networks that is the communication between any Unmanned Air Vehicles besides the random movement of UAV in this network. In this paper focused on the mean of FANET network and the main routing protocols on this modern area, then compare between two routing protocol AODV and DSR. The result led to AODV is better than DSR routing in three parameters: PDR, E2E delay and throughput. In addition AODV more appropriate for FANET environment than DSR with different number of nodes in the FANET network.

Keywords- *MANET,VANET, FANET, Routing Protocol.*

Introduction

In case of calamitous occurrence, when there are lucky in centre point that lead the service out or basically not available, for resolving these issues used a group of flying nodes that known as UAVs can provide a speedy deployable in addition self-managed ad hoc network [1]. As shown in figure (1) the flying ad hoc network (FANET) is a subset of ad hoc network like other ad hoc network such as (MANET) and (VANET) on the main features like wireless medium and random deployment but also the FANET have special characteristic to identification of FANET network [2]. FANET may include heterogeneous or homogenous Unmanned air Vehicles (UAVs) that are capable to interconnect with each other in the area, besides interacts through their environments to obtain some kind of valuable information [1]. FANET do not usage, fundamental controlled scheme [3].
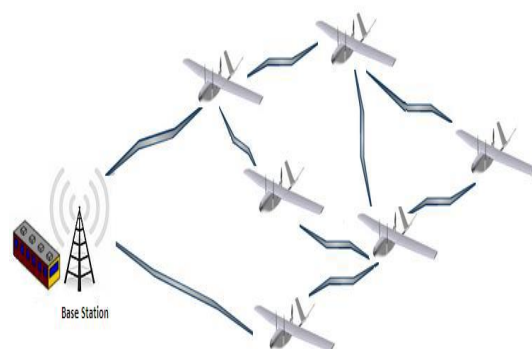
Fig.(1): Flying Ad hoc Network(FANET).

Hadeel .M

1.   Wireless Ad Hoc Network

Mobile Ad-hoc Network: MANET: are crowed of nodes that connected between them by wireless communication channel. In1970 "DARPA" the first concept form of MANET that depended on infrastructure less networks [4]. The nodes are free and random mobile in any deployment changes repeatedly. There are many challenging issues in mobile ad-hoc networks such as power control, security delay sensitivity [3]. As shown in figure (2).

Fig.(2): Mobile Ad hoc Network (MANET).

Vehicular Ad-hoc Network: VANET: is subsection from MANET, each node in VANET called Vehicular on the road (network)[5]. It related with MANET in many features, but also different in other features. The VANET used today's because there are many biggest problems in traffic management [6]. VANET achieved two methods of communication: the first on depended on fixed infrastructure and vehicle node. Another method chastely wireless infrastructureless networks [7]. Vehicular ad- hoc network has numerous application such as: Safety applications (Collision avoidance, Traffic Management and Co-operative driving) and User applications (Electronic toll collection, Entertainment Applications, Internet Access and Locating fuel station) [5]. As shwn in figure (3).

Fig.(3):Vehicular Ad hoc Network(FANET).

Flying Ad hoc Network: FANET is a sub-classification of vehicular ad hoc network. That means the biggest network MANET then VANET after that the FANET came [4]. Because VANET and FANET have the main feature of MANET with some of the differences. The node in FANET called Unmanned Aerial Vehicles(UAV)[8]. Each node in fly network can fly autonomously with no pilot on it, it operated by programmed flight plans or by dynamic automation systems [9]. FANET are infrastructureless networks with no central point. This network has many applications such as location aware services, rescue operations and security services [10]. As shown in table (1) that explain the main difference between types of Ad hoc network.

Table(1):Comparison between Ad-Hoc Networks

AD HOC NETWORK TYPES		
FANET	**MANET**	**VANET**
Node called Unmanned Aerial Vehicle (UAV)	Node called mobile node	Node called Vehicle node
High Movement	Low Movement	Moderate Movement
Very large of nodes consume energy	Limited of nodes consume energy	Limited of nodes consume energy
Rapid deployment	Slow deployment	Rapid deployment
Geospatial localization (GPS, AGPS)	Geospatial localization (GPS)	Geospatial localization (GPS, AGPS)
Lower than MANET node density	Low node density	Higher node density

Hadeel .M

2.   Unmanned Aerial Vehicle (UAV)

FANET have a group of UAV that distinguish as the size is small with fast deployment in addition the flexibility of nodes [11]. The UAV as a team when mobile according to trajectories defined through separable responsibilities that should be allocated to perform a comprehensive mission. There are two types of UAV: The first one called single-UAV or small UAV system that depended on a star deployment network that make UAV is a focus point [5]. An earth node may indirectly interconnect through others over the UAV. The main problem in this topology if the main point (focus point) fails all the system the UAV has to come back to the base [2]. On the other hand, this system has many advantages such as lower cost and speedily than the second type of UAV [3]. Conversely, in multi-UAV systems, the speed low than single system and more cost, but rather than the UAVs can share responsibilities amongst themselves besides this increases the fault tolerance of the UAV system. As the first type, this system also has advantages such as the dynamic topology of the network, but the communication among UVAs in FANETs it's still problematic [7]. This problem will be solved by using two protocols one between UAV and the central point and the second used between the UAVs itself [12]. As shown in table (2) that explain the main difference.

Table (2): The main difference between Multi-UAV System and Small UAV System

UAV Type of FANET		
Feature	**Multi-UAV System**	**Small UAV System**
Cost	Large cost	Lower cost than Multi-UAV
Scalability	Easy	Limited
Speed	High	Low
Small radar cross-section:	Very small radar cross-sections(more than one)	Usually one large radar cross-section
Survivability	Better than if one UAV failed the other UAVs will survive the system.	Less than Multi-UAV System

3.   Routing Protocols On FANET

Routing in FANET as well as MANET and VANET network must be classified by four main modules as in figure (4):
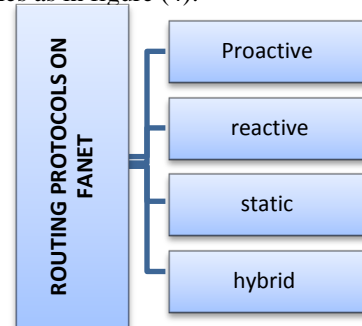
Fig(4):FANET routing protocol.

- **Proactive routing protocol depended on routing table that are from time to time refreshed such as:**
  - Destination Sequenced Distance Vector (DSDV): This routing protocol must be all UAV in FANET network know everything about each other. The technique is different in the process than the main proactive approach because when used this protocol in FANET the sequence number assigned through the target node so as to remove the loop of routing happened via make alterations in the deployment of network [8].
  - Directional Optimized Link State Routing (DOLSR): Any node in the FANET network must be know information about each other node. But this protocol has two messages, the first one control messages that used to know any different in deployment of FANET network[3]. The second one is hello message, which is sent from time to time to check the connect with neighbors in communication region. Multipoint Relay used in DOLSR when somewhat node requirements to transmission the data to other nodes, it will choice an MPR to frontward the routing messages [10].

Journal of AL-Qadisiyah for computer science and mathematics   Vol.10   No.1   Year 2018
ISSN (Print): 2074 – 0204   ISSN (Online): 2521 – 3504

Hadeel .M

- **Reactive routing protocol usually discovers the route on demand only:**
- Dynamic Source Routing (DSR): This routing protocol was applied through Brown et al. In [16]. This Routing based on multi-hop in FANET network. Any source node in FANET save the route to target node on the header of the data. To avoid any confectionary in FANET the UAV transfer the data with a request ID. Apply the DSR on FANET network it cannot be easy[7].
- Ad-hoc On-demand Distance Vector (AODV): AODV is one of famous protocol in reactive routing , the main feature of AODV that keeps one record for any node in the AODV table and AODV keeps only the path of the next hop which maximizes bandwidth in the FANET network. This routing based on three steps, the first one called the discovery process used to discover the route from the source to the target node and to avoid the loop. The second step, transferring the data, in the last step called routing maintaining that used to fix and refresh the routing tables [11].
- **The third routing protocol is static that have a permanent routing table there is no refreshed with time:**
- Load Carry and Deliver Routing (LCAD): LCDR is one of famous routing protocols in FANET network. The method of this protocol depended on transmission information by using flying UAV between two points in a ground. But this transmission must be happened with one hop[1]. The distance between these two point (begin and target) based on the UAV rapidity. On the other hand LCDR secure because only one hop between begin and target nodes[12].
- Multilevel Hierarchical Routing (MLH): This protocol based on UAVs clusters that mean the process of transfer data between the UAVs and a ground station. The cluster head   separate operations between each cluster in specific ranges. This routing protocol useful when large network that is main different from load carry and delivering routing [9].
- Data-Centric Routing (DCR): This routing protocol based on one-to-many that led to communication between some data required by numerous UAVs in the FANET network. As the multilevel hierarchical routing the DCR clusters besides works as follows [6]. This DCR has weakness is the redundant data sent on FANET network. On the other side, the feature of the DCR is the message transfer procedure is not blocked among UAVs that called flow decoupling and the second feature is space decoupling the ID besides the location of the UAVs in FANET network . The last feature, there is no required to be UAVs online entirely time [8].

- **The last one called hybrid routing protocol is a mixture between   proactive in addition to reactive protocol:** such as Zone Routing Protocol (ZRP),Temporarily Ordered Routing Algorithm (TORA)[5].

4.   Application scenario of FANET

Flying Ad Hoc Network (FANET) with built-in sensors to reconnoiter 3D space, the   UAV scheme requirement scan its location and react in real-time to regulate position and formation. Surveillance,   search   and   saving   tasks   in misadventure recovery, and objective localization.

5.   Proposed Solution

In this paper, we proposed system, routing protocols DSR and AODV are designated briefly besides the performance constraints of this protocol are also covered. This part shows how DSR, AODV protocols define mechanisms to their route strategy depended on the reactive category. This proposed system useful to decrease the connected cost in base location control besides efficiency of routing. Any node in FANET achieves protocols on the way to evaluate the performance, these protocols have dissimilar parameters such as delay, bandwidth and overhead. In this system the FANET will select the effective protocol on the way to broadcast the packet as shown in figure(5).
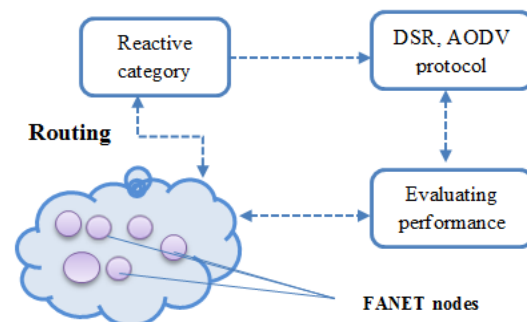
Fig(5):Architecture Diagram.

Hadeel .M

6. Simulation

The NS2 simulator used for calculating, analysing and evaluating the effectiveness with the performance of AODV and DSR. The ns2 have types of connecting protocol such as: UDP, multicast routing and TCP. Also NS2 covered both main type of network like wired and wireless network. Ns2 depended on c++ as backend with OTcI interpreter.

However, these two protocols have different parameter with dissimilar in performance area as follow:

- ▪ **Packet delivery ratio**: it's the ratio of data packet receiving through the targets to those created by the source nodes. The equivalent used for the packet delivery ratio mathematically.

Packet delivery ratio= Total of data packet receiving through the each target/ Total of data packets generated through the each source**.**

- ▪ **End to End delay (E2E Delay):** its depended on the time line. It takes the middling time of the data packets that consume to arrive the target node in FANET. Any delay may be occurs through the way between nodes to reach the target.

The average of the E2E= Total of the time consumed to send packets for each target**/** N.

- ▪ **Throughput:** Its defining the total number of successful data packet delivery above a Communication channel.

Throughput= N/1000

Where N is the number of bits reached successfully through every target.

Table (3): Simulation Parameters

NS2	
Parameter	**Value**
Simulator	NS2 (Version-2.35)
Protocols	AODV and DSR
Channel Type	Channel/Wireless Channel
Simulation duration	150s
Traffic Type	CBR
Data Payload	512 Bytes / packet
Number of Nodes per simulation	50, 100, 200
Node Speed	5, 15,25 (Meter/Sec) Max of

7. Analysis and Examination

The result, as estimation shows the AODV routing is better than DSR routing protocol because the performance of the DSR is decreasing frequently whereas the packet delivery ratio is increasing in AODV. On the other hand the delay in AODV will be highest than DSR in FANET network. In throughput metric the AODV routing is effective at what time compared to DSR routing when apply on FANET environment as in figure (6),(7).
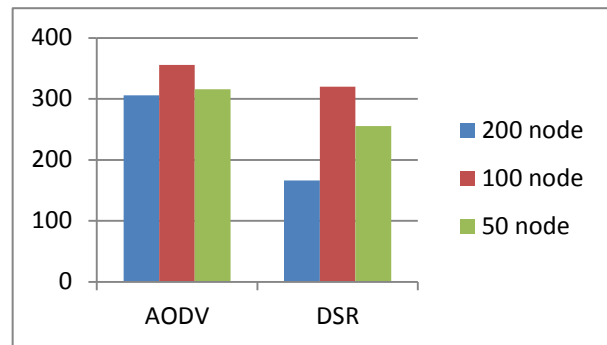
Fig(6):Throughput between AODV and DSR.
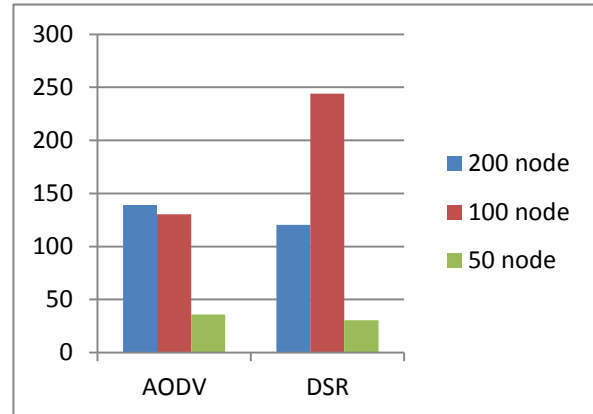
Fig(7). E2E delay between ADOV and DSR.

Conclusion

The paper has a study to the new network called FANET its modern area developing fast, we compare between the main ad- hoc wireless network VANET, MANET and FANET. Furthermore, Mobility is the greatest interesting problematic for FANET network. On the other hand, in this research there are different parameter in different number of nodes with two types of routing protocol. The estimation result focus on the AODV routing is better than DSR routing on FANET network, because the first routing is flexible for the environment of the FANET and could be developing this protocol to be more suitable.

In future we could develop many ideas in this modern FANET area such as:

1- Merge between two routing protocols and apply these two routing on FANET network and made new routing just for FANET.
2- Apply the Decentralized Cloud Approach in FANET network.
3- Secure the path between UAVs and station to prevent any malicious node from reach to any data. This point important, specially in military application.
4- Optimize on the UAVs in FANET.
5- Calculate the packet drop in ADOV and DSR in FANET .
6- Approve the DSR and AODV routing used in FANET when distance is long of communication for coverage area.

References

1. K. Kumari, B. Sah and S. Maakar, "A Survey: Different Mobility Model for FANET", International Journal of Advanced Research in Computer Science and Software Engineering, 2015.
2. Naveen, S. Maakar, "Concept of Flying AD-Hoc Network: A Survey", Proceedings of National Conference on Innovative Trends in Computer Science Engineering (ITCSE-2015) held at BRCMCET, Bahal on 4th April 2015.
3. M. Yassein and N.Damer, "Flying Ad-Hoc Networks: Routing Protocols, Mobility Models,Issues",International Journal of Advanced Computer Science and Applications, Vol. 7, No. 6, 2016.
4. C. Barrado, R. Messeguer, J. López, E. Pastor, E. Santamaria and P. Royo, "Wildfire monitoring using a mixed air-ground mobile network", IEEE Pervasive Computing, 2010.
5. Singh et al,"A Comprehensive Survey on Fanet : Challenges and Advancements", International Journal of Computer Science and Information Technologies, 2015.
6. Md. Hasan, Md. Hossain and M. Atiquzzaman, "On the Routing in Flying Ad hoc Networks", IEEE Proceedings of the Federated Conference on Computer Science and Information Systems, 2015.
7. K. Kumari, S. Maakar and B. sah, "A Brief Survey of Mobility Model for FANET", National Conference on Innovative Trends in Computer Science Engineering held at BRCMCET4th ,April 2015.
8. Sudip, Misra and Gopidi Rajesh," Bird Flight- Inspired Routing Protocol for Mobile Ad Hoc Networks", ACM Transactions on Autonomous and Adaptive Systems, Vol. 6, No. 4, Article 25, October 2011 .
9. G. Heitz, D. Floreano and B. Rimoldi " Dynamic Routing for Flying Ad-Hoc Networks (FANETs): A survey," Ad Hoc Networks, vol. 11, no. 3, pp. 1254–1270, 17 June 2014.
10. I. Bekmezci, O. Sahingoz, Ş Temel,"Flying ad-hoc networks (FANETs): A survey." Ad Hoc Networks 11. No 3 1254-1270,2013.
11. O. KSahingoz. "Routing ptocols in flying Ad-hoc networks (FANETs): Concepts and challenges". Journal of Intelligent & Robotic Systems, pp. 513-27.April 2014.
12. Ozgur, Koray and Sahingoz, "Networking Models in Flying Ad-Hoc Networks (FANETs): Concepts and Challenges", Springer Science, September,2013.

مقارنة بين كفاءة بروتوكول التوجيه في الشبكات الجوية المخصصة (فانيت)

هديل محمد طاهر النعيمي
جامعة الانبار- العراق

المستخلص :

الشبكات الجوية المخصصة (FANET) هي عبارة عن مجموعة من المركبات الجوية بدون طيار (الطائرات بدون طيار) تحلق في السما وتشكل على هيئة شبكة تدعى FANET وكل طائرة تمثل ك(Node) في الشبكة. تطور هذا النوع من الشبكات الطائرات بدون طيار تطورا سريعا. ان تطور هذا النوع من التكنولوجيا يتطلب مهام او تحديات مختلفة عن الشبكات الاخرى مثل تكاليف النمو والصيانة والإندماج. يعد هذا النوع من الشبكات ذات خصائص ومميزات تجعلها مختلفة عن الشبكات الاخرى حيث ان من اهم صفاتها هي المرونة العالية ، منخفضة التكلفة، إلى جانب اخر انها سريعة الترتيب أو تنظيم الشبكة. ومن ناحية أخرى، هناك مشاكل رئيسية في هذه الفئة من الشبكات و هي التواصل بين المركبات الجوية بدون طيار بعضها مع بعض بالإضافة إلى الحركة العشوائية للطائرات بدون طيار في هذه الشبكة.

في هذا البحث تم التركيز على متوسط شبكة فانيت وبروتوكولات التوجيه الرئيسية على هذه التكنولوجيا الحديثة، ثم قارن بين اثنين من بروتوكول التوجيه AODV و DSR. أدت النتيجة إلى AODV أفضل من DSR التوجيه في ثلاث من اهم المقاييس الاساسية في الشبكات وهي : PDR ، E2E التأخير والإنتاجية(Throughput). وبالإضافة إلى ذلك AODV أكثر ملاءمة لبيئة فانيت من DSR مع عدد مختلف من العقد(Nodes) في شبكة فانيت.

Video Frames Edge Detection of Red Blood Cells: A Performance Evaluation

Karrar Neamah Hussein
Dir. Scholarship & Cultural Relations
Baghdad, Iraq
karrarneamah@yahoo.com

Abstract

The boundary structure (shape and size) and numbers of Red Blood Cells (RBCs) play a significant role in controlling human physiology. Several blood related diseases including sickle hemoglobin, polycythemia, thalassemia, anemia, and leukemia that occur due to the alteration of RBCs structures need precise detection, analysis, and subsequent inhibition. Diverse boundary analyses that have already been developed to detect the frames edge of blood samples remained ineffective. Thus, an automated system needs to be designed for exact detection of the RBCs edges. The edges being the main features of image often provide vital information to separate regions within an object or to detect changes in illumination. Accordingly, edge detection is regarded as an important step in the analysis of images and extraction of valuable information. In this paper, we evaluated the performance of video frames edge detectors and compared it with different gradient based techniques including Robert, Sobel, Prewitt and Canny, Zero-crossing (Laplacian, Gaussian and fuzzy logic) by applying them on video of RBCs. Two criteria such as mean square error (MSE) and peak signal to noise ratio (PSNR)were exploited to achieve good quality of video frames edge detectors for RBCs. Canny edge and fuzzy logic based techniques revealed the optimum performance towards the detection of video frames edge of RBCs.

Keywords: Edge detection, Fuzzy logic, Video frames edge, MSE, PSNR.

Karrar .N

1.   Introduction

In recent times, digital image processing have been received a great attention in diversified fields [1]. Including computer vision office, industrial automation, face detection, features detection, lane departure warning system, remote sensing, natural resources survey, management, criminology, astronomy, meteorology and medical imaging [2]. Cumulative use of digital imaging systems has contributed significantly in the domain of medical diagnostics and greatly expanded in health care sector. Thus, computer aided diagnostic appeared as a routine means in clinical field [3]. Therefor rapid advancement in the electronic and photonic technology has allowed the invention of sophisticated diagnostic tools including Magnetic Resonance Imaging (MRI) or Computed Tomography (CT). Initially developed analogue imaging methods such as endoscopy or radiography are presently supported with digital sensors [4]. Despite such progress, a fully automated and accurate technique for RBCs edges detection is far from being developed.

Digital Images (DIs) are comprised of individual pixels, wherein the discrete color values or brightness are assigned. Using appropriate information communication networks and protocols, such DIs can be processed efficiently and made accessible at several places simultaneously. These protocols include picture archiving and communication systems (PACS) as well as the digital imaging and communications in medicine (DICOM) [5]. In medicine, the DI processing is now used for analyzing a significant volume of images to achieve high quality information for disease diagnosis and subsequent treatment. This helps considerably to the physicians, researchers, and medical practitioners to derive more diagnostically useful information [6].

Numerous blood related human diseases that occur from RBCs structural changes need to be detected, analyzed, and cured. RBCs are rich in iron-containing biomolecule called hemoglobin which bind oxygen and responsible for the red color of the blood. Approximately 2.4 million new erythrocytes are produced per second in an adult [7]. Human diseases are expressed through the abnormality or anomaly of RBCs. Changes in the RBCs shape, size, or number often cause diseases such as Sickle Hemoglobin, Sickle cell disease, Polycythemia, and Thalassemia. In this regard, an efficient blood samples frames edge detection tool is prerequisite. The image edges that render central information require careful evaluation.

In this paper, we assessed the performance of video frames edge detectors for RBCs and compared it with various existing art-of-the techniques. RBCs being the most significant components of human blood for delivering oxygen to the body tissues are considered in the present study.

2.   Edge Detection Techniques for Red Blood Cells [RBCs]

Over the years, diverse RBCs edges detection techniques have been developed such as Robert, Sobel, Prewitt, Laplacian of Gaussian (LoG), Canny and Fuzzy Logic (FL). It is vital to focus on the various RBCs edges detection preprocessing steps to make a systematic comparison of the resulting edges. In the present method, first the videos of red blood cells are utilized under a microscope. Then, the input video files are converted into frames (still images).

Karrar .N

Afterward, the noise from these frames is removed using median filter [8]. Next, the thresholding method is used to change these images into grayscale with a resolution of (300×220) pixels. Outcomes from each of the abovementioned edge detection technique are compared using two criteria. The quality and efficiency of these edge detector schemes are evaluated in terms of mean square error (MSE) and peak signal to noise ratio (PSNR). Figure 1 depicts the basic architecture of the edge detection scheme used in this study.
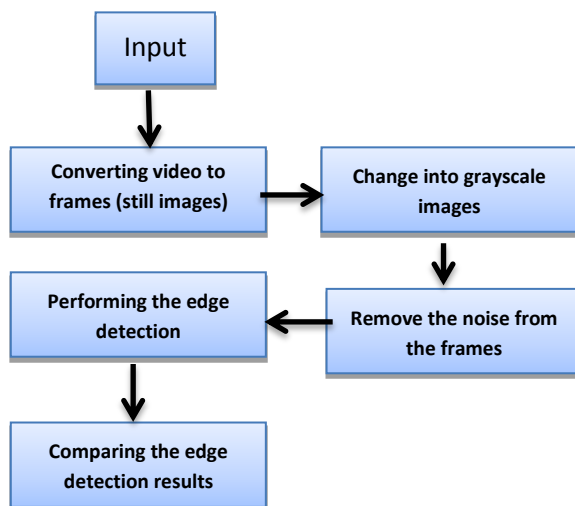
Figure 1: Schematic presentation showing the workflow for edge detection scheme using video file.

Median filter has been used to remove the noise, which is very useful for digital image processing applications. It consists of a window slides through the data and the median value inside the window acts as output of the filter. Being nonlinear in nature, median filter possesses several advantages including the maintenance of the edge and efficiency of noise removal with strength against impulsive type noise [9].

It is considered as one type of smoothing techniques similar to linear Gaussian filtering. Although all such filters are efficient in eliminating the noise in the smooth regions of the signal but they affect negatively at the edges. Thus, to preserve the properties of the video frames edges the median filter is selected [10].

3.   Development of Edge Detectors

Edge detection process can reduce the amount of data in an image by simultaneously preserving the structural information involving object boundaries. Due to these reasons edge detectors are greatly beneficial in image analysis operations and object recognition [11]. Presently, several algorithms are available for edges detection, wherein each one has some advantages and disadvantages over the others. For instance, Robert, Sobel and Prewitt operators are based on the intensity gradient magnitude calculation at each image pixel. In such schemes, the gradient value is compared to the threshold value. If the value of the gradient is higher than a threshold value then a pixel location is classified as an edge, otherwise the pixel location is specified as not an edge [12].

The Laplacian of Gaussian operators are applied by choosing one mask and making a convolution to the original image with the mask. The positive or negative sign of the outcome from two adjacent pixel locations renders directional information in terms of brighter side of the edge. Subsequently, zero crossing is utilized to determine the alteration through zero in the values of the edges points [13]. Wide usage of these operators is limited by their sensitiveness to noise. To surmount the noise problems, Canny proposed a method where image convolution was used with the first order derivatives of Gaussian filter for smoothing in the local gradient direction followed by edge detection and thresholding[14].

3.1   Roberts Edge Detector

This is a simple and fast detection scheme for 2-D spatial gradient measurement on the image. It selects the areas of high spatial gradient, which often conform to the edges. The input of the Roberts operator is a grayscale image, whereas each pixel value in the output specifies the estimated absolute quantity of spatial gradient of the original input image at that point [11,12]. Theoretically, Roberts's operator is comprised of a pair of (2×2) convolution masks as illustrated in Figure 2.

1+	0
0	-1

0	1+
-1	0

Gy   *Gx*
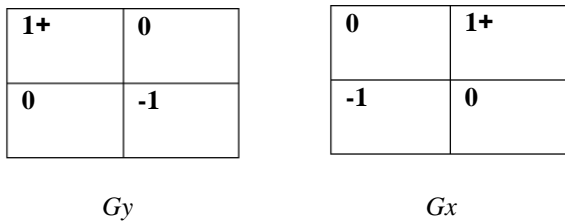
Figure 2: Roberts Cross convolution masks.

These masks have been proposed to respond the maximum of edges working in 45° to the pixel grid, where one mask is used for each of the two vertical orientations. The masks can be used individually to the input image for separate measurements of the gradient contents in each direction (called *Gx* and *Gy*) [12]. Mathematically, Roberts's operator is defined as:

$$G(x,y) = \left\{ \left[\sqrt{f(x,y)} - \sqrt{f(x+1,y+1)} \right]^2 - \left[\sqrt{f(x+1,y)} - \sqrt{f(x,y+1)} \right]^2 \right\}^{\frac{1}{2}} \quad (1)$$

3.2   Sobel Edge Detector

This operator performs a 2-D spatial gradient measurement on an image. It focuses on the areas of high spatial gradient that match to the edges. Generally, it is used to estimate the absolute gradient magnitude at each point in an original grayscale image. This operator is consisted of a pair of (3×3) convolution masks as displayed in Figure 3,

where the first mask is just the second one rotated by 90°.Sobel operator resembles the Roberts cross operator.

$$Gx = \begin{bmatrix} -1 & 0 & +1 \\ -2 & 0 & +2 \\ -1 & 0 & +1 \end{bmatrix} \quad Gy = \begin{bmatrix} +1 & +2 & +1 \\ 0 & 0 & 0 \\ -1 & -2 & -1 \end{bmatrix}$$

Figure 3: Sobel convolution masks.

These kernels have been proposed to respond the maximum of edges working horizontally and vertically relative to the pixel grid with one mask for each of the two vertical directions. These masks can be used individually to the input image, to obtain discrete measurements of the gradient component in each direction (called *Gx* and *Gy*). It is used to calculate the absolute magnitude of the gradient at each pixel and the direction of that gradient [14]. The edge magnitude and the edge direction are defined via the relation:

$$\text{EDGE MAGNITUDE} = \sqrt{S_1{}^2 + S_2{}^2} \quad (2)$$

$$\text{EDGE DIRECTION} = \tan^{-1}\left(\frac{S_1}{S_2}\right) \quad (3)$$

3.3   Prewitt Edge Detector

Prewitt operator is used for detecting two types of edges such as Horizontal and Vertical. This operator produces an image, wherein the higher grayscale value refers to the existence of an edge between two objects. This operator is similar to the Sobel operator but with different mask coefficients. Besides, it contains a pair of (3×3) convolution masks as follows:

$$Gx = \begin{bmatrix} -1 & 0 & +1 \\ -1 & 0 & +1 \\ -1 & 0 & +1 \end{bmatrix} \quad Gy = \begin{bmatrix} +1 & +1 & +1 \\ 0 & 0 & 0 \\ -1 & -1 & -1 \end{bmatrix}$$

Figure 4: Prewitt convolution masks.

At each pixel location, two numbers are found with p1 (corresponding to the result from the vertical edge mask) and p2 (corresponding to the result from the horizontal edge mask). These numbers are used to determine the edge magnitude and the edge direction using the expression[15].

$$EDGE\ MAGNITUDE = \sqrt{P_1{}^2 + P_2{}^2} \quad (4)$$

$$EDGE\ \ DIRECTION = \tan^{-1}[\tfrac{P_1}{P_2}] \qquad (5)$$

3.4 Laplacian of Gaussian

The Laplacian of an image focuses on the regions of intensity that has fast change and thus useful for detecting the edges. To minimize the noise sensitivity of an image the Laplacian is often utilized with a Gaussian Smoothing filter. Usually, this operator uses a single gray level image as input and produces a gray level image as output. The Gaussian function is used as low-pass smoothing filter of the image and the Laplacian operator acts as high-pass filter according to the second derivative of zero to detect the edges. Gaussian filter function is defined as [16]:

$$LOG(x,y) = -\frac{1}{\pi\sigma^4}\left[1 - \frac{x^2+y^2}{2\sigma^4}\right]e^{-\left(\frac{x^2+y^2}{2\sigma^4}\right)} \quad (6)$$

After the noise minimization from the input image using Gaussian filter, the Laplacian convolution masks are applied on the image. Afterward, the threshold value is calculated. Finally, the zero crossing method is applied to determine the change through zero in the values of the edges points [15]. Generally, three small masks are used as depicted in Figure5.

$$\begin{bmatrix} 0 & -1 & 0 \\ -1 & 4 & -1 \\ 0 & -1 & 0 \end{bmatrix} \quad \begin{bmatrix} -1 & -1 & -1 \\ -1 & 8 & -1 \\ -1 & -1 & -1 \end{bmatrix} \quad \begin{bmatrix} -2 & 1 & -2 \\ 1 & 4 & 1 \\ -2 & 1 & -2 \end{bmatrix}$$

Figure 5: Laplacian convolution masks.

3.5 Canny Edge Detector

This edges detection technique is based on three criteria. After converting an input image into gray image, the Gaussian convolution is used for noise reduction and to smooth image. The maximum value of the first derivative corresponds to the minimum of the first derivative. It means that the points with radical change of gray-scale (strong edge) and points with simple change of grayscale (weak edges) correspond to the second derivative zero-crossing point. Thus, these two thresholds are used to detect strong edges and weak edges. Actually, the Canny algorithm is not exposed to noise interference due to its true weak edges detection capacity [14,17].

$$G''(X) = \left(-\frac{X}{\sigma^2}\right)e^{-\left(\frac{X^2}{2\sigma^2}\right)} \qquad (7)$$

3.6   Fuzzy Logic

Fuzzy logic (FL) is defined as a superset of classical (Boolean) logic which are expanded to handle the concept of partial time values between completely true and *completely false*. It deals with reason that is approximate rather than exact, where variables of FL may have a true value that ranges between 0 and 1. Certainly, FL is a powerful problem solving technique with diverse applicability, especially in the fields of control and decision making [18].

Fuzzy image processing can be defined as a collection of all approaches that recognize and represent the images. The representation and processing of image based on the chosen fuzzy method and on the problem under consideration. In most of these techniques, adjacent points of pixels are assumed in some classes and then fuzzy system inference are implemented using suitable membership function defined for each class.

Karrar .N

Fuzzy image processing is comprised of three main stages such as image fuzzification, fuzzy technique, and image defuzzification. The fundamental step of fuzzy image processing is the modification of membership values. Therefore, the coding of image data (fuzzification) and decoding of the results (defuzzification) are the vital steps for image processing using FL [19].

Edges in the images that constitute a significant gray level change needs precise detection. For edge detection a set of nine pixels which is a part of (3×3) or (5×5) window of an image to a set of fuzzy conditions are useful to focus on all the edges of an image. In the fuzzy edge detection, points affiliated to a common area must be white, otherwise they must be black, where black and white are the fuzzy variables. For integrated area concept, the intensity variation is considered between the pixel at the kernel of the neighborhood and its neighbors. This helps to compare the pixels values, which are present on the edge in a gray scale image. Figure 6 provides a graphical representation of the rules used in FL where ZE is the variety of the independent variables of the fuzzy set. The box leveled Z_5 represents the intensity of the center pixel which is determined to be the output value with WH (white) or BL (black) [20].
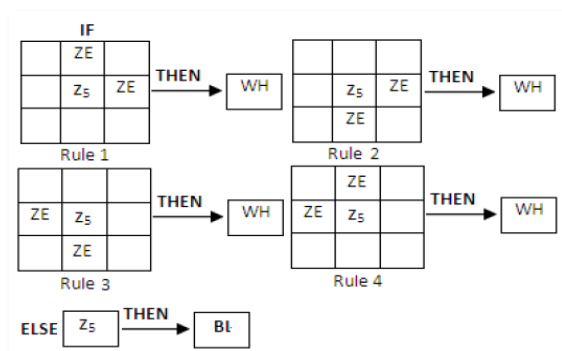
Figure 6: Schematic representation showing the rules of FL.

4.   Parameters for Performance Evaluation of the Edge Detection Method

4.1   Mean Squared Error (MSE)

Generally, is defined as the difference between the estimated and the true value of the quantity under study. MSE can be match to the predicted value of the squared error loss. The MSE (estimated) of the predictor is defined as:

$$MSE = \frac{1}{N}\sum_{i=0}^{n}(\hat{Y}_i - Y_i)^2 \quad (8)$$

where $\hat{Y}$ is a vector of n predictions, Y is the vector of the true values, and N is the total number of realizations. The MSE of the estimator is defined as:

$$MSE(\breve{\boldsymbol{\theta}}) = E[(\breve{\theta} - \theta)^2] \quad (9)$$

where θ is the computed magnitude of the parameter for a given sample (sample-dependent) and $\breve{\theta}$ is the corresponding unknown value. This definition is based on the unidentified parameter. The MSE in this context is a property of an estimator (of a way to get an estimate) the MSE is equivalent to the total of the difference and the squared bias of the estimator or of the expectations, in the condition of the MSE of an estimator [21]. It yields:

$$MSE(\breve{\theta}) = Var(\breve{\theta}) + \left(Bias(\breve{\boldsymbol{\theta}},\theta)\right)^2 \quad (10)$$

4.2 Peak Signal-to-Noise Ratio (PSNR)

Commonly, the PSNR is used to measure the quality of reconstruction of loss compression codecs where the signal is the main data and the noise is the error that is introduced by compression. Therefore, when comparing compression codecs, PSNR approximates human perception of reconstruction quality. Though a higher PSNR typically refers to restructuring of higher quality but in some conditions it differs [22].

Karrar .N

The MSE and the PSNR are the two metrics used to measure error standards for determining the image quality or comparing among images. The MSE determines the cumulative squared error between the original image and the resulting image. The PSNR is a measure of the peak error. A lower MSE value indicates an accurate image features. To obtain the PSNR values, first the MSE values of the block are computed using:

$$MSE = \frac{\sum_{M,N}[I_1(m,n)-I_2(m,n)]^2}{M*N} \quad (11)$$

Where M and N represent the number of rows and columns in the input images, respectively. The block calculates the PSNR using the relation:

$$PSNR = 10 \log 10 \left(\frac{R^2}{MSE}\right) \quad (12)$$

Where R is the maximum fluctuation in the input image data type [23].These popular standards are chosen and the performance evaluation of RBCs video frames edges detection schemes.

5.   Results and Discussion

Experiments are conducted using MATLAB code to determine the quality and clarity of edge detection in the video image for RBCs boundaries. Two videos for RBCs under a microscope are considered. The blood samples are collected from laboratory. One sample contained normal RBCs with521 frames in 16 minutes and the other enclosed abnormal RBCs with 219 frames in 9 minutes. Each video consisted of many frames which are randomly chosen and applied in the experiments. First, the videos are changed to frames and then the colored frames are changed to grayscale images. Next, the noise from the frames is removed using median filter to preserve the edges.

Afterward, all the aforementioned edge detectors are applied on the frames. The edge pixels to size ratio of the image, MSE and PSNR for each operator is calculated to determine the effectiveness of the operator in detecting the edges of the RBCs. Experimental results are summarized in Table 1.Figure 7 compares the original color image with the converted gray scale image after using the median filter. Figures 8-13 compares the outcome of various edge detectors with MSE for normal RBCs frame number 250.

Table 1: Comparative analysis among various edge detectors for the second sample (frame number 250) of normal RBCs under microscope.

Edge detector	Ratio of edge pixels to size of image (%)	MSE	PSNR
Roberts	29.22	0.0321	63.2675
Sobel	31.74	0.0282	63.6363
Prewitt	31.74	0.0270	63.7998
LoG	48.40	0.0268	63.8607
Canny	75.43	0.0265	63.8381
Fuzzy	64.14	0.0226	63.5697
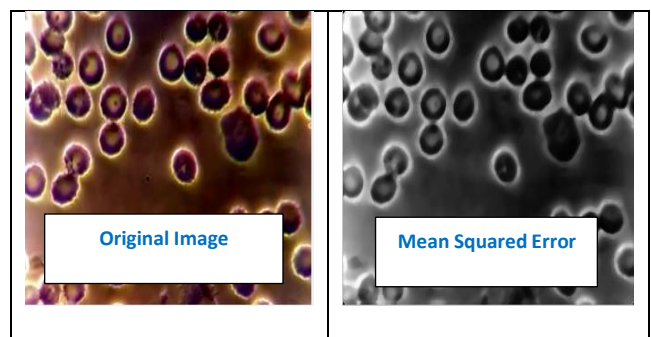
Figure 7: The original image and median filter image for normal RBCs frame number 250.
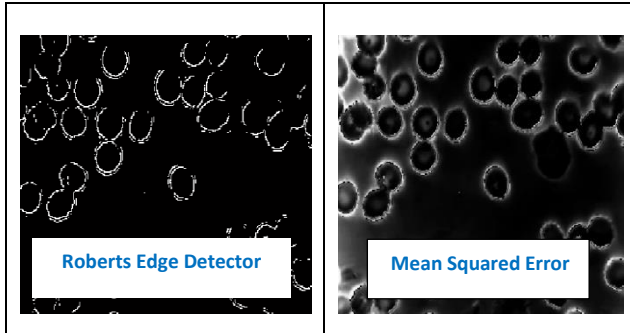
Figure 8: Roberts edge detector and MSE   for normal RBCs frame number 250.
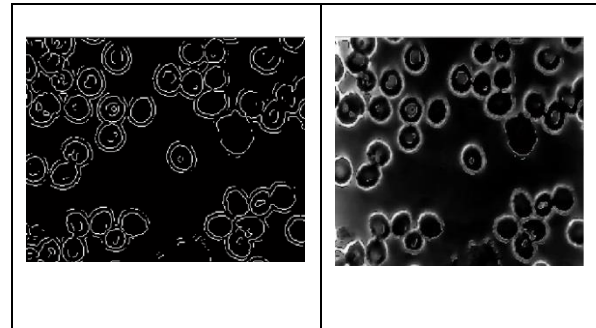
Figure 11: LoG Edge Detector and MSE for normal RBCs frame number 250.
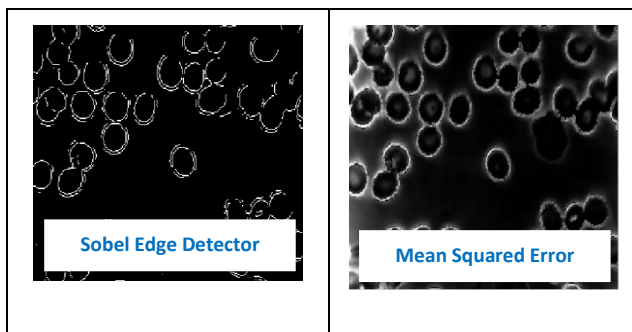
Figure 9: Sobel Edge Detector and MSE for normal RBCs frame number 250.
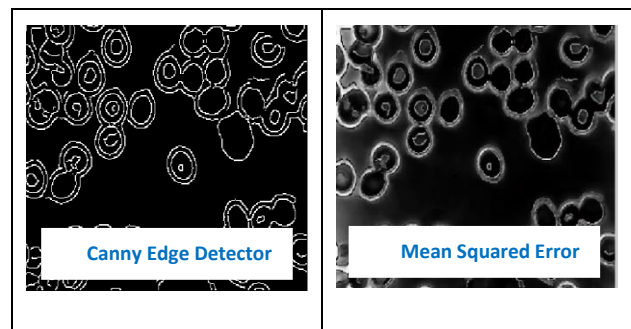
Figure 12: Canny Edge Detector and MSE for normal RBCs frame number 250.
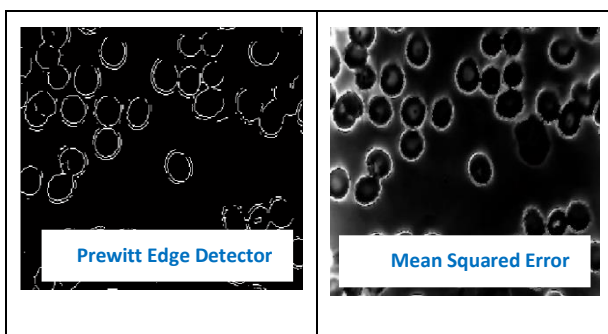
Figure 10: Prewitt Edge Detector and MSE for normal RBCs frame number 250.
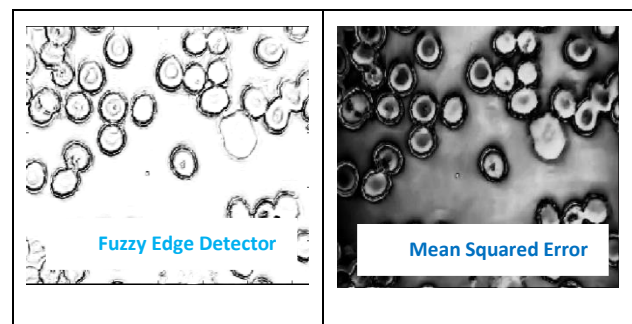
Figure 13: Fuzzy Edge Detector and MSE for normal RBCs frame number 250.

Karrar .N

6.   Performance Evaluation

In the present study, two medical videos of Red blood cells (RBCs) are selected. The first one is for normal RBCs and the other is for abnormal RBCs. After converting these videos to frames, grayscale images are obtained and the noise is removed. Finally, all edge detectors are applied to these images. The original medical images (frames) of normal RBCs from video and subsequent removal of noise from the images using median filter. Figure 8 revealed a clear difference in terms of clarity. Similar observations are made for abnormal RBCs from video and for noise removed images using median filter. The images for edges which are obtained by applying Roberts, Sobel, Prewitt, LoG, Canny and fuzzy edges detectors on all RBCs frames and the calculated mean squared error displayed a clear difference among various method (Figures 8-13).

The results (Table 1) for the ratio of edge pixels to size of image, mean squared error (MSE) and peak signal-to-noise ratio (PSNR) for the resultant image revealed the improvement of one method over the other. An increase in the ratio of edge pixels to size of image indicated the enhanced efficiency of the edge detector and vice versa. Moreover, any lacking of MSE signified the decreased efficiency of the edge detector and vice versa. An increase in the PSNR signified the enhanced efficiency of the edge detector and vice versa. In the Roberts detector, the edges of the object are not smooth enough. Sobel detector produced less information of edges. Prewitt detector provided better edges than Sobel and Roberts.

Laplacian of Gaussian detector rendered useful information of edges, while Canny created better edges with higher PSNR values, which confirmed the superiority of the method in RBCs frames edge detection. The FL revealed great accuracy in detecting the edges of RBCs and achieved lowest values of MSE, indicating its lacking of error estimation in the edge detection. Furthermore, FL displayed some distinct features than others operators, without same limitations like fixed edge thickness and threshold. It is established that FL is flexible to implement where the edge thickness can simply be changed by changing the rules and output parameters.

7.   Conclusions

This paper compared the performance of various schemes useful for RBCs video frames edge detection. Using edge detection, the sharp discontinuities are located, where such discontinuities are sudden changes in pixel intensity that distinguish the boundaries of objects in an image. The boundaries of RBCs are examined to determine whether they are normal or abnormal because it is known that several human diseases occur due to the change in the shape, size or number of RBCs. The efficiency of various operators in detecting the borders of RBCs is compared. MATLAB R2014a coding is used for frames of video and the computational results are analyzed in terms of MSE and PSNR. Based on the experimental results, the following conclusions are drawn:

i)   Robert operator produced smooth edges of RBCs as compared to other operators.

ii)   Sobel provided less information of edges for RBCs than other operators. It is more sensitive to the diagonal edge is than the horizontal one. Although Sobel edges spurious but they are relatively less intense compared to original one.

iii) Roberts operator has missed a few edges and the Sobel operator detected thicker edges than Robert. This indicated that Sobel is slightly better than Roberts scheme.

iv)   Prewitt operator rendered better information than Robert but is more sensitive to horizontal and vertical edges. All images of RBCs showed a difference in the ratios of pixels edges to Sobel and Prewitt. Prewitt and Sobel detectors approximately revealed same level of performance without significant difference.

v)   Canny detector exhibited greatly smooth edges of RBCs and performs better than all others. Images evaluation showed that a low threshold produces the false edges and high threshold misses the important edges. Moreover, Canny for edge detection is computationally more expensive than Laplacian of Gaussian (LOG), Sobel, Prewitt, and Robert's operator because of the chosen three criteria. In short,

vi)   Canny revealed a better edge detection than other operators. The highest value of PSNR clearly showed that the edge detected image in Canny has enclosed less noise than other operators.

vii) Laplacian of Gaussian (LoG) provided quite similar information to Canny, but the edges are unsmooth.

viii) FL operator revealed lowest MSE, indicating its highest accuracy for video frames edges detection of RBCs. It is asserted that the Canny and FL detectors are appropriate to use as edge detectors for RBCs.

References

[1]   Adrian, R. J. (2005). Twenty Years of Particle Image Velocimetry. Experiments in Fluids, 39(2), 159-169.

[2]   National Research Council. (2013). Future us Workforce For Geospatial Intelligence. National Academies Press.

[3]   Szabo, T. L. (2004). Diagnostic Ultrasound Imaging: Inside Out. Academic Press.

[4]   Dougherty, G. (2009). Digital Image Processing For Medical Applications. Cambridge University Press.

[5]   Deserno, T. M. (2010). Fundamentals of Biomedical Image Processing. In Biomedical Image Processing (Pp. 1-51). Springer Berlin Heidelberg.

[6]   Mair, T. S., & Kinns, J. E. N. (2005). Deep Digital Flexor Tendonitis in the Equine Foot Diagnosed By Low- Field Magnetic Resonance Imaging In The Standing Patient: 18 Cases. Veterinary Radiology & Ultrasound, 46(6), 458-466.

[7] Underwood, E. (2012). Trace Elements in Human and Animal Nutrition. Elsevier. 2, 459-461.

[8] Cheng, E. D., Challa, S., & Chakravorty, R. (2011). Parallel Microscopic Cell Image Segmentation and Multiple Fusions. International Journal of Signal And Imaging Systems Engineering, 4(2), 96-114.

[9] Jayaraj, V., & Ebenezer, D. (2010). A New Switching-Based Median Filtering Scheme and Algorithm For Removal Of High-Density Salt And Pepper Noise In Images. Eurasip Journal on Advances in Signal Processing, 2010(1), 690218.

[10] Arias-Castro, E., & Donoho, D. L. (2009). Does Median Filtering Truly Preserve Edges Better Than Linear Filtering. The Annals of Statistics, 1172-1206.

[11] Kaur, E. K., Mutenja, V., & Gill, E. I. S. (2010). Fuzzy Logic Based Image Edge Detection Algorithm in Matlab. International Journal of Computer Applications, 1(22), 55-58.

[12] Nadernejad, E., Sharifzadeh, S., & Hassanpour, H. (2008). Edge Detection Techniques: Evaluations and Comparison. Applied Mathematical Sciences, 2(31), 1507-1520.

[13] Huang, C. Y., & Wu, M. J. (2006). Image Segmentation. Ece, 533, 1-3.

[14] Vincent, O. R., & Folorunso, O. (2009, June). A Descriptive Algorithm For Sobel Image Edge Detection. In Proceedings of Informing Science & It Education Conference (Vol. 40, Pp. 97-107).

[15] Bhatia, M., Yadav, D., Gupta, P., Kaur, G., Singh, J., Gandhi, M., & Singh, A. (2013, September). Implementing Edge Detection For Medical Diagnosis of A Bone In Matlab. In Computational Intelligence and Communication Networks, 2013 5th International Conference on (Pp. 270-274). IEEE

[16] Vincent, O. R., & Folorunso, O. (2009, June). A descriptive algorithm for sobel image edge detection. In Proceedings of Informing Science & IT Education Conference (Vol. 40, pp. 97-107).

[17] Maini, R., & Aggarwal, H. (2009). Study and Comparison of Various Image Edge Detection Techniques. International Journal of Image Processing , 3(1), 1-11.

[18] Mohanty, P. K., & Parhi, D. R. (2013). Controlling the Motion of An Autonomous Mobile Robot Using Various Techniques: A Review. Journal of Advance Mechanical Engineering, 1(1), 24-39.

[19] Aborisade, D. O. (2011). Novel Fuzzy Logic Based Edge Detection Technique. International Journal of Advanced Science and Technology, 29(1), 75-82.

[20] Khaire, P. A., & Thakur, N. V. (2012). A Fuzzy Set Approach For Edge Detection. International Journal of Image Processing, 6(6), 403-412.

[21] Hoerl, A. E., & Kennard, R. W. (2000). Ridge regression: biased estimation for nonorthogonal problems. Technometrics, 42(1), 80-86.

[22] Gupta, M., & Garg, A. K. (2012). Analysis of image compression algorithm using DCT. International Journal of Engineering Research and Applications $(IJERA)$, 2(1), 515-521.

[23] Huynh-Thu, Q., & Ghanbari, M. (2008). Scope of validity of PSNR in image/video quality assessment. Electronics letters, 44(13), 800-801.

إطارات الفيديو كشف حافة خلايا الدم الحمراء: تقييم الأداء

كرار نعمه حسين
دائرة البعثات والعلاقات الثقافية
karrarneamah@tahoo.com

المستخلص :

يلعب هيكل الحدود (الشكل والحجم) وأعداد خلايا الدم الحمراء (كرات الدم الحمراء) دورا هاما في السيطرة على فسيولوجيا الإنسان. العديد من الأمراض المرتبطة بالدم بما في ذلك الهيموغلوبين المنجلي، كثرة الحمر، الثلاسيميا، وفقر الدم، وسرطان الدم التي تحدث بسبب تغير هياكل كرات الدم الحمراء تحتاج الى الكشف الدقيق والتحليل الاحق. تحليلات حدود متنوعة التي تم تطويرها بالفعل للكشف عن حافة إطارات عينات الدم ظلت غير فعالة. وبالتالي، يجب تصميم نظام آلي للكشف الدقيق عن حواف كرات الدم الحمراء. الحواف كونها السمات الرئيسية للصورة غالبا ما توفر معلومات حيوية لفصل المناطق داخل كائن أو للكشف عن التغيرات في الإضاءة. وبالتالي، يعتبر الكشف عن الحافة خطوة هامة في تحليل الصور واستخراج المعلومات القيمة. في هذا البحث ، قمنا بتقييم أداء إطارات الفيديو كاشفات الحافة ومقارنتها مع تقنيات التدرج مقرها مختلفة بما في ذلك روبرت، سوبيل، بريويت و كاني، صفر عبر (لابلاسيان، غاوسية والمنطق غامض) من خلال تطبيقها على الفيديو من كرات الدم الحمراء. وقد استغل معياران من قبل متوسط الخطأ المائل (MSE) ونسبة الإشارة إلى الضوضاء (PSNR) لتحقيق نوعية جيدة من أطر الفيديو للكشف عن الحافة لكرات الدم الحمراء. حافة وتقنيات منطقية غامض كشفت الأداء الأمثل نحو الكشف عن إطارات الفيديو حافة كرات الدم الحمراء.

Technology of the Coordinator's Construction for Distributed Transactions in the Web Service Conditions

Ali Mohammed Saleh Ahmed
University of Diyala
Internet and Computer Center
dr.alisaleh80@gmail.com

Firas Mohammed Aswad
University of Diyala
College of Basic Education
altae13@yahoo.com

Abstract:

   The article is devoted to the transactions management in the heterogeneous distributed information environments is considered and the construction tool of the transaction coordinator on the basis of the scripting LUA language in the conditions of Web service is offered.

   The LUA scripting language, in context of creation of LTM transaction coordinator using the modified query language LQL, has sufficient tools available in modern scenarios programming languages, When determining the library of LTM transaction coordinator built in conditions of LUA machine, using modernized scripting LQL.

Ali .M / Firas .M

Introduction

The priorities of company's activity change day by day: companies are being reorganized, break new ground and expand applications capacity, for example, developing a new web services. Under these changes, an organization faces the problem of effective and cost-beneficial resources provision to build them in line with priorities. It requires arriving at a solution, which allows the access to the informational structure at the time and location where there is a need for it, by implementing and

optimizing access to information, regardless of its physical structure. Thus, there is a need for information integration across the distributed environment, either within a single server or in a heterogeneous IT environment, for a number of independent systems or a combination of several solutions.

1- Providing access to information structure

For the solution of this problem, we are considering the integration process of all databases into a single service database, while the actual location of the considered database remains unchanged. At the creation of this structure information remains in its initial source where, it is being modified. Most data sources are a single integrated virtual database, masking the number and types of DBMS differences. An integrated solution for service DBMSs allows accessing directly the data not only of the most famous DB providers, such as Linter, Paradox, Clipper, MS SQL Server, MUMPS, Oracle, but also of modern DBMS vendors, without determination of the actual physical location of data from a web service.

As there is no need to duplicate any information into a service web-DBMS, this integration provides the most rapid way to information integration. This integration also configures a supporting zone of such information that exists in legacy web-applications, or in applications that require a local owner and simply cannot be consolidated. When using such an approach of integration of heterogeneous distributed DBMS two concepts arise: local transactions and global transactions [3].

Division of transactions of general type into local and global appeared in connection with the application of the distributed multilink systems. Local transactions in case of a mismatch with service DBMS are known as transactions controlled by databases. From the point of view of a software support, which uses universal API, to access a database the local transactions are generated and terminated in conjunction with a certain call to DBMS. Usually, the open management of local transactions is implemented by the call of such methods as "to save transaction in DB" or "to roll back transaction from a DB". This mode of operation is typical for building applications of "client-server" architecture. If the transaction termination procedure is implemented in a single command, then DBMS uses a single phase mode of transaction termination. With such approach, there is no way to create a transaction, which "joints" actions using several connections simultaneously.

Ali .M / Firas .M

In "client-server" architecture the implementation of procedure of single-phase local transactions use is possible until no distributed DBMS is used. At the moment of such architecture, the client application code creates a connection to DBMS, a function is created either implicitly or explicitly, that begins a local transaction. Then selection of data, and as a result, completion of transaction is made. If it was the last, and all the necessary actions have been executed, the connection with the DBMS breaks.

If a distributed DBMS is used that defines the implementation of data change procedure in several DBMSs in one transaction context — so the possibility to form a universal transaction shall be provided for this task solution, to be executed for several databases of this type. This implementation procedure is conventionally called "two-phase commit local transactions".

2- Implementation of Transaction Coordinator

Requirements enhancement to difficult projects design technologies, to increase of their reliability and scalability level, as well as to capacities of a creation of heterogeneous RDBMS, have led to changes of the situation as follows: complete complex technologies of real time distributed systems design emerged. The most famous and perfect ones are CORBA, J2EE and .NET. Previously, the definition of the transaction for a RDBMS was extended to an entire IS, which is a small part of such system. Not only information content in long-term storages became transactional — final objects, of which all information system consists, became the same.

Owing to such system development, a task of personal operation emerged at level of provided distributed object transactions and transactions at level of heterogeneous databases [2]. To operate such object transactions in multilink information systems, there is a special component, which is usually called the transaction coordinator. In the developed information system the transaction coordinator is realized on the basis of the scripting programming language LUA, which allows solving a problem of transaction model with two-phase end. This programming language has been choose because of its ease of use, simple syntax, and thus sufficient power: the language supports objects, meta-tables make its type ultimately flexible and use of API-functions allows excellent integration, increase of scripts and expansion of basic language capabilities. LUA can be used together with "client-server" applications, written in various high level programming languages, including the support of web languages, such as PHP, Perl, Python, Ruby, ASP.NET, and Groovy. The considered language of the transaction coordinator is simple in training, thanks to extension possibility with help of C-functions, can be applied to wide range of tasks, using object-oriented programming mechanisms with support of prototypes.

3- Information system setup phases

When determining the library of LTM transaction coordinator built in conditions of LUA machine, using modernized scripting LQL language, there are several actions to set the system work. The sequence of these actions is given below[7].

Ali .M / Firas .M

3.1. Loading of the main configuration file. In the directory of executable software a search of a file named conf/ORB.conf shall be done. Then its values are read to system buffer by special system tools.

3.2. Initialization of ORB space. At this stage a stack of necessary libraries omniORB 4.3 is being compiled. Further, using the loaded settings, the initialization method omniORB is called, which in turn prepares the CORBA environment for interaction with the general information system of web-application.

3.3. Initialization of the LUA machine. As the LUA-language interpreter is required, the need of loading of main concepts into memory arises, that accomplishes by methods of calling lua_open () function from LUA-libraries stack. This operation creates a new state and returns the index. In case of memory lack as a result of work the zero index will be defined.

3.4. Loading of necessary libraries. Considering item 3 in which process of creation of a new independent status of LUA for which to be made loading of standard alternative libraries, such as functions for operation with lines, mathematics, additional functions of debugging, the function for operation with an operating system constructed in the scripting LUA language or on another JAVA the compatible to the general loader provided interpreter was realized.

3.5. Creation of a container of alias. At this stage, the procedure of creation of an object of a special class, which is developed especially, is made and contains a full range of alias to the DBMS, is engaged in their creation, deleting and search in system. The object of the considered container registers unique a method in LUA-machine. The challenge of the provided instruction is necessary for addition of references to the distributed databases the considered information system in a container.

3.6. Registration of external instructions in the LUA machine. In considering this step alone, because of the need to register previously prepared operation for the interpreter. After this step there is a procedure of modernization of standard LUA language in the LQL language.

3.7. Loading of alias file. The file an alias is presented in the form of the list of descriptors on remote DBMS. As a result of which accomplishment in the interpreter, an object of a container of references will contain a set of objects of alias when which using the appeal to required components of a general information system is created. If to consider the class diagram for an object of an alias - we define that a base class for it is LQLObject, which realizes functionality on fixing external and additional instructions in the LUA interpreter. Further, using parent methods, an object of the class LQLAlias creates own global meta-data sheet with a unique identifier (name) comprising instructions of the virtual machine for access to the distributed DBMS. The metastable represents the usual table in LUA in which admissible operations over value are presented.

Ali .M / Firas .M

One of the global classes, responsible for the operation of information systems in the framework of the task is Alias class that provides interaction with the environment as follows: it encapsulates an object reference to the CORBA skeletons HSystem.DriverManager and HSystem.Connection. Using CORBA object references of the classes there is a transaction in SQL DBMS with which the currently set direct connection. This mechanism is implemented in the framework of Operation AHas: query (), which by means of delegated LQLAlias class for further registration in the LUA interpreter. After the end of the considered process the unique reference to an object to become available in the language formation of inquiries.

3.8. Creation of the environment of performance transactions. The constructed runtime environment of transactions is intended for storage of running states of each local transaction in the conditions of a distributed query to DBMS which at the time of execution of a distributed query to an information system of real time monitors operation of each operation in the interpreter. As soon as in the conditions of search the instruction of accomplishment of a local request to RDBMS meets, the environment of accomplishment places complete subject to the local transaction in the container. If there are errors during the execution of a distributed query - rolls back all transactions are in the container. In the absence of error situations - records every transaction in your database, for later execution.

3.9. In case of successful implementation of each earlier considered stage (item 1-p.8) forming a global object of the class LQLGlobal which is an internal class of the global LQL environment is made. Using dynamic conversion to the ILQLGlobal interface, the pointer on the recorded object returns to the web application. If the ORB initialization phase, the machine initialization LUA error, the information model built throws an exception, which sets the rules saying that from now on will not operate the library, respectively, web-application specifies a null pointer.

The Results

The article deals with the problems of transaction management in heterogeneous distributed IT environments and offers means of building transaction coordinator based on LUA scripting language in a Web-service.

The following results were obtained:

1.   The architecture of web-service applications for multiprocessor and cluster solutions that are scalable and provides high performance when inter-module interaction in the DBMS.

2.   Hierarchical model of access to data and internal information exchange in a web-service interface that provides rapid generation of data based on queries to the DBMS information environment.

3.   The concept of the transaction was extended to information systems in general, not just to DBMS as a part of such systems.

4.   This solution provides enhanced operational efficiency allowing several applications to work jointly.

Ali .M / Firas .M

Conclusion

Thus, the LUA scripting language, in context of creation of LTM transaction coordinator using the modified query language LQL, has sufficient tools available in modern scenarios programming languages: mathematical transactions completion, managing structures, iterator and standard libraries for string objects handling, return and data collection. All this absolutely meets requirements of creating the considered information system.

References

[1] V.L. Burkovskiy, A.N. Dorofeev, S.V. Seminin, Simulation and algorithmization of control of heterogeneous databases in the distributed information systems [Text] // Voronezh, VSTU, (2003) – p.71.

[2] S.A. Rikov, V.L. Burkovskij, A.A. Golikov Control of the heterogeneous distributed objects of information systems of real time // Voronezh: VSTU, (2012) – p.193.

[3] Rikov S.A. Mathematical and software information systems of real time with the heterogeneous environment of the distributed DBMS – Voronezh: VSTU, (2011) – p.185.

[4] Lokshin, M.V. Technique of receiving time estimates of execution of requests in the parallel DBMS with data replication [Text] // Control systems and information technologies. – (2014). -№ 4. – p.41-44.

[5] Ritter D. The Middelware Muddle. DBMS magazine, May, (1998), p. 15.

[6] Rykov SA, AA Golikov, Burkovsky VL Implementation LQL query language for interaction with a homogeneous medium // Electrotechnical complexes and control systems, Voronezh, H.2, (2010).-p.53-55.

[7] Golikov AA Rykov SA Lomov EO, Burkovsky VL "Building a Distributed Transaction Coordinator in a heterogeneous environment based on LUA» // Journal of Vilnius Gediminas Technical University, v.5, №4,(2009).- p.202-203.

[8] Ozhan G., Dogac A., Kilic E., Ozcan F., Nural S., Dengi C., Halici U., Aspinar B., Koksal P., Mancuhan S., Evrendilec C. Making Oracle7, Sybase and Adabas Interoperable through CORBA: MIND Project. In Proc. Of European Oracle User Group Conference, Amsterdam, April (1996) p. 1047-1058.

[9] Pitoura E., Bukhres O., Elmagarmid A. Object Orientation in Multidatabase Systems. Report CSD-TR-93-084, Department of Computer Science, Purdue University.

[10] Pons J., Vilarem J. Mixed concurrency control: Dialing with heterogeneity in distributed database systems. In Proceedings of the Fourteenth International VLDB Conference, August (1988), Los Angeles p.144.

[11] Lokshin MV Study of parallel execution of SQL-queries with advanced data caching // Modern Information Problems in Economics and Safety: Proceedings of the XVIII International Open Science Conference, USA, Mississippi, Lorman, "Science Book Publishing House", in January (2013), p. 69-72.

تكنولوجيا بناء منسق للمعاملات الموزعة في شروط خدمة الويب

علي محمد صالح احمد   فراس محمد اسود

جامعة ديالى   جامعة ديالى

مركز الحاسبة والانترنت   كلية التربية الاساسية

altae13@yahoo.com   dr.alisaleh80@gmail.com

المستخلص :

هدف البحث هو إدارة المعاملات في بيئات المعلومات الموزعة غير المتجانسة ويعتبر أداة البناء المنسق على أساس لغة البرمجة LUA في ظروف او شروط خدمة الانترنت.

لغة البرمجة LUA في سياق إنشاء منسق المعاملات LTM باستخدام لغة الاستعلام المعدلة LQL، والتي لديها أدوات كافية متاحة في سيناريوهات لغات البرمجة الحديثة ، وعند تحديد مكتبة لمنسق المعاملات LTM بنيت في ظروف LUA machine، وذلك باستخدام تحديث البرمجة LQL.

ان أولويات نشاط الشركات تتغير يوما بعد يوم حيث يتم إعادة تنظيم الشركات، وكسر أرضية جديدة، وتوسيع قدرات التطبيقات، على سبيل المثال، من خلال تطوير خدمات الويب الجديدة. وفي ظل هذه التغييرات، تواجه المنظمة مشكلة توفير موارد فعالة ومفيدة من حيث التكلفة لبناءها بما يتفق مع الأولويات. يتطلب التوصل إلى حل يسمح بالوصول إلى البنية الإعلامية في الوقت والمكان تكون هناك حاجة إليها، من خلال تنفيذ وتحسين الوصول إلى المعلومات، بغض النظر عن هيكلها المادي. وبالتالي، هناك حاجة إلى تكامل المعلومات عبر البيئة الموزعة، سواء داخل خادم واحد أو في بيئة تكنولوجيا المعلومات غير المتجانسة، لعدد من الأنظمة المستقلة أو مزيج من عدة حلول.

الكلمات المفتاحية: لغة LQL، لغة LUA، نظام ادارة قاعدة البيانات، CORBA، IS، خدمة الويب.

3D anaglyph image watermarking approach

Bahaa Kareem Mohammed
Kut technical institute
Midlle technical university
Bahaaka87@gmail.com

Hala A. Naman Al-taee
College of Engineering
Wasit University
halaaitaee@yahoo.com

Alaa Abdulhussein Daleh Al.magsoosi
Education college
Wasit university
Almusawialaa231@gmail.com

Abstract

In this paper, a binary watermark is embedded and extracted using principal component analysis along with non-subsampled contourlet transform. Before the use of aforementioned techniques, the binary watermark is scrambled, for which we have used Arnold transform. This will by default add a level of security measures without a password. The approach as presented in the following paper is very efficient, novel, robust and blind. We have also considered the possibility of image processing attacks, hence we have employed non subsampled contourlet transform for the same. The scheme is tested on various images and we have come to a conclusion that this scheme is very performance oriented when compared to the existing watermarking techniques using 3D anaglyphic images.

Keywords—PCA (Principal Component Analysis), DCT (Discrete Cosine Transform), NSCT (Non Subsampled Contourlet Transform) , DFB (Directional Filter Banks)

I.   Introduction

In the current digital age, where internet and technologies have grown to a very large extent providing a lot of services to every individual, we can easily see increasing misuse and ill-usage of such technologies. To give some examples about the same, we can always look up to multimedia content such as image, videos, audio etc. The main victim of such losses are the ones who have created the information. This is where copyright protection comes into picture. It now becomes more important to make intact the copyright of its original owner. This is where we drive motivation for providing a watermarking technique for 3D anaglyph images.

In simple words, watermarking is a process of adding some message (which is to be transmitted) into another message (which acts as a cover for original message) so that it hides. There are multiple applications for this technique. Complete embedding and extraction procedures that involves adding a message into a cover and then taking it out again is termed as a complete watermarking approach. We also need to take care about an important aspect of watermarking, which is it should not degrade the cover in any case, at least not visible to naked eyes.

Bahaa K/Hala A. N/Alaa A

In the given paper, we have tried to present a novel and blind watermarking scheme for 3D anaglyph image. The scheme is robust and can be used for protecting the copyrights. In the proposed methodology, we will input a 3D anaglyph image. Sub band will be extracted from this image by the use of N-level non subsampled countourlet transform. Then we apply PCA which helps us to search the significant coefficients in the sub bands selected. Finally we embed the watermark into these coefficients. At the receiver's side, blind watermark extraction, as stated before, is applied so as to get back the binary watermark image hidden inside the cover data. We have tested the suggested algorithm for various attacks as well. Some of the commonly used attacks were cropping, histogram equalization, gaussian noise etc.

The paper is organized as follows. In the next section, we have discussed about preliminary information about the important and relevant concepts. The next section i.e. section number 3 discusses about the proposed methods about watermarking scheme. Section 4 deals with comparison with the existing systems. And in the end, we have conclusions in section 5.

II.   preliminaries

A. Nonsubsampled Countourlet Transform

Nonsubsampled countourlet transform, commonly known as NSCT is characterized by the following integral properties: flexible, multiscale, multidirectional, efficient transform and shift invariant. The main items it consists of is a filter bank that helps to make subbands out of a 2D frequency plane. The mechanism behind construction of these subbands is as follows: it first takes out the nonsubsampled directional filter bank and nonsubsampled pyramid structure, it then combines them both so as to get the best frequency hence achieving better subband decomposition. Atrous filtering system is used to implement it, which is shown in equation 1 below.

As mentioned earlier, the shift invariant nature of filtering is a property of multiscale of the nonsubsampled countourlet transform which helps in achieving a decomposition of the sub band. The results are pretty redundant because at each stage of the process, 1 band pass image is generated. In accordance to the process the filters are up-sampled, we get a shift invariant and highly directional expansion along with a nonsubsampled directional filter bank. The output in return will eliminate both down-samplers and up-samplers in the directional filter bank. This also turns off both the down-samplers and up-samplers in each of the 2 channel filter bank in the directional filter bank structure in tree form.

B. Principal Component Analysis

The following information describes the vital steps to be taken for implementation of principal component analysis. Each of the image pixel value is subtracted from the mean value of all pixels, in order to centralize the pixel values. This will help us to calculate the covariance matrix. Then we calculate the eigenvectors and eigenvalues of the covariance matrix obtained from previous step. In order to find the principal component of this data, we pull out the eigenvector with the highest eigenvalue. We then transpose eigenvectors and multiply this on the left of the transposed original data.

C. Arnold Transform

The sole purpose of Arnold transform is to add a level of security to the operation. It is an image scrambling methods. The 2 main characteristics of Arnold transform are periodicity and simplicity. Therefore, if we have the periodicity information we can easily restore the source original image. This will be done by a number of iterations. Keeping the image security property in mind, this is used in various applications.

$$y[n] = \sum_{k \in sup \ p(h)} h[k]x[n - Sk]$$

(1)

Bahaa K/Hala A. N/Alaa A

III.   proposed watermarking scheme

Following is an explanation of the proposed watermarking scheme. As discussed in the above sections, we are employing Arnold transform to add the security feature to the operation. It provides a non-password security. It is applied on the watermark image which is in binary form. As with the most watermarking schemes, this scheme is also divided in 2 main parts: embedding the watermark in cover image and extracting the watermark in watermark embedded cover. We start by employing a pair of stereo images obtained from Middlebury stereo images dataset. These 2 separate stereo images are joined together to make 1 complete 3D anaglyph image by the process of linear projection. This 3D anaglyph image will be considered as the cover image for embedding operation. We then move forward with transforming this cover image by making use of N-level non subsampled countourlet transform. This transform will give us multiple sub bands. We are going to select the sub band with the minimum variance, and use it for the embedding process.

A. Embedding

Following steps needed to be followed for the embedding procedure. A detailed flow diagram is provided in figure 1.

- 3D anaglyph image is obtained. We use the left and right stereo images and combine them by the use of linear projection method as discussed earlier.

- Apply N-level non subsampled countourlet transform to the cover image obtained in above step.

- Select the sub band with minimum variance.

- Apply PCA to the selected sub band.

- Scramble the binary watermark image (whose size is 32 X 32) using Arnold transform. Apply *p* number of transitions.

- Scrambled binary watermark image is embedded into the selected sub band obtained after PCA transform

- Apply inverse PCA to the sub band which is modified in previous step.

- N-level inverse non subsampled countourlet transform is applied to sub bands, which produces the watermarked cover image (3D anaglyph)
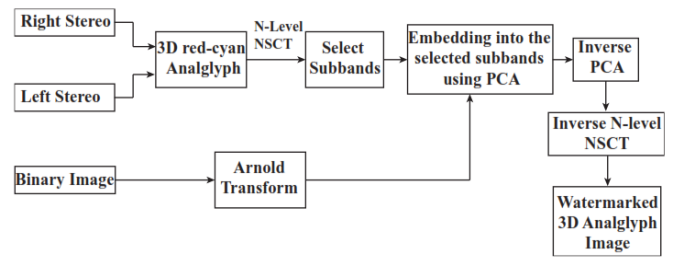
Fig. 1.   Proposed embedding procedure.

B. Extracting

Following steps needed to be followed for the extraction procedure. A detailed flow diagram is provided in figure 2. Please note the while extraction process, no information is used from source data. This is a blind and robust watermarking scheme. We make use of the 3D watermark cover image obtained after embedding. We do make use of the level N of non-subsampled countourlet transform and the p iterations of Arnold transform. They are used as the secret keys.

- Apply N-level non subsampled countourlet transform to the 3D anaglyph cover image.

- Select the sub band with minimum variance

- Apply PCA to this sub band

- Watermark pixels are extracted from this output

- Inverse 2D Arnold transform is applied p number of times, assembling the watermark embedded.
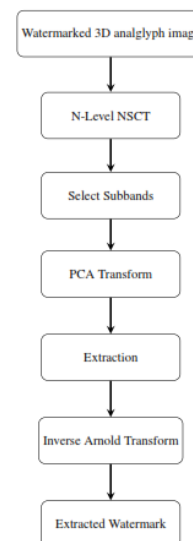
Fig. 2.   Proposed extraction procedure.

Bahaa K/Hala A. N/Alaa A

IV.   results and discussion

In calculating the results for the analysis, we have used various original 3D anaglyph images in the process. These images are used to evaluate the performance of the system. The original 3D anaglyph images are of the size 370 x 460 x 3. We have then applied liner projection on the pair of 3D anaglyph images and then, the output is resized to 256 x 256 x 3, which is to be used as the final cover image. A binary image watermark is used whose dimension is 32 x 32. For the N level non subsampled countourlet transform, the level of transform that we have used is 4. Hence the particular sub band that is selected is calculated at level 4 of the non subsample countourlet transform.
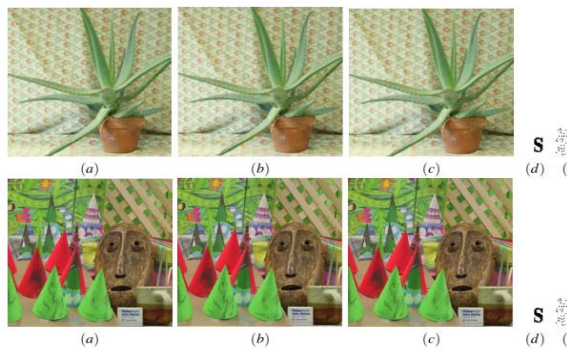
Fig. 3.   (a) Left stereo image (b) Right stereo image (c) Generation of 3D anaglyph image (d) Original watermark image (e) Scrambled watermark after arnold transform (f) Reconstructed watermark

A. Imperceptibility

If we are to check the PSNR value of the original watermark and the reconstructed watermark, then the value so obtained must be more than 51db. This is a sign of an imperceptible watermarking system. In the proposed system, we have managed to get a PSNR value of 69db. Hence it can be very easily said that out proposed system is highly imperceptible.

B. Robustness

In terms of how a watermarking system holds against the intentional attacks from an outside hacker or a non authorized entity determines the robustness of that watermarking scheme. We were able to work on the robustness of this system by comparing the original watermark with the watermark obtained after the image processing attack. We have measured the robustness with the help of normalized correlation and have managed to get an NC value of 0.9 for most of the attacks.

C. Security

Arnold transform adds a level of seurity to our system. We have to transform/scramble the original watermark image using p iterations of arnold transform. Then at the receiver side, we have to again apply arnold transform p iterations to reconstruct the original watermark again from the scrambled version of it. This is how we obtain the original watermark image back from its unscrambled version.

TABLE I.   COMPARISON OF PSNR VALUES OF WATERMARKED 3D ANAGLYPH IMAGES

Images	Doll	Cones	Tsukuba	teddy	Venus	Baby1
PSNR value(dB)	69.2284	69.1916	69.031	69.1916	69.0913	69.2943

TABLE II.   NORMALIZED CORRELATION VALUES AFTER THE ATTACKS

| Attacks	Aloe	Baby	Flowerpot	Lamp shade	Midd1	Doll	Rocks	Wood	Plastic	Monopoly
Averaging Filtering([7×7])	1	1	1	1	1	1	1	1	1	1
Median Filtering([7×7])	1	1	1	1	1	1	1	1	1	1
Sharpening(50%)	1	1	1	1	1	1	1	1	1	1
Color Quantization	0.99924	0.99812	0.99953	0.99832	0.99815	0.9983	0.9996	0.99993	0.99841	0.99872
Gaussian Noise	1	1	1	1	1	1	1	1	1	1
JPEG Compression	1	1	1	1	1	1	1	1	1	1
Rotation(50deg)	0.9995	0.9995	0.9995	0.9995	0.9995	0.9995	0.9995	0.9995	0.9995	0.9995
Cropping(50%)	1	0.9981	0.9982	0.9995	0.9989	0.99983	0.9998	1	0.9985	0.9981
Scaling	0.99804	0.99881	0.99834	0.99991	0.99898	0.99954	0.99859	0.99818	0.99978	0.99962
Contrast Adjustment	1	1	1	1	1	1	1	1	1	1
Translation	1	1	1	1	1	1	1	1	1	1
Resizing	1	1	1	1	1	1	1	1	1	1
Impulse Noise	0.99867	0.99954	0.99807	0.99813	0.99923	0.99829	0.99856	0.99934	0.99904	0.99933
Histogram Equalization	1	1	1	1	1	1	1	1	1	1
No Attack	1	1	1	1	1	1	1	1	1	1

TABLE III.   COMPARISON WITH OTHER WATERMARKING SCHEMES

Images	Proposed method			Bhatnagar			Liu and Tan			IVY		
	Cones	Tsukuba	Dolls	Cones	Tsukuba	Dolls	Cones	Tsukuba	Dolls	Cones	Tsukuba	Dolls
No Attack	1	1	1	1	1	1	1	1	1	1	1	1
Averaging filter([7×7])	1	1	1	0.8503	0.8543	0.8422	0.7560	0.7502	0.7547	0.9514	0.9401	0.9517
Median Filtering([7×7])	1	1	1	0.9406	0.9357	0.9372	0.8091	0.8171	0.8003	0.9937	0.9898	0.9910
Gaussian Noise	1	1	1	0.8491	0.8514	0.8435	0.8169	0.8118	0.8157	0.9499	0.9583	0.9420
JPEG Compression	1	1	1	0.9719	0.9763	0.9757	0.9440	0/9497	0.9475	1	1	0.9999
Cropping	0.99978	0.99978	0.99974	0.9649	0.9856	0.9558	0.6472	0.6420	0.6441	0.9754	0.9799	0.9629
Resizing	1	1	1	0.9475	0.9455	0.9424	0.7511	0.7678	0.7517	0.9876	0.9689	0.9559
Rotation(50degree)	0.9995	0.9995	0.9995	0.8909	0.8970	0.8891	0.6838	0.6887	0.6853	0.9812	0.9989	0.9887
HE	1	1	1	0.9597	0.9548	0.9593	0.9593	0.9672	0.9508	0.9912	0.9919	0.9809
Contrast Adjustment	1	1	1	0.9768	0.9777	0.9744	0.9517	0.9599	0.9537	0.9760	0.9800	0.9718
Sharpening	1	1	1	0.9956	0.9963	0.9964	0.9906	0.9876	0.9931	0.9999	0.9989	0.9979

Bahaa K/Hala A. N/Alaa A
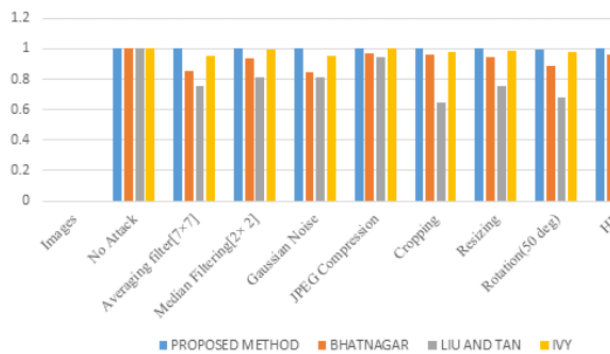
Fig. 3.   Comparison of proposed watermarking scheme with other schemes

V.   conclusion and future work

In this paper, we have implemented a watermarking scheme for 3D anaglyph cover image. For keys, we have used the level of non-subsampled contourlet transform and the number of iterations of the arnold transform. This is suffice to say that in order to obtain the original watermark embedded in the cover image, an individual needs these 2 keys. This will help in copywriting the information. As a future work, we can look for incremental PCA.

References

[1] Laudon, K. C., and J. P. Laudon, "Ethical and social issues in information systems, " Management Information Systems: Managing the Digital Firm pp.169,(2012).

[2] I. Cox, M. Miller, J. Bloom, M. Miller, Digital Watermarking: Principles Practice, Morgan Kaufmann, (2001)

[3] Tao, Hai, et al, "Robust image watermarking theories and techniques: A review." Journal of applied research and technology vol. 12 no.1,pp. 122-138, (2014)

[4] M. Arnold, S. Wolthusen and M. Schmucker, Techniques and Applications of Digital Watermarking and Content Protection, Artech House Publishers,(2003)

[5] Luo, Ming, "Robust and blind 3D watermarking", (2006).

[6] Devi, Hidangmayum Saxena, and Khumanthem Manglem Singh. "A Brief Survey on 3D Watermark- ing Techniques"

[7] Ying, Wang, Zheng Xue-feng, and Liu Hai-Yan, Robust 3D Watermarking Based on Geometry Im- age , In 4th IEEE International Conference on Wireless Communications, Networking and Mobile Computing (2008).

[8] Cai, S.,   Shen, X,"Octree-based robust watermarking for 3D model", In Journal of Multimedia, vol.6no.1, pp. 83-90(2011).

[9] Harte, Thomas, and Adrian G. Bors, "Watermarking 3D models", In IEEE International Conference on Image Processing,vol. 3(2002).

[10] Tamane, Sharvari C., and Ratnadeep R. Deshmukh,"Blind 3D Model Watermarking Based on Multi- Resolution Representation and Fuzzy Logic", arXiv preprint arXiv: 1203, 2485 (2012).

[11] Song, Han Sae, Nam Ik Cho, and Jong Weon Kim,"Robust watermarking of 3D mesh models", In IEEE Workshop on Multimedia Signal Processing(2002).

[12] Mitrea, Mihai,"Toward robust spread spectrum watermarking of 3D data", (2004)

[13] Wang, Xinyu, and Shun Du,"A Non-blind Robust Watermarking Scheme for 3D Models in Spatial Domain", Electrical Engineering and Control. Springer Berlin Heidelberg, pp.621-628,(2011).

[14] Motwani, Rakhi C., and Frederick C. Harris Jr, "Robust 3D Watermarking Using Vertex Smoothness Measure", In IPCV, pp. 287-293(2009).

[15] Singh, Law Kumar, Deepak Chaudhry, and Gopalji Varshneya, A Novel Approach of 3D Object Watermarking Algorithm using Vertex Normal" ,In International Journal of Computer Applica- tions,vol.60no.5(2012)

[16] Kalivas, A., Tefas, A., Pitas, I, Watermarking of 3D models using principal component analysis, In IEEE International Conference on Multimedia and Expo, vol.1, pp. 637-640,(2012).

[17] Kuo, Chen-Tsung, et al,"A blind robust watermarking scheme for 3D triangular mesh models using 3d edge vertex detection",In Asian Journal of Health and Information Sciences vol.4 no.1, pp.36- 63,(2009)

[18] Zafeiriou, Stefanos, Anastasios Tefas, and Ioannis Pitas,A blind robust watermarking scheme for copyright protection of 3D mesh models, In IEEE International Conference on Image Processing, vol.3,(2004).

[19] Liu, Yang, Balakrishnan Prabhakaran, and Xiaohu Guo,"Blind invisible watermarking for 3D meshes with textures", In 17th IEEE International Conference on Image Processing (ICIP),(2010).

[20] Feng, X. Q., and Yanan Liu,"A robust, blind and imperceptible watermarking of 3D mesh models base on redundancy information", Int J Digital Content Technol Appl 6.2, 201, pp.172-179.

[21] Kim, Min-Su, et al,"Watermarking of 3D irregular meshes based on wavelet multiresolution analysis, Digital Watermarking", Springer Berlin Heidelberg, pp. 313-324,(2005).

[22] Praun, Emil, Hugues Hoppe, and Adam Finkelstein, "Robust mesh watermarking, In Proceedings of the 26th annual conference on Computer graphics and interactive techniques. ACM Press/Addison- Wesley Publishing Co., (1999).

[23] Yang, Ying, and Ioannis Ivrissimtzis,"Polygonal mesh watermarking using Laplacian coordinates", Computer Graphics Forum. Vol. 29. No. 5. Blackwell Publishing Ltd,(2010).

[24] Lin, Chao-Hung, et al, "A novel semi-blind-and-semi-reversible robust watermarking scheme for 3D polygonal models." The Visual Computer 26.6-8, pp. 1101-1111,(2010).

[25] Ohbuchi, R., Mukaiyama, A., Takahashi, S., A frequency-domain approach to watermarking 3D shapes, In Computer Graphics Forum, vol.21no.3, pp. 373-382,(2002)

[26] Fu, Y.,Robust image watermarking scheme based on 3D-DCT, In Sixth IEEE International Confer- ence on Fuzzy Systems and Knowledge Discovery, vol. 5, pp. 437-441,(2009).

[27] Tefas, A., Louizis, G., Pitas, I,3D image watermarking robust to geometric distortions, In IEEE Inter- national Conference onAcoustics, Speech, and Signal Processing (ICASSP),vol. 4, pp. IV-3465,(2002)

[28] Jaipuria, S. J. ,"Watermarking for Depth Map Based 3D images using wavelet transform", In IEEE International Conference on Communications and Signal Processing, pp. 181-185, (2014).

[29] Kim, Hee-Dong, et al. "Robust DT-CWT watermarking for DIBR 3D images", In IEEE Transactions on Broadcasting, vol.58 no.4 pp.533-543,(2012).

[30] Prathap, Ivy, and R. Anitha, "Robust and blind watermarking scheme for three dimensional anaglyph images," Computers Electrical Engineering, vol.40 no.1, pp.51-58(2014).

[31] Bhatnagar, Gaurav, Jonathan Wu, and Balasubramanian Raman. "A robust security framework for 3D images." Journal of visualization vol.14 no.1 , pp.85-93,(2011)

[32] Abbas, Tawfiq A., Majid Jabbar Jawad, and Sud Sudirman, "Robust Watermarking of Digital Vector Maps for Copyright Protection".

[33] Liu, Ruizhen, and Tieniu Tan. "An SVD-based watermarking scheme for protecting rightful owner- ship." IEEE transactions on multimedia vol. 4 no.1, pp. 121-128, (2002)

[34] Do, Minh N., and Martin Vetterli. "The contourlet transform: an efficient directional multiresolution image representation." IEEE Transactions on image processing vol.14no.12 , 2091-2106,(2005).

[35] Arthur L.da Cunha, Jianping Zhou, Minh N.Do,The Nonsubsampled Contourlet Transform: Theory, Design and Applications, IEEE Transactions on Image Processing, Vol.15, no.10, Oct (2006).

[36] Herve Abdi, Lynne J Williams, "Principal component Analysis", Wiley Interdisciplinary Reviews: Computational Statistics.

[37] Li, T Liang He, "Arnold Transform based image scrambling method", International Conference on Multimedia, (2013).

[38] http://vision.middlebury.edu/stereo/data/

علاء عبدالحسين دليح   هالة عبدالعظيم نعمان   بهاء كريم محمد

جامعة واسط   جامعة واسط   الجامعة التقنية الوسطى

كلية التربية   كلية الهندسة   المعهد التقني الكوت

المستخلص :

العلامة المائية الثنائية يتم تضمينها واستخراجها باستخدام تقنيات التحليل للمكونات الرئيسية جنبا الى جنب مع استخدام تحويل الشكل الخارجي للعينات الغير فرعية ، قبل استخدام التقنيات المذكورة أعلاه العلامه المائية الثنائية شوشت لذلك نحن استخدمنا تحويل ارنولد. و هذا بشكل افتراضي يضيف مستوى من الاجراءات الامنية بدون كلمة مرور .منهاج البحث كما هو موضح في الورقة التالية هي فعالة جدا و جديدةو قوية . وتم اخذ في نظر الاعتبار الامكانية الهجمات باستخدام معالجة الصور وبالتالي قمنا بتوظيف تحويل الشكل الخارجي للعينات الفرعية لنفسها . المخطط تم اختباره على صور متنوعه وحصلنا على استنتاجات ان أداء هذا المخطط موجه جداً عندما نقارن بتقنيات العلامه المائية الحالية او السابقة باستخدام النقش ثلاثي الابعاد على الصور .

An Efficient Classification Algorithms for Image Retrieval Based Color and Texture Features

Iman Abduljabbar Saad
Electronic Computer Center
Al-Mustansiriyah University, Baghdad, Iraq

Abstract:

Content-Based Image Retrieval CBIR system commonly extracts retrieval results respecting to the similarities of the extracted feature of the given image and the candidate images. The proposed system presented a comparative analysis of five types of classifiers which used in CBIR. These classifiers are Multilayer Perceptron (MP), Sequential Minimal Optimization (SMO), Random Forest (RF), Bayes Network (BN) and Iterative Classifier Optimizer (ICO). It has been investigated to find out the best classifier in term of performance and computation to be the suitable for image retrieval. The low level image features which include texture and color are used in the proposed system. The color features involve color-histogram, color-moments and color-autocorrelogram while texture features involve wavelet transform and log Gabor filter. Also the system will include hybrid of texture and color features to get efficient image retrieval. The system was tested using WANG database, and the best average precision achieved was (85.08%) when combining texture and color features and using the (RF) classifier.

Keywords: - Color descriptors, Textures descriptors, Classifiers algorithms.

1. Introduction

Nowadays, there have been major developments in image acquisition techniques as well as the expansion of data storage units for very huge databases. In order to retrieve and manage this large number of images with high efficiency, an effective retrieval system was necessary [1]. The method of automatic image annotation is used for automatically generating number of labels for describing the image content. Low level features typically used for images annotated with labels. Machine learning techniques provided facilitates to annotate the image by learning the correlation between features of image and annotated labels [2].

A large number of researchers aim to retrieve images based on its content and tried to automate the process of image analysis. Problems related to the image retrieval consist of two sections; (feature extraction and classification). Many different techniques and algorithms have been used by lot of researchers to extract image features and classification to improve recall and accuracy [3].

Image retrieval method, which depends primarily on the image content, has been suggested in this paper to find related images. The visible image's content is analyzed based on low level features that obtained from the image. Based on methods of automatic image annotation, there are various algorithms for automated image retrieval and classifications are used.

Iman .A

2.   Related Work

This section of the paper includes some published researches written in the field of CBIR.

[4] Proposed method depend on the color moments features and Wang database for an image retrieval. In this method the image is partitioned into four parts. After that, the color moments are extracted of each part and clustered into four classes. The mean moment is extracted for each class and considered as such as an image primitive. The entire primitives are applied as features and every class mean is combined into a one class mean. In this work the average precision gain was 31.09

[5] Proposed method used texture and color for CBIR technique. They used Zernike chromaticity distribution to capture color features. Where, texture features are extracted using a rotation-invariant and scale-invariant image descriptor in Contourlet domain. The average precision gain in this work was 51.02.

[6] Proposed a new method depend on 2D Dual-Tree Discrete Wavelet Transform (2D DT DWT). In the first, all images are converted from RGB color space to YCbCr color space. Then, the 2D DT DWT is applied to each color band. For all images in the database, the features such as mean, energy, entropy and standard deviation are extracted from each color bands of the image. The Euclidean distance is used in the image matching process to find the closer relevant images. WANG database was used and the average precision gain in this work was 33.86.

[7] Proposed method used neural network based back propagation and global image properties. At first, the neural network is trained about the images' database features. Image's features that considered in this method are GLCM (Gray Level Co-occurrence Matrix), color histogram and edge histogram. The results are shown an improvement in image retrieval about precision and recall.

[8] Proposed method depended on color and texture features and used Discrete Wavelet Transform and the Self Organizing Map (SOM) artificial neural networks. The average precision when using WANG database was 55.88.

[9] In this paper, the performance of Sparse Banded Filter matrices are evaluated by comparing it with the standard edge detection filters through CBIR. 7 classes out of the 10 classes of WANG database are used. The features are extracted depended on edge detection and Singular Value Decomposition. The average precision when using WANG database was 23.69%.

[10] Proposed approach for CBIR based on color and texture data. In this regard, color histogram and color moment are used as color feature; further, PCA statistical method is applied to reduce dimensions. The average precision when using WANG database was 62.4%.

This paper is organized as follows: The first section of the paper presents the proposed method. The second section discusses the experimental result .Finally, in the last section; the main conclusion concerning the proposed approach is given.

3.   Proposed Method

In this work, two types of features and five types of classifier are used to compare their performances in increase image retrieval accuracy. The first type of feature is color features which include HSV histogram, color moments and color Autocorrelogram, while second type is texture features which based on transform method that includes Gabor wavelet and Wavelet transforms. The classification algorithms that used in this work are Iterative Classifier Optimizer (ICO), Bayes Network (BN), Random Forest (RF), Multilayer Perceptron (MP) and Sequential Minimal Optimization (SMO). Figure (1) shows the diagram of proposed method.

Iman .A
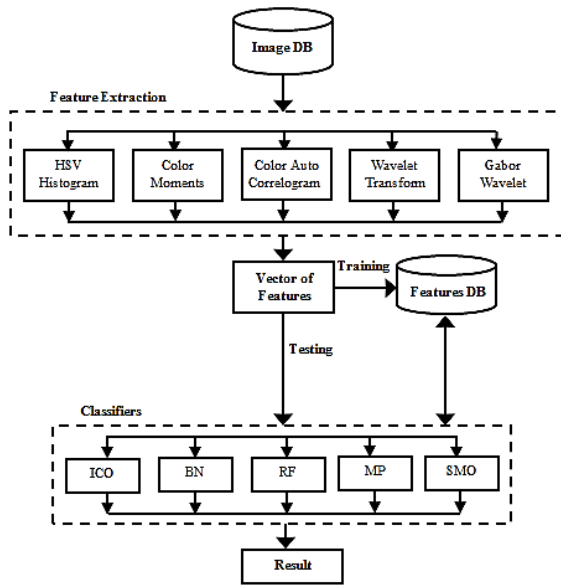
Figure (1): Block Diagram of Proposed Method.

I. Color Feature Extraction

For extraction of color feature, three different methods have been used; histogram, autocorrelogram and color moments which describe as follows:

A. HSV color space

HSV space is a way to describe color that considered more intuitive than other color spaces. HSV contains three components (Hue, Saturation and Value) [11]. HSV color space is derived from RGB values using the following equations [12]:

$$H = \cos^{-1}\left\{\frac{\frac{1}{2}[(R-G)+(R-B)]}{\sqrt{(R-G)^2 + (R-B)(G-B)}}\right\} \quad (1)$$

$$S = 1 - \frac{3}{R+G+B}\lfloor MIN(R,G,B)\rfloor \quad (2)$$

$$V = \frac{1}{3}(R+G+B) \quad (3)$$

The proposed method computes histogram for each band separately such as *H* band, *S* band and *V* band. The histogram count number of pixels corresponds to a specific color in quantized color's space. To reduce computing time required for histogram, the color space must be quantizing into a limited number of levels. HSV color space quantized by using uniform quantization from 360 levels into 8 levels for *H* while 2 levels for each *S* and *V*.

B. Color Moments

The ground of the color moments depends on the color distribution in the image which represents probability distribution that can be distinguished by different moments. Color moments can be classified into number of order as follows: first order, second order, third order and higher orders. The mean (first order) and standard deviation (second order) color moments have been used in the proposed method. They are extracted for each band of RGB color space; Red, Green and Blue bands [2]. Mathematically, the early two moments are described as follow:

$$u_i = \frac{1}{N}\sum_{j=1}^{N} f_{ij} \quad (4)$$

$$\sigma_i = \frac{1}{N}\sum_{j=1}^{N} \left((f_{ij} - u_i)^2\right)^{\frac{1}{2}} \quad (5)$$

Where *N* represents the number of pixels in image, f_{ij} represents the value of ith color component of the image pixel *j* [13].

C. Color Autocorrelogram

Color autocorrelogram, is counseled to describe not merely the color allocations of pixels, but additionally the spatial correlation of color's pairs. The elements in the autocorrelograms are frequencies of the occurrence of the two identical color levels at a given distance. In proposed approach autocorrrelogram is used because of its smaller size [13]. For faster retrieval, the color is quantized to 64 colors.

II. Texture Feature Extraction

For extraction texture feature, two different methods have been used; discrete wavelet transform and log Gabor filter.

A. Discrete Wavelet Transform

The wavelet transforms commutated for a 2D signal level by using sub-sampling and recursive filtering. The signal for each level decomposed into four frequency sub bands, Low-Low, Low-High, High-Low and High-High [13].

Iman .A

This signal is decomposed into two ranges when passing through these filters: the low-pass filter and high-pass filter. Rough information of the signal is extracted by the low-pass filter that corresponds to the average operation while detailed information is extracted from the signal using a high-pass filter that corresponds to the variation operation [14]. In the proposed method four level of decomposition is applied.

B. Gabor Wavelet

The Gabor Wavelet consists of a group of Gabor filters which a set of wavelets capturing energy at different frequencies and directions. Localized frequency description is provided from signal expansion. Texture features is extracted from capturing local features-energy from this signal. So, Gabor wavelet has good characteristics in space position, space frequency and direction selectivity [13].

III. Classifier Types

In this work, there are five types of classification algorithms are used and it is described as follow:

A. Sequential Minimal Optimization (SMO)

Sequential Minimal Optimization algorithm is used for training a support vector classifier. It is a simple algorithm that used for quickly solves the Support Vector Machine Quadratic Programming (SVM QP) problem. The SMO does not require any extra matrix storage and no numerical QP optimization. At every step, SMO chooses two Lagrange multipliers to jointly optimize, finds the optimal values for these multipliers, and updates the SVM to reflect the new optimal values. The advantage of SMO lies in the fact that solving for two Lagrange multipliers can be done analytically [15].

B. Random Forest (RF)

Random Forest is a set learning methods that used for regression and classification. The basic concept of the random forest's methodology is the constructing a forest of random decision trees; which are created by randomizing the spilt at each node of decision tree. Each tree is likely to be less accurate than a tree created with exact splits. But,

by combining several of these "approximate" trees in an ensemble, we can improve the accuracy, often doing better than a single tree with exact split [16] [17].

C. Bayes Network (BN)

Bayes Network is called Naïve Bayes algorithm which is based on Bayes theorem; it is useful for large data sets. Attributes are independent, which is presence of one particular feature in a class, is independent of any other features in that class. This is a statistical based learning algorithm; it is efficient, strong, fast and considerably accurate in real world scenario [18], this algorithm works better on categorical data, easily handle missing data. Dimensionality of data is very high and helps in solving predictive problems; there is no repetitive parameter estimation [19].

D. Iterative Classifier Optimizer (ICO)

Iterative classifier uses cross validation and optimizes the number of iteration for the given classifier; it is capable of handling missing, nominal, binary classes and attributes like numeric, nominal, binary, empty nominal [20]. In this paper test, ICO is used 10 iterations.

E. Multilayer Perceptron (MP)

Multilayer Perceptron is classifier based on using back propagation for classification. MP is a feed-forward neural network composed of an input layer of nodes, two or more layers of perceptron and the output layer. The layers between the input and output layers are called hidden layers [21]. It depends on supervised learning process which conducted through change the connection weights after handling each data's piece, depending on the amount of error that results in the output target and compared with the expected results. It has a lot of successful applications in solving complex problems in the real world [22].

Iman .A

IV. Feature selection

The most important issues in the field of retrieving images is found features vector that have a great power of distinction. In practice there are a larger numbers of candidate features are extracted, then the best of them is selected. In this paper, to select the best set of features, the CFS (Correlation based Feature Selection) algorithm is used. The selected features set has low inter correlation and very correlated with the class [23].

4. Experimental Result

This section was devoted to present and discuss several classification algorithms to compare their performance in image retrieval accuracy. These classification algorithms are Multilayer Perceptron (MP), Sequential Minimal Optimization (SMO),

Random Forest (RF), Bayes Network (BN) and Iterative Classifier Optimizer (ICO). The process of classification is performed by three algorithms based on color features, texture features and combination of them. These three algorithms produced different results which are explained in this section.

The WANG database is used which consist of 1000 images belong to 10 different classes where each class includes 100 images of 384 x 256 pixels dimension, Figure (2) shows examples of WANG database. The database is divided into two categories: Train Data and Test Data; test dataset contain the images which we want to Query (in this work 20% from each class images are used for testing) and train dataset contain the images that the user wants (in this work 80% from each class images are used for training).

Class1:Africans	Class2:Beaches	Class3:Building	Class4:Buses	Class5:Dinosaur
Class6:Elephants	Class7:Flowers	Class8:Horses	Class9:Food	Class10:Mountain

Figure (2): Example Image of WANG Database classes.

Retrieval results are examined by the known "precision and recall" criteria, which are described as follows:

Precision = no. correct of image/ no. retrieval images

Recall = no. correct of image/no. all image related

Iman .A

A. Implemented Color Features

In the first proposed algorithm, the training and testing have been done on features extracted from various color components; HSV Histogram, Autocorrelogram and Color Moments. With HSV Histogram, for saving the time, each of *H*, *S* and *V* is quantized to be equivalently to 8x2x2 and get a 32-dimensional color feature vector.

Where with Color Autocorrelogram, the image is quantized into 64 colors = 4x4x4 in RGB space and four predefined distances between neighbour pixel intensities [1 3 5 7], so, there is 64-dimensional color feature vector. In case of using Color Moments, first two color moments are extracted from each one of (Red, Green and Blue) planes of image that will led to 6-dimensional color feature vector. The results of the Precision and Recall are shown in Table (1) depending on the color features vector which consists of 102 features.

Table (1): Precision and Recall results for Classification Techniques Using Color Features.

Classes	Classifier Type									
	MP		SMO		RF		BN		ICO	
	Precision%	Recall%	Precision%	Recall%	Precision%	Recall%	Precision%	Recall%	Precision%	Recall%
Africans	70.6	70.6	56.5	76.5	70	82.4	77.8	82.4	70	82.4
Beaches	73.7	60.9	80	69.6	76	82.6	73.9	73.9	63.3	82.6
Buildings	72.2	68.4	65	68.4	60.9	73.7	73.7	73.7	56.5	68.4
Buses	55.6	66.7	66.7	66.7	91.7	73.3	100	73.3	69.2	60
Dinosaurs	100	100	100	100	93.8	100	93.8	100	100	100
Elephants	73.1	82.6	85	73.9	85	73.9	84	91.3	76.5	56.5
Flowers	100	84.6	95.8	88.5	100	88.5	95.8	88.5	92.6	96.2
Horses	85.7	100	73.9	94.4	85.7	100	90	100	82	100
Foods	71.4	62.5	63.2	50	72.7	66.7	70.8	70.8	68.8	45.8
Mountains	69.6	80	76.2	80	88.9	80	85	85	82.4	70
Average Precision	77.19	77.63	76.23	76.80	82.47	82.11	84.48	83.89	76.11	76.19
Model Build Time(Second)	33.3		0.46		0.77		0.18		9.99	

According to the output results listed in Table (1), when applying algorithm on the tested dataset, indicate that the best average (precision =84.48%, recall=83.89%) has been gain when using BN classifier with low time (0.18) second. It is noted that class4 (Buses) of images have higher precision rate (100) with just BN classifiers type, class5 (Dinosaurs) have higher precision and recall rate (100%) for most classifiers types because these images have simple background, therefor the nature of images has good effect on the results. Class7 (Flowers) have higher precision rate (100%) for MP and RF classifiers types, where class8 (Horses) of images have higher recall rate for all classifiers types except SMO.

B. Implemented Texture Features

In the second algorithm, the training and testing have been done on texture features. Gabor filters are applied on the image with four scales of frequency and six orientations. The Mean-squared energy and mean amplitude for each scale and orientation is calculated and created a texture feature vector of length 48. When applying Wavelet, fourth-level decomposition is achieved, so, 1x20 feature vector containing the first two moments (mean and standard deviation) of wavelet's coefficients are created and consist of 40 features. The results of the Precision and Recall are show in Table (2) depending on the texture features vector which consists of 88 features, when applying algorithm on the tested images.

Iman .A

Table (2): Precision and Recall results for Classification Techniques Using Textures Features.

Classes	Classifier Type									
	MP		SMO		RF		BN		ICO	
	Precision%	Recall%	Precision%	Recall%	Precision%	Recall%	Precision%	Recall%	Precision%	Recall%
Africans	66.7	47.1	52.9	52.9	55.6	58.8	35	41.2	31.6	35.3
Beaches	73.1	82.6	54.2	56.5	56	60.9	53.6	65.2	63.2	52.2
Buildings	66.7	63.2	55.6	52.6	63.2	63.2	50	36.8	50	57.9
Buses	73.7	93.3	78.6	73.3	86.7	86.7	54.2	86.7	72.7	53.3
Dinosaurs	100	100	100	100	100	100	100	100	100	100
Elephants	83.3	87	70.4	82.6	71.4	87	68.2	65.2	69.6	69.6
Flowers	89.3	96.2	89.3	96.2	96	92.3	92.3	92.3	100	96.2
Horses	88.9	88.9	73.7	77.8	76.5	72.2	87.5	77.8	83.3	83.3
Foods	82.4	58.3	56.3	37.5	50	29.2	43.8	29.2	47.6	41.7
Mountains	56.5	65	59.1	65	58.3	70	42.1	40	44.4	60
Average Precision	**78.06**	**78.16**	**69.01**	**69.44**	**71.37**	**72.03**	**62.67**	**63.44**	**66.24**	**64.95**
Model Build Time(Second)	23.1		0.21		0.63		0.07		9.32	

The results listed in Table (2), show that the high average (precision =78.06%, recall=78.16%) has been gain when using MP classifier with time (23.1) second. Also, it is noted that class5 (Dinosaurs) of images have higher precision and recall rate (100%) for all classifiers types because these images have simple background, where, class7 (Flowers) of images have higher precision rate for ICO classifiers type. The all classifier types which based on color features gave better results on all classes than classifier types which based on texture features.

C. Implemented Hybrid Features

In the third algorithm, for enhancing system's performance of the image retrieval, training and testing have been done with combination of color and textural features (Hybrid). The results of the Precision and Recall are show in Table (3) depending on the features vector of color and texture which consists of 190 features.

Table (3): Precision and Recall results for Classification Techniques Using Hybrid Features.

Classes	Classifier Type									
	MP		SMO		RF		BN		ICO	
	Precision%	Recall%	Precision%	Recall%	Precision%	Recall%	Precision%	Recall%	Precision%	Recall%
Africans	82.4	82.4	54.2	76.5	76.9	58.8	75	70.6	80	70.6
Beaches	69.2	78.3	80	87	67.7	91.3	65.4	73.9	75.	78.3
Buildings	81.3	69.4	85.7	63.2	70	73.7	47.6	52.6	61.5	84.2
Buses	93.3	93.3	92.3	80	83.3	100	76.5	86.7	78.6	73.3
Dinosaurs	100	100	100	100	100	100	100	100	100	100
Elephants	90.9	87	87	87	90.9	87	80	87	81.8	78.3
Flowers	100	100	96.3	100	100	96.2	100	96.2	96.2	96.2
Horses	96.7	100	94.7	100	94.7	100	93.8	83.3	85.7	100
Foods	76.2	74.7	85	70.8	85.7	50	55.6	41.7	70.6	50
Mountains	78.9	85	85	85	78.3	90	81	85	95	95
Average Precision	**86.9**	**87**	**86**	**85**	**84.8**	**84.7**	**77.5%**	**77.7**	**82.4**	**82.6**
Model Build Time(Second)	58.2		0.55		1.77		0.2		18.9	

Iman .A

The results listed in Table (3), show that the high weighted average (precision =86.9%, recall=87%) has been gain when using MP classifier with time (58.2) second. Also, it is noted that class4 (Buses) of images have higher recall rate (100) with just RF classifiers type, class5 (Dinosaurs) of images have higher precision and recall rate (100%) for all classifiers types, class7 (Flowers) of images have higher precision and recall rate (100%) for all classifiers types except ICO, where Class8 (Horses) of images have higher recall rate (100%) for all classifiers types except BN.

In order to reduce the computation time, the selection feature algorithm is used to find best feature vector. The length of feature vector is reduced from 190 features to 59 best features. The results of the Precision and Recall are show in Table (4) depending on the features vector of the best color and texture features, when applying algorithm on tested images.

Table (4): Precision and Recall results for Classification Techniques Using Part of Hybrid Features.

Classes	Classifier Type									
	MP		SMO		RF		BN		ICO	
	Precision%	Recall%	Precision%	Recall%	Precision%	Recall%	Precision%	Recall%	Precision%	Recall%
Africans	78.6	64.7	72.2	76.5	82.4	82.4	82.4	82.4	73.3	64.7
Beaches	85.7	78.3	72	78.3	70.8	73.9	63	73.9	70.8	73.9
Buildings	72.2	68.4	81.3	68.4	73.7	73.7	61.1	57.9	60	78.9
Buses	73.7	93.3	92.9	86.7	86.7	86.7	93.3	93.3	84.6	73.3
Dinosaurs	100	100	100	100	100	100	100	100	100	100
Elephants	80.8	91.3	76.9	87	87.5	91.3	72.4	91.3	80.8	91.3
Flowers	96	92.3	96.3	100	100	96.2	96.3	100	100	100
Horses	94.4	94.4	90	100	88.2	88.9	94.1	88.9	94.7	100
Foods	71.4	62.5	78.9	62.5	78.9	62.5	73.3	45.8	75	50
Mountains	69.6	80	85	85	82.6	95	90	90	85.7	90
Average Precision	82.2	82.52	84.6	84.44	85.08	85.06	82.6	82.35	82.5	82.21
Model Build Time(Second)	15.55		0.42		0.48		0.07		6.19	

The results listed in Table (4), show that the high average (precision =85.08%, recall=85.06%) has been gain when using RF classifier with time (0.48) second. Also, it is noted that class5 (Dinosaurs) of images have higher precision and recall rate (100%) for all classifiers types, where class7 (Flowers) of images have higher precision and recall rate for most classifiers types, Class8 (Horses) of images have higher recall rate (100%) for two classifiers types SMO and ICO.

General averages of precision and recall when using each classifier type (MP, SMO, RF, BN and ICO) with each feature type (color features, texture features and hybrid) for all 10 classes of the dataset is plotted, as shown in Figures (3) and (4).

Iman .A
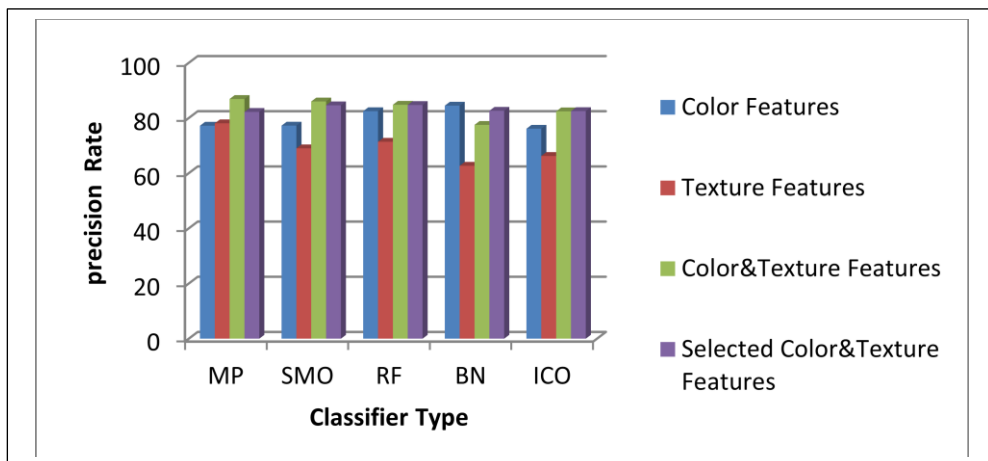
Figure (3): Bar graph showing the average of precision per classifier type.
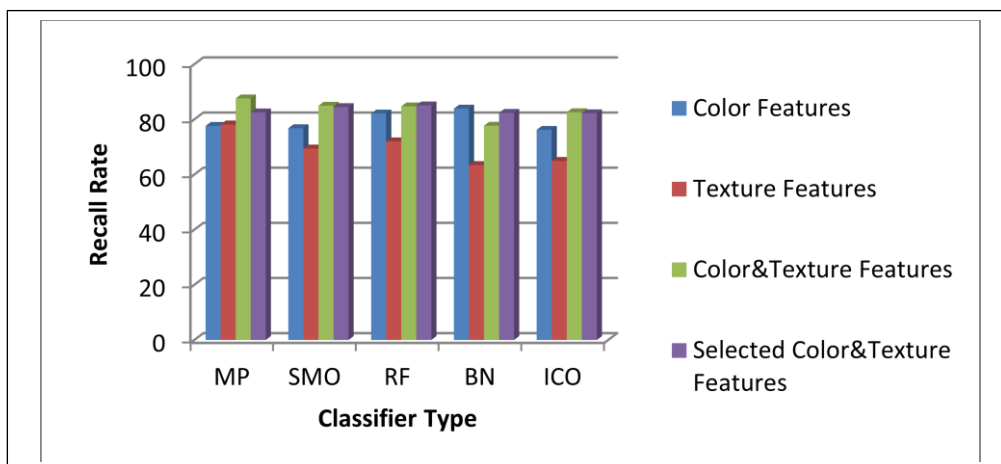
Figure (4): Bar graph showing the average of Recall per classifier type.

Figures (3) and (4) show that, high average (precision & recall) results of this system were when hybrid of color and textures features along with MP classifier is used, and when using selected best features of color and textures along with RF classifier type.

5. Conclusions

In this work, the results show that all classifiers types based on hybrid features of color and texture have given better results than using color features only or texture features only in image retrieval because color information and relative position of pixels are considered very important. The results of the average of precision and recall showed that

MP classifier type was the best one from the others in the image retrieval with high complexity time when using all color and textures features. Where, the RF classifier type was the best one from the others in the average of precision and recall with low complexity time, when using the best selected features of the color and textures. Also, it's found that the complexity of the image is very affected on the image retrieval results. Table (5) lists the average precision values attained by the proposed method compared with those given in previous studies, taking into consideration that in these studies same datasets have been used. The listed results demonstrate that the proposed method in this paper outperforms other methods.

50

Iman .A

Table (5): A Comparison between the performance results of proposed method with other methods applied on the same database.

Classes	Precision% [4]	Precision% [5]	Precision% [6]	Precision% [8]	Precision% [10]	Precision% Proposed Method
Africans	13.3	40.9	27	27.8	55	82.4
Beaches	26.15	39.4	33.4	54.2	48	70.8
Buildings	11.05	30.5	35	34.4	38	73.7
Buses	17.25	73.7	32.2	52.6	60	86.7
Dinosaurs	17.25	58.8	30.4	52.6	93	100
Elephants	34.9	49.1	38.4	55.6	52	87.5
Flowers	49.5	71.1	29.6	82.8	77	100
Horses	20.8	52.5	34.6	74.8	83	88.2
Foods	15.6	31.2	40	30.4	70	78.9
Mountains	25.9	63	38	50	48	82.6
Average Precision	23.17	51.02	33.86	51.52	62.4	85.08

References

[1] M. Waghmare and K Patidar, "A System for the Retrieval of Images from Large Database", International Journal on Recent and Innovation Trends in Computing and Communication, Vol. 4, Issue.1, PP. 26 – 29, 2016.

[2] N. S. Naik, S. S. Kulkarni and A. L. Kadam, "Content Based Image Retrieval Using Color, Texture and Hybrid Features", International Journal of Engineering Research and Development, Vol. 12, Issue 6, PP.31-38, June 2016.

[3] S. A. Husain and F. S. Akbar, "A Comparative Analysis of Feature Sets for Image Classification Using Back Propagation Neural Network", International Journal of Information and Electronics Engineering, Vol. 5, No. 1, January 2015.

[4] H. H. Bhuravarjula and V.N.S. Kumar, "A Novel Content Based Image Retrieval Using Variance Color Moment", International Journal of Computational Engineering Research, Vol.1, PP.93-99, 2012.

[5] X. Wang, H.Yang and D.Li ," A new content-based image retrieval technique using color and texture information", Computers & Electrical Engineering, Vol.39, No.3, PP.746-761, 2013.

[6] S.K. Thirunavuk, R.P. Ahila, S. Arivazhagan and C. Mahalakshmi, "Content Based Image Retrieval Based on Dual Tree Discrete Wavelet Transform", International Journal of Research in Computer and Communication Technology, Vol.2, PP.473-477, 2013.

[7] A. Nagathan and I. Manimozhi, "Content-Based Image Retrieval System using Feed-Forward Backpropagation Neural Network", International Journal of Computer Science Engineering, Vol. 2 No.04, July 2013.

[8] A. Huneiti and M. Daoud, "Content-Based Image Retrieval Using SOM and DWT", Journal of Software Engineering and Applications, Vol.8, PP.51-61, 2015.

[9] H .T. Suseelan, S. Sudhakaran, V. Sowmya and Dr. K. P. Soman, "Performance Evaluation of Sparse Banded Filter Matrices using content based image retrieval", Institute of Integrative Omics and Applied Biotechnology, Vol.7, Issue 3, PP.11-18, 2016.

[10] M. S. Navabi and Z. A. Brooghani, "Content-Based Image Retrieval through Combined Data of Color Moment and Texture", IJCSNS International Journal of Computer Science and Network Security, Vol.17 No.2, February 2017.

[11] M. Deswal and N. Sharma,"A Fast HSV Image Color and Texture Detection", International Journal of Science and Research, 2012.

Iman .A

[12] M. Soni and P. Singh,"Content Based Image Retrieval Using Combined Gabor and Image Features", International Journal of Computer Science and Technology, Vol.7, Issue 3, July - Sept 2016.

[13] A. Singla1and M. Garg,"CBIR Approach Based On Combined HSV, Auto Correlogram, Color Moments and Gabor Wavelet", International Journal Of Engineering And Computer Science, Vol.3, Issue 10 October, PP. 9007-9012, 2014.

[14] H. B. Jehlol, "Image Retrieval Using Association Rules", M.Sc. thesis, Iraqi Commission for Computers And Informatics, Informatics Institute for Postgraduate Studies , Iraq, 2013.

[15] V. Duraisamy and R. B. Durai, "Sequential Minimal Optimization: A Fast Algorithm for Training Support Vector Machines", International Journal of Information Sciences and Application,Vol.3, No.2 ,PP. 93-97, 2011.

[16] K. Jayech and M. A. Mahjoub, "Clustering and Bayesian network for image of faces classification", International Journal of Advanced Computer Science and Applications, Special Issue on Image Processing and Analysis, 2011.

[17] K. Goeschel, "Reducing false positives in intrusion detection systems using data-mining techniques utilizing support vector machines, decision trees, and naive Bayes for off-line analysis", Southeast Con., Norfolk, VA, PP. 1-6, 2016.

[18] J. Han, Micheline and J. Pei, "Data Mining: Concepts and Techniques", Morgan Kaufmann Publishers Inc, USA, 3rd edition, 2012.

[19] S. Senthil, B.G. Deepa and B. Ashwarya ,"Comparison of Classification Algorithms for Predicting Breast Cancer", IJSRD - International Journal for Scientific Research & Development, REVA University, Bangalore, India, Vol. 4, Issue 12, 2017.

[20] R. A. OMONDI and C. J. RAJAPAKSE, "FPGA Implementations of Neural Networks", 1St edition, Springer publishing company, 2010.

[21] K. Sharma, A. Kaur and S. Gujral, "Brain Tumor Detection Based On Machine Learning Algorithms", International Journal of Computer Applications (0975 – 8887) Vol. 103 – No.1, October, 2014.

[22] M. A. Hall, "Correlation-based Feature Selection for Machine Learning", the university of Waikato, Hamilton, NewZealand, 1999.

[23] A. J. Mouhamd, "Image Compression Using Wavelet Transform", M.Sc. thesis, College of Science, The University of Al-Mustansiriyah, 2005.

خوارزميات تصنيف كفوءة لأسترجاع الصور اعتماداً على الخصائص اللونية والنسيجية

ايمان عبد الجبار سعد

مركز الحاسبة الالكترونية

الجامعة المستنصرية، بغداد، العراق

المستخلص:

أنظمة استرجاع الصور بالاعتماد على محتوى الصور تستخرج عادةً نتائج الاسترجاع من خلال اوجه التشابه بين خصائص الصورة المراد استرجاعها وخصائص الصور المرشحة. النظام المقترح يقدم مقارنة تحليلية لخمسة أنواع من خوارزميات التصنيف التي استخدمت في نظام استرجاع الصور بناءً على المحتوى، هذه المصنفات هي Multilayer Perceptron (MP), Sequential Minimal Optimization (SMO), Random Forest (RF), Bayes Network (BN) and Iterative Classifier Optimizer (ICO)، حيث يتم التحقق لأيجاد خوارزمية تصنيف مناسبة من حيث الاداء والسرعة لاسترجاع الصور. في النظام المقترح تم استخدام خصائص الصورة منخفضة المستوى متمثلة بخصائص اللون مثل (color-histogram, color-moments and color-autocorrelogram) وخصائص النسيج مثل (Wavelet transform and log Gabor filter)، كذلك يشمل النظام على هجين من الخصائص اللونية والنسيجية معاً لأسترجاع الصور بشكل كفوء. تم اختبار النظام باعتماد قاعدة البيانات (WANG) حيث كان افضل معدل للدقة في الاسترجاع هو (85.08%) من خلال دمج الخصائص اللونية مع الخصائص النسيجية وباستخدام المصنف (RF).

Image Encryption Using Columnar Transportation Technique and Bits Reversing

Mohammed Hasan Abdulameer
Department of computer science,
Faculty of education for girls, university of kufa, Iraq

Abstract

Security has become very important aspect during data transmission and storage. Cryptography is used to maintain security. Columnar Transportation Technique is one of the most common methods that used in image encryption. In this paper, we proposed an encryption technique based on columnar Transportation and bits reversing, and named the method (CTR). Different colored images are used in the experiments. Experimental results showed that the proposed method is a secure and effective as a color image encryption method.

Mohammed .H

I.   Introduction

Security of images has gained much attention for many years, and the "illegal data access has become big issue and widespread in communication networks. So that, data security in storage and transmission of digital images is extremely needed, such as in transmitting medical images, military images transmissions, and confidential video conferencing [1][2][3]. Digital images, nowadays it's a very popular for using in computers and other digital devices. For image processing applications, it is always worth to minimize the computational time and storage. There are many studies and techniques to encrypt images which were achieved great results [4][5]. However, the classical cipher methods are still slow to process image and video data in commercial systems. An algorithm to enhance the security in transmission digital images was proposed by Rodriguesa et al [6] .Their approach was based on Advanced Encryption Standard (AES) stream ciphering applied in the Huffman coding. Their proposed structure permits decryption of an explicit area of image and that led to a substantial decrease in processing time in encrypting and decrypting process. Moreover, it provides a steady bit rate and retain the JPEG bit-stream acquiescence. To reflect a high level security and features of parallel processing with better image encryption and non-distortion, Ammar et al [1] introduced a new method as an image encryption technique. It was established on a non-traditional random number generators and a residue number system (RNS) sequence, which are clustered as a chaotic system. Acharya et al [7] have proposed an advanced of hill cipher named as (AdvHill) encryption algorithm which uses an involuntary key matrix.[7]. Their proposed method was an effective against plaintext attacks. Singh and Nand [8] introduced an approach where the image file is considered as a stream of bits. These are constructed as grids of variable sizes.

Their proposed method transforms each grid into encrypted grid by applying Helical and columnar transposition. This paper proposes an approach called (CTR) to simulate analyzing and ciphering the entire image by re-ordering the data of image matrix; using Columnar Transportation technique and bits reversing in order to choose an effective key as one of available ciphering/deciphering keys.

I.   The proposed Methodology

The general block diagram of the proposed methodology is illustrated in the figure (1) below:
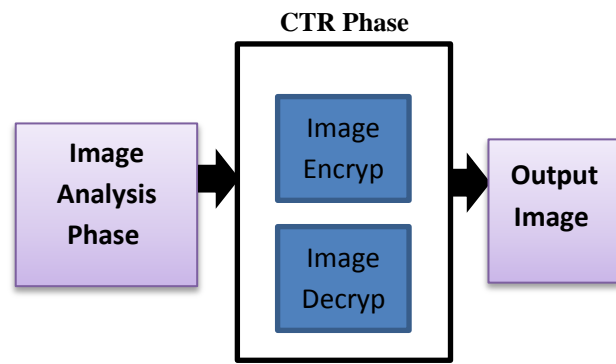
Figure (1): the proposed Methodology.

1. **Image Analysis phase**: it is the first phase in the proposed methodology which comprises many steps as described in the following flowchart:
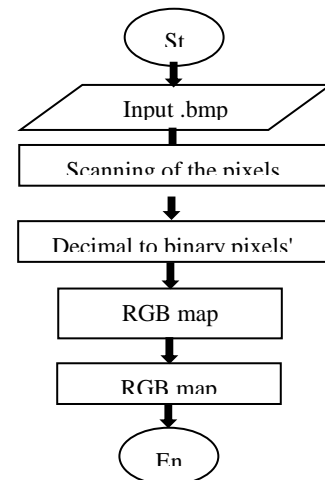
Figure (2): flowchart of the image analysis

steps

Journal of AL-Qadisiyah for computer science and mathematics   Vol.10   No.1   Year 2018
ISSN (Print): 2074 – 0204   ISSN (Online): 2521 – 3504

Mohammed .H

a) **Input .bmp image:** In this processing step, each image is mapped into the popular type of bitmap (24 bit for each pixel (RGB)) which is used in most operating systems such as windows. We used different sizes of the applied image from the dataset such as (768×512) [9] as shown in the table (1).

Table (1): Some images sizes used in the proposed method

127×128
549×523
581×461
768×512

b) **Scanning pixels:** In this step, the method scans the entire coordination of the image through the width and the height in order to get the original data matrix**.**

c) **Decimal to Binary pixels form:** In this stage, the method converts all the pixels' values from decimal into binary form concurrently with the previous step.

d) **RGB pixels map division and buffering:** In this step, each pixel's value divided into three parts of colors binary matrixes named as color names R, G, and B.

The general equations for the previous steps are:

$$I_{Size(n*m)} = \begin{array}{l} n = I_{width-1} \\ m = I_{high-1} \end{array} \tag{1}$$

To convert the decimal form of value to the binary form

$$I_{RGB}(r.c) \sum_{i=0}^{n} \sum_{j=0}^{m} I(r.c) \tag{2}$$

And for each pixel in equation 2, we get the binary form of it based on equation 3

$$I_{Bin}(r.c)$$
$$= \sum_{k=1}^{24} \begin{array}{ll} \text{if } I_{rgb}(r.c) \bmod 2=0 & \text{if } K\leq8:I_R(0)\text{and if } K\leq16:I_G(0) \text{ and if } K\leq24:I_G(0) \\ \text{else } I_{rgb}(r.c) \bmod 2=1 & \text{if } K\leq8: I_R(1)\text{and if } K\leq16:I_G(1) \text{ and if } K\leq24:I_G(1) \\ I_{rgb}(r.c)=I_{rgb}(r.c) \text{ div } 2 \end{array}$$

$$\tag{3}$$

$$I_{Binary\ of\ RGB}(r.c) = I_{Binary\ of\ R}(r.c) +$$
$$I_{Binary\ of\ G}(r.c) +$$
$$I_{Binary\ of\ B}(r.c) \tag{4}$$

2. CTR method phase:

There are two main procedures for this phase, the CRT image encryption for ciphering each input image and the CRT image decryption for deciphering each input image that is ciphered.

Journal of AL-Qadisiyah for computer science and mathematics   Vol.10   No.1   Year 2018
ISSN (Print): 2074 – 0204   ISSN (Online): 2521 – 3504

Mohammed .H

2.1. **Image Encryption:**

The general flowchart of CTR image encryption as shown in figure (3):
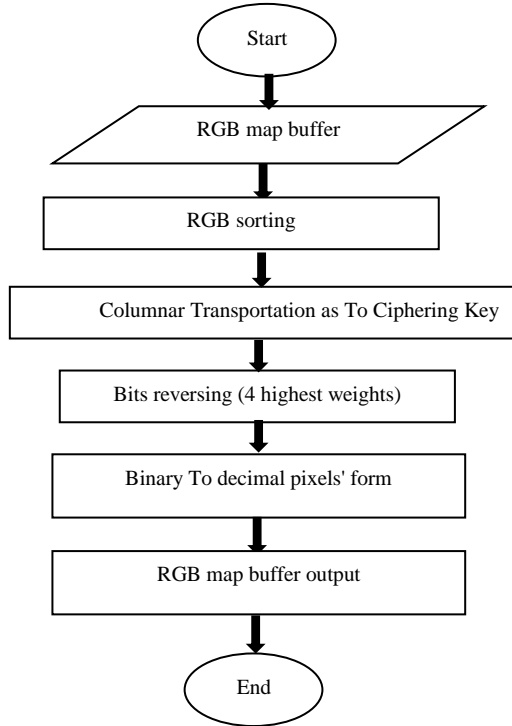
Figure (3): flowchart of CTR image encryption

A. **RGB sorting step:** this step starts with sorting all pixels' data by organize the 24 bits for each pixel into (3*8) array in order to convert them to ciphering key in Columnar transportation using equation 5:

$$I_{RGB\ Sort}(n.m) = \sum_{i=0}^{n}\sum_{j=0}^{m}\sum_{k=1}^{3}\sum_{l=1}^{8} I_{Binary\ of\ RGB}(k.l) \quad (5)$$

B. **Columnar transportation**: Re-arrange the 8' columns of the binary array as to the applied ciphering key (length is: 8) for each pixel sorted in equation 5 by applying equation 6:

$$P_{RGB\ Sort} = \sum_{k=1}^{3}\sum_{l=1}^{8} P_{Columnar\ Transport}(k.l) \quad (6)$$

C. **Bits reversing (4 highest weights)**: It is a significant step in the proposed method that reverse the last 4 bits' positions values (5,6,7,8) from 1 to 0 and verse vise for each pixel sorted in equation 6 by applying equation7 below:

$$P_{Bit\ inverse} = \sum_{k=1}^{3}\sum_{l=5}^{8} if\ P(k,l) = 1, then\ P(k,l) = 0, \\ Else\ P(k,l) = 1 \quad (7)$$

D. **Binary to decimal pixels' form:** after the previous step, we convert the 24 bit of applied pixel to its decimal value for each pixel sorted in equation7 via applying equation 8 as below:

$$P_{Dec}(r.c) = \\ \sum_{k=1}^{24} if\ I_{rgb}(k) = 1\ then\ sum = sum + p\ (initial = 1) \\ p = 2 \times p \quad (8)$$

E. **RGB map buffer output:** collect all image data as in the equation 9 and saving it as ciphered image.

$$I_{decimal\ of\ RGB}(r.c) = I_{dec\ of\ R}(r.c) \\ + I_{Bec\ of\ G}(r.c) \\ + I_{dec\ of\ B}(r.c) \quad (9)$$

1.2 Image Decryption:

The general flowchart for CTR image decryption is illustrated in figure (4):
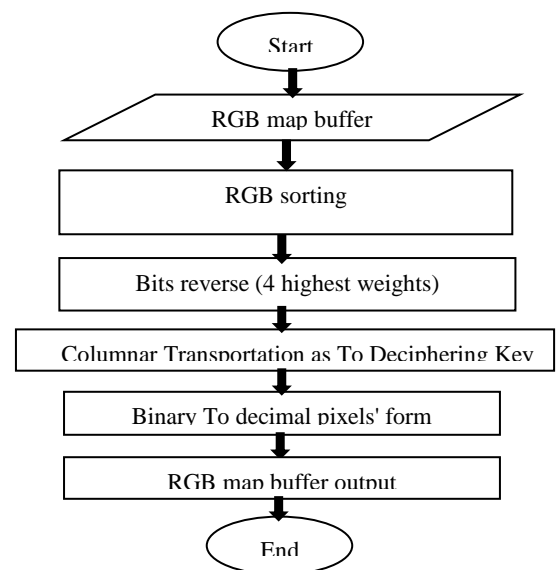
Figure (4): flowchart steps of CTR image decryption

A. **RGB sorting:** arrange the 24 bits for each pixel into (3×8) array to convert them as deciphering key in columnar transportation step as above in equation 5.

B. **Bits reverse (4 highest weights):** reverse the last 4 bits' positions (5,6,7,8) from 1 to 0 and verse vise as in explained above in equation 6.

C. **Columnar transportation**: Re-arrange the 8' columns of the binary array as deciphering key from the equation 7 above.

D. **Binary to decimal pixels' form:** convert the 24 bit of applied pixel into its decimal values as in equation 8.

E. **RGB map buffer output:** collect all the image data and saving it as ciphered image as in the equation 9.

3. **Output Image:** it is the final phase that shows either the ciphered or deciphered image after applying CTR method procedures.

II.   Implementation and Experimental results

This section shows the experimental results of the proposed CTR approach for the selected images from the dataset of colored images [9]. The figures 5 and 6 present the images before and after applying CTR method.
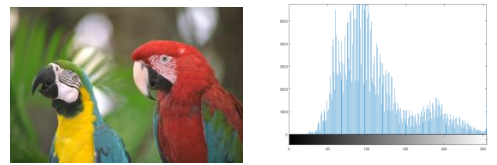
(a)Original Parrot image with histogram
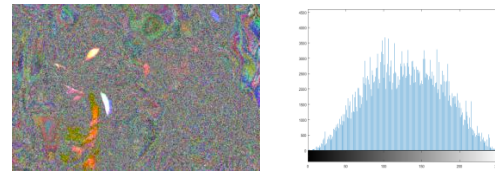
(b) Parrot image after applying CTR method with histogram
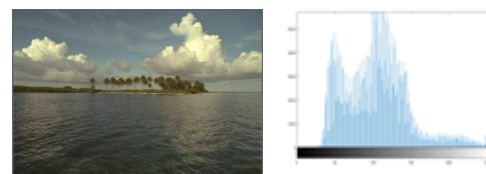
(a)Original Land image with histogram
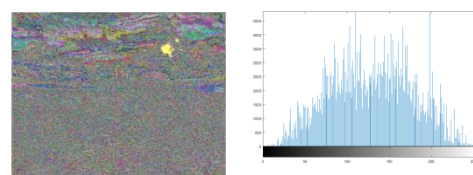
(b) Land image after applying CTR method with histogram

Figure (5): Two images encryption and decryption by CTR method with their histogram

Mohammed .H
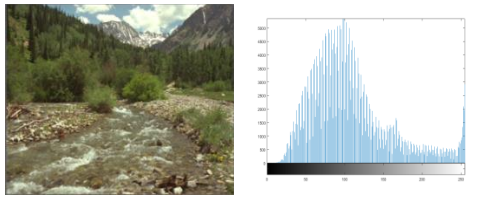
(a)Original Mount image with histogram
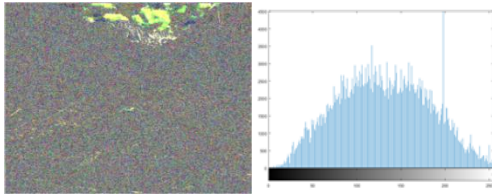
(b) Mount image after CTR algorithm with histogram
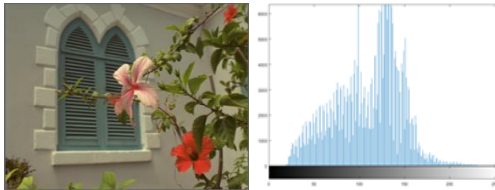
(a)Original Window image with histogram
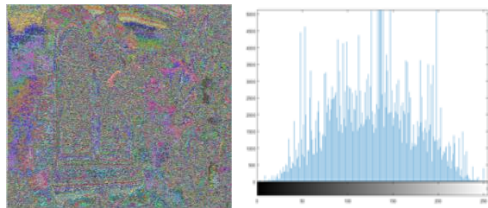
(b) Window image after CTR algorithm with histogram

Figure (6): Two images encryption and decryption by CTR method with their histogram

Moreover, table 2 shows the decimal values of the cropped 5×5 pixels of Parrot image and table 3 demonstrate the RGB binary values corresponding to cropped 5×5 pixels in table 2.

Table (2): Decimal values of the cropped 5×5 pixels of Parrot image

pixels	Pix0	Pix1	Pix2	Pix3	Pix4
Pix0	14929332	14929332	14929078	15060664	14994871
Pix1	14929587	14863539	14929078	14994871	14929078
Pix2	14929332	14863539	14929078	14994871	14994871
Pix3	14929332	14929332	14994871	15126457	15126457
Pix4	14863539	14929332	14994871	15060664	15126711

Table (3): RGB binary values corresponding to cropped 5×5 pixels in table 2.

pixels		Pix0	Pix1	Pix2	Pix3	Pix4
Pix0	R	00101101	00101101	01101101	00011101	11101101
	G	10110011	10110011	00110011	01110011	10110011
	B	11000111	11000111	11000111	10100111	00100111
Pix1	R	11001101	11001101	01101101	11101101	01101101
	G	01110011	00110011	00110011	10110011	00110011
	B	11000111	01000111	11000111	00100111	11000111
Pix2	R	00101101	11001101	01101101	11101101	11101101
	G	10110011	00110011	00110011	10110011	10110011
	B	11000111	01000111	11000111	00100111	00100111
Pix3	R	00101101	00101101	11101101	10011101	10011101
	G	10110011	10110011	10110011	11110011	11110011
	B	11000111	11000111	00100111	01100111	01100111
Pix4	R	11001101	00101101	11101101	00011101	11101101
	G	00110011	10110011	10110011	01110011	00001011
	B	01000111	11000111	00100111	10100111	01100111

Mohammed .H

IV. Discussion

The strength of the CTR method in ciphering is depends on the power of the ciphering key, and to explain that; we will summarize some points;

first, the length of the key will be same as the size of the bits of each color. That will mean the length will be eight numbers ranging in [1,2,3,3,4,5,6,7,8]. Each one of them have the same position of the original bit. When the user chooses the ciphering key as the form [12345678], then it will be in the same ordering of the original bits of the image's pixels. That's means there is no change in the positions of bits for the ciphering image and the original image. In addition, the deciphering key must be the same to ciphering key. **Second,** depend on the columnar transportation of the positions of the ciphering key, we will get powerful ciphering key. **Third,** due to the importance of the last positions of the binary form of each color, we must take into account changing the positions of these 4 highest weights when trying to choose a ciphering key. **Four,** the eight digits for each ciphering key mean there are many transportations between the positions. It may get a ciphering key with one transport such as (21345678), the decipher keys (reverse keys) for the cipher keys above will be the same. Table (4) below show that the positions of the first and the second bits are changed. Changing between four bits means two positions changed such as (21435678). The changing to six and eight bits also possible such as (21436578), (21436587). There are thirty-two possible ciphering keys. **Finally,** the power of ciphering depends on substitution the maximum transportations, in this case the CTR method will be very effective in ciphering and this relating with the nature of the original image data. For example, the key (37821546) is a powerful ciphering key and the reverse key of it is (54176823). The powerful ciphering key for certain source image may be unreliable for another source image.

Table (4): Bit changing to create ciphering keys.

Bits changes	Ciphering key								Deciphering key							
One bit change	2	1	3	4	5	6	7	8	2	1	3	4	5	6	7	8
Two bits changes	2	1	4	3	5	6	7	8	2	1	4	3	5	6	7	8
Six bit changes	2	1	4	3	6	5	7	8	2	1	4	3	6	5	7	8
Eight bit changes	2	1	4	3	6	5	8	7	2	1	4	3	6	5	8	7
More bit changes (**Strong Key**)	3	7	8	2	1	5	4	6	5	4	1	7	6	8	2	3

V. Conclusion:

Columnar Transportation and bits reversing (CTR) method has been proposed in this paper. The method simulate analyzing and ciphering the entire image. This achieved by re-ordering the data of image matrix and choose an effective key as one of available ciphering/deciphering keys. Eight different colored images have been collected and used in the experimental results. The results showed high performance in the encryption for the selected images. Furthermore, the CTR was reliable in analyzing and encrypting variety of image features. Moreover, it was an easier to manage use of available keys in order to investigate the desired cipher sample of any color image. To extend this work, we suggest combining the proposed CTR with another method for more security performance and use large dataset to show more stability.

Mohammed .H

VI. References:

[1] A. Ammar, A. S. S. El-Kabbany, M.I. Youssef and A. Emam, "A Novel Secure Image Ciphering Technique Based On Chaos", 4th WSEAS Int. Conf. on Information Science, Communications and Applications, Miami, Florida, April 21-23, (2004).

[2] Hasan Thabit Rashid and Hind R. M.," New Algorithm for Image Ciphering by Detecting the Edges of Color Image", The Scientific Karbala Journal, Vol: 144, No: 774. (2008).

[3] Hasan Thabit Rashid and Hind R. M.," Ciphering of Stopping and the Attrition Voices Phonemes in Coding Image", 1st Conference for the Secret of the Information and the Ciphering, Islamic University, Najaf, Iraq,Vol: 16, No: 20, April 2008.

[4] El-Zoghdy SF, Nada YA, Abdo AA, "How Good Is The DES Algorithm In Image Ciphering", International Journal of Advanced Networking and Applications. 2(5):796-803,(2011).

[5] Kester, Quist-Aphetsi. "Image Encryption based on the RGB PIXEL Transposition and Shuffling." International Journal of Computer Network and Information Security 5, no. 7, p.43, (2013).

[6] Bhairvee Singh, Parma Nand, India, "Image Encryption and Decryption Using Helical and Session Based Transposition with Key Wrapping ", INTERNATIONAL GLOBAL JOURNAL FOR ENGINEERING RESEARCH, NOV, VOL. 10, NO. 2, (2014).

[7] Acharya, Bibhudendra, Saroj Kumar Panigrahy, Sarat Kumar Patra, and Ganapati Panda. "Image encryption using advanced hill cipher algorithm." International Journal of Recent Trends in Engineering 1, no. 1 (2009).

[8] J.M. Rodriguesa, W. Puecha and A.G. Borsb,"A Selective Encryption for Heterogenous Color JPEG Images Based on VLC and AES Stream Cipher", CGIV'06: 3rd European Conference on Colour in Graphics, Imaging and Vision, Jun, Vol. 2006. No. 1, pp.34-39, (2006).

[9] The Data set of Toyama_database-MICT Image Quality Evaluation Database (2008).

تشفير الصور باستخدام تقنية النقل العمودية وعكس البتات

محمد حسن عبدالأمير
قسم الحاسبات /كلية التربية للبنات /جامعة الكوفة

المستخلص :

أصبح الأمن جانبا هاما جدا أثناء نقل البيانات والتخزين ويستخدم التشفير للحفاظ على الأمن. تقنية النقل العمودية هي واحدة من الطرق الأكثر شيوعا التي تستخدم في تشفير الصور. في هذه البحث، نحن نقترح تقنية التشفير على أساس النقل العمودي وعكس البتات تسمى طريقة سي ار تي . وتستخدم الصور الملونة المختلفة في التجارب. وأظهرت النتائج التجريبية أن الطريقة المقترحة هي آمنة وفعالة كطريقة تشفير للصورة الملونة.

2D to 3D conversion using a pair of images

"KLT algorithm as a case of development and study"

Sarmad Nihad Mohammed

University of Kirkuk

Department of Computer Science, College of Computer Science

Sarmad_mohammed@uokirkuk.edu.iq

Abstract., This paper investigate how motion between two images is affecting the reconstruction process of the KLT algorithm which we used to convert 2D images to 3D model. The reconstruction process is carried out using a single calibrated camera and an algorithm based on only two views of a scene, the SFM technique based on detecting the correspondence points between the two images, and the Epipolar inliers. Using the KLT algorithm with structure from motion method shows the incompatibility of it with the widely-spaced images. Also, the ability of reducing the rate of reprojection error by removing the images that have the biggest rate of error. The experimental results are consisting from three stages. The first stage is done by using a scene with soft surfaces, the performance of the algorithm shows some deficiencies with the soft surfaces which are have few details. The second stage is done by using different scene with objects which have more details and rough surfaces, the algorithm results become more accurate than the first scene. The third stage is done by using the first scene of the first stage but after adding more details for surface of the ball to motivate the algorithm to detect more points, the results become more accurate than the results of the first stage. The experiments are showing the performance of the algorithm with different scenes and demonstrate the way of improving the algorithm where it found more points from images, so it builds more accurate 3D model.

Keywords. SFM, Conversion Algorithms, 2D into 3D, Computer Vision, KLT algorithm.

Sarmad .N

1.Introduction. The ability of the vision of living creatures in receiving the real world as a three-dimensional scene motivates pioneers of the computer vision community to determine methods to simulate this ability. The solutions to this problem are divided into two groups, the first by acquiring a three-dimensional model directly from the real world by using special cameras such as a stereoscopic dual-camera with the ability to generate a three-dimensional model directly from a real-world scene. The second is by using two-dimensional data as inputs for algorithms designed particularly for the conversion of two-dimensional models into three-dimensional models. The role of these algorithms is to reconstruct a three-dimensional model based on the structure of the two-dimensional data which is missing the third dimension (the depth information) of the real world. The missing depth information is the result of the inadequacy of the traditional camera to obtain the third dimension from a captured scene, hence the role of algorithms to overcome this problem.

2. Why Do We Need to Convert the Two-Dimensional into Three-Dimensional. In general, there is more than one reason to convert two-dimensional images into three-dimensional models. The enormous amount of two-dimensional data in the past and the present in addition to the traditional devices for capturing scenes from the real world are the most important reasons. At this point, a trend where the role of conversion algorithms from 2D to 3D for generating three-dimensional models is becoming more popular. The accuracy of these algorithms, which differ from each other, depends on elements such as time consumption and the precision of the output model. [1]

The way that the mind behavior to generate the 3D model from the real world are considered as a base to compute the 3D geometry from 2D geometry or the structure from motion. The nonlinear approach is a technique which is employ this behavior to recover the structure and motion by minimize the value of the nonlinear cost function [2].

3.   Challenges   Facing   Conversion Techniques. The challenges facing the techniques of conversion from the two-dimensional model to the three-dimensional model are divided into two groups. The first group covers every algorithm and several problems which must be solved by applying these algorithms. The second group of challenges involves specific types of algorithms considered to be high quality conversion techniques.

The first group of challenges includes three tasks which are solvable with every conversion algorithm. These tasks include [3][4]:

- **Apportionment of depth.**
- **Check of convenient disparity**
- **Padding of the exposed regions**

The second group (as shown below) of these challenges could be named as typical problems, which require high quality conversion algorithms in order to execute them. Those problems such as:

- **Semi-transparent objects (glass)**
- **Repercussion**
- **Foggy translucent objects**
- **Thin objects such as fur or hair**
- **Noise effects such as film grain**
- **The quick and unorganized motion in a scene**
- **Small pieces such as snow, rain and explosions**

Sarmad .N

4. 2-D and 3-D. The process of transformation from 3D space to a 2D plane can be illustrated with a pinhole model (Figure 1), which consists of a plane R, called the image plane and a point C, the optical center, which does not belong to the image plane.
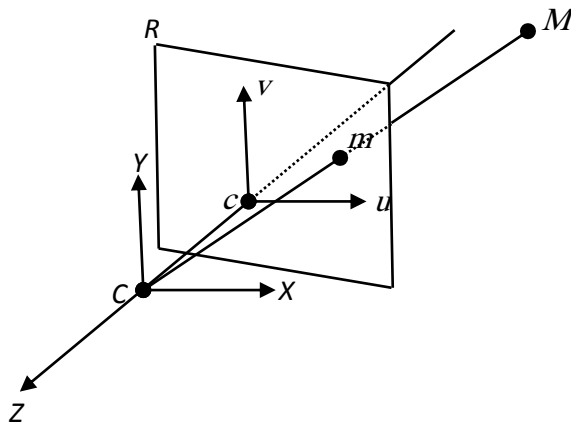
Figure 1 Pinhole $Model^1$

M object has a projection on the image plane R at the m point, and that projection represented by intersection of the optical ray (C, M) and the image plane R. The principal point c represents the center of the perpendicular of the optical axis on the image plane. The camera coordinate system (CCS) could be carried out with the center C and two axes (X and Y) which are parallel to the image plane (u, v) and the third axis Z corresponds the optical axis. The distance between the center C and the image plane represent the focal length f. [5]

5. The Relationship between the Camera and the Real World. In general, all images that we have represent the reflection of any object in our world, so those images represent the results of the relationship between cameras and the real world, and each point in the image has a corresponding point in the real world. Clearly, the position of any object in an image depends on its position in the real world.

In fact, after the camera captures any scene, we obtain a 2D image coordinate $P(u,v)$ from 3D points (scene coordinates) $P(X,Y,Z)$. [6]

6. Camera Calibration. Camera calibration is the process of estimating the internal camera parameter (intrinsic parameter) that relates the direction of rays through the optical center to coordinates on the image plane. The importance of the internal camera parameter lies in the need for building 3D models of the world using a camera with a known intrinsic parameter [6].

7. STATE-OF-THE-ART. The procedure of obtaining structure from a set of images began in the 1980s [7-10]. Normally, structure from motion is initially approached by placing a set of obvious characteristics that are found in two image structures. This is commonly denoted as the correspondence problem solution. Then, the proportional motion of these characteristic correspondences is given the structure of the environment [11]. The conventional estimation of structure from motion mostly uses two images obtained from a single camera to slant the field of view of 45 to $60°$ [12-14]

8. Related Works. Using the structure and motion together under the name of structure from motion to reconstruct the three-dimensional model from multiple images is considered to be a significant topic in computer vision research. The pioneers in the field of computer vision have proposed many techniques to fill the lacunae in the structure from motion approach.

Zhengyou Zhang [18] used structure and motion from two perspective views based on the essential parameters, a fundamental matrix and Euclidean motion.

The problem with this technique is that the results mostly are not good enough due to the sensitivity of the second step to the incipient guess and the difficulty of obtaining an accurate incipient estimate from the first step. In order overcome this problem, Zhengyou Zhang proposed an approach by imposing the fundamental matrix (zero-determinant constraint). Unlike [18], Frank et al [19] introduced another technique by using the structure from motion without correspondence. This method exceeded the traditional techniques that require the presence of a known correspondence point [12] or calibrated images from a known camera viewpoint [13] or known shape [14]. Furthermore, this method deals with non-sequential images which are taken from vastly different viewpoints.

Masahiro [15] introduced a method of using the structure from motion in map reconstruction. This method was a system of three-dimensional simultaneous localization and mapping (SLAM), which is based on the SFM scheme. The steps of this method are as follows:

- Basic Framework
- Feature Tracking
- Initial Estimation

The first step considers the three-dimensional SLAM as a set of images obtained from a monocular camera. The three-dimensional map

is represented as three-dimensional points from the feature points tracked through the set of images. The second step occurs based on KANADE-LUCAS-TOMASI [16]. The third step occurs by using the factorization method [17].

The precision and robustness of this method is based on the selection of the baseline distance, so the proper baseline selection depends on standards for object shape reconstruction and the camera pose estimation.

9. The Proposed Method. According to the title of the paper, the technique of reconstructing a three-dimensional model from a pair of two-dimensional images depends on structure and motion. In order to obtain this information, there are a number of steps to follow. First, we need a static scene with an object of known size (in our scene, the object is a ball of size 10 cm) this size is considered as a scale factor to reshape the 3D model, and a calibrated camera to obtain two views. After obtaining the real data in two images, the work of the KLT algorithm begins at this step. The workings of this algorithm are presented in the following sections as the next diagram representing.
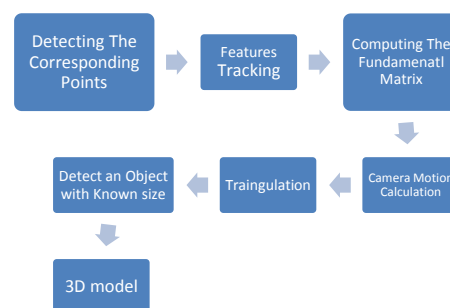
Processing Diagram

Sarmad .N

9.1 Detection of The Correspondence Points. In order to continue to the others step, it is necessary to find the correspondence points. Therefore, the best features need to be detected in order to track from image to image. This process is carried out by using the minimum eigenvalue algorithm as proposed by C. TOMASI & J. SHI [23], and as the below equation shows:

$$R = \min(\lambda_1, \lambda_2)$$

where (λ_1, λ_2) represents the eigenvalues and the window (corner) is accepted if those eigenvalues are greater than the predefined threshold value (λ) as shown below:

$$\min(\lambda_1, \lambda_2) > \lambda$$

According to the C. Tomasi & J. Shi method, the strongest corners will be found in the image, which is a grayscale image.

9.2 Features Tracking. This step begins after finding the strongest corners (best features) from the first image. The role of this process is to track those features in the second image. This process is carried out by using the KLT algorithm   (KANADE-LUCAS-TOMASI) [24]. The goal of this algorithm is to find the specific location of a specific point in the second image according to the first image. This is achieved with the following equation:

$$\bar{V}_{opt} = G^{-1}\bar{b}$$

9.3 Computing the Fundamental Matrix. The computation of the fundamental matrix from the correspondence points which are detected is the first step, the next equation is used to compute the fundamental matrix F:

$$X'^T FX = 0$$

Where X' and X represents corresponding points of a pair images.

9.4 Camera Motion Calculation. In this section, we will estimate the position and orientation of a calibrated camera. Normally, there are two views, hence there are two poses. Both poses are relative to each other as denoted by the fundamental matrix F. The camera poses are computed up to scale and the position denoted a unit vector.

9.5 Triangulation. The three-dimensional positions of the matched points can be determined by triangulating.

9.6 Detect an Object with Known Size. This process is carried out by using the MSAC algorithm (M-estimator sample consensus). The fitting of a sphere to an inlier point cloud using an object with known size is here a ball of size 10 cm.

10. Experimental Results. The experiments were carried out on an ordinary PC equipped with the following specifications:

- System Type: 64-bit operating system, x64-based processor.
- Edition: Windows 10 Home.
- Processor: Intel (R) Core (TM) i3-2310M CPU @ 2.10 GHz.
- RAM: 4.00 GB.

The input images were obtained from a digital camera (NX3000) equipped with:

- 20.3 MP APS-C CMOS Sensor.
- 16-50 mm Power Zoom Lens.
- 1/4000 sec Shutter Speed.

All experiments were carried out using the MATLAB R2015b software package. The methodology of the paper was based on the technique of 'structure from motion 'using KLT algorithm, but by using a single calibrated camera with the camera calibration application in MATLAB and by obtaining two views of the scene with a little motion for the second view. The algorithm that will create the three-dimensional model of the scene, from a pair of two-dimensional images following several steps, as the next section shows.

- The first step is carried out by loading a pair of images of the scene obtained by using the above camera.

- Next, the camera parameters are obtained by loading the camera calibration. To understand the mean reprojection error, which represent the difference in distance between the

actual scene and the estimated one, we show below the equation of mean projection error:

$$\sum d\,(x_i,\hat{x}_i)^2 + d\,(x_i',\hat{x}_i')^2 \ \dots\dots\dots\ 1$$

The unit of the reprojection error in pixel, so less than one it will be acceptable rate as shown in figure 2.
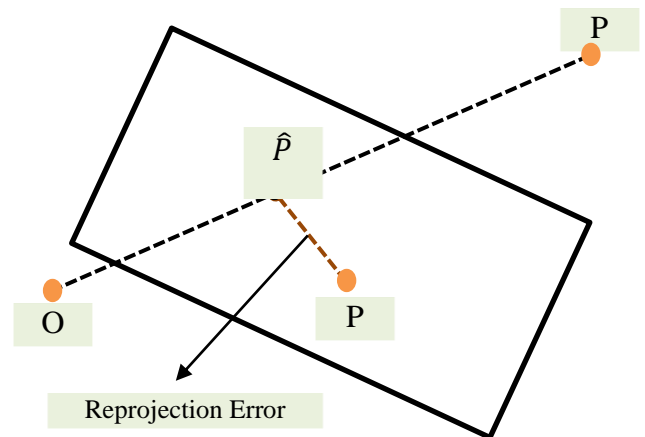
Figure 2: The reprojection error

- Camera calibration.
- In order to avoid any lens distortion effects on the accuracy of the final reconstruction, MATLAB offers a simple function for this purpose which
straightens any lines that may deform due to the radial distortion of the lens.

- At this step, the algorithm detects the corresponding points between the two images. This process can be carried out in a number of ways; however, here, the motion occurs not too far from the first position, so the KLT algorithm (KANADE–LUCAS–TOMASI) is suitable to create the point correspondences.
- Computing the fundamental matrix is carried out at this point and according to the results, the inlier points are obtained, and those points match the Epipolar constraints.
- The computation of the camera position, which consists of the translation and rotation, is carried out by using the CameraPose function in MATLAB.
- The three-dimensional locations of the matched points found in the fourth step are reconstructed using the triangulation function.
- The Plot Camera and the PcShow functions are used to display the three-dimensional point cloud.
- In order to detect the actual scale factor, the algorithm uses an object with known size, so the scene contains a ball with a known radius (of 10 cm). The PcFitSphere function fits a sphere to the point cloud to detect the ball.
- The final step is the metric reconstruction, which mean the coordinates of the three-dimensional points will be in centimeter due to the actual radius of the ball which was 10 cm.

The following images show the results of the above steps with multiple different scenes, and each image has a title to clarify its identity. The time consumed by the algorithm to reach the results was different in each test, where the 1st test consumed 102 seconds, the 2nd test consumed 280 seconds, and the 3rd one consumed 131seconds. The results are shown below:

Figure 3: The original images

Figure 4: The Undistorting images

Journal of AL-Qadisiyah for computer science and mathematics   Vol.10   No.1   Year 2018
ISSN (Print): 2074 – 0204   ISSN (Online): 2521 – 3504

Sarmad .N
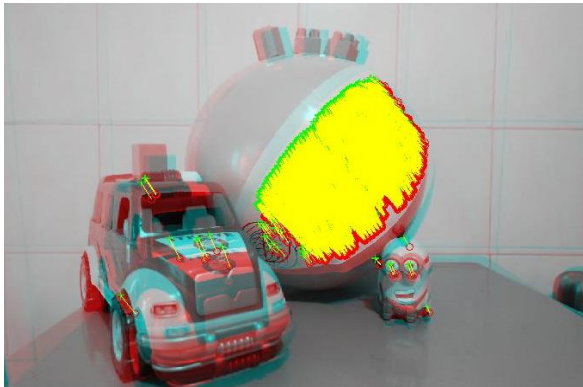
Figure 5: Strongest corners from the first image

Figure 8: Estimated size and location of the ball

Figure 6: The Tracked features
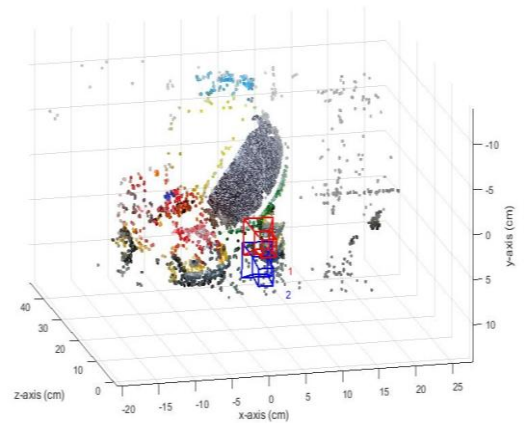
Figure 9A: Metric reconstruction of the scene

Figure 7: The Epipolar inlier
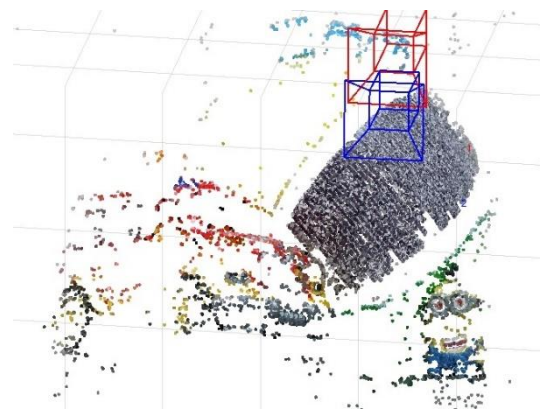
Figure 9B: Metric reconstruction of the scene with another position

In order to test the algorithm with another scene, which consisted of different ball with rugged surface and objects with more details, we repeat the execution of the code and the results were as shown:

Sarmad .N

Figure 10: The original images (second test)
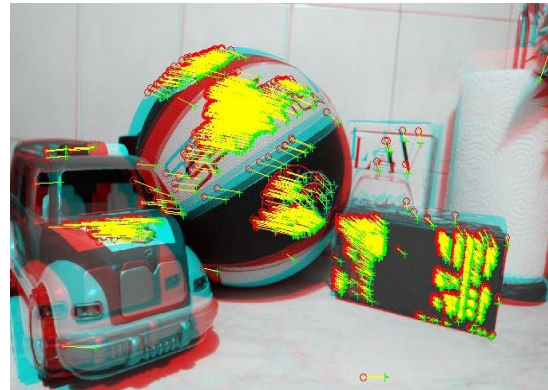
Figure 13: Tracked features (second test)

Figure 11: Undistorted images (second test)

Figure 14: Epipolar inlier (second test)

Figure 12: Strongest corners from the first
image (second test)
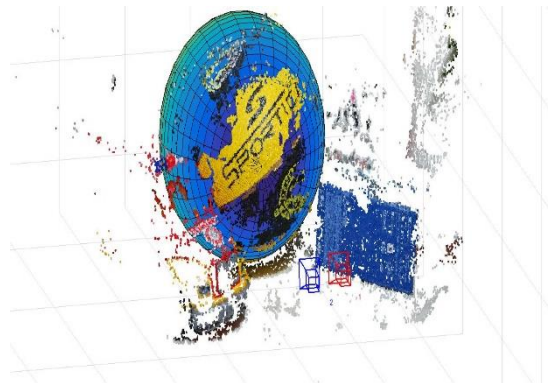
Figure 15: Estimated size and location of the
ball (second test)

Sarmad .N
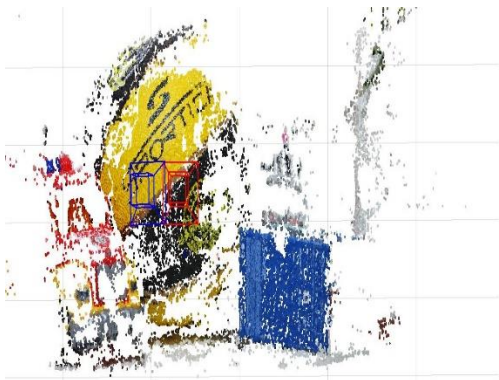
Figure 16A: Metric reconstruction of the scene
(second test)

Figure 18: The undistorted images (3rd test)
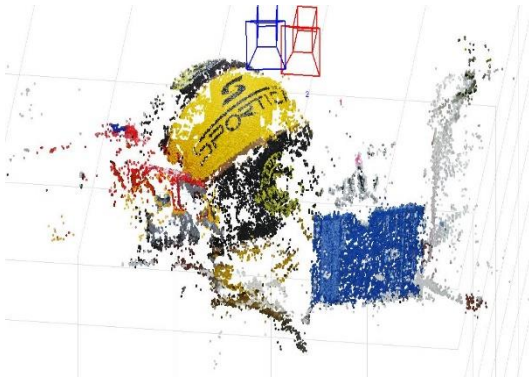
Figure 16B: Metric reconstruction of the scene
with another position (second test)

Figure 19: Strongest corners from the first
image (3rd test)

The first scene (Figure 3) contained a ball with
a soft surface which had some parts with only
one color. We added some details to this ball
in order to induce the algorithm to detect more
matching points, and the results were as shown
below:
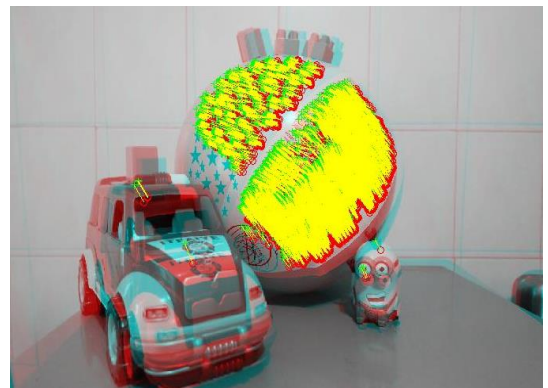
Figure 20: The Tracked features (3rd test)

Figure 17: The original images (3rd test)

Journal of AL-Qadisiyah for computer science and mathematics   Vol.10   No.1   Year 2018
ISSN (Print): 2074 – 0204   ISSN (Online): 2521 – 3504

Sarmad .N

Figure 21: The Epipolar inlier (3rd test)

Figure 22: Estimated size and location of the ball (3rd test)

Figure 23A: Metric reconstruction of the scene (3rd test)

Figure 23B: The metric reconstruction of the scene with another position (3rd test)

As we said when the distance between the images is not too far, so the KLT algorithm will work properly, but when the distance become more than 5 cm (distance between the camera and the scene was 50 cm) the algorithm fails to match the points between the images as shown in the figure 24.

Figure 24: KLT algorithm error

Sarmad .N

11.Real Data and Numerical Results

- **First Test**: In Figure 3, we show two real images of a constructed composite scene. This scene represents a difficult set of data due to its soft surface. We have covered the images with matched points using the KLT algorithm technique. When the sixth step of the algorithm is applied to the matched points of the real data, the motion estimate is a single matrix (1×3) for translation and a double matrix (3×3) for rotation, as shown below:

$$t = \begin{bmatrix} -0.27 \\ 3.16 \\ 0.3 \end{bmatrix}$$
$$R = \begin{bmatrix} 0.99 & 0.005 & -0.034 \\ -0.002 & 0.99 & 0.096 \\ 0.035 & -0.095 & 0.99 \end{bmatrix}$$

As Zhengyou Zhang [32] used the same technique that we followed in our method and according to the available numerical data from his method, the translation and rotation data was as shown below:

$$t = [\,-9.6, 1.85, -1.75]^T$$
$$R = [-2.1, 4.2, 1.04]^T$$

The remaining data obtained from the experimental results are as follows:

		M.P. error 0.77
All colors		19961856x3 uint8
Ball Prop.	Parameters	[0.57, -0.91,10.6,3.13]
	Center	[0.57, -0.91,10.6]
	Radius	3.13
Camera parameters	Radial Distortion	[-0.099,0.12]
	Tangential Distortion	[0, 0]
	Estimate Skew	0
	Intrinsic Matrix	[3.9,0,0;0,3.9,0;2.7,1.85,1]
	Focal length	[3.9,3.9]
	Principal Point	[2.7,1.85]
Fund. Matrix		[1.3, -3.07,0.01; -7.28, -2.6,0.001; -0.01, -2.1,0.9₁
Scale Factor		3.18

The Numerical Result Data (First Test)

- **Second Test**: The second test carried out by using another scene as shown in the figure 10, and the numerical results data as shown below:

$$t = \begin{bmatrix} -3.3 \\ 0.14 \\ -0,47 \end{bmatrix}$$
$$R = \begin{bmatrix} 0.99 & -0.02 & -0.08 \\ 0,02 & 0.99 & 0.015 \\ 0.087 & -0.018 & 0.99 \end{bmatrix}$$

		M.P. error 0.77
All colors		19961856x3 uint8
Ball Prop.	Parameters	[-0.99, -0.68,9.7,2,92]
	Center	[-0.99, -0.68,9.7]
	Radius	2.92
Camera parameters	Radial Distortion	[-0.099,0.12]
	Tangential Distortion	[0, 0]
	Estimate Skew	0
	Intrinsic Matrix	[3.9,0,0;0,3.9,0;2.7,1.85,1]
	Focal length	[3.9,3.9]
	Principal Point	[2.7,1.85]
Fund. Matrix		[2.02, 6.49, -0.001; -4.02, -3.88,0.01; 2.33, -0.01, 0,99]
Scale Factor		3.41

The Numerical Result Data (2nd Test)

- **Third Test:** The third test carried out by using the first scene but with adding some more details as shown in the figure 17, and the numerical results data as shown below:

$$t = \begin{bmatrix} -0.25 \\ 3.34 \\ -0,01 \end{bmatrix}$$
$$R = \begin{bmatrix} 0.99 & 0.002 & -0.031 \\ 0,001 & 0.99 & 0.11 \\ 0.031 & -0.11 & 0.99 \end{bmatrix}$$

Sarmad .N

		M.P. error 0.77
All colors		19961856x3 uint8
Ball Prop.	Parameters	[0.69, -0.98,9.64,2,98]
	Center	[0.69, -0.98,9.64]
	Radius	2.98
Camera parameters	Radial Distortion	[-0.099,0.12]
	Tangential Distortion	[0, 0]
	Estimate Skew	0
	Intrinsic Matrix	[3.9,0,0;0,3.9,0;2.7,1.85,1]
	Focal length	[3.9,3.9]
	Principal Point	[2.7,1.85]
Fund. Matrix		[1.7, 3.06 ,0.01; -5.49, -4.03,0.003; -0.01, -0.00, 0,99]
Scale Factor		3.35

The Numerical Result Data (3rd Test)

12. Discussion: The image resolution used in the algorithm was 5472×3648. Initially, the algorithm begins in the first test with loading a pair of images (Figure 3), followed by the camera calibration stored in the camera parameters object loaded, which included the camera intrinsic matrix, the radial distortion and the estimated skew. According to the value of the skew, which here is zero, there is no distortion in the lines of the lens. The next process aims to remove any bends in the lines of the lens, and as the skew is zero, there is no need for this step (4). Later, the feature points will have been detected in this step from the first image (Figure 5) and, as mentioned above, are carried out by using the KLT algorithm.

The point tracker is created to find the correspondence points between the images (Figure 6). In order to specify the Epipolar constraints, the fundamental matrix is estimated, and by computing the fundamental matrix, the inlier points will be established and matched to the Epipolar constraints (Figure 7). Before the final step in the algorithm, the camera position (R, t), which represents the external parameters, are computed. Later, by using the sphere function to fit the point cloud in order to find the size and location of the ball in the scene (Figure 8).

Finally, the coordinates of the three-dimensional points in centimeters are determined according to the actual size of the ball (Figure 9 A and B). The final result of reconstruction of the three-dimensional model was not good due to the holes in the model; therefore, it was necessary to fill the uncovered areas

Zach et al [20] in their methods using four different datasets, and by adding more points where are reduced the of error, except the third dataset where the error is increased, and this issue is left without explaining in their paper. Those results shown in the next table.

Dataset	#Images	#3D points	Init. Image error	#Added points	Final image error
1	175	43553	2.17	1497	2.14
2	186	47756	6.18	5605	4.89
3	99	31876	1.77	5747	6.75
4	191	60997	3.3	1556	2.4

The results of Zach et al method[12]

Journal of AL-Qadisiyah for computer science and mathematics   Vol.10   No.1   Year 2018
ISSN (Print): 2074 – 0204   ISSN (Online): 2521 – 3504

Sarmad .N

In our method we used different types of scenes in order to demonstrate the behavior of the algorithm. The numbers of three-dimensional points, which are the algorithm obtained from the first scene (figure 3), are 19333 points. After adding more details to the first scene, and by using the same algorithm (figure 17), the numbers of three-dimensional points are increased from 19333 points to 22195 points. In the second test we are using different scene (figure 10), which is have more colors and details, the result of using such a scene was obtaining more 3D points. Where the numbers of 3D points are increased from 22195 points to 59413 points. Next three tables are clarifying all those results which were carried out from the three tests.

The original scene (1st Test)		
3D points	Image points	Matched Points
19333	30306	19333
The original scene after modifying (3rd Test)		
3D points	Image points	Matched Points
22195	39402	22195
Different scene with more details (2nd Test)		
3D points	Image points	Matched Points
59413	247519	59413

Numbers of points according to different scenes

Zach et al [20] in their method were added more points in order to reduce the rate of error, where the approach of the proposed method in this paper is motivate the algorithm to obtain more matched points by using scenes rich in details.

The limitations of the previous algorithm were found in the fourth step of the feature detection, where the KLT algorithm will not work probably if the space between the obtained images is too great (Figure 10). Next, the tracker features had some difficulties detecting the soft surfaces in the scene (Figure 6), so we added some details to this surface in order to motivate the algorithm to detect more matching points (Figure 17). Then, the same steps which mentioned above were executed. As the final result of the third test shown in the figures 23 A, B, the algorithm detects more points and reconstruct new model with more points.

The second test was carried out by using a different scene (Figure 10), after executing the algorithm, the results were more accurate than the first test due to the details of the scene which was had more colors than the first scene (figure 3).

13. Conclusion: In this paper, we concentrated on the KLT algorithm based on two views. The experimental results in the previous section have some limitations that need improvement and complementary solutions.

The results of the experiments show the insufficiency of KLT algorithm when the distance between images becomes more than 5 cm. Also, we figure out the possibility of reducing the rate of reprojection error by removing the images that have the biggest rate of error.

The experimental results are consisting from three stages. The first stage is done by using a scene with soft surfaces, the performance of the algorithm shows some deficiencies with the soft surfaces which are have few details. The second stage is done by using different scene with objects which have more details and rough surfaces, the algorithm results become more accurate than the first scene. The third stage is done by using the first scene of the first stage but after adding more details for surface of the ball in order to motivate the algorithm to detect more points, the results become more accurate than the results of the first stage. The experiments are showing the performance of the algorithm with different scenes and demonstrate the way of improving the algorithm.

In spite of the limitations mentioned above, the algorithm creates three-dimensional models that depend on only two views with the model being meaningful according to the original scene. Moreover, the work of the algorithm is quite good due to the rating of the mean projection error, which was 0.94 and decreased into 0.77.

14. Future Work: Researchers in this field may use this paper in investigations of two-dimensional to three-dimensional conversion algorithms. They can deal with the limitations mentioned herein by finding alternative algorithms instead of using the KLT algorithm to cope with widely-spaced images, or improve the 3D-model for greater accuracy. Also, they can estimate the depth information using other algorithms, and comparing the results with the current one in order to clarify the strengths and weaknesses of each algorithm.

References

[1] Ji Zhang et al, (2011), "**Pose-Free Structure from Motion Using Depth from Motion Constraints**", IEEE TRANS. ON IMAGE PROCESSING, VOL. 20, NO. 10, PP 2937-2953.

[2] Tony Jebara et al, (1999), "**3D Structure from 2D Motion**", IEEE SIGNAL PROCESSING MAGAZINE, VOL. 16, ISSUE: 3, PP 66 – 84.

[3] Scott Squires, (2011), "**2D to 3D Conversion**", ADAPT Web Site, effectscorner.blogspot.com.

[4] Jon Karafin, (2011), "**State-Of-The-Art 2D to 3D Conversion and Stereo VFX**", International 3D Society University, Presentation 3DU-Japan event in Tokyo.

[5] Olivier Faugeras and Quang-Tuan Luong, (2001), "*The Geometry of Multiple Images*".

[6] Simon J.D. Prince, (2012), "*Computer Vision Models, Learning and Inference* ".

[7] LONGUET-HIGGINS, (1981), "*Computer Algorithm for Reconstructing a Scene from Two Projections*," Nature 293, PP:133–135.

[8] Prazdny, (1983), "*On the Information in Optical Flows*," Computer Vision, Graphics, and Image Processing VOL 22, No 2, PP:239 – 259.

[9] Tsai et al, (1981), "*Estimating Three-Dimensional Motion Parameters of a Rigid Planar Patch*," Acoustics, Speech and Signal Processing, IEEE Trans on 29, PP:1147-1152.

[10] Soatto et al, (1998), "Reducing "*structure from motion*" a general framework for dynamic vision. Part 1: modelling.," International Journal of Computer Vision 20, PP:993-942.

Sarmad .N

[11] Joseph and J. Sean, (2013), "*Structure from Motion in Computationally Constrained Systems*", Micro- and Nanotechnology Sensors, Systems, and Applications V, edited by Thomas George. Saiph Islam, K. Dutta, Proc. of SPIE Vol. 8725, 87251G.

[12] M. Pollefeys, (1999), "*Self-Calibration and Metric Reconstruction in Spite of Varying and Unknown Intrinsic Camera Parameters*", Int. J. of Computer Vision, VOL.32, No.1, PP:7-25.

[13] K. Kutulakos, (1999), "*Theory of Shape by Space Carving*", In Proc. Seventh Int. Conf. on Computer Vision, PP:307-314.

[14] D. Lowe, (1991), "*Fitting Parameterized Three-Dimensional Models to Images*", IEEE Trans. on Pattern Analysis and Machine Intelligence, VOL.13, No.5, PP:441-450.

[15] Zucchelli, (2002), "*Optical flow based structure from motion*", Numerical Analysis and Computer Science. Stockholm: (Royal Institute of Technology).

[16] Astrom et al, (2000), "*Solutions and Ambiguities of the Structure and Motion Problem for 1D Retinal Vision*," J. Math. Imaging Vis. VOL 12, No 2, PP:121-135.

[17] Li et al, (2006), "*Structure from Planar Motion*", IEEE Trans on Image Processing 15, PP:3466-3477.

[18] Zhengyou Zhang, (1997), "*Motion and Structure from Two Perspective Views: From Essential Parameters to Euclidean Motion Via Fundamental Matrix*", Journal of the Optical Society of America, VOL.14, No.11, PP:2938-2950.

[19] Frank Dellaert et al, (2000), "*Structure from Motion without Correspondence*", Computer Science Department & Robotics Institute Carnegie Mellon University, Pittsburgh PA 15213, IEEE 1063-6919/00.

[20] Christopher Zach et al, (2012), "*Discovering and Exploiting 3D Symmetries in Structure from Motion*", IEEE Conference, Computer Vision and Pattern Recognition, DOI: 10.1109/CVPR6247841, PP: 1514-1521.

[21] Klingner et al, (2013), "*Street View Motion-from-Structure-from-Motion*", IEEE Int. Conference on Computer Vision, DOI 10.1109/ICCV, PP: 953-960.

[22] Yongjun Zhang et al, (2015), "*Optimized 3D Street Scene Reconstruction from Driving Recorder Images*", Remote Sens. 7, PP: 9091-9121, ISSN 2072-4292 DOI: 10.3390/RS70709091.

[23] C. TOMASI & J. SHI, (1994), "*Good Features to Track*," Proc. of CVPR'94, PP: 593-600.

[24] Derek Hoiem, 2012, "*Feature Tracking and Optical Flow*", Computer Vision, CS 543/ECE 549, Illinois Univ.

تحويل الصور الثنائية الابعاد الى نماذج ثلاثية الابعاد بإستخدام زوج من الصور
"خوارزمية كي ال تي كحالة تطوير ودراسة"

سرمد نهاد محمد
جامعة كركوك
كلية العلوم ، قسم علوم الحاسوب

المستخلص :

تدرس هذه الورقة كيفية تأثير الحركة بين صورتين لمشهد واحد على عملية تشكيل النموذج الثلاثي الابعاد بإستخدام خوارزمية كي إل تي (KLT) والتي استخدمت لتحويل صور ثنائية الأبعاد إلى نموذج ثلاثي الأبعاد. تتم عملية إعادة تشكيل النموذج الثلاثي الابعاد باستخدام كاميرا واحدة وخوارزمية تقوم على استخدام اثنين فقط من الصور لمشهد واحد، واعتماد تقنية (SFM) على أساس الكشف عن النقاط المشتركة بين الصورتين، و إيبيبولار إنليرس. استخدام خوارزمية (KLT) مع طريقة (SFM) يدل على عدم قدرة الخوارزمية على النجاح في العمل عندما تكون المساحة بين الصورة الاولى والثانية شاسعة. كما وتم تقليل معدل الخطأ عند اعادة تسقيط المشهد من الواقع الى الكاميرا عن طريق إزالة الصور التي لديها أكبر معدل الخطأ. تم العمل على تشكيل نموذج ثلاثي الابعاد بأستخدام ثلاثة مشاهد مختلفة على ثلاثة مراحل. المرحلة الأولى تمت باستخدام مشهد ذو أسطح ناعمة، ويظهر أداء الخوارزمية بعض أوجه القصور مع الأسطح الناعمة التي ليس لها سوى القليل من التفاصيل. اما المرحلة الثانية تمت باستخدام مشهد مختلف مع الكائنات التي لديها المزيد من التفاصيل والأسطح الغير ملساء، وهنا نتائج الخوارزمية اصبحت أكثر دقة من المشهد الأول. المرحلة الثالثة تمت باستخدام المشهد الأول في المرحلة الأولى ولكن بعد إضافة المزيد من التفاصيل على سطح الكرة لتحفيز الخوارزمية لكشف المزيد من النقاط، وهنا اصبحت النتائج أكثر دقة من نتائج المرحلة الأولى. وتظهر التجارب أداء الخوارزمية مع مشاهد مختلفة وتظهر طريقة تحسين الخوارزمية حيث وجدت المزيد من النقاط من الصور، لذلك تم تشكيل النموذج الثلاثي الابعاد بصورة أكثر دقة.

Design and Implementation of Smart Dust Sensing System for Baghdad City

Hussien A. Mohammed
University of Information Technology and Communication
dr.hussien.a.mohammed@uoitc.edu.iq

Abstract

The atmosphere in the world and especially in Iraq is yearly exposed to many dust storms that cause dust floated, which negatively affects the health of people, animals and agriculture. In this research, a system is proposed that used sensor to continuously measure the level of dust in the air of Baghdad city 24 hours /7 days a week. Then analyzing these measurements to determine the level of risk impact on people health especially people with respiratory diseases. The proposed system has the ability of sending warning text message expressing the level of potential threat to the people.
In order to accelerate the rapid processing, an accurate Arduino Uno microcontroller was used to measure the density of the dust and make the required processing. In addition to, using the Global System for Mobile Communications (GSM) type SIMS900 as SMS sender.
The advantages of this system is represented by its ability to alert the people about air pollution in real time, ease of use (where mobile devices are available to most people in Baghdad) and the low cost of sending a message.

Keywords: Dust Sensor, Dust Storms, GSM, Mobile Communications, SMS.

1. Introduction

Often sand and dust storms (SDS) influence some countries because their geographical position. These dust storms hit many countries and unfortunately, it hit Iraq and last for days. In summer season, the climate in Iraq is dry, hot and dusty. A northwest wind drive dust storms and this wind known in Arabic language by "Shimali" (means wind come from the north). At any time of the year, may rip via the River valleys of Tigris and Euphrates in central and southern of Iraq and storm almost continuously through June and July as shown in figure 1. Sometimes, "Shimali" might blow in the months of August and September. These winds can continue for more than one day,

strength during the day, weak at night, and sometimes create ruined dust storms [1].

In addition to, the Iraqi Ministry of Environment recorded 122 dust storms and 283 dusty days. The forecasts predict 300 dusty days and dust storms yearly may occur in the next ten years [2].

Living in environment with such condition causes lung illnesses including asthma and constrictive bronchiolitis [3]
Further, 300 million people in the whole world suffer from asthma as estimated by the American Academy of Allergy Asthma and Immunology.
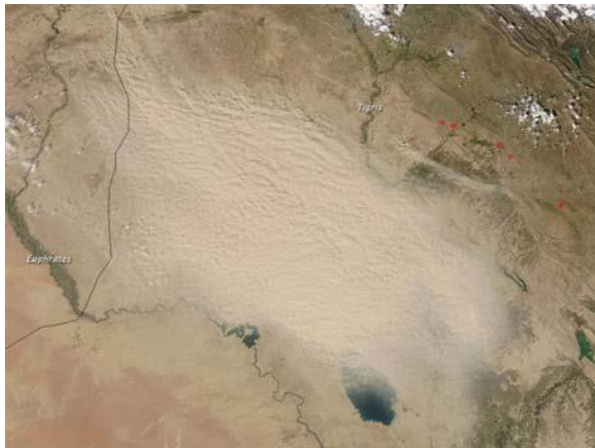
Figure 1. Dust Storm View

Asthma is regarded as burden in high-income countries because it cost the government too much. While, the most deaths which caused by asthma occur in countries of low and middle-income. However, there is not reliable epidemiological investigation and studies to define the number of people who suffer from asthma in many developing countries. Moreover, it is hard to diagnose and tackle the asthma disease in developing countries.

This is attributed to the limited available data and high expense that required to overcoming this disease. In general, a physician requires around six months for each individual to be diagnosed by asthma [4].

A study started in September 2013 and lasted to March 2014. This study targeted people aged 4-15 years who attending school. All individuals aged 4-15 years in the selected group were invited to participate in the study. The student's schools were randomly selected from two cities in Iraq Baghdad and Rumadi. This study investigates the spread of asthma symptoms in children that include: ever wheezed, current wheezing, speech limitation, ever diagnosed with asthma, dry cough and exercise-induced asthma. The results were as presented in table 1 [5].

Table 1. The Asthma Symptoms Prevalence in Children at Iraqi Schools

Asthma Symptoms	Boys (No.=307)	Girls (No. =486)	Total (No. = 793)
ever wheezed	21.2%	17.7%	19.0%
current wheezing	16.3	13.2%	14.4%
speech limitation	2.9%	1.9%	2.3%
ever diagnosed with asthma	19.9%	16.9	18.0%
dry cough	19.2 %	11.1	14.2%
exercise-induced asthma	16.3%	10.9	13.0%

Furthermore, the U.S. Environmental Protection Agency presented a guide of Air Quality Index (AQI) impacts on human health.

Table 2 describes the effects of increasing AQI on human health.

Hussien .A

Table 2. The effects of Air Quality Index on Human Health

Value of AQI	Health Level	Actions to Protect Your Health
(0–50)	Good	None
(51–100*)	Moderate	Unusually sensitive people should consider reducing prolonged or heavy outdoor exertion.
(101–150)	Unhealthy for Sensitive Groups	The following groups should reduce prolonged or heavy outdoor exertion: • People with lung disease, such as asthma • Children and older adults • People who are active outdoors
(151–200)	Unhealthy	The following groups should avoid prolonged or heavy outdoor exertion: • People with lung disease, such as asthma • Children and older adults • People who are active outdoors Everyone else should limit prolonged outdoor exertion
(201–300)	Very Unhealthy	The following groups should avoid all outdoor exertion: • People with lung disease, such as asthma • Children and older adults • People who are active outdoors Everyone else should limit outdoor exertion.
(301–500)	Hazardous	Everyone should avoid all physical activies outdoors

Usually, when AQI values are less 100, the air quality is regarded well. As value of AQI is increasing, the effects are getting more risk to human health [7].

Moreover, the recent advances in cellular networks has opened up new era of devices that use wireless networks for particularistic intents. The term Machine 2 Machine (M2M) means two communicated machines and it used for Machine to Mobile too, in addition to other concepts. The combination of M2M and internet of things presented new revolution of technology that would be producing various business in future. It will resulting in increase the number types of applications. M2M technology offers the ability of sending the world physical information between two machines through the communication networks and other platforms.

As a result, a monitoring system that able to sense the environmental condition outdoors for allergic people (or people with asthma) is required. Especially with the recent developing in computer technology, sensors and information systems [6] that facilities introducing such controlling system.

The rest of this paper are structured as follows: Section 2 explained the related work. Proposed system presents in section 3. Section 4 details analyzing results. Dust sensor is described in section 5. Proposal Implementation explained in section 6. Conclusion is described in section 5.

2. Related work

The authors in [8] studied the storms of sand and dust in Iraq and the near areas. They classified the major factors that caused the sand and dust storms development. In addition to, presenting these storms effects on the economic losses and human's health.

In [9] the authors used micro electro-mechanical sensors and wireless network sensor to design and implement a smart dust sensor.

The authors in [10] measured the temperature, humidity, atmospheric pressure and dust density by developing a new technique for weather station. A web server is developed in order to process the recorded data which are collected by sensors. Finally, the new system has the ability of alerting user by web page or by text messages.

The research in [11] presented new technique that sense the dust intensity in air. This proposal based on Radio Frequency Identification technology (RFID) to transmit sensed data via wireless network. RFID technology includes wireless sensors so it get the benefits of small and cheap RFID tags to the wireless sensor networks.

Journal of AL-Qadisiyah for computer science and mathematics   Vol.10   No.1   Year 2018
ISSN (Print): 2074 – 0204   ISSN (Online): 2521 – 3504

Hussien .A

3. Proposed system

The proposed system consists of three components: dust sensor (operation and evaluated), processing, and the process result is send to Allergic People via network (GSM). Figure 2 shows the block diagram of proposed system. It is consists of microcontroller, dust sensor, GSM that communicates to Mobile phone, and power supply.

The dust sensor sense the outdoor environment periodically (means every 5 minutes or based on required setting). Then, send sensed data to controller which analyses them and send alert message to user mobile. The content of message is vary based on the received data (Excellent weather, Good weather, Unhealthy weather, Dangerous weather, or Emergency weather). Figure 3 shows the proposed system architecture. The dust sensor measures the dust regularly (for example every 1 minute)   then specify the measured value on human health based on table 2. Hence take the action upon the specified value of dust.

Figure 2. The Block Diagram of the Proposed System.
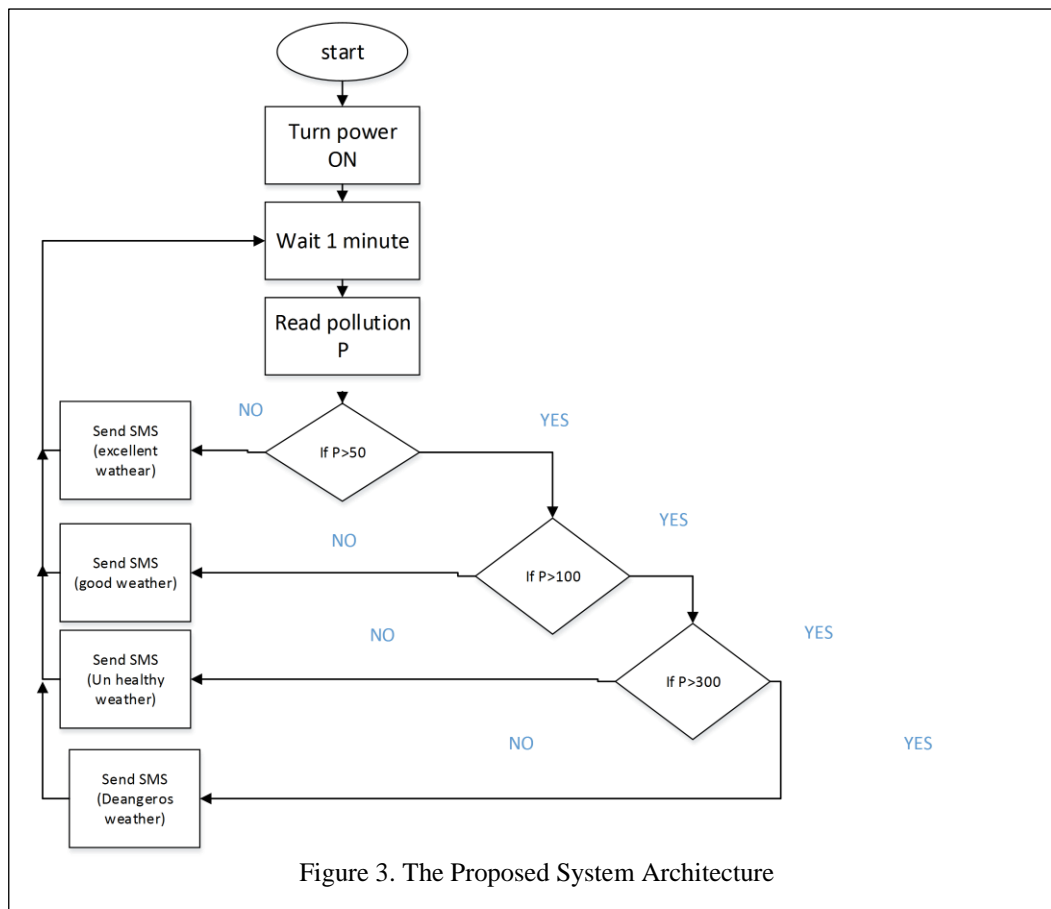
Figure 3. The Proposed System Architecture

4. Dust sensor

Infrared electromagnetic wave (IR) is used for counting the density of dust particle. The transmitted beam of IR groves may be contain this particle where the scattered light is detected by using photodiode. Optical lens is used to focusing and collecting beam upon detector as show on figure (4).
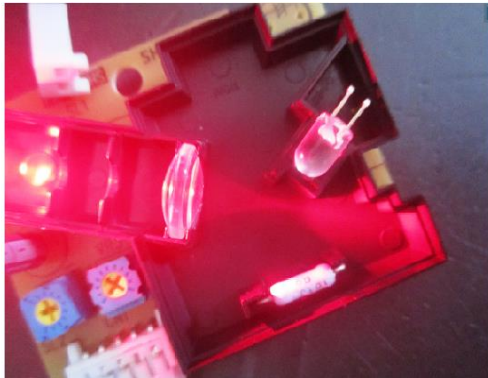
Figure 4. The Construction of Dust Sensor

The used heat generator is represented by Resistor of 100 Ω, which is allowed to circulate in to sensor groves. The IR photo diode is transmit train of pulses as a plus width modulator (PWM). The sensor detects particle of a diameter (1-10µm), where the detectable range of particle is depending on the detectable range setting of dust concentration $0 – 1.4$ mg/m³and the raise time of this sensor is about 1 mint after power on. The suitable supply voltage is 5 volt direct current. The output signal without dust is shown in figure (5).

Figure 5.The Output of Dust Sensor without Dust

Dust will be detected when it scattered the IR light as shown in figure (6). The pulse width of the output is proportional to the dust density.

Figure 6.The Pulse Width with Dust

A. Sensor output

The output of the sensor is fluctuated between low and high stat when dust particles enter the groves of sensor. Otherwise the output of the sensor is not fluctuated.

Low plus (LO) proportional with dust construction, when measured what they call LO pulse occupancy (LPO), the constriction of dust can be determined for 30 second time period can be used to measure LOP as show in figure (7).

Low ratio [%] = t (sec) / 30 (sec)* 100
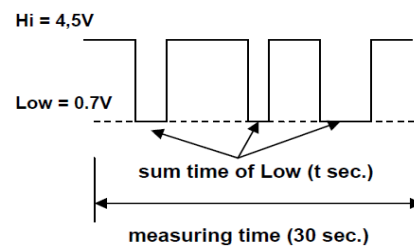
Figure (7) Low Ratio

Low ratio represent the value of dust particle that can be measured, as a number of particle and its diameter are show in figure (8)
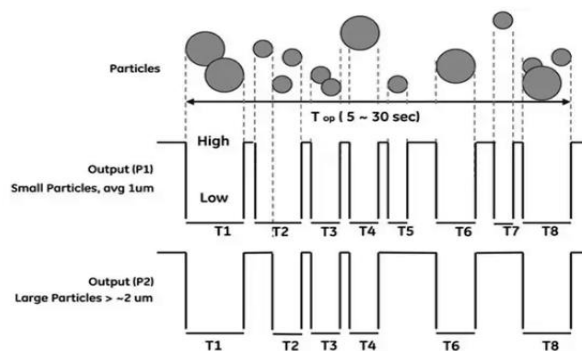
Figure (8) low ratio measurement with assumed two different particle diameter

Hussien .A

B.   Dust density measurement and process

In order to measure the density of the dust under test, electronics microcontroller is used of type (Arduino Uno). The output of dust sensor is connected to it as shown in figure (9).
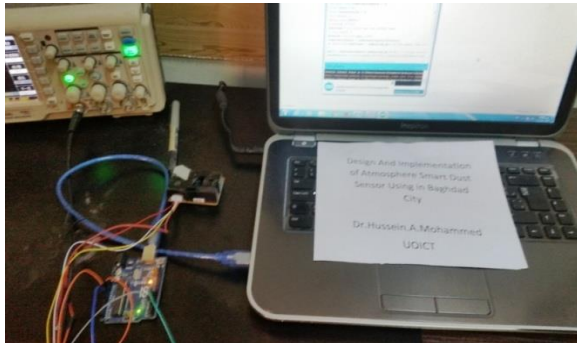
Figure 9. The Connection of Dust Sensor with Arduino Microcontroller Board

The Arduino deriver software has been downloaded and installed on personal computer to communicate with microcontroller bored by connecting it using (USB port). The output of this software appear on a monitor named (serial monitor). Figure 10 shows serial monitor when it is presenting the output of dust sensor in case of concentration =0.62pcs/0.01cf.When increase the construction of a dust density the serial monitor of Arduino microcontroller
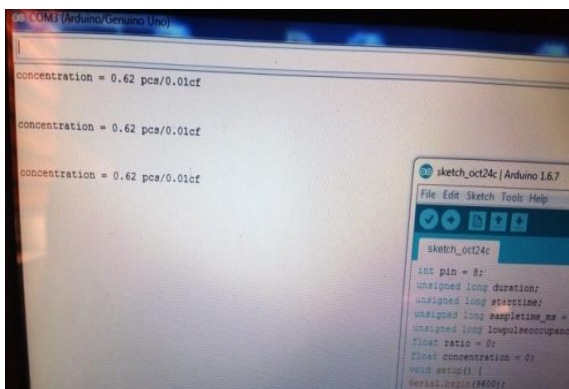
Figure 10.The Serial Monitor Presenting the Output 0.62 pcs/0.01cf of Dust Sensor

Figure 11.The Serial Monitor Presenting the Output

5.   Proposal Implementation

The Arduino platform has been chosen to implement the proposal system because it's open source prototype platform. Arduino programming language is used to programmer the microcontroller on the board where this language is based on Wiring and the Arduino environment Processing. The Arduino Uno is a microcontroller that based on the ATmega328.

There are many advantages when using this type of microcontroller in term of low power CMOS, 8-bit based on the (AVR) that enhance the reduced instruction set computer RISC architecture which provide a small, highly-optimized set of instructions which is produce a power full instructions in a single clock per cycle. In addition to, the throughputs of this category is about million instructions per second (MIPS). Therefore the power consumption automatic versus processing speed.

The features of microcontroller are32K bytes Programmable Flash, Read-While-Write capabilities, 1K bytes EEPROM, 2K bytes SRAM, three flexible Timer, internal and external interrupts

The implementation of microcontroller includes two steps, which are described as follows:

A.   Software Design

Software design consist of two parts: programming Arduino Uon and then Reading the measurements of sensor in order to forward the gathering data when requested.

Microcontroller is programmed to send status of a sensor i.e. number of readings, time interval and to be used to get sensor readings. In addition to using the microcontroller as a storage to save data in it and retransmit (in GSM network) when it required. Therefore it increase its reliability.

B.   Hardware Connection

The microcontroller is connect to GSM board by using Arduino board to enable it from sending and receiving SMS with ratio of dust based on collected and processed data.

SIM900 board is implemented to send SMS as shown in figure (11).The SIM900 shield has a modem and transfers processed data to the GSM network by connect the modem to subscriber identification module (*SIM*) card that placed in GSM board (low level communication). Then connect to the mobile company (Zain). The last connects to Mobile company Servers which will send a SMS to patient.

The resulted message can be sent to the asthma patients with dust level by using the Arduino program. The modem need 12v,1A, in order to operate reliable. The baud rate of GSM board is set is to 19200 symbols per second, the transmitter of Arduino Uon pin TX is connected to the GSM receiver pin RX. While the receiver of Arduino Uon pin RX is connected to transmitter pin TX of GSM

Figure 12. The implemented SIM900 Board

6.   Conclusion

In this paper, a portable system has been designed and implemented that can monitor the level of air dust in real time 24 hours / 7 days in Baghdad city. The proposed system deploy dust sensor to sense the dust level in air, process and transmit the information to a mobile devices through the mobile company. This new approach provide real time, accurate and automated machine to mobile communication that means the sensors can send data to Phone devices via GSM technology. The dust sensor can be placed anywhere and the data of dust density can be gathered and sent SMS text message upon the read data. The proposed system can be used to monitor quality of the air in many aspects. It can be used in street, home, hospital and many other places for daily monitoring. The system will contribute to reduce the risk of health condition for many patients and in some cases save their lives. In addition to, the proposed system will reduce the patient stay at hospital if s/he need to, since they will be ready to take all the required procedures when receiving and reading the sms. The sms may include instructions for them on how to act when dust storms occur.

References

[1] Varoujan K. Sissakian, Nadhir Al-Ansari, and Sven Knutsson, "Sand and dust storm events in Iraq", Natural Science, Vol.5, No.10, 1084-1094 (2013) http://dx.doi.org/10.4236/ns.2013.510133.

[2] Kobler, M. (2013) Dust storms of Iraq, UN Secretary General for Iraq, A ministerial meeting in Nairobi, Kenya. http://www.term123.com/dust-storms-of-iraq/#mh32BcOB4S6cRkIG.99

[3] Harrington, A. D., M. P. Schmidt, A. M. Szema, K. Galdanes, S. E. Tsirka, T. Gordon, and M. A. A. Schoonen (2017), The role of Iraqi dust in inducing lung injury in United States soldiers—An interdisciplinary study, GeoHealth, 1, 237–246, doi:10.1002/2017GH000071.

[4] Maris Brummel, "Asthma in Developing Countries", the Borgen Project, 4 MAR 2014. https://borgenproject.org/about-us/

[5] Dr Aya Rahman Lafta and Dr Mohammed Shamssain, "Comparison of the Prevalence Rates of Asthma and Allergies Between UAE and Iraqi Schoolchildren", EUROPEAN JOURNAL OF PHARMACEUTICAL AND MEDICAL RESEARCH, ejpmr, 2016,3(3), 15-22.

Journal of AL-Qadisiyah for computer science and mathematics   Vol.10   No.1   Year 2018
ISSN (Print): 2074 – 0204   ISSN (Online): 2521 – 3504

Hussien .A

[6] Ron Williams and Vasu Kilaru "Air Sensor Guidebook" National Exposure Research Laboratory U.S. Environental Protection Agency,2014

[7] U.S. Environmental Protection Agency Office of Air Quality Planning and Standards Outreach and Information Division Research Triangle Park, NC, "A Guide to Air Quality and Your Health ", February 2014 EPA-456/F-14-002

[8] Varoujan K. Sissakian1, Nadhir Al-Ansari, Sven Knutsson, "Sand and dust storm events in Iraq", V. K. Sissakian et al. / Natural Science 5 (2013) 1084-1094.

[9] Roopal Gautam1, Sandhya Kumari2, Shuchi Chaudhar, "SMART DUST: AN EMERGING TECHNOLOGY", International Journal Of Advance Research In Science And Engineering, IJARSE, Vol. No.2, Issue No.10, October 2013

[10] S. H. Parvez, J. K. Saha, M.J. Hossain, H. Hussain, Md. M. A. Ghuri, T. A.Chowdhury, Md. M. Rahman, N.Z. Shuchi8, A. Islam, M. Hasan And B. Paul, "A Novel Design and Implementation of Electronic Weather Station and Weather Data Transmission System Using GSM Network", WSEAS Transactions on Circuits and System, https://www.scribd.com/document/334915699/a085801-435.

[11] Shyam D. Bawankar, Sonal B. Bhople & Vishal D. Jaiswal, "Mobile Networking For "Smart Dust" With RFID Sensor Networks", International Journal of Smart Sensors and Ad Hoc Networks (IJSSAN), ISSN No. 2248-9738 (Print), Vol-2, Iss-3,4, 2012.

تصميم وتنفيذ نظام تحسس غبار ذكي لمدينة بغداد

حسين عبد الرضا محمد
جامعة تكنولوجيا المعلومات والاتصالات
dr.hussien.a.mohammed@uoitc.edu.iq

المستخلص :

يتعرض الغلاف الجوي في العالم، وخاصة العراق، لكثير من العواصف الترابية التي تسبب الغبار ، مما يؤثر سلبا على صحة الناس والحيوانات والزراعة. هذا البحثيقترح نظام يستخدم جهاز الاستشعار لقياس مستوى الغبار في الهواء في مدينة بغداد باستمرار خلال وبعد عواصف الغبار. ثم تحليل هذه القياسات لتحديد مستوى تأثير المخاطر على صحة الناس وخاصة الأشخاص الذين يعانون من أمراض الجهاز التنفسي.النظام المقترح لديه القدرة على إرسال رسالة نصية تحذيرية تبين مستوى التهديد المحتمل.

من أجل معالجة سريعة، تم استخدام متحكم اردوينو أونو لقياس كثافة الغبار وإجراء المعالجة المطلوبة، بالإضافة إلى استخدام النظام العالمي للاتصالات المتنقلة نوع SIMS900 لارسال رسائل نصية لمرضى الربو ميزة هذا النظام تمثل قدرته على تنبيه المرضى حول الظروف الجوية في الوقت الحقيقي، وسهولة الاستخدام (حيث تتوفر الأجهزة المحمولة لمعظم الناس في بغداد)، وانخفاض تكلفة إرسال الرسائل .

Design and Implementation of Efficient and High-Speed Multiplication Circuits Based on Vedic Algorithms

Muthana Yaseen Nawaf Isawi

University of Kirkuk
Department of Computer Science, College of Science
Muthana2085@yahoo.com

Abstract. The increasing speed of computer processors with each passing day has required the design of arithmetic circuits to be verified as high performance. For this reason; by being observed the computer arithmetic, it enabled faster algorithms to come out and verifications of hardware in terms of the facilities that technology provides. The main aim of the computer arithmetic is the design of the circuits and algorithms that will increase the speed of the numerical process. To this end, the design of arithmetic multiplication circuits with a faster and higher bit length is presented through the efficient bit reduction method in this paper. The developed fast and efficient algorithms for arithmetic multiplication process by using the efficient bit reduction method have been observed in this work. By making changes in some multiplication methods that are based on Vedic math's, the higher bit length circuits of multiplication circuits in the literature which are 4 bits have been developed by using some basic properties of multiplication like decomposition and bit shifting. Analysis of arithmetic circuits is implemented by verifying functionally with VHDL simulations, getting output signal waveform and measurements of delay time. All the circuits of hardware that are observed have been described via VHDL and the performances of multiplication circuits that are synthesized have been presented via FPGA.

Key Words. Vedic algorithms, bit reduction, digital multiplier, VHDL, FPGA.

1.Introduction. To speak of today's engineering world, multiplication-based operations are some of the most commonly used functions and have recently been used in many Digital Signal Processing (DSP) applications such as Convolution, Fast Fourier Transform, Filtering and in the Arithmetic Logic Unit (ALU) of microprocessors [1, 2]. The most commonly used process is the multiplication process speed and designing the low-power multiplication circuit has been the focus of attention in recent years [3]. To minimize power consumption and delay in digital systems are required optimization at every stage of the design. This optimization means choosing the best algorithm for the situation, which means the highest level of design, the topology and finally the technology used in the implementation of the digital circuits. Based on these components, different types of available multiplication circuits are designed [4, 5].

Muthana .Y

The use of multiplication methods has been documented in the civilizations of Egypt, Babylon, India, and China [3]. In the early days of the advent of computers, multiplication was generally applied through a series of operations (addition, subtraction, and shifting). There are many algorithms proposed in the literature to perform the multiplication process, each offering different advantages and performing differently in terms of delay, circuit complexity, chip area and power consumption [5, 6]. The structure of the multipliers is generally divided into three categories. The first is a serial multiplier that focuses on the hardware and uses as minimum chips as possible. Second is parallel multipliers (tree and array) that perform mathematical operations at high speed. But the disadvantage of these multipliers is that they use a larger chip area. The third is the serial-parallel multiplier, which stands as a good alternative between the serial multiplier that takes a long time and the parallel multiplier that takes a large chip area [1, 5]. This paper presents a high-speed efficient multiplier implementation based on Vedic multiplication algorithms (Urdhva Tiryakbhyam Sutra and Nikhilam Sutra). In addition, various algorithms for arithmetic multiplication using efficient bit reduction method have been investigated. The commonly used Vedic multiplication algorithm and classical Booth multiplication algorithm have been chosen as arithmetic multiplication operations. However, in order to understand the working logic of the algorithms, the basic principles of multiplication algorithms, hardware implementation circuits and performance properties are given. However, the proposed Vedic algorithm we have developed based on Vedic mathematics is presented in detail.

2. Vedic Algorithms and Booth Multiplier

2.1 Vedic Mathematics: Vedic mathematics is part of the four Veda "wisdom books". It makes explanations about some mathematical terms such as geometry, trigonometry, arithmetic, quadratic equations, factorization and even calculus [7].

Vedic mathematics is basically composed of 16 Sutra, which deals with the branches of mathematics such as arithmetic, algebra, geometry.

These methods can be applied directly to geometry, trigonometry, differential, integral, conics, and applied mathematics of various types. Since Vedic formulas (Sutra) are claimed to be based on the natural principles working conditions of the human mind, they offer a very interesting field and some efficient algorithms that can be applied to various branches of engineering such as programming and digital signal processing [7, 8].

2.2 Urdhva Tiryakbhyam Sutra: The multiplier is based on the Urdhva Tiryakbhyam algorithm of the ancient Indian Vedic mathematics. Urdhva Tiryakbhyam Sutra is a general form that can be applied to all cases of multiplication such as binary, hex, decimal and octal. The word means "Vertical & Crosswise" [7]. It is based on a new idea that helps to produce all the partial products and then to make the simultaneous additions of these partial results. Thus, the partial products and the parallelism in the production of their summaries can be achieved using Urdhava Tiryakbhyam. Since the partial results and their summations are calculated in parallel, the multiplier is independent of the clock frequency of the processor. On this count, the multiplier will need the same time to calculate the result, so it will be independent of the clock frequency [7, 9]. The main advantage is the reduction of the need for microprocessors to manage increasingly rising clock times. While a higher clock frequency usually results in an increased operating power, the disadvantage is that it increases the power dissipation which causes the device management to increase in temperature. The advantage of the multiplier is that as the number of bits increases, the gate delay and area increase more slowly than the other multipliers. Therefore, it is efficient in terms of time, space and power [8, 10].

Now we will see how this algorithm is used with binary numbers. An example (1101 * 1010) is given in Table 1.

Muthana .Y

Table 1: Using Urdhva Tiryakbham for binary numbers

X = 1101, Y = 1010	METHODOLOGY
x_3 x_2 x_1 x_0 **Multiplicand** y_3 y_2 y_1 y_0 **Multiplier** P6 P5 P4 P3 P2 P1 P0 $p_0 = x_0 y_0;$ $c_1 p_1 = x_1 y_0 + x_0 y_1;$ $c_2 p_2 = c_1 + x_2 y_0 + x_1 y_1 + x_0 y_2;$ $c_3 p_3 = c_2 + x_3 y_0 + x_2 y_1 + x_1 y_2 + x_0 y_3;$ $c_4 p_4 = c_3 + x_3 y_1 + x_2 y_2 + x_1 y_3;$ $c_5 p_5 = c_4 + x_3 y_2 + x_2 y_3;$ $c_6 p_6 = c_5 + x_3 y_3$	

2.3 Nikhilam Sutra: It means "all from 9 and last from 10". Basically, starting from the leftmost digits, each number is subtracted from 9 and the last number is subtracted from 10 [2, 7]. The Sutra algorithm is based on two different methods of multiplying numbers. The first is to find the nearest base of two numbers in multiplication., and the second is the subtraction method. Although the Nikhilam Sutra is applicable to all multiplication operations, it is essentially effective when the numbers are large and the complexity of the multiplication process is less [11]. We will illustrate Sutra by taking the multiplication of two decimal numbers (89 * 92) is show in Figure 1.
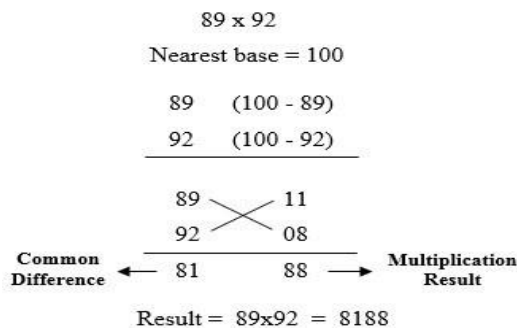
Figure 1: Multiplication using Nikhilam Sutra

2.4 Proposed Vedic Algorithm: In the binary arithmetic, a new reduced bit multiplication algorithm has proposed by modified the Nikhilam Sutra algorithm using some basic features such as decomposition and bit shifting. Based on the proposed algorithm, a 4x4-bit multiplication operation can be reduced to a single 2x2-bit multiplication operation. As a result, this algorithm reduces the delay for carry propagation more than any 4x4 bit multiplication. In the 4-bit proposed multiplication algorithm [4], it can be extended for larger numbers with some changes depending on the steps in the algorithm. The algorithm of proposed Vedic multiplier for the multiplication of two 8-bit numbers is given below.

(**a) Initialization**

Initialize: flag1 = flag2 = flag3 = flag4 = flag5 = flag6 = flag7 = flag8 = flag9 = flag10 = flag11 = flag12 = flag13 = 0

Muthana .Y

(b) Preprocessing

Input 8-bit binary numbers a and b

n1 = Number of least significant consecutive zeros in a

n2 = Number of least significant consecutive zeros in b

n = n1 + n2

 a'= Right shift a by n1

 b'= Right shift b by n2

(c) Processing

1. IF (a' > 128 & b' > 128) THEN

     a'=255-a'; b=255-b'; flag1=1;

2. IF (a' > 64 & b' > 128) THEN

      b'=b'-128; flag2=1;

   [IF (b' > 64 & a' > 128) THEN a'=a'-128;]

3. IF (a' > 64 & b' > 64) THEN

     a'=128-a'; b=128-b'; flag3=1;

4. IF (a' > 32 & b' > 64) THEN

      b'=b'-64; flag4=1;

   [IF (b' > 32 & a' > 64) THEN a'=a'-64;]

5. IF (a' > 32 & b' > 32) THEN

     a'=64-a'; b'=64-b'; flag5=1;

6. IF (a' > 16 & b' > 32) THEN

      b'=b'-32; flag6=1;

   [IF (b' > 16 & a' > 32) THEN a'=a'-32;]

7. IF (a' > 16 & b' > 16) THEN

     a'=32-a'; b=32-b'; flag7=1;

8. IF (a' > 08 & b' > 16) THEN

      b'=b'-16; flag8=1;

   [IF (b' > 08 & a' > 16) THEN a'=a'-16;]

9. IF (a' > 08 & b' > 08) THEN

     a'=16-a'; b=16-b'; flag9=1;

10. IF (a' > 04 & b' > 08) THEN

      b'=b'-08; flag10=1;

   [IF (b' > 04 & a' > 08) THEN a'=a'-08;]

11. IF (a' > 04 & b' > 04) THEN

     a'=08-a'; b=08-b'; flag11=1;

12. IF (a' > 02 & b' > 04) THEN

     b'=b'-04; flag12=1;

   [IF (b' > 02 & a' > 04) THEN a'=a'-04;]

13. IF (a' > 02 & b' > 02) THEN

     a'=04-a'; b=04-b'; flag13=1;

14. IF (a'=01) THEN p'=b' | IF (b'=01) THEN

    p'=a'

     GOTO Step 16

15. Perform 4bit multiplication: p'=a'*b';

16. IF (flag13= 1) THEN

      p'= [LHS=04-(a'+b')+ Carry of RHS] | [RHS=(2 bit)p'];

17. IF (flag12= 1) THEN p'=a'*04+(a'*b');

18. IF (flag11= 1) THEN

      p'= [LHS=08-(a'+b')+ Carry of RHS] | [RHS=(3 bit)p'];

19. IF (flag10= 1) THEN p'=a'*08+(a'*b');

20. IF (flag9= 1) THEN

      p'= [LHS=16-(a'+b')+ Carry of RHS] | [RHS=(4 bit)p'];

21. IF (flag8= 1) THEN p'=a'*16+(a'*b');

22. IF (flag7= 1) THEN

      p'= [LHS=32-(a'+b')+ Carry of RHS] | [RHS=(5 bit)p'];

23. IF (flag6= 1) THEN p'=a'*32+(a'*b');

24. IF (flag5= 1) THEN p'= [LHS=64-(a'+b')+ Carry of RHS] | [RHS=(6 bit)p'];

25. IF (flag4= 1) THEN p'=a'*64+(a'*b');

26. IF (flag3= 1) THEN p'= [LHS=128-(a'+b')+ Carry of RHS] | [RHS=(7 bit)p'];

27. IF (flag2= 1) THEN p'=a'*128+(a'*b');

28. IF (flag1= 1) THEN p'= [LHS=255-(a'+b')+ Carry of RHS] | [RHS=(8 bit)p'];

29. p = Left shift p' by n bits

30. Return the product p

31. **End**

Muthana .Y

In the preprocessing stage, the multiplier and the multiplied binary numbers are shifted directly to the right to remove the least significant consecutive zero bits. This reduces the calculation time by reducing the number of multiplier and multiplicand bits. The effect of the raised zero bits is combined more efficiently by shifting the last output to the left with the bits in the equal number.

To illustrate this multiplication table, consider the multiplication of two binary numbers (11000000 * 11000000).

$a = (1100\ 0000)_2 = (C0)_{16} = (192)_{10}$

$b = (1100\ 0000)_2 = (C0)_{16} = (192)_{10}$

Preprocessing:

$a' = 11$ $n1 = 6$;   shift a to the right by 6 bit because the number zero is six;
$b' = 11$ $n2 = 6$;   shift a to the right by 6 bit because the number zero is six;
$n = n1 + n2 = 12$

Processing:

Since number a 'and b' is greater than $(10)_2$, step 13 is taking place.

IF $(a' > 02\ \&\ b' > 02)$ THEN

$a' = 100 – a'$; $b' = 100 – b'$;
$a' = 0100 - 0011$; $a' = 0001$;
$b' = 0100 - 0011$; $b' = 0001$;

$p' = a' * b'$;
$p' = 0001 * 0001$; $p'(RHS) = 0001$;

IF $(flag13 = 1)$ THEN $p'= [LHS=04-(a'+b')+$ Carry of RHS] | [RHS=(2 bit)p'];

$(a'+b') = 0001+0001 = 0010$
Co of RHS= 0
$p' = [\ 0100 – 0010 + 0\ ] | [\ 01\ ]$
$p' = [10] | [01]$

$p' = 1001$ Now we will shift the final result to the left according to n.
$n = 12$
$p = 1001\ 0000\ 0000\ 0000 = (36864)_{10}$

2.5 Booth Multiplication Algorithm: The Booth multiplication algorithm is a very efficient multiplication in signed numbers. The Booth algorithm is a method that reduces the numbers of generated partial products [1, 3]. The Booth algorithm is based on the fact that the multiplicative number presented in a certain range is converted to a higher base number and the number of digits is reduced [12]. In the Booth algorithm, the three-bit parts of the multiplier are scanned and the operations corresponding to the values of these parts are performed. This reduces the summation time and accelerates the multiplication process [3, 12]. Table 2 shows the 4-base (3 bit scans) Booth Recording process. The multiplier number encoded by the Booth Recording process is formulated below.

$$Z_i = -2X_{i+1} + X_i + X_{i-1}$$

Table 2: BOOTH-4 Recording Process

X_{i+1}	X_i	X_{i-1}	Z_i
0	0	0	+0A
0	0	1	+A
0	1	0	+A
0	1	1	+2A
1	0	0	-2A
1	0	1	-A
1	1	0	-A
1	1	1	+0A

As an example, 1000011101 is taken as a multiplier. The coding obtained by selecting 3 digits is as follows. where the start bit $X_{-1} = 0$ is taken.

Muthana .Y

Figure 2: Hardware structure of the 4-base Booth algorithm

3. The Multipliers Implementation

3.1 (8x8) bit Urdhva Tiryakbhyam Multiplier:
The 8x8 bit multiplication is generated by using
four 4x4 bit multiplier blocks. Just as in the case of
a 4x4 multiplication block, the numbers a and b are
divided into smaller pieces at n / 2 = 4 bits long.
These newly formed 4-bit pieces are inserted as
input into the 4x4 multiplier block, where again

these new pieces are divided into smaller pieces of
n / 4 = 2 bits long and added to the 2x2
multiplication block. The result that produced from
the output of the 4x4 multiplication block is sent to
an addition tree for addition as shown in Figure 3
[6, 11].

3.2 (8x8) bit Proposed Vedic Multiplier:
The general architecture structure of the proposed
Vedic multiplication circuit for the 8-bit
multiplication is shown in Figure 4.

Figure 3: Block Diagram of 8x8 Urdhva Multiply block

Muthana .Y

Figure 4: Hardware architecture of the proposed Vedic multiplier

Journal of AL-Qadisiyah for computer science and mathematics   Vol.10   No.1   Year 2018
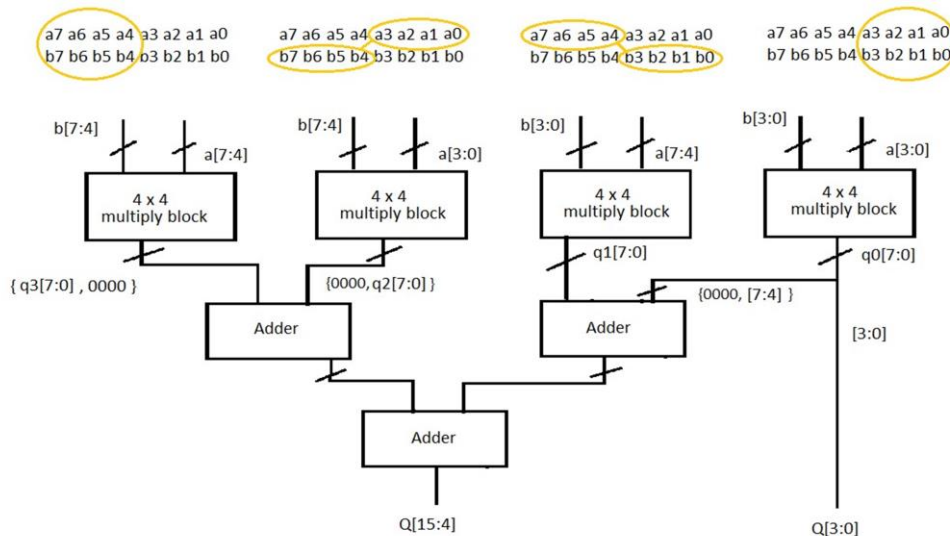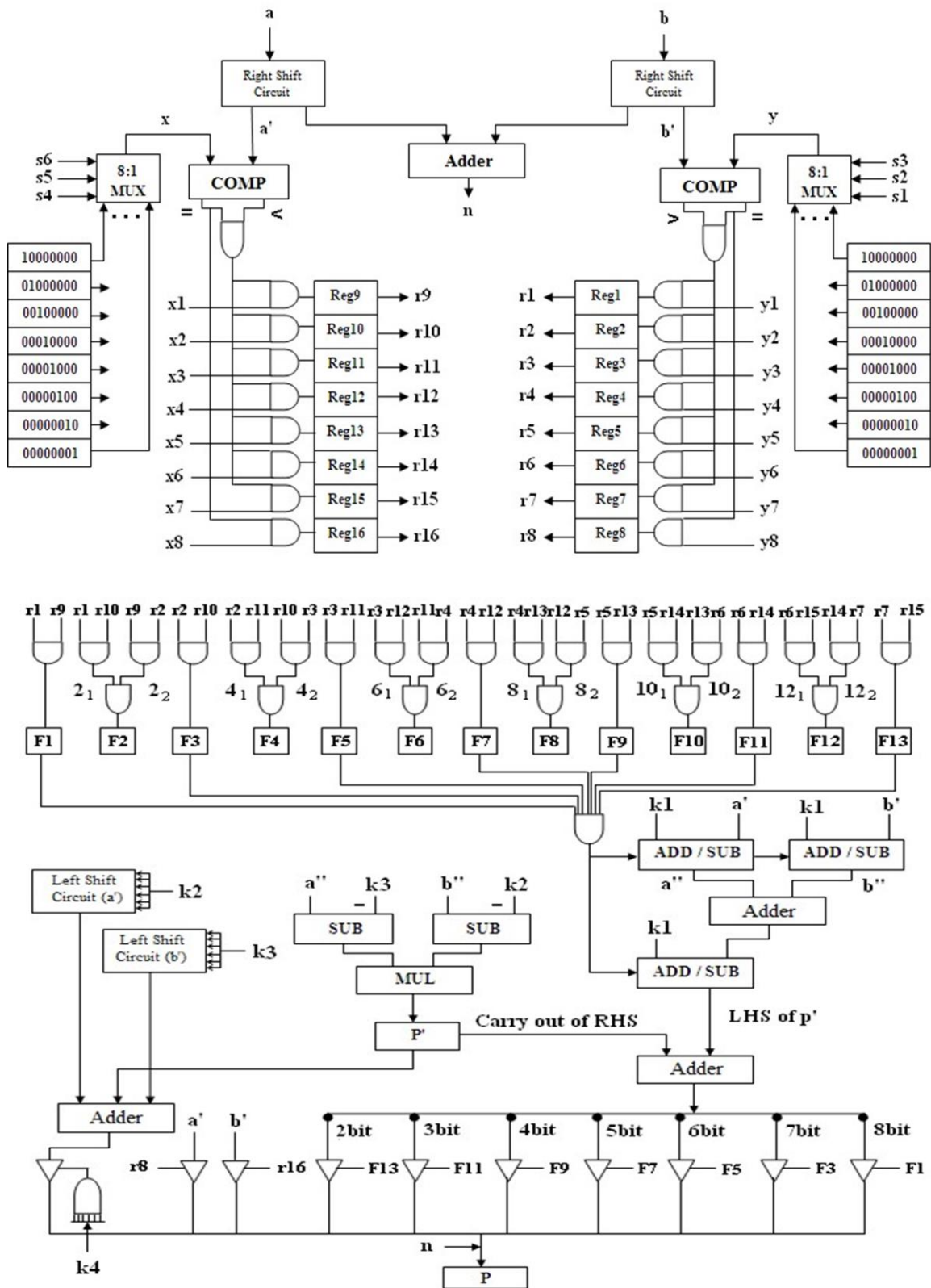**ISSN (Print): 2074 – 0204   ISSN (Online): 2521 – 3504**

Muthana .Y

In the Figure 4 k1 represent [F1, F3, F5, F7, F9, F11, F13, 0, 0], k2 = [22, 42, 62, 82, 102, 122, 0, 0], k3 = [21, 41, 61, 81, 101, 121, 0, 0] and k4 = [f2, f4, f6, f8, f10, f12].

4. Performance Comparison

All multiplier algorithms are tested and simulated by using VHDL and MAX + plus II environment (3s100evq100-5 configuration). And Performance analysis is performed using the Xilinx FPGA Spartan 3E (XC3S100E, Package VQ100, Speed - 5) device. The VHDL and MAX + plus simulations

of Urdhva, Booth and proposed Vedic multiplication algorithms are shown in Figures 5, 6 and 7 for 8 bit operands, respectively. Here, it is seen that arithmetic multiplication circuits are functionally verified.

The multiplier circuits are synthesized on the FPGA kit and their performance was obtained. As a performance criterions, from input to output the longest delay time and the total unit gate count (chip area) has been taken as a criterion. The delay here represents the delay on the FPGA kit. The Table 3 shown below is FPGA hardware performance of multiplication methods.
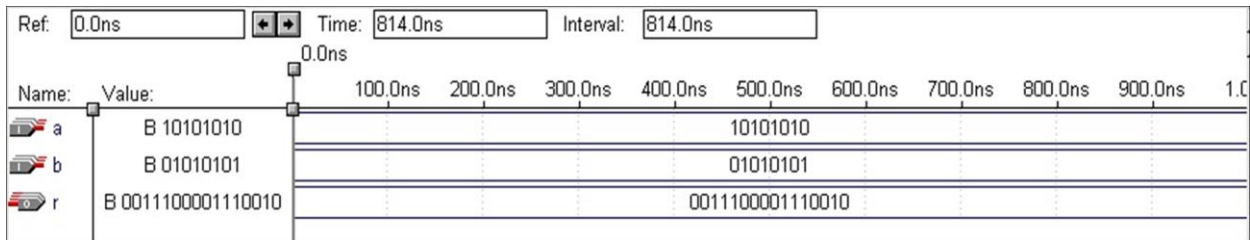
Figure 5: Timing diagram of 8x8 Urdhva multiplier
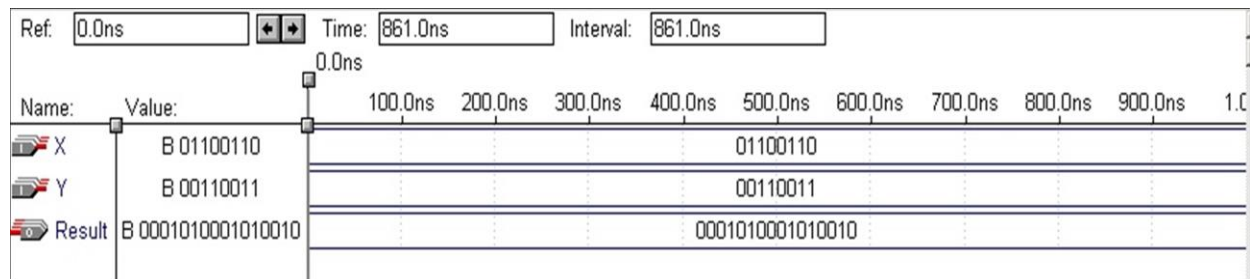
Figure 6: Timing diagram of 8x8 Booth multiplier
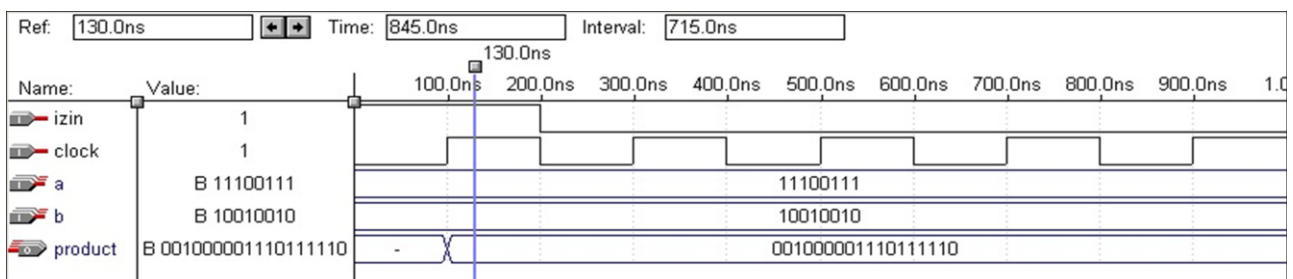
Figure 7: Timing diagram of 8x8 proposed Vedic multiplier

Muthana .Y

Table 3: FPGA implementation results

Device Utilization Summary (FPGA: Spartan 3E XC3S100E, Package VQ100, Speed -5)							
Type of Multiplier		**Urdhva**		**Booth**		**Proposed**	
Number of bits	**Available**	**4bit**	**8bit**	**4bit**	**8bit**	**4bit**	**8bit**
Number of Slices	960	16	75	18	93	13	47
Number of Slice Flip Flops	1920	0	0	0	0	8	15
Number of 4 input LUTs	1920	28	133	32	164	27	89
Number of bonded IOBs	66	16	32	16	32	15	27
Number of GCLKs	24	0	0	0	0	2	2
Number of IOs		16	32	16	32	18	34
Delay (ns)		11.005	21.544	12.767	23.934	6.947	9.887
Chip Area		228	634	217	592	260	1164

Figure 8 shows the delay time (T) depending on the bit length of the multiplication algorithms, Figure 9 shows the required chip area (A) based on the bit length, and the productivity AxT (power consumption) graph obtained by multiplying these two values. Here, when calculating the delay time T, the iteration counts of the algorithms, the number of shifting, and the re-coding times are taken into account.

According to the results obtained, the fastest of the multiplication algorithms is the proposed Vedic multiplication algorithm, but the excess chip area that is used with this speed increment is emerging. As the slowest algorithm, the Booth multiplication algorithm works slower. However, this algorithm requires minimum chip area. Urdhva multiplication algorithm is an algorithm that requires medium delay and medium chip area. Figure 10 shows that on the AxT graph used as the basic performance criterion, the minimal power consumption circuit belongs to the circuit implemented by the proposed Vedic method.
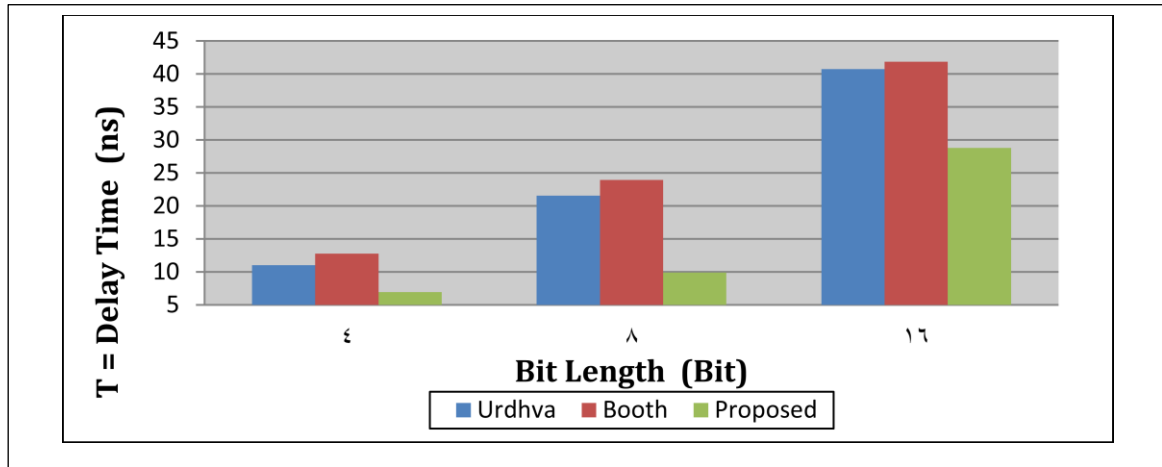
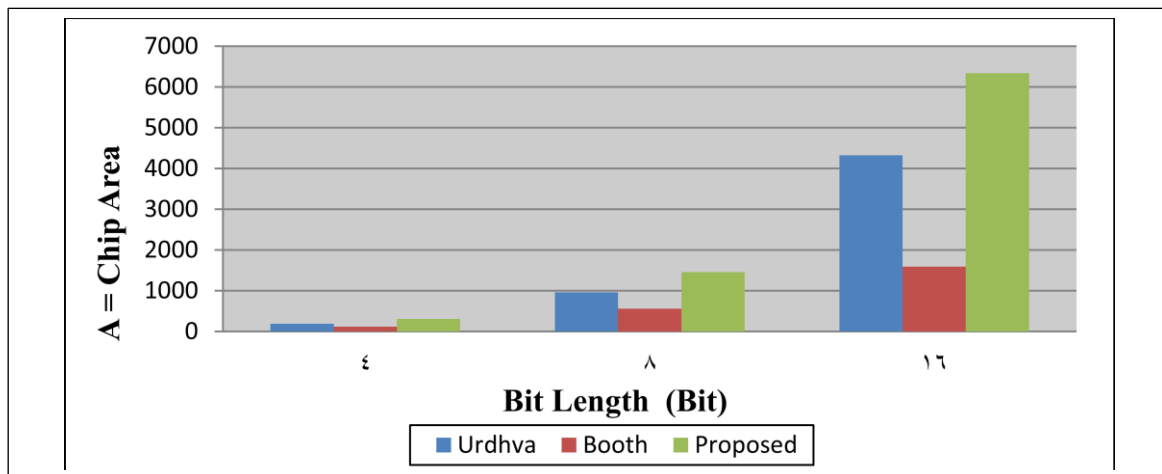**Muthana .Y**

Figure 8: Delay (T) graph of multiplication algorithms

Figure 9: Chip Area (A) graph of multiplication algorithms
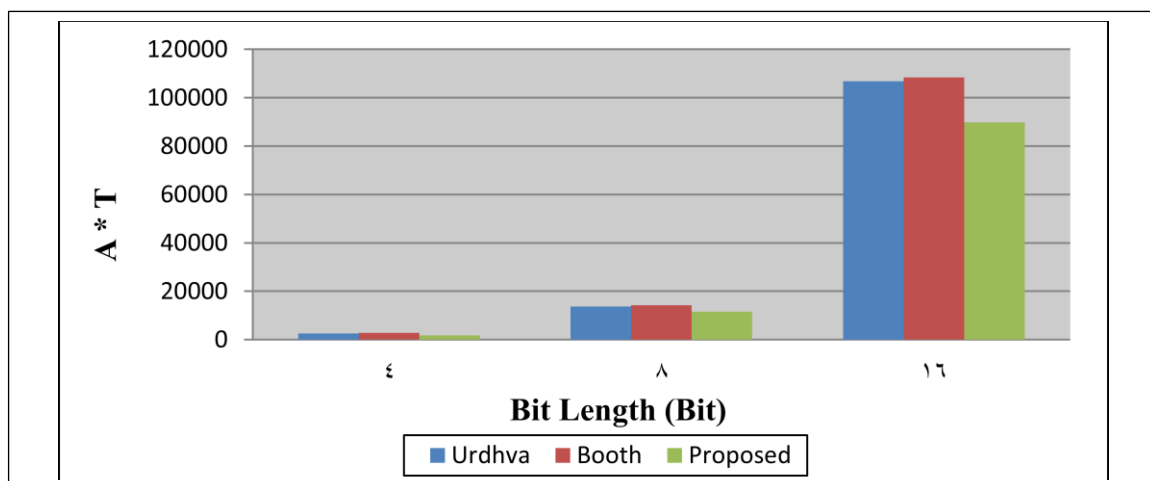

Figure 10: Power consumption (A*T) graph of multiplication algorithms

Muthana .Y

5. CONCLUSION

In this study, multiplication algorithms that based on Vedic Mathematics and based on the principle of efficient bit reduction are examined. Performance analysis of the algorithms was performed by simulating all the multiplication circuits in VHDL language. In addition, all hardware multiplication circuits have been synthesized by using FPGA kit to determine the performance of the circuits. In the Multiplier circuits, it can be concluded that the fastest one (i.e. the lowest delay time) is the proposed Vedic multiplier circuit, while the slowest one is the Booth multiplier circuit. On the other hand, it has been seen that the Booth multiplier uses the least number of the unit gates (i.e. it can be produced with the least cost). If the amount of power consumed in the chip is taken into consideration, the proposed Vedic multiplier circuit is best; The Booth multiplier circuit has been determined to have the worst performance. The Urdhva multiplier circuit exhibits a medium delay and a medium cost performance at the same time.

7. REFERENCES

[1] G.-K. Ma, F. J. Taylor, "**Multiplier Policies for Digital Signal Processing**", IEEE ASSP Mag., Vol. 7, no. 1, pp. 6–20, (1990).

[2] P. D. Chidgupkar and M. T. Karad, "**The Implementation of Vedic Algorithms in Digital Signal Processing**", Global J. of Engg. Edu., Vol. 8, no. 2, pp. 153-157, (2004).

[3] A.D. Booth, "**A Signed Binary Multiplication Technique**", Qrt. J. Mech. App. Math.,, Vol. 4, pp. 236–240, (1951).

[4] Harpreet Singh Dhillon and Abhijit Mitra, "**A Reduced-Bit Multiplication Algorithm for Digital Arithmetic**", International Journal of Computational and Mathematical Sciences 2, pp. 64-69, (2008).

[5] Wallace, C.S., "**A suggestion for a fast multiplier**", IEEE Trans. Elec. Comput., Vol. EC-13, no. 1, pp. 14–17, (1964).

[6] H. Thapliyal and M. B. Srinivas, "**High Speed Efficient N×N Bit Parallel Hierarchical Overlay Multiplier Architecture Based on Ancient Indian Vedic Mathematics**", Enformatika Trans., Vol. 2, pp. 225–228, (2004).

[7] Swami Bharati Krsna Tirtha, "**Vedic Mathematics**", Motilal Banarsidass, Varanasi, India, (1965).

[8] Asmita Haveliya, "**A Novel Design for High Speed Multiplier for Digital Signal Processing Applications (Ancient Indian Vedic mathematics approach)**", International Journal of Technology and Engineering System (IJTES), Vol. 2, no.1, pp. 27-31, (2011).

[9] Pushpalata Verma, K. K. Mehta, "**Implementation of an Efficient Multiplier based on Vedic Mathematics Using EDA Tool**", International Journal of Engineering and Advanced Technology, Vol. 1, pp. 75-79, (2012).

[10] M.C. Hanumantharaju, H. Jayalaxmi, R.K. Renuka, M. Ravishankar, "**A High Speed Block Convolution Using Ancient Indian Vedic Mathematics**", International Conference on Computational Intelligence and Multimedia Applications, Vol. 2, pp. 169-173, (2007).

[11] G.Ganesh Kumar and V.Charishma, "**Design of High Speed Vedic Multiplier using Vedic Mathematics Techniques**", International Journal of Scientific and Research Publications, Vol. 2, pp. 1-5, (2012).

[12] Rubinfield L.P., "**A proof of the Modified Booth's Algorithm for Multiplication**", IEEE Trans. Computers, Vol.25, no.10, pp. 1014-1015, (1975).

Muthana .Y

تصميم وتنفيذ دوائر ضرب الفعالة وعالية السرعة بالاعتماد على خوارزميات فيديك

مثنى ياسين نواف
جامعة كركوك / كلية العلوم / قسم علوم الحاسوب
Muthana2085@yahoo.com

المستخلص :

مع مرور الايام تطلبت السرعة المتزايدة لمعالجات الكومبيوتر الى تصميم الدوائر الحسابية ذات الاداء العالي. وقد أتاح هذا الشرط إعادة النظر في الحساب الحاسوبي، ومكن من ظهور خوارزميات سريعة، وبعض تطبيقات الاجهزة الذي توفره التكنولوجيا .والغرض الرئيسي من الحساب الحاسوبي هو تصميم الدوائر والخوارزميات التي من شأنها زيادة سرعة المعالجة الرقمية. تحقيقا لهذه الغاية، هذا البحث يقدم تصميم وتنفيذ دوائر الضرب الحسابية ذات السرعة العالية جداً وبطول بت أعلى من خلال استخدام طريقة خفض بت فعالة وذلك من خلال إجراء تغييرات في بعض أساليب عملية الضرب التي تقوم على الرياضيات الفيدية، فقد تم تطوير دوائر الضرب ذات 4 بت الى بت أعلى من الدوائر الضرب باستخدام بعض الخصائص الأساسية في عملية الضرب مثل التحليل وازاحة البتات. تم كتابة وتنفيذ كودات خوارزميات الضرب في لغة توصيف العتاد للدارات المتكاملة عالية السرعة المعروفة (VHDL) وتنفيذ تحليلات الأداء لدوائر الضرب الحسابية عن طريق التحقق الوظيفي من خلال المحاكاة XILINX و الميدان المتقشف لمصفوفات البوابات القابلة للبرمجة (FPGA)، والحصول على إشارة الخرج الموجي وقياسات أوقات التأخير.

Proposed method for Analyze the QR code and Detection of Vulnerabilities

Sarah Saadoon Jasim

Middle Technical University
Computer Science/Technical college of

Management – Baghdad/Dept. of IT

Abstract

A 2D matrix that is designed via keeping two points under consideration is QR code, in other words, it stores a large amount of data as compared to 1D barcodes. A Denso-Wave Corporation in Japan has been developed the QR code; the various marker of QR codes over traditional barcodes owns a large storage capacity, read faster, 360-degree reading, printing of small size, correction of error, and supports more languages. The use of QR codes has been expanding over the world because of these benefits. This paper tries to highlight the characteristics, working, significance, and vulnerabilities of the QR codes. After applying the proposed method, the irrelevant positions were detected, then it was removed without any effect on the QR code reading, and these positions are used to hide text or image; indicating that the proposed new method has shown some important characteristics which will affect the security and confidentiality of the QR-code.

Keywords: QR Code, Irrelevant positions.

Sarah .S

1. **Introduction**

In 1994 one of the Japanese Toyota group companies has created a QR code; QR code (Quick Response code) is a two-dimensional barcode [1]. In both the vertical and horizontal direction information is encoded, thus controlling up to several hundred times thus storing more data than a traditional barcode; using a camera to the access the data is by taking an image of the code (e.g. built into a smartphone) and this image is processing by a QR reader [2]. The function of symbols is similar to conventional barcodes;   however, there is an ability to store additional data inside it. Criteria of forty versions have been defined on the different space of QR code [1]. In June 2000 propagated an international standard ISO/IEC 18004, has been focused on QR codes. QR codes are used firstly in the application of production control of automotive parts and since their development, in a lot of usages, a wide range is found in different regions. Generally, QR codes have been spread widely on declarations, products, and posters. In 2010, the International Air Transport Association (IATA) for worldwide airports integrated the QR code into passenger boarding passes. In hospitals were used QR code used especially for patient identification in Hong Kong. Another example of QR code was applied to the trains for ticketing system and airlines or to the bills for e-payment [3].

Recently, the QR code becomes extremely popular in digital image watermarking which can be used as a cover image or as a watermark. In our work, we focus on using the QR code as a cover image for hiding the information [4].

2. **Literature review**

Priyanka Gaur, Shamik Tiwari (2014) presents a novel method for QR barcode recognition using the texture features and neural network. All the operations are performed on the MATLAB platform. Performance of proposed methodology is evaluated using a database of QR code images. ZXing library is also used for recognition purpose, which shows the satisfactory results. Zxing library can decode all of them correctly. For the images with blur 86.66% recognition rate is achieved. The recorded recognition rate for the detected deformed barcode images is 70% [5].

D. Antony Praveen Kumar and M. Baskaran. (2016) Present the process is improving the steganography method using QR-code data input pattern image and LSB technique in RGB image. So, the proposed system process has done the message transferring effectively in a secure manner based on Least Significance Bit method and QR code pattern image. Finally, the resulted work is to increase the system performance level compare to existing methodology [6].

The Authors in Ref [7] analyze the QR codes based on their significance and use. They discuss the work of QR codes such that making the reader familiar with the QR codes; such that a many complex information can be stored in this small area. With increased awareness about the utility of these codes, we can look forward to using them in more general areas.

Sarah .S

In the work [8], an information form was used that combines cryptography and steganography; such that QR codes are applied to encode the message encrypted. The steganography of a nested image with the QR codes is been performed on an appropriate cover image and it is clear from the results that the Stego image was created a similar to the cover image, and these images cannot be identified by the eye of a human. From the selected images are proved MSE (mean square error) and RMSE (root means the error box) values.

3. Quick Response code (QR code)

QR code called matrix code and its a two-dimensional encoding of data. This automatically readable matrix code consists of two boxes (black and white). It has been storing the data as a form of contact information, Uniform Resource Locator (URL), links to images or videos, clear text, and etc. [9].

3.1. The architecture of QR Code:

Each QR code is similar to the square models. the square of models divided into the two parts: area of encoding and models functions. Function models concentrate on positions that represent data encoding in a cryptographic region.
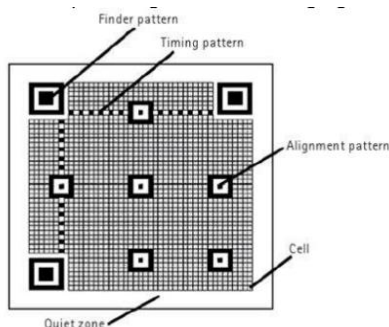
Fig (1) Architectural QR-code

In Figure (1) illustrates the QR code structure. patterns of the function include (finder, timing, and alignment) models. A finder patterns are three major structures based on three corners in the QR-code; for determining the correct orientation of a symbol uses Finder models. To detect the side of the pattern by a decoder software are used Timing models. In the case of an image, distortion uses the Alignment models to decode correctly a symbol via software decoder. The remainder of the area, which is not the function pattern; it is the encrypted area which the data codewords are stored and errors are corrected in code words [9]. The Quiet Zone is spacing area and its importance of the scanning program to differentiate between the QR code and surrounding of it's.

3.2. Qualities of QR Code:

The following some general qualities or characteristics in the QR code that must be identified:

a) Large space of storage: the QR code could be stored approximately 7,089 characters of data and where this size of data is huge compared with a 1D barcode.

b) Encryption a set of characters for the data:

・ The data of numeric or the digits from 0 to 9.

・ The digits from 0 to 9; The letters from A to Z (upper case); other characters (space, :, %, *, +, -, /,_, $) or called data of alphanumeric.

・ Characters of Kanji.

c) Small Size for print: one of the characteristics of QR codes in the horizontal and vertical directions is storing the information, and depending on this characteristic with the same size of data, the space obtained via QR code is one to four times less than space obtained via One-dimensional barcode.

d) The Degree reading of the QR code is 360: from the characteristics of the QR code is reading from any direction; and it was applied by the finder samples found at three corners of the code. These samples help to determine characteristics of QR code.

e) Correction of error and ability of the restoring: data can be retrieved in case if part of the code is been harming or contaminated; the procedure of error detection can be centralizing on the correct data area; L, M, Q and H are four levels of QR code of error correction. The weakest in level L and the strongest in level H such as the error correction capability [10].

4. Uses and importance of QR code:

The QR code readers provide a straightforward representation with an appropriate access to data. Therefore, the QR codes are used widely for the declaration of products, links to companies' website, and competition for sign up pages. The printing of QR code on the building may enable the guestor for knowing the building's history, and it might give data about its architect or about how to build the building. There are various ways to use the QR codes [9]:

✓ In business company cards: QR code on the business cards is an excellent location. Meet someone at any pooling, get automatically on their communication data and saved on your smartphone by scanning a QR code.

✓ Advertisements of the magazine: in any magazine, a product announcement in addition to the QR code might bring the attention of the reader to the site of the company; and the client might reading about this product and purchasing it.

✓ Restaurants and Cafes: The prioritize client in the restaurants or any cafe shop offering a specific or free rebate in addition to a ready meal via the use of a QR code printed on their dining tables.

✓ Manufacturers of equipment: we can add QR code to the instruction manual by the manufacturer of the product that transport people to electronic content and help use products.

✓ Talking Labels: If you print a QR code on your talk labels, the product poster becomes alive. A code may be taking the guestor to a video or may be shown images of interesting to the product that may affect buyers.

5. Proposed Methodology

The main objective of our proposed system is to discover the irrelevant positions that do not affect the QR code reading, and these positions are used to hide text or image. The work of a QR code involves two parts encoding and decoding of the data. The Fig (2) shows the schematic flow diagram of the proposed work.

Sarah .S

A. QR-code Creation:

In this process, load the image of QR code directly, or choosing a type of code that you want to create by entering the data to attach it to the symbol; then, click on button "Creating of QR Code". After that, QR code is generated in the program. Fig. 3 shows how a QR code can generate.

(a) Loading of QR-Code (b) Creating of QR-Code

Fig (3) (Creating, Loading) QR Code

B.   QR-code   Histogram   equalization   and Binarization:

In the case of loading the image of QR code; the processes of histogram equalization and binarization are important to remove the existing noise in QR code image. The equalization of the histogram is a common technicality to improve the appearance of the poor image, a function similar to the histogram extension process and gives satisfactory results for images with a wide range of gray levels such that the Histogram Equalization is a technicality that makes the resulting image as simple as possible as flat. The theoretical basis of the histogram equalization is based on probability theory, where it is treated as a probability distribution of gray levels. The histogram equalization process consists of four steps (see Fig 4):
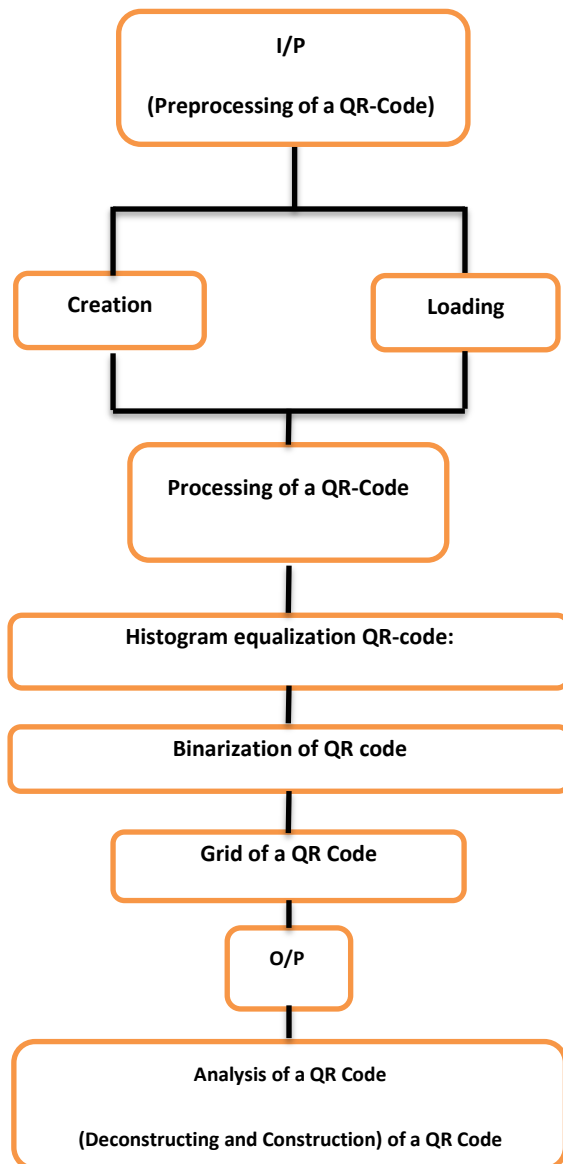

Fig (2) Block diagram of the proposed system

5.1. Preprocessing of a QR Code

At this stage, there is a set of pre-processes that should be taken into our consideration to create the QR code, and these pre-processes are presented as follows:

- Find the Running Sum of the histogram values.

- Divide the resulting values from step (a) on the total number of image elements normalize.

- Multiply the values by step (b) with the value of the larger gray level and rotate the result to the nearest integer.

- Match the values of gray levels with the results of step (c).

Fig (4) Histogram equalization QR-code

With the QR code binarization process, the images are converted to grayscale and converted to black and white (binary image) according to the value of threshold 130, as shown in Fig 5.

Fig (5) Binarization QR-code

C. **Grid of a QR Code**

This process explained the grid, height, and width of QR code for knowing the number of pixels and finding the positions that can be used for hiding the information; in addition to convert the QR code to the binary system. This process is represented in the following steps:

- Clip of a QR Code to delete the white areas surrounding the QR-code (as shown in Fig 6).

Fig (6) Clip QR-code

- Ridge of a QR Code: at this step, we find the width and the height of the QR-code; through which the QR-code is divided into a grid of white and the black boxes (see Fig 7). The Ridge of a QR Code is constructed by using Equation (1):

$$Ridge\ QR\text{-}code = width*height \qquad (1)$$

Fig (7) Ridge QR-code

Sarah .S
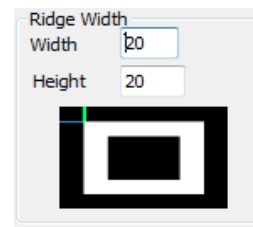
- Draw ridge of a QR Code: in this step, the pixels are drawn based on the previously computed grid to determine the number of positions (blocks) to be used for hiding information without any effecting on the QR code (see Fig 8).

Fig (8) Draw ridge of QR-code

5.2. Analysis of a QR Code

The final process is done by firstly, deconstructing the QR Code and using a mask of (3 * 3) to take all the possible probabilities in QR code to find the number of positions for hiding information as represented in equation (2);

$$Number\ of\ hidden\ blocks = Ridge\ QR\text{-}code*Number\ of\ blocks \tag{2}$$

Secondly, a construction of the QR Code is done (see Fig 9, 10).

Fig (9) Finding the Number of hidden blocks in the QR-code
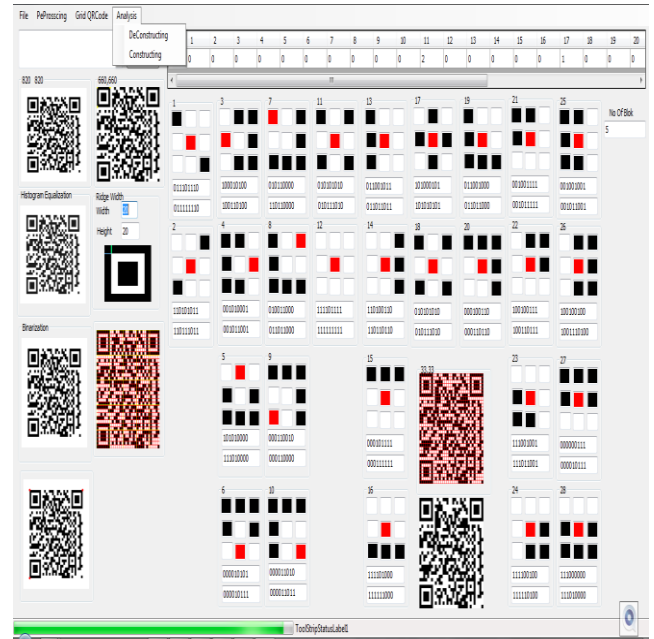
Fig (10) The overall proposed system
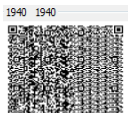
6. Experimental results

To evaluate the proposed system, a lot of loaded QR codes are used, and after applying our method, we can get the irrelevant positions as demonstrated in Table 1. And Table 2 shows the original QR-codes and the QR-codes without the irrelevant blocks.

Sarah .S

Table (1) Show number of pixel of irrelevant blocks

Number of bits	Number of blocks	Number of hidden blocks
32	9	576
56	13	832
88	8	512
112	9	576
120	13	5200
272	16	6400
352	13	5200
616	30	12000
704	39	15600
1200	23	368
3080	103	41200

Table (2) Show original QR-code and QR-code after eliminating the irrelevant blocks

Number of bits	QR-code			Final QR-code	(Pass/ Not Pass) of QR-code
	Original	x	y		
32		200	200		Pass
56					Pass
88		200	200		Pass
112					Pass
120		660	660		Pass
272		820	820		Pass
352		820	820		Pass
616		1060	1060		Pass
704		1140	1140		Pass
1200		200	200		Pass
3080		1940	1940		Not Pass

Sarah .S
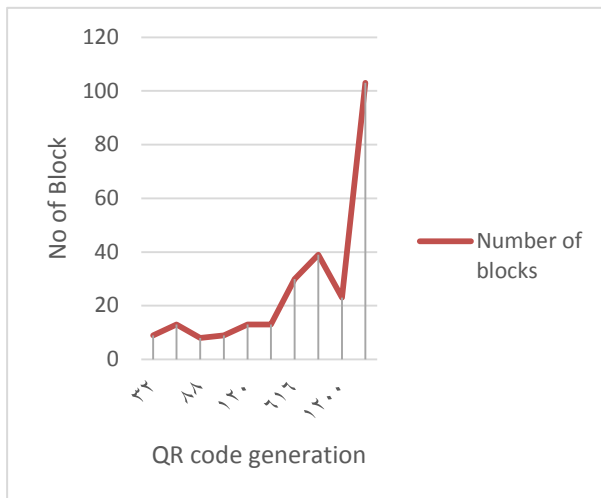
Fig (11) The number of blocks for the generated QR codes

The diagram above shows the number of blocks that have been changed (i.e. removed from the QR code) within a set of generated QR code. Which in turn did not affect the process of reading and retrieving information from the code through the scanner? So, this paper shows that there are a number of irrelevant blocks that can be used to hide the data without any effect in the process of retrieving QR code data.

7. Conclusion

In this paper, a set of unimportant points (irrelevant positions) was discovered in QR Codes; after removing it, QR codes will not be affected and still be readable normally. The removing of these irrelevant positions makes the proposed method faster in coding, discovery and reduce the size of the QR Codes.

References

[1] David Pintor Maestre, "QRP: An improved secure authentication method using QR codes", Universitat Oberta de Catalunya, 08018, Barcelona, Spain,dpintor@uoc.edu, June 8, 2012.

[2] Kieseberg P., Leithner M., Mulazzani M., Munroe L., Schrittwieser S., Sinha M., AND Weippl E., "QR Code Security', the 8th International Conference on Advances in Mobile Computing and Multimedia, Paris, France - November 08-10-2010, Pages 430-435. doi>10.1145/1971519.1971593.

[3] Falkner S., Kieseberg P., E. Simos D., Traxler C., and Weipp E., "E-voting Authentication with QR-codes", International Conference on Human Aspects of Information Security, Privacy, and Trust HAS 2014: LNCS 8533, pp. 149–159, 2014. https://link.springer.com/chapter/10.1007/978-3-319-07620-1_14.

[4] Jumana W., Dong Jun H., Sarah S., Saad H., and Hiyam H., " An Immune Secret QR-Code Sharing based on a Twofold Zero Watermarking Scheme". International Journal of Multimedia and Ubiquitous Engineering Vol.10, No.4 (2015), pp.399-412. http://dx.doi.org/10.14257/ijmue.2015.10.4.38.

[5] Gaur P., Tiwari S., "2D QR Barcode Recognition Using Texture Features and Neural Network", International Journal of Research in Advent Technology, Vol.2, No.5, May 2014 E-ISSN: 2321-9637.

Sarah .S

[6] D. Antony Praveen K., and M. Baskaran, "Data Hiding Using LSB with QR Code Data Pattern Image", International Journal of Science Technology & Engineering | Volume 2 | Issue 10 | April 2016 ISSN (online): 2349-784X.

[7] Kulkarni S. S.and Malagi C., "Creation and Analysis of QR Code", Bonfring International Journal of Software Engineering and Soft Computing, Vol. 6, Special Issue, October 2016.

[8] B Karthikeyan, Kosaraju C. A., Gupta S S., "Enhanced Security in Steganography using Encryption and Quick Response Code", This full-text paper was peer-reviewed and accepted to be presented at the IEEE WiSPNET 2016 conference.

[9] Sangeeta Singh, "QR Code Analysis", International Journal of Advanced Research in Computer Science and Software Engineering, Volume 6, Issue 5, May 2016 ISSN: 2277 128X.

[10] International Standard ISO/IEC 18004, "Information technology Automatic identification and data capture techniques Bar code symbology QR Code", Reference number - ISO/IEC 18004:2000(E), First Edition 2000-06-15.

<div dir="rtl">

الطريقة المقترحة لتحليل رمز الاستجابة السريعة والكشف عن مواطن الضعف

المستخلص :

رمز الاستجابة السريعة هي مصفوفة ذات بعدين التي تم تصميمها باعتبارها اساسا نقطتين، وبعبارة أخرى، فإن رمز الاستجابة السريعة يخزن كمية كبيرة من البيانات بالمقارنة مع الباركود ذات البعد الواحد. وقد طورت شركة دينسو في اليابان رمز الاستجابة السريعة مقارنة مع الباركود التقليدية حيث تمتلك سعة تخزين كبيرة، قراءة أسرع، وقراءة 360 درجة، طباعة صغيرة الحجم، وتصحيح الاخطاء، ويدعم المزيد من اللغات. وبسبب هذه الفوائد تم التوسع في استخدام رمز الاستجابة السريعة في جميع أنحاء العالم . هذه البحث يحاول تسليط الضوء على خصائص، عمل، أهمية، ومواطن الضعف لرمز الاستجابة السريعة. بعد تطبيق الطريقة المقترحة، تم الكشف عن المواقع غير المهمة، ثم تمت إزالتها دون أي تأثير على قراءة رمز الاستجابة السريعة، وتستخدم هذه المواقع لإخفاء نص أو صورة. مشيرا إلى أن الطريقة الجديدة المقترحة أظهرت بعض الخصائص الهامة التي سوف تؤثر على أمن وسرية رمز الاستجابة السريعة.

كلمات البحث: رمز الاستجابة السريعة، والمواقع غير المهمة.

</div>

Modification of two Parameters Rayleigh into three Parameters one Through Exponentiated

Waleed meaya rodeen
Basra university
Collage of management and economic
Statistics department

Abstract
The continuous probability Rayleigh distribution is one of the important Is an important distribution that can be used To analyze signal data and statistical error data as well as time to failure, so we work on modifying two parameters Rayleigh (α, θ) into three parameters one's $(\alpha, \theta, \lambda)$ through exponentiated, the new $p.d.f$ obtained, also the formula for r[th] moments about origin is derived, to be used in estimating of parameters and also of reliability function. All derivation required were explained and the estimators by maximum likelihood and moments were obtained using different sets of initial values and the replicate of each experiment is $(R = 1000)$, the results are compared by using mean squared error (MSE).
Keywords: Three Parameters Rayleigh, moments Estimators, (MOM), Maximum Likelihood Estimator (MLE), reliability Function $[R_T(t)]$, Mean Squared error (MSE).

1. Introduction

The Rayleigh distribution is one of the continuous probability distribution, which is one of the family of distribution introduced by, Burr (1942), it is used in analysis of signal and also in representing statistical errors of all types. Rayleigh distribution has many applications in representing statistical model for life time data (Lawless, J.F.[1982])[7], Dey, S. and das, M.K. (2007)[4], explain Bayesian approach interval for Rayleigh distribution. The $p.d.f$ of two parameters Rayleigh (α, θ) is given by;

$$f(x; \alpha, \theta) =$$
$$2\alpha\theta^2 x\, e^{-(\theta x)^2}\left(1 - e^{-(\theta x)^2}\right)^{\alpha-1} \qquad x, \alpha, \theta > 0$$
(1)
$$\qquad\qquad 0 \qquad\qquad o/w$$

Where (α) is the shape parameter and (θ) is the scale parameter.
The p.d.f in equation (1) may have different shape according to value of (α), if $(\alpha \leq \frac{1}{2})$, the p.d.f in equation (1) is decreasing curve, and when $(\alpha > \frac{1}{2})$, it is skewed to right.

The cumulative distribution function corresponding to equation (1) is;

$$F(X; \alpha, \theta) = pr(X \leq x) = \left(1 - e^{-(\theta x)^2}\right)^{\alpha}$$
(2)
Also survival function is;
$$S(X; \alpha, \theta) = 1 - \left(1 - e^{-(\theta x)^2}\right)^{\alpha}$$
(3)
Also when $(\alpha\ \&\ \theta > 0)$, we can define the hazard function;
$$h(X; \alpha, \theta) = \frac{f(X; \alpha, \theta)}{S(X; \alpha, \theta)}$$
(4)
The $p.d.f$ in equation (1) can be transformed to a three parameters Rayleigh through using exponentiated transformation by adding another shape parameter (λ), using
$$G_X(x) = [F(x, \alpha, \theta]^{\lambda} = \left[\left(1 - e^{-(\theta x)^2}\right)^{\alpha}\right]^{\lambda} =$$
$$\left(1 - e^{-(\theta x)^2}\right)^{\alpha\lambda} \qquad\qquad (5)$$
$$g(x) = \alpha\lambda\left(1 - e^{-(\theta x)^2}\right)^{\alpha\lambda-1}\left(e^{-(\theta x)^2} 2x\theta^2\right)$$
$$= 2x\alpha\lambda\theta^2 e^{-(\theta x)^2}\left(1 - e^{-(\theta x)^2}\right)^{\alpha\lambda-1} \qquad \alpha, \theta, \lambda >$$
$$0\ and\ \alpha\lambda > 1 \qquad\qquad (6)$$
Equation (6) is the new $p.d.f$ of exponentiated Rayleigh which have applications in signal and errors analysis. The survival function is:
$$S(X; \alpha, \theta, \lambda) = 1 - (F(X; \alpha, \theta)^{\lambda}$$

Waleed .M

2. Moment Estimator Method

We find the formula for the rth moments, about origin;

$$\mu'_r = E(x^r) = \int_0^\infty x^r f(X; \alpha, \theta)$$
(7)

After some steps we have;

$$\mu'_r = \frac{\alpha}{\theta^r} \sum_{i=0}^{\alpha-1} \frac{C_i^{\alpha-1}(-1)^{\alpha-1-i}}{(\alpha-i)^{\frac{r}{2}+1}} \Gamma\left(\frac{r}{2}+1\right) \qquad \alpha > 1$$
(8)

$$\mu'_r = E(x^r) = 2\alpha\lambda\theta^2 \int_0^\infty x^{r+1} e^{-(\theta x)^2} \left(1 - e^{-(\theta x)^2}\right)^{\alpha\lambda-1} dx \qquad (9)$$

Since

$$(1-t)^n = \sum_{j=0}^n C_j^n (-1)^j t^j$$

Then;

$$\left(1 - e^{-(\theta x)^2}\right)^{\alpha\lambda-1} = \sum_{j=0}^{\alpha\lambda-1} C_j^{\alpha\lambda-1} (-1)^j \left(e^{-(\theta x)^2}\right)^j$$

$$\mu'_r = 2\alpha\lambda\theta^2 \sum_{j=0}^{\alpha\lambda-1} \int_0^\infty x^{r+1} e^{-(\theta x)^2} C_j^{\alpha\lambda-1}(-1)^j \left(e^{-j\theta^2 x^2}\right) dx \qquad (10)$$

$$\mu'_r = 2\alpha\lambda\theta^2 \sum_{j=0}^{\alpha\lambda-1} C_j^{\alpha\lambda-1}(-1)^j \int_0^\infty x^{r+1} e^{-\theta^2(i+j)x^2} dx$$

Let $\quad Z = \theta^2(1+j)x^2 \quad \Rightarrow \quad x = \frac{\sqrt{Z}}{\theta\sqrt{1+j}} \quad \Rightarrow$

$$dx = \frac{1}{2\theta\sqrt{Z}\sqrt{1+j}} dZ$$

$$\mu'_r = k \int_0^\infty \left(\frac{\sqrt{Z}}{\theta\sqrt{1+j}}\right)^{r+1} e^{-Z} \frac{1}{2\theta\sqrt{Z}\sqrt{1+j}} dZ$$

$$= k \frac{1}{2\theta^{r+2}\left(\sqrt{1+j}\right)^{r+1}\sqrt{1+j}} \int_0^\infty \sqrt{Z}^r e^{-Z} dZ$$

$$\mu'_r = \frac{2\alpha\lambda\theta^2 \sum_{j=0}^{\alpha\lambda-1} C_j^{\alpha\lambda-1}(-1)^j}{2\theta^{r+2}\left(\sqrt{1+j}\right)^{r+2}} \int_0^\infty Z^{\frac{r}{2}} e^{-Z} dZ$$

$$= \alpha\lambda \sum_{j=0}^{\alpha\lambda-1} C_j^{\alpha\lambda-1}(-1)^j \frac{\Gamma\left(\frac{r}{2}+1\right)}{\theta^r} \left(\frac{1}{\sqrt{1+j}}\right)^{r+2} \qquad \alpha\lambda > 1 \quad (11)$$

By solving $\left(\mu'_r = \frac{\sum_{i=1}^n x_i^r}{n}\right)$ for $(r = 1,2,3)$ and $\alpha\lambda > 1$, we can obtain moments estimates for three parameters of (E − Ray).

3. Maximum Likelihood Estimator

Let $(x_1, x_2, \dots, x_n)$ be a r. s. from $p.d.f, \; f(x; \alpha, \theta)$, then;

$$L = \prod_{i=1}^n f(x_i) = 2^n \alpha^n \lambda^n \theta^{2n} \prod_{i=1}^n x_i \, e^{-\theta^2 \sum_{i=1}^n x_i^2} \prod_{i=1}^n \left(1 - e^{-\theta^2 x_i^2}\right)^{\alpha\lambda-1} \qquad (12)$$

$$\log L = n\log 2 + n\log \alpha + 2n\log \theta + n\log \lambda + \sum_{i=1}^n \log x_i - \theta^2 \sum_{i=1}^n x_i^2$$

$$+ (\alpha\lambda - 1) \sum_{i=1}^n \log\left(1 - e^{-\theta^2 x_i^2}\right)$$

$$\frac{\partial \log L}{\partial \alpha} = \frac{n}{\alpha} + \sum_{i=1}^n \log\left(1 - e^{-\theta^2 x_i^2}\right) = 0$$

$$\hat{\alpha}_{MLE} = -\frac{n}{\sum_{i=1}^n \log\left(1 - e^{-\theta^2 x_i^2}\right)}$$
(13)

$$\frac{\partial \log L}{\partial \theta} = \frac{2n}{\theta} - 2\theta \sum_{i=1}^n x_i^2 + (\alpha\lambda - 1) \sum_{i=1}^n \frac{(-1)\left(e^{-\theta^2 x_i^2}\right)(-2\theta x_i^2)}{\left(1 - e^{-\theta^2 x_i^2}\right)} = 0$$

$$(\alpha\lambda - 1) \sum_{i=1}^n \frac{(-1)\left(e^{-\theta^2 x_i^2}\right)(-2\hat{\theta}x_i^2)}{\left(1 - e^{-\theta^2 x_i^2}\right)} = \hat{\theta} \sum_{i=1}^n x_i^2 - \frac{n}{\hat{\theta}}$$

$$\hat{\theta}^2 \left[\sum_{i=1}^n x_i^2 - (\alpha\lambda - 1) \sum_{i=1}^n \frac{(-1)\left(e^{-\theta^2 x_i^2}\right)(-2\hat{\theta}x_i^2)}{\left(1 - e^{-\theta^2 x_i^2}\right)}\right] = n$$

By using newton raphson method to get the parameter estimator of θ

4. Simulation

The estimation and comparison has been done through simulation procedures, were the values are generated from;

$$G_X(x) = [(1 - e^{-(\theta x)^2})^\alpha]^\lambda$$
$$u_i = [(1 - e^{-\theta^2 x^2})]^{\alpha\lambda}$$
$$u_i^{\frac{1}{\alpha\lambda}} = (1 - e^{-\theta^2 x^2})$$
$$e^{-\theta^2 x^2} = 1 - u_i^{\frac{1}{\alpha\lambda}}$$
$$-\theta^2 x^2 = \ln\left(1 - u_i^{\frac{1}{\alpha\lambda}}\right)$$
$$x^2 = -\frac{1}{\theta^2} \ln\left(1 - u_i^{\frac{1}{\alpha\lambda}}\right)$$
$$x_i = -\frac{1}{\theta} \sqrt{\ln\left(1 - u_i^{\frac{1}{\alpha\lambda}}\right)}$$

Waleed .M

The initial values are;

α	λ	θ
3	0.5	0.8
4	0.8	1.5
3.5	2	2

Table (1): Estimation of ($\alpha = 3, \theta = 0.6, \lambda = 0.5$)

n	$\hat{\theta}_{MLE}$	$\hat{\theta}_{MOM}$	$\hat{\lambda}_{MLE}$	$\hat{\lambda}_{MOM}$	$\hat{\alpha}_{MLE}$	$\hat{\alpha}_{MOM}$
	0.6604	0.51593	0.5506	0.5560	2.4756	2.8660
	0.6403	0.52274	0.5643	0.5641	2.4814	2.9520
	0.5031	0.51499	0.5602	0.6203	2.4703	2.9830
3	0.8703	1.04061	0.8613	0.6614	2.9611	2.8820
0	0.8832	1.4035	0.9921	1.0021	3.0112	1.3846
	0.9994	1.0362	1.3011	1.0314	3.0611	1.4157
	1.4683	1.5266	1.2920	1.1121	3.5211	1.3992
	1.5962	1.9821	1.0122	1.2306	3.5311	1.3672
	1.6401	1.9932	1.0089	1.5216	3.8020	1.4407
	1.6612	1.9961	1.5283	1.5220	3.8840	1.4402
	0.48776	0.5006	1.4407	1.4837	1.1254	1.5267
	0.49582	0.5832	1.4408	1.4962	1.3621	1.5382
	0.51084	0.9486	1.4425	0.9437	1.6410	1.5171
6	0.8736	0.5044	0.8963	0.9882	1.0407	1.5189
0	0.9921	0.9936	0.8902	0.9945	1.0475	1.2346
	0.9914	1.0052	0.8831	1.6931	1.5743	1.2204
	1.4001	1.0069	0.8801	1.4825	1.5675	1.0666
	1.4231	1.5022	0.8711	1.5119	1.0161	1.2431
	1.4303	1.5311	0.6531	1.4945	1.4241	1.3352
	1.4996	1.4958	0.6420	1.8462	1.2563	1.2453
	0.49784	0.5042	0.5046	0.4871	2.1106	1.4837
	0.49987	0.4991	0.5049	0.4973	2.004	1.4810
	0.49417	1.0081	0.4998	0.4917	2.001	1.4707
	0.9981	1.0005	0.4999	0.9855	1.889	0.9463
	0.99046	1.0411	1.0005	0.9965	1.992	1.6472
9	1.00231	1.5432	1.0024	0.9943	1.0115	1.5321
0	1.51951	1.5171	1.0114	0.9931	1.5341	1.55221
	1.501009	1.51891	1.5348	1.5171	1.51718	1.4841
	1.50372	1.3264	1.51716	1.51886	1.51706	1.4742
	1.64021	1.4302	1.5189	1.5002	1.5051	1.3762

Table (2): Estimators of Reliability Function.

n	α	λ	θ	$\hat{R}_{MLE}$	$\hat{R}_{MOM}$	$Best$
		0.5	0.8	0.68323	0.59871	MLE
	3	0.8	1.5	0.76112	0.66082	MLE
		0.6	2	0.79014	0.89314	MOM
		0.5	0.8	0.99061	0.88541	MLE
30	4	0.8	1.5	0.9843	0.93061	MLE
		0.6	2	0.60075	0.77431	MOM
		0.5	0.8	0.99941	0.98405	MLE
	3.5	0.8	1.5	0.78063	0.69904	MLE
		0.6	2	0.66421	0.63415	MLE
		0.5	0.8	0.77435	0.90763	MOM
	3	0.8	1.5	0.84306	0.77531	MOM
60		0.6	2	0.872310	0.99078	MLE
		0.5	0.8	0.843301	0.884693	MOM
	4	0.8	1.5	0.706492	0.77084	MLE
		0.6	2	0.77145	0.84773	MLE
		0.5	0.8	0.78715	0.77806	MLE
	3.5	0.8	1.5	0.84734	0.84707	MOM
		0.6	2	0.85321	0.9993	MOM
		0.5	0.8	0.99061	0.99341	MOM
	3	0.8	1.5	0.84667	0.84732	MOM
		0.6	2	0.83552	0.84352	MOM
90		0.5	0.8	0.847076	0.84352	MLE
	4	0.8	1.5	0.776171	0.77061	MLE
		0.6	2	0.89031	0.84315	MLE
		0.5	0.8	0.88061	0.9091	MOM
	3.5	0.8	1.5	0.84553	0.9312	MOM
		0.6	2	0.84321	0.9906	MOM

Waleed .M

Table (3): Mean square error for $\hat{R}$.

n	α	λ	θ	$\hat{R}_{MLE}$	$\hat{R}_{MOM}$	$Best$
30	3	0.5	0.8	0.0041809	0.002567	ML
		0.8	1.5	0.0026424	0.0031071	ML
		0.6	2	0.002747	0.0033751	MOM
	4	0.5	0.8	0.003617	0.00214	ML
		0.8	1.5	0.004122	0.00431	MOM
		0.6	2	0.001513	0.00221	MOM
	3.5	0.5	0.8	0.001643	0.004151	MOM
		0.8	1.5	0.003512	0.00421	MOM
		0.6	2	0.003415	0.00396	MOM
60	3	0.5	0.8	0.000436	0.000412	ML
		0.8	1.5	0.000434	0.000251	ML
		0.6	2	0.000104	0.000161	ML
	4	0.5	0.8	0.000974	0.000994	MOM
		0.8	1.5	0.000762	0.000636	ML
		0.6	2	0.000152	0.000051	ML
	3.5	0.5	0.8	0.000734	0.000626	ML
		0.8	1.5	0.000346	0.000215	ML
		0.6	2	0.000789	0.000313	ML
90	3	0.5	0.8	0.000919	0.0001021	ML
		0.8	1.5	0.000514	0.000231	ML
		0.6	2	0.000501	0.000282	ML
	4	0.5	0.8	0.000747	0.0002031	ML
		0.8	1.5	0.000671	0.000115	ML
		0.6	2	0.000621	0.000071	ML
	3.5	0.5	0.8	0.000606	0.0000241	ML
		0.8	1.5	0.000264	0.0000112	ML
		0.6	2	0.000255	0.0000151	ML

Conclusion

- ☒ Rayleigh distribution is a good probability distribution for representing signal data, also time to failure for medical physical experiments when failure happens after ($t > \alpha\ for\ example$), but in our research we work on modifying two parameters Rayleigh into three one's.

- ☒ Reliability estimators by moments and maximum likelihood indicates that ($\hat{R}_{MLE}$) is better than ($\hat{R}_{MOM}$) with percentage (75%), while ($\hat{R}_{MOM}$) with (25%).

- ☒ The sample size taken are ($n = 30,60,90$), with different sets of initial values obtained under condition ($\alpha\lambda > 1$).

- ☒ The results are compared by statistical measures mean squares errors.

References
[1]Abd – Elfatta, A.M., (2011), "Goodness of fit test for the generalized Rayleigh distribution with unknown parameters", Journal of Statistical Computation and Simulation, Vol.81, No.3, 357 – 366.
[2]Abdul-Moniem I. B. and Abdul-Hameed H.F. (2012),"On Exponentiated Lomax Distribution".Inter. Jou. Of Math. Archive -3(5), pp:2144-2150.
[3]Azeem Ali, Syed AnwerHasnain, and Munir Ahmad, (2015), MODIFIED BURR III DISTRIBUTION, PROPERTIES AND APPLICATIONS, Pak. J. Statist.Vol. 31(6), 697-708.
[4]Dey, S. and Das, M.K. (2007), "A note on Prediction Interval for a Rayleigh Distribution: Bayesian Approach", American Journal of Mathematical and Management Science, 27(1&20, 43 – 48.
[5]Flaih A., Elsallaukh H., Mandi E. and Milanova M. (2012),"The Exponentiated Inverted WeibullDistribution", Appl. Math. Inf. Sci., vol. 6, no. 2, pp:167-171.
[6]Kundu, D. and Raqab, M.Z., (2005), "Generalized Rayleigh Distribution: Different Methods of Estimations", Computational Statistical and Data Analysis, 49, 187 – 200.
[7]Lawless, J.F., (1982), "Statistical Models and Methods for life time data", Jhon Wiley & Sons, New York.
[8]MOHAMMAD Z. RAQAB – MOHAMED T. MADI, (2009), "Bayesian analysis for the exponentiated Rayleigh distribution", METRON - International Journal of Statistics 2009, vol. LXVII, n. 3, pp. 269-288.
[9]Raqab, M.Z., (2005), "Generalized Rayleigh Distribution Different Methods of Estimation", Computational Statistics and Data Analysis, 49,187 – 200.
[10]Raqab M.Z. and Madi M.T. (2009), "Bayesian Analysis for the Exponentiated Rayleigh Distribution", METRON-Inter. J. of stal., vol. 67, no.3, pp:269-288.
[11]Rosaiaah, K., Kantam, R.R.L. and Santosh Kumar, Ch., (2007), Reliability of Test plants for exponentiated log logistic distribution", Economic Quality Control, Vol. , 165 – 175.
[12]Reza Azimi1, FarhadYaghmaei and DarioshAzim, (2012)," Comparison of Bayesian Estimation Methods for Rayleigh Progressive Censored Data Under the Different Asymmetric Loss Function", International Journal of Applied Mathematical Research, 1 (4) (2012) 452-461.
[13]SankuDey, TanujitDey, Sudhansu S. Maiti, (2015), "Bayes Shrinkage Estimation of the Parameter of Rayleigh Distribution for Progressive Type-II Censored Data", Austrian Journal of Statistics, Volume 44, 3–15.

[14]Sanko Dey (2008), "Minimax Estimation of the parameter of the Rayleigh distribution under quadratic loss function", Data Science Journal, Vol. 7, 23.

[15]Shankar Kumar Shrestha, Vijay Kumar, (2014), "Bayesian Analysis for the Generalized RayleighDistribution", International Journal of Statistika and Mathematika, Volume 9, Issue 3, pp 118-131.

[16]Smail Mahdi, (2006), "Improved Parameter Estimation in RayleighModel", Metodološkizvezki, Vol. 3, No. 1, 63-74.

وليد مية رودين
جامعة البصرة / كلية الادارة والاقتصاد / قسم الاحصاء

الملستخلص

يعتبر توزيع رايلي من التوزيعات المستمرة المهمه التي تستخدم في بيانات اوقات الفشل ، اذ تم عمل تحديث على توزيع رايلي باستخدم التحويل الاسي للحصول على توزيع بثلاث معالم وتم اشتقاق صيغة للعزم R للحصول على مقدرات العزوم وكذلك تقدير المقدرات للنموذج باستخدام دالة الامكان الاعظم وقد تم استخدام قيم ابتدائية مختلفة وبعدد تكرارات التجربة لـ(R=1000) وتم مقارنه النتائج بالاعتماد على معيار متوسط مربعات الخطاء(MSE)

The superiority of fuzzy exponential faimly distributions in measuring the reliability of the machines

Adnan Shamkhi Jaber
University of Babylon
College of Economics
& Business Management
Department of Statistics

Safa Fahm Talal
University of Baghdad
College of Economics
& Business Management
Department of Statistics

Abstract:

The study of the efficiency of the reliability of systems or productive systems in scientific life has a significant and important role in the scientific and technological development of these systems. This study deals with the superiority of mass fuzzy exponential distributions (exponential, wibble, kama, natural logarithmic) in measuring the reliability of the machines of the successive system.

The applied study included data taken from the Diesel Station north of Diwaniyah, which is the time of failure and taken to a single block consisting of five machines operating respectively.

The most important results of the study are that the data follow the distributions of the mass fuzzy exponential and the best distribution is the natural distribution logarithmic as the owner of the highest reliability as it turns out that the machines decreased significantly and largely because of the lack of preventive maintenance of these machines because of lack of equipment backup materials as a result of the austerity policy as well as the poor fuel used in operation.

Keywords: Fuzzy   reliability - Wibull   distribution - fuzzy   gama   distribution - fuzzy   groups

Introduction

The Reliability has become an important aspect of the life and effectiveness of equipment and machinery. The interest increased during the Second World War and expanded in the recent years as a result of rapid developments and the use of electronic devices and complex systems. The time of this development has been increased interest in studying the causes of holidays that result in the cessation of machines and devices at different , the breakdown of these machines and devices   leads to material losses as well as low production ,

The Parallel production systems consist of many production systems and the effectiveness of these systems can be determined by reliability. Validity suggests that the system is effective or ineffective.
The concept of reliability is the possibility of the ability of the machine or the device to complete the operations of non-failure (malfunction) either statistically, the reliability is the possibility that the machine or the device is working to accomplish a certain work for a period of time until the breakdown in this machine, Its occurrence is how long it will take to be repaired. Mistakes have an effect in the decision-making process to solve any problem. In practice, most of the problems faced by researchers may suffer from a lack of information or inaccuracy in the collection process. Adversely affect the solution of these problems.

Adnan .S / Safa .F

The phenomenon that has the fuzzy character estimate the remaining time of the cancer patient misery of treatment for survival may determine the doctors a number of months and four months to stay alive and then will die life until we find that this patient may leave life before or after this time and hence the soul , The variable age of the patient is a misty variable, and other phenomena that have the fuzzy characteristics, the estimate of the operation period of the machine through the operating life of the machine and the expected time period in which the machine works without failure, such as working for two years, but this machine may fail before the period due to certain circumstances as high temperature or because of poor fuel and other factors that led to the breakdown of the machine ahead of time for breakdown, and here we find that estimate the function of the machine reliability and probably two years is hazy number.

Research problem :
The Diesel station north of Diwaniyah suffers from sudden stops at its engines, which have a negative impact on the production of electric power , as well as the lack of accuracy in times of breakdown   and operation and we will study the fuzzy reliability .

The Search's Goal:
1- Calculating the reliability function of the system and the normal way of blurred failure times, which follow the exponential distributions of mass exponential   and using the functions of belonging and non-trigonometric affiliation

2- Studying the distributions of mass fuzzy exponential and finding the preference of the exponential distributions of the Fuzzy groups   in the calculation of the reliability of the successive system.

The theoretical aspect :
1. Introduction:
The reliability function [2] is defined as the probability that a vehicle will remain in a given system after time t, if our symbol of reliability function is:

$$R(t) = p(T > t) \qquad t \geq 0$$

$$1 - \int_0^t f(t)dt \quad \ldots\ldots\ldots \quad (1)$$

As representing $f(x)$ the probability density function(*p.d.f*) of the random variable reliability x_i any vehicle represents the vehicle's ability to continuity work to certain time periods without stop working before but in fact can be the vehicle to stop working before the time period identified here will show the type of uncertainty in Determination of the duration of the vehicle's suspension, which is due to the presence of fuzzy at the time of suspension of the vehicle and therefore the reliability to be estimated will be a fuzzy reliability.

This chapter deals with some of the basic concepts in the fuzzy groups and clarifies the concept of ambiguous reliability. It also includes the study of some distributions of fuzzy failure times (The Mass exponential)

2 - Some Basic Concepts In Fuzzy Set

The Fuzzy group theory is a generalization of classical group theory. The set group can include the classical group as a special case. The fuzzy group theory mathematical deals with form strict group theory to describe Fuzzy terminology in Fuzzy groups of linguistic modifiers to represent the disparity slightly in meaning, we find that the concept of the degrees of membership or concept of values of organic probabilistic we can get it in a simple as it can represent a membership of some elements in the overall groups and that this membership change from full membership to non-membership and either have full membership or ownership of membership or perhaps a partial membership, and thus any phrase is described as a mathematical function of a group of couples, each of which value .

There are some concepts of Fuzzy groups which we will discuss in detail as follows:

2-1 Fuzzy Groups Fuzzy Set
((Zimmerman)) identified the Fuzzy groups as a set of elements   that can be specific or non-specific so that each element that belongs to Group A and will be the degree of membership in one or non-specific to the group and the degree of membership of zero, and allows varying degrees between zero and one.

Thus, the group theory is characterized by the presence of the function of affiliation so that each element of the total group is associated with a number in the range [0,1] represents the achievement of that element of the characteristic which is trying to sub-group to represent it mathematically If we had a space that includes all the elements of a comprehensive group   ,

$$X = \{x_i\} \qquad i = 1, 2, ..., n$$

$$A = \{x_i , \mu_A(x_i) , x_i \in X , \mu_A(x_i) \in (0,1)\} \ldots\ldots\ldots (2)$$

A is called a blurred group and is called   a function of belonging. We note that a function $\mu_A(x_i)$ that is asso-ciated with x_i that represents the degree of belonging of that element   to group A [8].

2-2 α-cut
Defined α as the lowest degree of belonging owned by any element of the cloud group A and the value is within the closed period [0,1] [7]

Adnan .S / Safa .F

3-2 Membership Functions :

The main motivations for the formation of fuzzy clusters are to deal with concepts of a hazy nature that cannot be categorically determined. Each group A is defined in terms of a comprehensive set X defined by a function called the membership function $x \in X$ and symbolized by $(\mu_{A^i} R)$ Each element $x \in X$ indicating a value in the closed period [0,1] characterizes the degree of membership of element X in A. The most famous of these formulas:

- Triangular-Shape Membership Function [13]

  It is a function of three parameters (a, b, c) and its general form

$$\mu_{A(x,a,b,c)} = \begin{cases} 0 & if \ x \prec a \\ \dfrac{x-a}{b-a} & if \ a \leq x \leq b \\ \dfrac{c-x}{c-b} & if \ b \leq x \leq c \\ 0 & if \ x \succ c \end{cases} \quad (3)$$

- Trapezoidal Function [13]

Is a function that has four parameters (a, b, c, d) and can be expressed as follows :

$$\mu_A(x,a,b,c,d) = \begin{cases} 0 & x < 0 \\ \dfrac{x-a}{b-a} & a \leq x \leq b \\ 1 & b \leq x \leq c \\ \dfrac{d-x}{d-c} & c \leq x \leq d \\ 0 & x > d \end{cases} \quad (4)$$

- Bell function [13] is a nonlinear exponential function that expresses the natural curve shape and its formula:

$$\mu(x) = ce^{-(\frac{x-a}{b})^2} \quad -\infty < x < \infty \quad (5)$$

There are other functions, such as the function of oversize and other functions.

The functions used in this research are the functions of the triangular member ship function non-member, ship Function and symbolizes these functions with the symbol and the variance in the form of two forms   : [11: pp352]: $v_A(x) \quad \mu_A(x)$

$$\mu_A^{\sim}(x) = \begin{cases} \dfrac{x-a_1}{a_2-a_1} & a_1 \leq x \leq a_2 \\ \dfrac{a_3-x}{a_3-a_2} & a_2 \leq x \leq a_3 \\ 0 & otherwise \end{cases} \quad (6)$$

$$v_A^{\sim}(x) = \begin{cases} \dfrac{a_2-x}{a_2-a_1'} & a_1' \leq x \leq a_2 \\ \dfrac{x-a_2}{a_3'-a_2} & a_2 \leq x \leq a_3' \\ 1 & otherwise \end{cases} \quad (7)$$
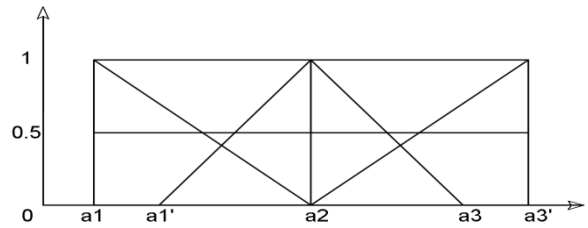
Figure (1): represents the function of belonging - not belonging to the fuzzy number (reference No. 11)

3 -The Fuzzy Reliability

The Fuzzy reliability is defined as follows:

The probability of working the vehicle with varying degrees of success and for a period of time t When calculating the reliability of any vehicle and for a specified period between t1 and t2, it is certain that the vehicle is working at time t1 but the vehicle may stop working before time t2 ie the time of stop t2 is something of uncertainty, For this reason, the value t2 is ambiguous and according to the group theory, the whole set of elements is fuzzy .

On this basis we will deal in this research with the concept of fuzzy reliability symbolized by the symbol $\tilde{R}$ and expressed as follows:

Let $\tilde{R}$ be part of a group A whereas A is a group of fuzzy event and if it expresses the performance of the vehicle to be operated and reflects the performance of a group   of vehicles. From the definition of fuzzy conditional probability we have [15]:

$$P(A \cap A_i) = P(A) . P(\tilde{A_i} | A) \quad (8)$$

By compensating equation (9) in equation (8) we get:

$$P(A) = R \ , \ P(A \cap A_i) = R \quad (9)$$

)

And assuming that $\tilde{A_i}$ it is the degree (R) in of belonging in and compensation $\mu_{\tilde{A}}(R)$ in $P(\tilde{A_i} | A)$:

$$\tilde{R} = P(\tilde{A_i} | A) . R \quad (10)$$

According to the definition of reliability we obtain:

$$\tilde{R} = R . \mu_{A_i}(R) \quad (11)$$

Adnan .S / Safa .F

In equation (8) we obtain:

$$R = \int_T^\infty f(t)dt \qquad (12)$$

$$\tilde{R} = \int_T^\infty f(t)dt \cdot \mu_{A_i}(R) \qquad (13)$$

We also assume that the random fuzzy variable represents the working time t of the system components. It is also assumed x to have a distribution function $f(x_i,\theta)$ and a cumulative distribution function $\tilde{F}_x(t)$ since [4: pp1295-1298]

$$\tilde{F}_x(t) = p(x \le t) \qquad (14)$$

Depending on the natural cumulative distribution function, the mathematical uncertainty is defined as follows:

$$F_x(t) = p(\mathrm{T} > t) = 1 - F_{x(t)} \qquad (15)$$

$$= \{ [1 - F_{\max}(x)(\alpha)], [1 - F_{\min}(x)(\alpha)], [\mu_{F(x)(\alpha)}] \} \qquad (16)$$

x : Normal random variable

$F_{\max}(x)(\alpha)$: Is the cumulative distribution function of the upper limit at the cutting level-α

$F_{\min}(x)(\alpha)$: Is the cumulative distribution function of the minimum at the cutting level-α

$F_{\min}(x)(\alpha)$: The degree of belonging to the cumulative distribution function at the level of cutting-α

4- Fuzzy Reliability calculation of systems :
The components of any functional system are generally related to several forms, such as sequential correlation and parallel correlation, and there are double-installation systems. Each of these forms has special mathematical treatment, the results of which are reflected in the results of the total system

4-2 Series System [5: pp74]
It consists of a set of components linked together in a way that can be represented in **Figure (2-2)**, which shows the connection of the system respectively, so that failure of one of the components causes the collapse of the entire system and that the success of the system depends on the success of the work of its components in this model to obtain the highest reliability so that The number of components is less than possible. If it is the uncertainty of the system   of components, the reliability of the system $\tilde{R}$ is calculated   as follows:

N represents the number of system dependencies

$$\tilde{R}_S = \Pi_{i=1}^n \tilde{R}_i \qquad (17)$$

Figure (2): Sequential scheme scheme (pp74: source 5)

4.2 Parallel System [5: pp74]
This system consists of a set of components that are related to each other so that the success of the system depends on the success of at least one component and lose the system function when the breakdown of all components at one time so the system's fuzzy reliability is:

$$\tilde{R}_P = 1 - \prod_{i=1}^n (1 - \tilde{R}_i) \qquad (18)$$

As:

$\tilde{R}_i$: Is the fuzzy reliability of the component i
n : The number of system dependencies The parallel system is represented as follows:
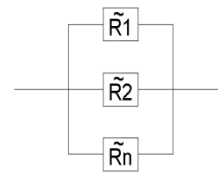
Figure 3: Parallel Link Scheme (PP75: Source 5)

5 - Distributions of the exponential mass
This study included a study of a number of important distributions in measuring reliability, including:

5.1 Fuzzy exponential Distributions
The exponential distribution is one of the most common distributions that is a special case of gamma distribution and is associated with some continuous distributions such as (Pareto Distribution). If the random variable x has a Pareto distribution with a parameter λ the random variable $z = \ln(x)$ is distributed in the exponential distribution $\frac{1}{\lambda}$. The risk function is a constant quantity, the probability density function for exponential distribution is as follows [16]:

$$f(t ; \lambda) = \lambda e^{-\lambda t} \quad t \succ 0 , \lambda > 0 \qquad (19)$$

As λ it is the parameter of measurement for exponential distribution. If the distribution parameter is ambiguous then the probability density function will be defined as the following formula [10: pp75]:

$$f(t) = \tilde{\lambda} e^{-\tilde{\lambda} t} \quad , t \succ 0, \lambda \succ 0 \qquad (20)$$

$$f(t; \tilde{\lambda}) =$$
$$\{ f(t)[\alpha], \mu_{f(t)} | f(t)[\alpha] f_{\min}(t)[\alpha], f_{\max}(t)[\alpha], \mu_{f(t)} \} \qquad (21)$$

$$f_{\min}(t)[\alpha] = \inf \{ f(t,\lambda)[\alpha] | \tilde{\lambda} \in \lambda[\alpha] \}$$

$$= \{ \lambda^{\mathrm{L}[\alpha]} e^{-\lambda^{\mathrm{L}[\alpha](t)}} \} \qquad .... \quad (22)$$

Adnan .S / Safa .F

$$f_{\max}(t)[\alpha]=\sup\left\{f(\text{t},\lambda)[\alpha]\big|\lambda\in\tilde{\lambda}[\alpha]\right\}$$

$$=\left\{\lambda^{\text{u}[\alpha]}e^{-\lambda^{\text{u}[\alpha](\text{t})}}\right\} \qquad (23)$$

As:

$\tilde{\lambda}$: Measurement parameter for exponential distribution

$f(x,\lambda)$: Fuzzy probability density function

$\lambda^{u}[\alpha]$: Measurement parameter for minimum exponential distribution

$\lambda^{u}[\alpha]$: Measurement parameter for upper limit of exponential distribution

The average is:

$$E(\text{t})=\left\{\frac{1}{\lambda}\mid\lambda\in\tilde{\lambda}[\alpha]\right\} \qquad (24)$$

The distribution variation is:

$$\text{var(t)}=\left\{\frac{1}{\lambda^2}\mid\lambda\in\tilde{\lambda}[\alpha]\right\} \qquad (25)$$

The aggregate function (C.D.F) is

$$F(\text{t};\tilde{\lambda})=\left\{F(t)[\alpha],\mu_{F(t)}\big|F(t)[\alpha]=F_{\min}(t)[\alpha],F_{\max}(t)[\alpha],\mu_{F(t)}=\alpha\right\}$$

$$F_{\min}(t)[\alpha]=\inf\left\{\text{F}(t_i,\lambda)[\alpha]\big|\lambda\in\lambda[\alpha]\right\}$$
$$=1-e^{-\lambda L[\alpha]} \qquad (26)$$

$$F_{\max}(t)[\alpha]=\sup\left\{F(x_i,\lambda)[\alpha]\big|\lambda\in\tilde{\lambda}\right\}$$
$$=1-e^{-\lambda u[\alpha]} \qquad (27)$$

From (25) and (26) we obtain :

$$F(t_i,\lambda)=\left[e^{-\lambda L[\alpha]t},e^{-\lambda u[\alpha]t}\right] \qquad (28)$$

The distributive reliability function of the distribution is calculated as follows [10: pp76]:

$$R_{\min}(t)[\alpha]=1-\sup\left\{F(t,\lambda)[\alpha]\big|\lambda\in\tilde{\lambda}[\alpha]\right\}$$
$$=e^{-\lambda L[\alpha]t} \qquad (29)$$

$$R_{\max}(t)[\alpha]=1-\inf\left\{F(t,\lambda)[\alpha]\big|\lambda\in\tilde{\lambda}[\alpha]\right\}$$
$$=e^{-\lambda u[\alpha]t} \qquad (30)$$

From (29) and (30)   we get:

$$R(t,\tilde{\lambda})=\left[e^{-\lambda L[\alpha]t},e^{-\lambda U[\alpha]t}\right] \qquad (31)$$

5.2 – Fuzzy Log-Normal Distribution[6][1]

This distribution is characterized by its close relationship to one of the most important statistical distributions and widespread, which is the normal distribution and can clarify the relationship as follows : If a random variable x has a normal distribution with parameters $X\sim N(\mu,\sigma)$, a random variable χ has the natural logarithmic distribution with the same parameters. Note that $y=e^{-x}$ the new parameters do not represent the mean and variance of the variable. The logarithmic distribution has the following probability density function:

$$f(t;\mu,\sigma^2)=\frac{1}{t\sqrt{2\pi\sigma^2}}e^{-\left(\frac{\ln(t)-\mu}{2\sigma}\right)^2};\ t\succ 0,-\infty\prec\mu\prec\infty,\sigma^2\succ 0 \quad (32)$$

If the time of life follows the lognormal distribution of the two parameters μ and σ , then exponential function potential is known :

$$f(x,\tilde{\mu},\tilde{\sigma})=\{f(x)[\alpha],\mu f(x)\mid f(x)[\alpha]_t[f_{\min}(x)[\alpha],f_{\max}(x)[\alpha],\mu f(x)=\alpha]\}$$

Throughout this function we could get (C.D.F)

$$F(t,\tilde{\mu},\tilde{\sigma})=\{F(t)[\alpha],\mu F(t)\mid F(x)[\alpha]=[F_{\min}(x)[\alpha],F_{\max}(x)[\alpha]],\mu(x)=\alpha\}$$

$$=\left\{\Phi\left(\frac{\log(t-\mu^u[\alpha])}{\sigma^u[\alpha]}\right),\Phi\left(\frac{\log(t-\mu^L[\alpha])}{\sigma^L[\alpha]}\right)\right\} \qquad (33)$$

μ^u= The expected minimum for failure time .

μ^L= The expected maximum for failure time.

σ^u = The standard deviation to the minimum for failure time .

σ^L= The standard deviation to the maximum for failure time

By using function (C.D.F) fuzzy we could get the fuzzy reliability as follows :

$$R(\text{t})[\alpha]=1-F(t,\mu,\sigma)$$

$$=\left\{1-\Phi\left(\frac{\log(t)-\mu^L}{\sigma^L}\right),1-\Phi\left(\frac{\log(t)-\mu^u}{\sigma^u}\right)\right\} \qquad (34)$$

And its average

$$E(t)=\left\{e^{\mu+\frac{1}{2}\sigma^2}\ /\ \mu\in\mu[\alpha],\overline{\sigma^2}\in\overline{\sigma}[\alpha]\right\} \qquad (35)$$

Adnan .S / Safa .F

And contrast:

$$\text{var(T)} = \left\{ [e^{\sigma^2} - 1][e^{2\mu+\sigma^2}] / \mu \in \bar{\mu}[\alpha], \sigma^2 \in \bar{\sigma}[\alpha] \right\} \quad (36)$$

Using the CDF function. We can calculate the reliability function of fuzzy coli:

$$\tilde{R}(t)[\alpha] = \left\{ 1 - \tilde{F}(t, \tilde{\mu}, \tilde{\sigma}) = \{1 - \phi(\frac{\log t - \mu^L}{\sigma^L}), 1 - \phi(\frac{\log t - \mu^u}{\sigma^u}) \right. \quad (37)$$

5-3(fuzzy Weibull distribution)

It is the most useful distribution of reliability analyzes by controlling the distribution parameters that enable us to make a fit for the distribution of(times) or (ages) . The Weibull distribution of 1951 was used by the researcher Wallodi Weibull for the experimental demonstration of changes in expansion Iron and also used to express the period of service spent by radio personnel. This distribution can be shortened to the exponential distribution when the shape parameter is equal to one and Wipple's distribution has an increasing failure rate when the shape parameter is greater than one and has a decreasing failure rate when the shape parameter is less than one.

The Variable Weibull $\omega = \alpha, \beta$ and in which field $0 < x < \infty$ its measurement parameter $\theta > 0$ an form $\beta > 0$ Therefore, the probability density function p.d.f is as follows [3: pp200]:

$$f\,(t) = (\beta t^{\beta-1}/\theta^\beta)\,e^{-\left(\frac{t}{\theta}\right)^\beta}\ \ t \succ 0 : \beta, \theta \succ 0 \quad (38)$$

In case the distribution parameters are fuzzy then the probability density function will be defined as [9: pp82]:

$$f\,(x, \tilde{\theta}) = \{ \frac{\beta}{\theta[\alpha]}(\frac{X}{\theta[\alpha]})^{\beta-1} e^{-\left(\frac{X}{\theta[\alpha]}\right)^\beta}[\alpha], \mu f\,(x) \mid \text{f(x)}[\alpha] \quad (39)$$

Using this function we can obtain the aggregate function C.D.F:

$$\text{F}(t, \tilde{\theta}) =$$
$$\{ \text{F}(t)[\alpha], \mu_{f\,(t)} \mid \text{F(x)}[\alpha] = [\text{F}_{\min}(t)[\alpha], \text{F}_{\max}(t)[\alpha]], \mu\text{F(t)} = \alpha \}$$

$$= \{ 1 - e^{-\left(\frac{t}{\theta^j[\alpha]}\right)^\beta}, 1 - e^{-\left(\frac{t}{\theta^L[\alpha]}\right)^\beta} \} \quad (40)$$

Depending on the CD.F mist function, we calculate the uncertainty reliability function for the failure times on the following formula:

$$\tilde{R}(t)[\alpha] = \left\{ e^{-\left(\frac{t}{\theta^L[\alpha]}\right)^\beta}, e^{-\left(\frac{t}{\theta^u[\alpha]}\right)^\beta} \right\} \quad (41)$$

and its average

$$\mid (\theta\Gamma(1 + \beta^{-1}) \mid \theta \in \tilde{\theta}[\alpha]) \quad (42)$$

Contrast :

$$\mid \theta^2[\Gamma(\beta+1)/\beta] - [\Gamma\{(\beta+1)/\beta\}]^2 \mid \theta \in \tilde{\theta}[\alpha]\} \quad (43)$$

5-4 (Fuzzy Gama distribution)

One of the most important Gamma distributions used in the field of reliability which is often used as a model for the distribution of failure times in electrical, mechanical, and electromechanical systems. This distribution has the following probability density function [2]:

$$f(t, \lambda, r) = \frac{\lambda^r t^{(r-1)} e^{-\lambda t}}{\Gamma(r)}\ , t \geq 0 \quad (44)$$

If the distribution parameters are fuzzy , then the density function p.d.f will be defined as follows

$$\tilde{f}(t, \lambda, r) = \frac{\lambda^r t^{(r-1)} e^{-\lambda t}}{\Gamma(r)}\ , t \geq 0\ , \lambda \in \tilde{\lambda}[\alpha]\ , r \in \tilde{r}[\alpha] \quad (45)$$

As :

λ Shape parameter

r Represents the measurement parameter

$\Gamma(r)$ gamma function

It could be identify the Gama Function as follows :

$$\Gamma(r) = \int_0^\infty t^{(r-1)} e^{-t}\ dt \quad (46)$$

This function is characterized by [12]:

1- Each r > 1 is $\Gamma(r) = (r-1).\Gamma(r-1)$

2-for each correct number(n) is $\Gamma(n) = (n-1)!$

3- $\Gamma(\frac{1}{2}) = \sqrt{\pi}$

Adnan .S / Safa .F

For the blended aggregate function of the Cama D.F distribution, it is defined as:

$$F(t,\bar{r},\bar{\lambda})=\{\frac{1}{\Gamma(r)}(r,\lambda t)\mid \text{r}\in \bar{r}[\alpha],\lambda\in\bar{\lambda}[\alpha]\} \qquad (47)$$

And distributional mean :

$$E(t)=\{\frac{r}{\lambda}\mid \lambda\in\bar{\lambda}[\alpha]\,,\,r\in\bar{r}[\alpha]\} \qquad (48)$$

The contrast

$$var(t)=\{\frac{r}{\lambda^2}\mid \lambda\in\bar{\lambda}[\alpha]\,,\,r\in\bar{r}[\alpha]\} \qquad (49)$$

The fuzzy reliability function of the fuzzy Gama distribution [4]:

$$\bar{R}(t)=\frac{1}{\Gamma(r)}\Gamma(r,\lambda t)\mid \lambda\in\bar{\lambda}[\alpha]\,,\,r\in\bar{r}[\alpha] \qquad 50)$$

It is defined at the α-level :

$$\bar{R}(t)[\alpha]=[R_1[\alpha],R_2[\alpha]] \qquad (51)$$

as :

$$R_1[\alpha]=\min \frac{1}{\Gamma(r)}\Gamma(r,\lambda t)\mid \lambda\in\bar{\lambda}[\alpha]\,,\,r\in\bar{r}[\alpha] \qquad (52)$$

$$R_2[\alpha]=\max \frac{1}{\Gamma(r)}\Gamma(r,\lambda t)\mid \lambda\in\bar{\lambda}[\alpha]\,,\,r\in\bar{r}[\alpha] \qquad (53)$$

Applied side :
1. Introduction :

   Due to the importance of the location and population density of the Middle Euphrates region and the urgent need for electric power, a diesel station was established in Diwaniyah in 2012 with a design card of 196MW. It consists of 48 engines (generating unit with a capacity of 4.02 MW) distributed over 8 blocks and each block consists of 6 motors connected in parallel with auxiliary devices Fuel purifiers, oil purifiers, water treatment unit, oil heaters, boilers, air compressors and fuel tanks of both types (Diesel and HFo oil). It was initially operating on the fuel oil (Diesel) and then the automatic

conversion of the operation of black oil for the low costs and economic feasibility.

2. Data collection stage :

   Data on working times were collected from the planning and maintenance department of one block which consists of six motors connected in parallel for a period of five months from 1/1/2015 to 1/6/2015. All non mechanical and non-electrical stops were excluded. In some cases, the machine may be disrupted and then return to work on the same day before issuing the order for that fault, thus producing inaccuracies. In running the holidays, we are told that the holidays are maintenance times.

The following table shows the times of holidays and one block.

	Eng.1	Eng.2	Eng.3	Eng.4	Eng.5
1	32~	56~	26~	17~	29~
2	105~	13~	42~	22~	26~
3	42~	83~	62~	42~	22~
4	85~	61~	67~	170~	52~
5	56~	326~	13~	88~	87~

Table (1) shows the breakdown times for the five machines

   By collecting data and information on the production machines at the diesel station north of Diwaniyah, the stopping hours were obtained. As shown in Table (4-1) we arranged these data upward and then calculated the function of belonging to these times as shown below and according to the formulas (6, 7)

$$13,22,26,29,32,45,52,56,61,62,67,85,87,88,105,170,326$$

$$\mu_{\Pi3}(t) \;=\; \begin{cases} \dfrac{t-3}{13-3} & 3\le t\le 13 \\[2mm] \dfrac{23-t}{23-13} & 13\le t\le 23 \end{cases}$$

$$v_{\Pi3}(t) \;=\; \begin{cases} \dfrac{13-t}{13-3} & 3\le t\le 13 \\[2mm] \dfrac{t-13}{23-13} & 13\le t\le 23 \end{cases}$$

In order to obtain the fuzzy reliability is extracted and   for fuzzy numbers as shown below:

$$13\alpha=3+10\alpha \quad,\;23-10\alpha \qquad 13\beta=13-10\beta \quad,\;13+10\beta$$

$$22\alpha=12+10\alpha \quad,32-10\alpha \qquad 22\beta=22-10\beta \quad,\;13+10\beta$$

$$26\alpha=16+10\alpha +36-10\alpha \qquad 26\beta=26-10\beta \quad,\;13+10\beta$$

Adnan .S / Safa .F

Thus, the function of fuzzy reliability is measured by using the trigonometric function and the non-affiliation function, and by the type of distribution the data takes

* Measurement of the fuzzy reliability of the failure times that follow the distal exponential mass distributions

• If the failure times are followed for the exponential distribution, we apply the formula (41) mentioned in the theoretical side and using the function of belonging and non-trigonometric affiliation

• If follow the best time to distribute and apply the formula (56) mentioned in the theoretical part

Using the function of belonging and non-trigonometry

• If the failure times are followed for the distribution of Gama, the formula (65) mentioned in the theoretical aspect is applied

Using the function of belonging and non-trigonometry

• If the failure times are followed for natural logarithmic distribution, the formula (47) mentioned in the theoretical side shall be applied using the function of belonging and non-trigonometric affiliation. In applying the above formulas,

1- The reliability of the system is significantly reduced as it does not return again because of the lack of preventive maintenance on these machines in order to increase their production capacity

2 – The fluctuation of the values of reliability uncertainty at different levels of the values of α as the value of the value increases the value α of the system

3 - It has been observed that the natural logarithmic distribution is the best in the measurement of the fuzzy dependence of the system because it is the owner of the highest priority.

Table (2): The values of uncertainty for the failure times that follow the exponential distribution and using the trigonometric function

α	0.1		0.2		0.3		0.4		0.5	
	MIN	MAX	MIN	MAX	MIN	MAX	MIN	MAX	MIN	MAX
1	0.9953251	0.9999356	0.9959653	0.9998836	0.9965431	0.9998085	0.9970616	0.9997053	0.9975239	0.9995686
2	0.9720468	0.9928779	0.9742092	0.9916701	0.9762698	0.99034	0.9782294	0.9888837	0.9800885	0.9872979
3	0.9505615	0.9795584	0.9535541	0.977261	0.9564473	0.9748222	0.9592405	0.9722414	0.9619331	0.9695182
4	0.8335587	0.8674438	0.8387506	0.8616576	0.8438936	0.8557929	0.8489854	0.8498538	0.8540237	0.8438443
5	0.5208156	0.5193613	0.5274864	0.5111798	0.5342103	0.5030882	0.5409864	0.4950874	0.5478137	0.4871786

Adnan .S / Safa .F

Table (3): The values of the uncertainty of the failure times that follow the exponential distribution and the non-trigonometric function

a	0.1		0.2		0.3		0.4		0.5	
Fuzzy R	MIN	MAX	MIN	MAX	MIN	MAX	MIN	MAX	MIN	MAX
1	0.1741521	0.1732936	0.1639001	0.1868645	0.1542517	0.2014982	0.1451712	0.2172779	0.1366252	0.2342933
2	0.05908045	0.04874455	0.0556025	0.05256183	0.0523293	0.05667803	0.04924878	0.06111659	0.0463496	0.06590274
3	0.02890183	0.02038604	0.02720044	0.02198251	0.0255992	0.023704	0.02409223	0.0255603	0.02267397	0.02756197
4	0.00347958	0.00161294	0.00327474	0.00173925	0.00308197	0.00187546	0.00290054	0.00202233	0.00272979	0.0021807
5	4.5165E-05	1.1069E-05	4.2506E-05	1.1935E-05	4.0004E-05	1.287E-05	3.7649E-05	1.3878E-05	3.5433E-05	1.4965E-05

(Table 5)The values of uncertainty are shown for the failure times that follow the Weppel distribution and using the function of trigonometry

α	0.1		0.2		0.3		0.4		0.5	
Fuzzy R	MIN	MAX	MIN	MAX	MIN	MAX	MIN	MAX	MIN	MAX
1	0.9999223	0.9999997	0.9999482	0.9999992	0.9999662	0.999998	0.9999785	0.9999957	0.9999913	0.9999867
2	0.9964003	0.9994885	0.9971235	0.9992819	0.997726	0.9990131	0.9982225	0.9986695	0.9982376	0.9986273
3	0.9825484	0.9949086	0.9849966	0.9937068	0.9871884	0.9923095	0.9891377	0.9907004	0.9886638	0.9908594
4	0.7956014	0.8603317	0.8057959	0.8512236	0.8158739	0.8419315	0.8258164	0.8324728	0.835604	0.8228651
5	0.2607925	0.3729729	0.2713716	0.3608502	0.2823301	0.3490501	0.2936722	0.3375728	0.305401	0.3264178

Adnan .S / Safa .F

(Table 6) shows the values of the fuzzy reliability of the failure times that follow the Weppel distribution and the use of the trigonometric function

a	0.1		0.2		0.3		0.4		0.5	
Fuzzy .R	MIN	MAX	MIN	MAX	MIN	MAX	MIN	MAX	MIN	MAX
1	0.9998868	0.9999993	0.9999184	0.9999983	0.999942	0.9999964	0.9999595	0.9999929	0.999987	0.9999722
2	0.9967806	0.9994327	0.9973647	0.9992366	0.9978583	0.9989889	0.9982726	0.99868	0.9982996	0.9986177
3	0.9846364	0.9949633	0.9866952	0.9938836	0.9885369	0.9926373	0.9901759	0.9912094	0.9895849	0.9916269
4	0.8099397	0.8697895	0.8204215	0.8606205	0.8307096	0.8511961	0.8407819	0.8415339	0.8316524	0.8506171
5	0.2404458	0.3683794	0.2531115	0.3540432	0.2663218	0.2663218	0.2800744	0.3265693	0.2943642	0.3134465

Table (7): The values for the uncertainty of the failure times that follow the distribution of Gama and the use of the trigonometric function

a	0.1		0.2		0.3		0.4		0.5	
Fuzzy >R	MIN	MAX	MIN	MAX	MIN	MAX	MIN	MAX	MIN	MAX
1	0.9999714	0.9999976	0.9999765	0.9999962	0.999982	0.999994	0.9999871	0.9999909	0.9999913	0.9999867
2	0.9958357	0.9995185	0.9965732	0.9993603	0.9972157	0.999163	0.9977684	0.9989208	0.9982376	0.9986273
3	0.9810243	0.995294	0.9831962	0.9943688	0.9852301	0.9933243	0.9871205	0.9921557	0.9888638	0.9908594
4	0.7971126	0.8632029	0.8032841	0.8561954	0.8096437	0.8492439	0.8161762	0.8423724	0.8228651	0.835604
5	0.2876003	0.3559262	0.2968061	0.3411782	0.3063416	0.3288409	0.316211	0.3169154	0.3054178	0.326401

Adnan .S / Safa .F

Table (8): The values of the uncertainty of the failure times that follow the natural distribution of logarithmic and using the trigonometric function.

α	0.1		0.2		0.3		0.4		0.5	
fuzzy R	MIN	MAX	MIN	MAX	MIN	MAX	MIN	MAX	MIN	MAX
1	0.9999903	0.9999994	0.9999907	0.9999988	0.9999924	0.9999979	0.9999946	0.9999964	0.9999966	0.9999943
2	0.9929952	0.9994304	0.9942914	0.9992063	0.9954253	0.998919	0.9964013	0.9985582	0.9972264	0.9981138
3	0.9703485	0.993583	0.9737067	0.9922001	0.9768976	0.9906374	0.9799025	0.9888919	0.9827052	0.9869634
4	0.7543248	0.8259274	0.7604414	0.8181854	0.7668029	0.8105954	0.7734009	0.8031789	0.7802255	0.7959561
5	0.3525427	0.3813772	0.3597718	0.37081	0.3672213	0.3605663	0.3748959	0.3506424	0.3828002	0.341034

Table (9): The values of fuzzy reliability of the failure times that follow the natural logarithmic distribution and using the trigonometric function

α	0.1		0.2		0.3		0.4		0.5	
fuzzy R	MIN	MAX	MIN	MAX	MIN	MAX	MIN	MAX	MIN	MAX
1	0.9999432	1	0.9999659	0.9999999	0.9999004	0.9999996	0.9999891	0.9999988	0.9999943	0.9999966
2	0.994669	0.9993216	0.9957954	0.998991	0.9967304	0.9985471	0.997496	0.9979669	0.9981138	0.9972264
3	0.9748288	0.9924294	0.9783675	0.9904815	0.9815617	0.9882218	0.9844225	0.9856342	0.9869634	0.9827052
4	0.7536585	0.8194801	0.764285	0.8097317	0.7748882	0.7999293	0.7854512	0.7900889	0.7959561	0.7802255
5	0.3035969	0.4186169	0.3125287	0.4093174	0.3217419	0.4002505	0.331242	0.3914127	0.341034	0.3828002

Adnan .S / Safa .F

Conclusions :

1- The results obtained in the applied side in the measurement of fuzzy reliability showed that the logarithmic distribution is the best distribution among distributions. The exponential mass is the distribution with the highest reliability

2 - Due to the results obtained in the application side, the function of fuzzy reliability decreases with time as well as the holidays which increase with time due to the lack of spare materials and the equipment needed to maintain these engines for its durability.

3- In this study, the study of the applied side showed the fluctuation of the value of the reliability function and the mean time by the difference of the value of alpha .

4 - It has been concluded that the production machines suffer from frequent delays by observing the rate of holidays during the five months as a result of the lack of preventive maintenance of these engines because of the lack of equipment backup materials, which leads to a shortage of capacity of these machines .

Arabic references :

1-Shakir , Maitham Muwafq Farkhri , Zeina Hakmat Chalub , Khalid Zghaitoon (2014) "Using the Hippocampal Arrangement Method for Solving the Issue of Allocation in the Industrial Sector in Baghdad", Journal of Modern College, University, Vol. 2"

2-Al-Ghanim Mohammed Taha Hamad , Al-Sabagh , Hiba Atya , (2009) , A Study of Speculative Variables and Multiplexed Regression", Tikrit Journal of Economic and Administrative Sciences, vol. 5, no. 14.

3-Al-Wakeel , Ali Abdul Hussein (2004) , " "Notes on the Weppel Distribution," Journal of Economic and Administrative Sciences, vol. 18, no. 67

References

1- A. Venkatesh[*] , S. Elango . (2013) . " Fuzzy Reliability Analysis for the Effect of TRH Based on Gamma Distribution " , A. Venkatesh et at Int. Journal of Engineering research and Applications , Issn : 2248- 9622, vol.3 , pp.1295- 1298 .

2- Amit Kumara, Shiv prasadYadav and Surendra Kumar . (2008). " Fuzzy system Reliability using Different type of   Vague set " , International journal of Applied science and Engineering , 6 , 1 : 71 – 83 .

3- Avenkatesh and S. Mohankumar ,(2013) , " Fuzzy reliability analysis for the effect of vasopressin Based on normal distribution " , Aryabhaha Journal of Mathematics and Informatics , Vol. 5 , No.2 .

4- Bo yuan and George, j.kilr ,(1995),"fuzzy set and fuzzy logic theory and application.publ.by prentice hall ptr.new jersey 07458.

5- Chirg , F.F , Rong j . , Jin S.S , (2014) , " Fuzzy system reliability analysis based on level (λ– 1) intreval – valued fuzzy numbers , information science 272 , 185 – 197 .

6- E.BalouiJamkhaneh . (2014) " analyzing system Reliaibity using fuzzy weibull lifetime Distribution " , International Journal of Applied Operational Research , Vol .4 , No .1 , PP 81- 90 .

7- EzzatallahBalouiJamkhaneh   .(2012). " Relaiaibbility estimation under the fuzzy environments " , The journal of mathematic and computer science , vol. 5, No.1 , 28 – 39

8- G.s.mahparta&t.k.roy   .(2009)." Reliability evaluation using triangular intuitionistic fuzzy numbers arithmetic operations", tnternational journal of computer , electrical,automation, control information engineering

9- HosseinPishro – nik ,(2008). " introduction to probability ", statistics and Random processes " .

10- Hung T Nguyen & Elbert A Walker.(2000)." A first course in fuzzy logic",

11- Klir Et Al.(1997),".

12- Kumar , V. & Huang , Y. , (1993) , " Reliability analysis of amine production system a case study " . proceedings Annual Reliaibility and maintainbility symposium 167- 172 .

13- Li Tingie and Gao He , " Fuzzr reliability " , Beijing Institute of Aeronautics and Astronautics , 1988

افضلية توزيعات العائلة الاسية الضبابية في قياس معولية المكائن

عدنان شمخي جابر   الباحثة صفا فاهم طلال
جامعة بغداد ــ كلية الادارة والاقتصاد ــقسم الاحصاء

المستخلص :

يدرس البحث قياس المعولية الضبابية كما تناول ايضا دراسة افضلية توزيعات العائلة الاسية الضبابية (الاسي، ويبل، كاما، الطبيعي اللوغارتيمي) في قياس معولية النظام المتتالي.

وقد اشتملت الدراسة التطبيقية على بيانات تم اخذها من محطة ديزل شمال الديوانية وهي عبارة عن أوقات الفشل والمأخوذة لبلوك واحد مكون من خمس مكائن تعمل على التوالي.

وتمثلت اهم نتائج الدراسة ان التوزيع الطبيعي اللوغارتمي هو افضل توزيع من بين توزيعات العائلة الاسية الضبابية، اذ يُعد التوزيع هو التوزيع صاحب اعلى معولية. وان الماكينات انخفضت معوليتها وبشكل كبير مع تزايد معدل العطل بسبب عدم اجراء ادامة لهذه الماكينات بسبب قلة التجهيزات بالمواد الاحتياطية نتيجة لسياسة التقشف المتبعة بالإضافة الى رداءة الوقود المستعمل في التشغيل.

Simulation Methods of Multivariate Normal Distribution

Fadhil Abdul Abbas Abidy
Technical College of Management
Al-Furat Al-Awsat Technical University

abidy_fadhil@yahoo.com

Ali Hussein Battor   **Esraa Abdul Reza Baqir**
Department of Mathematics
College of Education for Girls
University of Kufa

alih.battor@uokufa.edu.iq   asraalghanm@gamil.com

Abstract:. In this paper, we are studying three simulation methods to generate observation for multivariate normal distribution, and these methods are: Matlab mvnrnd, decomposition and conditional methods, and we put simulation programs for each method by Matlab 2015a software, and comparison between these methods by depend on many criterions as MSE, AIC, skw, kur. As well as the run speed criterion for each method to get the best method.

1- Introduction:

Wolfgang Bischoff and Werner Fieger generalization the result of the Castillo and Galambos for multivariate random vectors [4], Patrick J., Matias, katarzyna [5], Chun-Chao Wang [6] and others wrote about the multivariate normal distribution and the simulation tests.

Multivariate distributions are studying with several variables (p)that is associated with each relationship and different degrees and thus dependent with a variance and covariance matrix Σ.[1] If Y has a multivariate normal distribution with mean vector μ and var-covariance matrix ∑, the density function is given by :

$$g(Y) = \frac{1}{\left(\sqrt{2\pi}\right)^p |\sum|^{\frac{1}{2}}} e^{-(Y-\mu)^{'}\sum^{-1}(Y-\mu)/2}$$

Where μ :Length-p row vector, $\sum: p \times p$ Matrix, $|\sum|$:Matrix determinant, and p is the number of variables. [2]

2- The concept of simulation

As a result of appearance several problems and statistical theories which are difficult find a logical analysis by mathematical proof, so it has been translated and transformation these theories to real societies, then they have chosen a number of independent random samples, To get the ideal solution for these problems, so practically these samples which are difficult find at the area because they Requires High cost, Time and effort hence some researchers have gone in the beginning of Twentieth century to apply technique the sampling experiment that which is known today simulation .The simulation process is a digital style to complete the experiments on the electronic calculator, which include types of logical and mathematical operations necessary to describe the behavior and structure of complex real system through a given time period.

Fadhil .A/Ali .H/Esraa .A

3- Comparative criteria:
1) Mean squared error (MSE)

If T is (statistic) estimate for the parameter θ then we called that $E[(T - \theta)^2]$ is
$$MSE = E[(T - \theta)^2]$$
$$= V(T) + [\theta - E(T)]^2$$
Now when the estimate T be unbiased estimator then $\theta = E(T)$, which mean that $[\theta - E(T)]^2$ is equal to zero and
$$MSE = V(T).$$
There is another formula for these estimators specially (for joint estimator) of it as

$$MSE_{model} = det \frac{1}{Rep} \sum_{i=1}^{Rep} ((T - \theta)(T - \theta)')$$

Where Rep: Replication of experiment

2) Akaike information criteria (AIC)
The form of this criteria is either
$$AIC = -2\log(MLE) + 2n \text{ ,or}$$
$$AIC = Nlog(MSE) + 2n$$
Where n: number of fitted parameters,
N: sample size.

3) Mardia's test statistic for skewness and kurtosis [6] [7]
If $X_1, X_2, \dots, X_n$ random sample of independent and identical p-variate vectors with unknown mean μ and unknown covariance matrix $\sum$. Mardia (1970-1974) defined the measure of multivariate skewness and kurtosis as follows:

$$b_{1,p} = \frac{1}{n^2} \sum_{i,j=1}^{n} g_{ij}^{3}$$

Where
$$g_{ij} = (x_i - \overline{x})' S^{-1}(x_j - \overline{x})$$
And
$$b_{2,p} = \frac{1}{n} \sum_{i=1}^{n} \{(x_i - \overline{x})' S^{-1}(x_i - \overline{x})\}^2$$

Under normality of $X_1, X_2, \dots, X_n$, asymptotically MVN ,A=n$b_{1,p}$ /6 has a X^2 distribution with f=p(p+1)(p+2)/6 degrees of freedom and the statistic $B = b_{2,p} - p(p + 2)/\sqrt{8p(p + 2)/n}$ has asymptotic standard normal distribution . Based on the statistic A and B, as test for multivariate normality jarque and bera (1987) proposed to use the statistic JB=A+B^2 which has asymptotic chi-square distribution with f+1 degrees of freedom. in addition, the distribution is symmetric (null

of skewness) around the curve when the value of skewness is zero (sk=0), and the value of kurtosis for the normal distribution in univariate case is 3,while the Mardia's kurtosis is p(p+2) for the multivariate distribution of p- variables, which is ku= 2(2+2)=8 when (p=2).but, the p_JB criterion has belong on the following hypothesis

H∘: the data is belong to MVN
If p-value <0.05 the hypothesis H∘ is reject.
Either p-value >0.05 the hypothesis H∘ is not reject.

4- Formulation of Simulation Model

We are choose Matlab 2015a as a program for this study to write a simulation model to generate observation for multivariate normal distribution and selecting default value for the parameters $\mu = \begin{bmatrix} 2.6 \\ 4 \end{bmatrix}$, $\Sigma = \begin{bmatrix} 1 & -1 \\ -1 & 2 \end{bmatrix}$ of this distribution, in addition to select sample size n= 15 , 50 ,100 and 200 respectively and choosing the number of replication as (R= 10000).

5- Simulation method
1- Matlab mvnrnd
This method depend on the following formula to get observation for multivariate normal distribution as
$$y = mvnrnd(mu, sigma\_cov, sample size)$$
Where mu: mean value vector for the distribution $sigma\_cov$: variance and cov_variance for the variable and we wrote a complete program for this method in matlab software.

2- Decomposition method

To generate observation of multivariate normal distribution by this method must be generate the vector $\underline{Z}$ from the relation $Z \sim N_p(0,1)$
and also generate the matrix T from the form $chol A$ in matlab program, such that A is var_cov matrix ,then get the variable X as
$X = \underline{\mu} + T\underline{Z}$ that submit to this distribution.

3- Conditional method[3]

The idea of this method is
- Generate x_1 from the marginal distribution of X_1.
- Generate x_2 from the conditional distribution of X_2, given $X_1 = x_1$.

The suitability of this method for a given bivariate distribution depends on there being an efficient method for generating from the required univariate distributions.

Fadhil .A/Ali .H/Esraa .A

Let $(X_1, X_2)'$ denote the bivariate normal vector with covariance matrix $\sum$ .define

$$Y_1 = (X_1 - \mu_1)/\sigma_1$$

$$Y_2 = \frac{(X_2 - \mu_2) - \frac{\sigma_2}{\sigma_1}(X_1 - \mu_1)\rho}{\sigma_2(1 - \rho^2)^{1/2}}$$

Then Y_1 and Y_2 are two independent standard normal variables, and we can express it by

$$X_1 = \sigma_1 Y_1 + \mu_1$$

$$X_2 = \sigma_2 \rho Y_1 + \sigma_2(1 - \rho^2)^{\frac{1}{2}} Y_1 + \mu_2$$

Univariate standard generators are widely available for this purpose.

More generally, let $X \sim N(\mu, \sum)$, i.e, X is a p-dimensional multivariate normal random vector with mean vector μ and covariance matrix $\sum$, let L be the lower triangular matrix of the cholesky decomposition of $\sum$, i.e a matrix such that $\sum = LL'$.(routines for computing L are available in many computer software packages.) given ρ independent univariate standard variates, $Y' = (Y_1, \ldots, Y_\rho)$, transform them

$$X = LY + \mu$$

To achieve $N_p(\mu, \sum)$ distribution.

5- Result of simulation

After we show the special methods to generate observation for multivariate normal distribution, we review the results that obtained it from these methods as:

Table (3-1): Simulation result of multivariate normal distribution by mvnrnd method

Sample size	$\hat{\mu}$	$\hat{\sum}$	$\hat{\rho}$	MSE	skw Sig. of skw	kur Sig. of kur	(P_JB)	time	AIC
15	[2.5975 4.0056]	[0.9971 1.9917]	-0.8330	3.1445	0.7875 0.7415	5.7207 0.1349	0.9483	0.9672	21.1848
50	[2.5996 3.9998]	[0.9997 1.9957]	-0.8064	0.0809	1.2377 0.0355	8.0727 0.4744	0.2818	0.9828	-121.6971
100	[2.5980 4.0029]	[0.9999 1.9970]	-0.5736	0.0101	0.1307 0.7031	7.5316 0.2791	0.6975	1.1076	-455.1037
200	[2.5994 3.9995]	[1.0003 2.0008]	-0.7019	0.0013	0.0201 0.9549	7.7267 0.3145	0.9884	1.2324	-1332.4

Table (3-2): Simulation result of multivariate normal distribution by decomposition method

Sample size	$\hat{\mu}$	$\hat{\sum}$	$\hat{\rho}$	MSE	skw Sig. of skw	kur Sig. of kur	(P_JB)	time	AIC
15	[2.5987 3.9979]	[0.9993 1.9968]	-0.7350	3.2092	0.4369 0.8955	5.7690 0.1401	0.9113	1.4508	21.4905
50	[2.5981 4.0010]	[0.9948 2.0012]	-0.7082	0.0848	0.2766 0.6799	6.0539 0.0427	0.6620	0.9672	-119.4022
100	[2.5986 4.0021]	1.0006 2.0010]	-0.7750	0.0101	0.2457 0.3933	7.6275 0.3207	0.5616	1.1856	-455.6912
200	[2.5992 4.0014]	[0.9999 2.0025]	-0.7266	0.0012	0.4234 0.0069	9.1161 0.0243	0.4155	2.3244	-1334.0

Fadhil .A/Ali .H/Esraa .A

Table (3-3): Simulation result of multivariate normal distribution by conditional method

Sample size	$\hat{\mu}$	$\hat{\Sigma}$	$\hat{\rho}$	MSE	skw Sig. of skw	kur Sig. of kur	(P_JB)	time	AIC
15	[2.6010 4.0007]	[0.9973 1.9966]	-0.7484	3.2385	0.5520 0.8477	0.9016 0.1548	0.7903	0.9204	21.6265
50	[2.6007 3.9996]	[1.0028 1.9972]	-0.6849	0.0842	0.2019 0.7939	7.2519 0.2542	0.7057	0.9516	-119.7166
100	[2.6014 3.9989]	[0.9997 1.9997]	-0.7280	0.0104	0.2071 0.4852	8.2721 0.3669	0.1768	1.0296	-452.1387
200	[2.6001 4.0002]	[1.0006 1.9998]	-0.6959	0.0012	0.0445 0.8295	8.0473 0.4666	0.8811	1.2480	-1334.2

Table (3-4): Comparison between the results in table (3-1),(3-2)and (3-3)

Sample size	methods	$\hat{\mu}$	$\hat{\Sigma}$	$\hat{\rho}$	MSE	skw Sig. of skw	kur Sig. of kur	(P_JB)	time	AIC
15	Matlab (mvnrnd)	[2.5975 4.0056]	[0.9971 1.9917]	-0.8330	3.1445*	0.7875 0.7415	5.7207 0.1349	0.9483*	0.9672	21.1848*
	Decomposition	[2.5987 3.9979]	[0.9993 1.9968]	-0.7350*	3.2092	0.4369* 0.8955	5.7690 0.1401	0.9113	1.4508	21.4905
	Conditional	[2.6010 4.0007]	[0.9973 1.9966]	-0.7484	3.2385	0.5520 0.8477	5.9016* 0.1548	0.7903	0.9204*	21.6265
50	Matlab (mvnrnd)	[2.5996 3.9998]	[0.9997 1.9957]	-0.8064	0.0809*	1.2377 0.0355	8.0727* 0.4744	0.2818	0.9828	-121.6971*
	Decomposition	[2.5981 4.0010]	[0.9948 2.0012]	-0.7082*	0.0848	0.2766 0.6799	6.0539 0.0427	0.6620	0.9672	-119.4022
	Conditional	[2.6007 3.9996]	[1.0028 1.9972]	-0.6849	0.0842	0.2019* 0.7939	7.2519 0.2542	0.7057*	0.9516*	-119.7166
100	Matlab (mvnrnd)	[2.5980 4.0029]	[0.9999 1.9970]	-0.5736	0.0101*	0.1307* 0.7031	7.5316 0.2791	0.6975*	1.1076	-455.1037
	Decomposition	[2.5986 4.0021]	1.0006 2.0010]	-0.7750	0.0102	0.2457 0.3933	7.6275 0.3207	0.5616	1.1856	-455.6912*
	Conditional	[2.6014 3.9989]	[0.9997 1.9997]	-0.7280*	0.0104	0.2071 0.4852	8.2721* 0.3669	0.1768	1.0296*	-452.1387
200	Matlab (mvnrnd)	[2.5994 3.9995]	[1.0003 2.0008]	-0.7019*	0.0013	0.0201* 0.9549	7.7267 0.3145	0.9884*	1.2324*	-1332.4
	Decomposition	[2.5992 4.0014]	[0.9999 2.0025]	-0.7266	0.0012*	0.4234 0.0069	9.1161 0.0243	0.4155	2.3244	-1334.0
	Conditional	[2.6001 4.0002]	[1.0006 1.9998]	-0.6959	0.0012*	0.0445 0.8295	8.0473* 0.4666	0.8811	1.2480	-1334.2*

Fadhil .A/Ali .H/Esraa .A

Table (3-5): Number times of excellence for each method and the total ratio to excellence

Sample size	Methods		
	Matlab (mvnrnd)	Decomposition	Conditional
15	3	2	2
50	3	1	3
100	3	1	3
200	4	0.5	2.5
Total of each method	13	4.5	10.5
Ratio	47%	16%	37%

Table (3-6): The average of all parameters and criterion of each method

Methods	mean1	mean2	var1	var2	roh	MSE	skw	kur	P_JB	time	AIC
Matlab (mvnrnd)	2.600	4.002	0.999	1.996	-0.714	0.809	0.544	7.263	0.729	1.073	-472.004
Decomposition	2.599	4.001	0.999	2.000	-0.736	0.826	0.346	7.142	0.638	1.482	-471.901
Conditional	2.603	4.000	1.000	1.998	-0.718	0.834	0.251	6.118	0.638	1.037	-471.107

Table (3-7): Number times of excellence for each method and the total ratio to excellence according to the average of each method

Methods	Matlab (mvnrnd)	Decomposition	Conditional
Total of each method	6	1	4
Ratio	55%	9%	36%

Fadhil .A/Ali .H/Esraa .A

6-   Discussion of the Results

Form the above tables we can discuss the following
result:

1- We can see in the tables (3-1),(3-2) and (3-3) that the valve of $\hat{\mu}$ and $\hat{\Sigma}$ are approach to the default value ,which $\mu = \begin{bmatrix} 2.6 \\ 4 \end{bmatrix}, \Sigma = \begin{bmatrix} 1 & -1 \\ -1 & 2 \end{bmatrix}$ when the sample size are increasing from the smaller (15) to greater (200) in all three methods .

2- Note that the criterion MSE, AIC in all simulation results in the tables (3-1),(3-2) and (3-3) above are inversely proportional to the sample size, which mean ,when sample size is increasing the criterion MSE ,AIC are decreasing .but the values of criterion skewness (sk) are approach to zero when the sample size is increasing in each method , also the values of kurtosis criterion(ku) are nearly from (8) in each method when the sample size start to be increasing, in addition , the values of the joint criterion (p_JB) in every method and in all cases of sample size are greater than (0.05) then we accept the hypothesis H∘, which
H∘: the data is belong to MVN
If p-value <0.05 the hypothesis H∘ is reject.
Either p-value >0.05 the hypothesis H∘ is not reject.

3- The table (3-4) shown the comparison between the simulation result of these methods ,such that the best value to the criterion MSE,AIC when sample size is(15),(50) is matlab (mvnrnd) method ,and when sample size increasing (100) the best value of MSE is in the same method above but AIC in decomposition method , also when sample size is more increasing (200) we can see the same value (0.0012)to criterion MSE in decomposition ,conditional method ,respectively and criterion AIC is just in conditional method .

4- In same table (3-4) of comparison the best value of criterion skewness when sample size is (100) and (200) in matlab (mvnrnd) method, but in decomposition when sample size is (15) while in conditional method when sample size is (50).

5- In table (3-5) we make a comparison to know the number of times of excellence and total ratio of excellence($ratio = \frac{sub\ number}{total\ number} * 100$) for each method and we get that the upper ratio to the matlab (mvnrnd) method (47%), while the second method (decomposition) have got on (37%), and so be the matlab (mvnrnd) method is the best method to generate observation of multivariate normal distribution.

6- After that we put table (3-6) to get the average of all the parameter and criterion of each method, this average got from accumulated the four values of parameter and criterion in addition to correlation in all case of sample size after that we divided it by four, for example to get the value (2.600) of mean 1 in the same table, we do that
Mean1=
(2.5975+2.5996+2.5980+2.5994)/4=2.600,
And so on for all other values, in addition to the table (3-7) contain the comparison of number of the times of excellence and the ratio to table (3-6) , and finally we deduced that the best method is matlab (mvnrnd)method because it get (55%) as a better ratio .

Fadhil .A/Ali .H/Esraa .A

7-   Appendixes (Programs)

```
clear all;num=1;
 while num<4
num=input('number of program 1 cond. 2 Dec.
3 Matlab?');
switch num
case  1
% program 1 Generate observation of
Multivariate Normal by conditional  with
Box_Muller Method
disp('Result of conditional method')
n=input('sample size?');% n is sample size.
Rep=input('R of Rep.?');% number of
replications
t0=cputime();rand('seed',n);
s_m=0;ssme =[0 0];ssva=[0 0];SS_MS=0;
mu=[2.6 ; 4];sigma=[1 -1;-1 2];
rho=sigma(1,2)/(sigma(1,1)*sigma(2,2))^0.5;
l=length(mu);
for r=1:Rep

U=unifrnd(0,1,2,n);U1=U(1,:);U2=U(2,:);ph=2
*(pi)*U1;R=(-2*log(U2)).^0.5;
   z1=R.*cos(ph);z2=R.*sin(ph);
      x1=mu(1,1)+z1*sigma(1,1)^0.5;
      y2=rho*z1+sqrt(1-(rho)^2)*z2;
      x2=mu(2,1)+sigma(2,2)^0.5*y2;
      x=[x1;x2]';me=mean(x);
      ssme=ssme+me;ssva=ssva+var(x) ;
      SS_MS=SS_MS+(me'-mu)*(me'-mu)';
end
   me=ssme/Rep
   var=ssva/Rep
   MSE=det(SS_MS)/(n-1)/Rep
   % MSE criterion for model
    AIC= n*log(MSE)+2*l
   % AIC criterion for model
    co=corr(x);rho_h=co(1,2)
    X=x;
[n,p] = size(X); alpha = 0.05;
difT = [];
for    j = 1:p
  difT = [difT,(X(:,j) - mean(X(:,j)))];
end;
S = cov(X);       % Variance-covariance matrix
D = difT * inv(S) * difT'; % Mahalanobis'
distances matrix
b1p = (sum(sum(D.^3))) / n^2; % Multivariate
skewness coefficient
b2p = trace(D.^2) / n; % Multivariate kurtosis
coefficient
v = (p*(p+1)*(p+2)) / 6;       % Degrees of freedom
g1 = (n*b1p) / 6;          % Skewness test statistic
(approximates to a chi-square distribution)
P1 = 1 - chi2cdf(g1,v);  % Significance value of
skewness
```

```
g2 = (b2p-(p*(p+2))) / ...
  (sqrt((8*p*(p+2))/n));       % Kurtosis test statistic
(approximates to a unit-normal distribution)
P2 = 1-normcdf(abs(g2)); % Significance value of
kurtosis
sk=b1p
ku=b2p
stats.Ps  = P1
stats.Pk  = P2
ks=skewness(X);ku=kurtosis(X)-3;
kwen=ks*ks';kur=ku*ku';
jb=n/6*(kwen+kur/4)
p_jb=1-chi2cdf(jb,v)
Mean_Ku=p*(p+2)*(p+1+n)/n
time=cputime()-t0
case 2
   % program 2 Generate observation of Multivariate
Normal by decomposition with inverse Method
disp('Result of Dec. method')
n=input('sample size?');
Rep=input('R of Rep.?');
t0=cputime();rand('seed',n);
s_m=0;ssme =[0 0];ssva=[0 0];SS_MS=0;
mu=[2.6 ; 4];sigma=[1 -1;-1 2];l=length(mu);A=sigma;
T=chol(A);
for r=1:Rep
   u=rand(n,2);Z=norminv(u,0,1);Y=Z*T;
for i=1:n
   for j=1:2
     X(i,j)=mu(j)+Y(i,j);
   end
end
   me=mean(X);
    ssme=ssme+me;ssva=ssva+var(X);
    SS_MS=SS_MS+(me'-mu)*(me'-mu)';
end
   me=ssme/Rep
   var=ssva/Rep
   MSE=abs(det(SS_MS))/(n-1)/Rep
   % MSE criterion for model
   AIC= n*log(MSE)+2*l
   % AIC criterion for model
   co=corr(X);rho_h=co(1,2)
[n,p] = size(X); alpha = 0.05;
difT = [];
for    j = 1:p
  difT = [difT,(X(:,j) - mean(X(:,j)))];
end;
S = cov(X);    % Variance-covariance matrix
D = difT * inv(S) * difT';% Mahalanobis' distances
matrix
b1p = (sum(sum(D.^3))) / n^2;  % Multivariate
skewness coefficient
b2p = trace(D.^2) / n; % Multivariate kurtosis
coefficient
v = (p*(p+1)*(p+2)) / 6;    % Degrees of freedom
g1 = (n*b1p) / 6;          % Skewness test statistic
(approximates to a chi-square distribution)
```

Fadhil .A/Ali .H/Esraa .A

```matlab
P1 = 1 - chi2cdf(g1,v);   % Significance value of
skewness
g2 = (b2p-(p*(p+2))) / ...
   (sqrt((8*p*(p+2))/n));     % Kurtosis test statistic
(approximates to a unit-normal distribution)
P2 = 1-normcdf(abs(g2)); % Significance value of
kurtosis
stats.Ps  = P1
stats.Pk  = P2
sk=b1p
ku=b2p
ks=skewness(X);ku=kurtosis(X)-3;
kwen=ks*ks';kur=ku*ku';
jb=n/6*(kwen+kur/4)
p_jb=1-chi2cdf(jb,v)
time=cputime()-t0
   case 3
   % program 3 Generate observation of Multivariate
Normal by Matlab function
disp('Result of MATLAB method')
n=input('sample size n?');
% n is sample size.
Rep=input('R of Rep.=');
t0=cputime();randn('seed',n);
s_m=0;ssme =[0 0];ssva=[0 0];SS_MS=0;
mu=[2.6 ; 4];sigma=[1 -1;-1 2];l=length(mu);
for r=1:Rep
   x=mvnrnd(mu,sigma,n);me=mean(x);
   ssme=ssme+me;ssva=ssva+var(x);
   SS_MS=SS_MS+(me'-mu)*(me'-mu)';
   end
   me=ssme/Rep
   var=ssva/Rep
   MSE=det(SS_MS)/(n-1)/Rep
   % MSE criterion for model
   AIC= n*log(MSE)+2*l
   % AIC criterion for model
 co=corr(x);rho_h=co(1,2)
   X=x;
[n,p] = size(X); alpha = 0.05;
difT = [];
for    j = 1:p
 difT = [difT,(X(:,j) - mean(X(:,j)))];
end;
S = cov(X);     % Variance-covariance matrix
D = difT * inv(S) * difT'; % Mahalanobis' distances
matrix
b1p = (sum(sum(D.^3))) / n^2;   % Multivariate
skewness coefficient
b2p = trace(D.^2) / n;  % Multivariate kurtosis
coefficient
v = (p*(p+1)*(p+2)) / 6;   % Degrees of freedom
g1 = (n*b1p) / 6;    % Skewness test statistic
(approximates to a chi-square distribution)
P1 = 1 - chi2cdf(g1,v);  % Significance value of
skewness
g2 = (b2p-(p*(p+2))) / ...
```

```matlab
   (sqrt((8*p*(p+2))/n));      % Kurtosis test statistic
(approximates to a unit-normal distribution)
P2 = 1-normcdf(abs(g2)); % Significance value of
kurtosis
sk=b1p
ku=b2p
stats.Ps  = P1
stats.Pk  = P2
ks=skewness(X);ku=kurtosis(X)-3;
kwen=ks*ks';kur=ku*ku';
jb=n/6*(kwen+kur/4)
p_jb=1-chi2cdf(jb,v)
Mean_Ku=p*(p+2)*(p+1+n)/n
time=cputime()-t0
   otherwise
      disp('End of select')
      break
end
        end
```

Reference

[1] Anderson, T.W., An Introduction to
   multivariate statistical analysis, John Wiley
   and Sons,(1984).

[2] Rencher, Alvin C., Methods of multivariate
   analysis, Second edition, Brigham young
   university, p. 83, (2002).

[3] N.Balakrishnan, chin-diew lai, continuous
   Bivariate distributions, Second edition,
   633,636, 2008.

[4] Bischoff, wolfgang , fieger ,Werner,
   Characterization of the multivariate normal
   distribution by conditional normal
   distributions, University of Karlsruhe,
    p.240, (1991).

[5] Patrick J. Farrell, Matias Salibian-Barrera
   and Katarzyna Naczk, On test for
   multivariate normality
   and associated simulation studies, Journal
   of statistical computation and simulation,
   Vol.77, No. 12, 1065-1080, (2007).

[6] Chun-Chao Wang, Amatlab package for
   multivariate normality test, Journal of
   statistical Computation and simulation,
   (2013).

[7] Hanusz, zofia and tarasinska,Joanna, On
   multivariate normality tests using skewness
   and kurtosis, colloquium biometricum44,
   139-148, (2014).
    zofia.hanusz@up.lublin.pl ,
    Joanna.tarasinska@up.lublin.pl

Fadhil .A/Ali .H/Esraa .A

طرائق محاكاة للتوزيع الطبيعي متعدد المتغيرات

فاضل عبد العباس العابدي   علي حسين بتور   إسراء عبد الرضا باقر

الكلية التقنية الادارية   كلية التربية للبنات

جامعة الفرات الاوسط التقنية   جامعة الكوفة

المستخلص :

تم في هذا البحث، دراسة ثلاث طرائق محاكاة لتوليد مشاهدات تخضع للتوزيع الطبيعي متعدد المتغيرات وهي:
Matlab mvnrnd، التجزئة والطريقة الشرطية وبناء برامج محاكاة لكل طريقة بأستخدام برنامج Matlab
2015a ، وتم مقارنة هذه الطرائق الثلاث بالاعتماد على عدة مقاييس منها مقياس معدل مربع الخطأ
MSE، مقياس اكاكي ومقياس الالتواء والتفرطح kur, skw، على التوالي بالاضافة الى مقياس سرعة التنفيذ لكل
طريقة.

قواعـد النشـر

- تعنى مجلة القادسية لعلوم الحاسوب والرياضيات بنشر البحوث العلمية الرصينة ذات العلاقة بعلوم الحاسبات ،الرياضيات ،الإحصاء والمعلوماتية والفيزياء الحاسوبية والتي لم تنشر أو تقدم للنشر سابقا .

- تخضع البحوث المقدمة للتقييم العلمي من لدن اختصاصين من داخل القطر وخارجه .

- يقدم البحث مطبوعا بنظام العمودين على ورق ابيض جيد قياس (A4) وبمسـافة مضـاعفة وبنظـام الـ word حصرا وان يكون نظام office 2010 وان يكون حجم الخط المستخدم في طباعة البحث (10) ونوعه Time New Roman ماعدا العنوان واسم الباحث يكون حجم الخط (12)(bold) ونوعه Time New Roman ، أما الجداول والإشكال فيكون الخط bold ونوعه Time New Roman وعند وجود المعادلات في البحث يجب إضافتها باستخدام محرر المعادلات .

- على الباحث (أو الباحثيين) تقديم ملخص لبحثه باللغتين العربية والانكليزية يتضمن عنوان البحث واسم الباحث أو الباحثيين وعناوينهم بحدود (150-200) كلمة .

- على الباحث (أو الباحثيين) ادراج البريد الالكتروني ويفضل ان يكون بريد رسمي .

- استخدام الباحث (أو الباحثيين) ذات البيانات الخاصة به (اسم الباحث ، المرتبة العلمية ، جهة الانتساب ، البريد الالكتروني الرسمي) والمستخدمة في بحوثه السابقة .

- يرتب البحث كما يأتي الخلاصة ، المقدمة ، المواد وطرائق العمل ، النتائج والمناقشة ، الخلاصة باللغة الثانية تتضمن عنوان البحث، اسم الباحث ومكان عمله .

- يتم ذكر المصادر في البحث بإتباع أسلوب الترقيم حسب أسبقية ذكر المصدر وتذكر المصادر في النهاية على الوجه الآتي :
اسم الباحث (أو الباحثيين) عنوان البحث اسم المجلة ، المجلد ، العدد ، رقم صفحتي بدء وانتهاء البحث ، سنة النشر بين قوسين .

- تنشر البحوث باللغة الانكليزية فقط وان يقدم الباحث أربع نسخ من البحث (ورقية + اقراص CD) .

- بعد الانتهاء من عملية التقييم والتصويبات وعند القبول النهائي يقدم البحث على قرص CD (office 2010 + pdf) مع نسخة ورقية نهائية .

- أن لا تزيد صفحات البحث المقدم للنشر عن عشر صفحات وبنظام العمودين وفي حالة تجاوز عدد صفحات البحث اكثر من ذلك يتم دفع خمسة الاف دينار عراقي لكل صفحة زيادة وان لايتجاوز العدد الاجمالي للبحث 20 صفحة .

- تعتمد المجلة تصنيف (Mathematics Subject Classificatio) في نشرها للبحوث العلمية .

- يقدم الباحث التصنيف المعتمد في المجلة لموضوع البحث .

- اجور التقييم والنشر للمجلة كالاتي :
اولا :- اجور التقييم (30000) الف دينار عراقي .
ثانيا :- اجور النشر حسب اللقب العلمي للباحث وكالاتي :
1- المدرس المساعد والمدرس (50000) الف دينار عراقي .
2- الاستاذ المساعد (75000) الف دينار عراقي .
3- الاستاذ (100000) الف دينار عراقي .

ملاحظة : عند تقديم البحث يدفع الباحث مبلغ (35000) الف دينار عراقي غير قابل للرد وفي حالة قبول نشر بحثه في المجلة يدفع بقية الاجور حسب لقبه العلمي .
كما ويدفع مبلغ (10000) الاف دينار عراقي غير قابل للرد اجور استلال ، وفي حالة اعادة فحص الاستلال للبحث مرة اخرى يعاد دفع المبلغ (10000) كأجور اعادة استلال .

مجلة القادسية لعلوم الحاسوب والرياضيات

هيئة التحرير

○ أ.م. د. محمد عباس كاظم   رئيس التحرير

○ د. قصي حاتم عكار   مدير التحرير

○ أ. د. (Gangadharan M.)   عضوا

○ أ.م. د. (N. Magesh)   عضوا

○ أ.م. د. رعد عزيز حسين   عضوا

○ أ.م.د. وقاص غالب عطشان   عضوا

○ أ.م. د. هشام رحمن محمد   عضوا

○ أ.م.د. لمياء عبد نور   عضوا

○ د. شروق جمعه سريح   عضوا

○ د. لمى صلال حسن   عضوا